![UCC University College Cork, Ireland / Coláiste na hOllscoile Corcaigh]

Towards a translational understanding of colonic bacteria in Crohn's disease pathology

A thesis presented to the National University of Ireland, Cork for the

degree of Doctorate of Philosophy

by

Keith O'Donoghue, B.Sc.

School of Microbiology,
School of Biochemistry & Cell Biology,
School of Medicine & Health,
and APC Microbiome Ireland
University College Cork, Cork, Ireland

Research supervisors:
Prof Marcus Claesson
Dr Susan Joyce
Dr Silvia Melgar
Head of School: Dr David J. Clarke
Head of School: Professor Justin V. McCarthy
Head of School: Professor Subrata Ghosh

March 2022

Contents

4

DECLARATION

This is to certify that the work I am submitting is my own and has not been submitted for another degree, either at University College Cork or elsewhere. All external references and sources are clearly acknowledged and identified within the contents. I have read and understood the regulations of University College Cork concerning plagiarism.

Signature: Keith O'Donoghue

Student Number: 110701619

Date: 31 March 2022

Declaration of input from other researchers

All animal experiments were conducted and carried out by APC Microbiome Ireland, UCC following prior approval from the University College Cork Animal Experimentation Ethics Committee.

Microbiota sequencing was performed by Dr Fiona Crispie at Teagasc with subsequent analysis and correlations contributed by Julia Eckenberger (Claesson Lab).

Bile acid Co-incubation experiments were performed by Katie O'Connor and Eabha Wall.

Acknowledgements

First and foremost, I would like to thank my supervisors, Dr. Silvia Melgar, Dr. Susan Joyce, and Prof. Marcus Claesson. Their enthusiasm, support, guidance, and wisdom were a constant source of drive and motivation throughout the years of study. Most of all, however, their understanding, compassion, and patience when times were tough were what really pulled me through, and I owe them a lot for the time they invested into giving good advice and being there when I needed help. Sincere thanks to all of you.

A massive thank you is needed for all the members of APC Spokes 4 and 7, past and present. An amazing group of people who were always willing to help with experiments (or donate some reagents) and are great fun on a night out. In particular, I would like to thank Alvaro, Valerio, Peter, Sarah, Karina, Naomi, Raminder, Gonzalo, Kevin, Mary, and Ana.

I would also like to thank my parents Billy and Joanie, thank you so much for constantly believing in me and encouraging me to pursue my goals. You have provided me with everything I could ever need down through the years and have been an unending source of support. Thank you to my sister Klara who always listened to my PhD woes with the utmost patience and understanding.

I am very privileged to have found wonderful friends in particular I would like to thank; Sean Daly for being a constant source of encouragement (and beautiful nonsense), and who would never let me doubt myself, Aoife for always listening about my PhD with such sincere and happy enthusiasm, John and Philippa for hosting the best parties, Dr. Andrew Ingamells and Dr. Tiffany Slater (my PhD compatriot) for nice relaxing cups of tea and PhD

chats in the countryside, and my brother in law David for his constant support and friendship.

However, my deepest appreciation goes to my wife, Linda. Even in the darkest of times your faith in me never wavered and your strength and resilience remain a constant source of inspiration to me. I do not think I would have been able to finish this PhD if I didn't have you to come home to every night. None of this would have been possible without your selflessness, strength, love, and support. I dedicate this thesis to you.

Publications and presentations

List of publications

Ryan FJ, Power EM, Laserna-Mendieta EJ, Ahern AM, Clooney AG, McMurdie PJ, Iwai S, Crits-Christoph A, Sheehan D, Moran C, **O'Donoghue KW**, *Flemer B, Zomer A, Fanning A, O'Callaghan J, Walton J, Temko A, Stack W, Jackson L, Joyce SA, Melgar S, DeSantis T, Bell JT, Shanahan F, Claesson MJ.* "Colonic microbiota is associated with inflammation and host epigenomic alterations in inflammatory bowel disease". Nat Commun. 2020 Mar 23;11(1):1512. doi: 10.1038/s41467-020-15342-5.

Manuscripts in preparation

Keith O'Donoghue, *Julia Eckenberger, Alvaro Lopez Gallardo, Valerio Rossini, Marcus Claesson, Susan Joyce, Silvia Melgar.* Gender-specific response to *Bacteroides vulgatus* colonisation results in altered microbiota composition and inflammation in a preclinical model of Crohn's disease. Target journal: *Gut Microbes*

Keith O'Donoghue, *Alvaro Lopez Gallardo, Silvia Melgar, Marcus Claesson, Susan Joyce.* Capability of Bacteroides species in modifying bile acid metabolism. Target journal: *Microbiology*

Aine Fanning, **Keith O'Donoghue**, Ana Ramon Vazquez, Mary Ahern, Ken Nally, Fergus Shanahan, Silvia Melgar. The short chain fatty acids acetate, propionate and butyrate differently regulate intestinal epithelial cell gene profile, function, and organoid development. Target journal: *Cells*

List of Presentations

<u>Keith O'Donoghue</u>, *Donjete Statovci, Gregory G. Mullamphy, Susan Joyce, Fergus Shanahan, Marcus J. Claesson, and Silvia Melgar*. Towards a translational understanding of colonic bacteria in Crohn's disease pathology. *Oral presentation* - New Horizons in Medical Research. A Scientific Conference organised by the School of Medicine, Research and Postgraduate Affairs Committee, UCC. December 8th, 2016, Cork, Ireland

<u>Keith O'Donoghue</u>, *Donjete Statovci, Gregory G. Mullamphy, Fergus Shanahan, Marcus J. Claesson, Susan Joyce, and Silvia Melgar*. Towards a translational understanding of colonic bacteria in Crohn's disease pathology. *Poster presentation* - Focused Meeting 2016 – Irish Division. Exploring the Microbe–Immune System Interface. September 1-2, 2016, Cork, Ireland

<u>Keith O' Donoghue</u>, *Susan Joyce, Fergus Shanahan, Marcus Claesson, Silvia Melgar.* Towards a translational understanding of colonic bacteria in Crohn's disease pathology. *Poster presentation*. 7th International Human Microbiome Consortium Meeting, June 26-26, 2017, Killarney, Ireland

<u>Keith O'Donoghue</u>. Towards a translational understanding of colonic bacteria in Crohn's disease pathology. *Oral presentation* - APC Microbiome Ireland Research Forum, Feb 9th, 2021, Cork, Ireland

<u>Keith O'Donoghue</u>, *Julia Eckenberger, Alvaro Lopez Gallardo, Valerio Rossini, Marcus Claesson, Susan Joyce, Silvia Melgar.* Toward a translational understanding of colonic Bacteroides species in Crohn's disease pathogenesis. *Poster presentation*. ICMI 2022, July 16-20, 2022, Seattle, Washington, USA

Abbreviations

16S rDNA	16s subunit ribosomal DNA
2CRS	Two-component regulatory systems
3D	Three dimensional
AA	Amino acid
ABCG5	ATP-binding cassette sub-family G member 5
ABCG8	ATP-binding cassette sub-family G member 8
AC	Adenylate cyclase
ACC	Acetyl-CoA carboxylase
Acetyl-CoA	Acetyl coenzyme A
ACN	Acetonitrile
AEEC	Animal Experimentation Ethics Committee
AF-1	Activation function-1
AF-2	Activation function-2
AIEC	Adherent Invasive *Escherichia coli*
AJ	Apical junction
ALA	ω3 a-Linolenic acid
AMP	Antimicrobial peptides
AMPs	Anti-microbial peptides
ANOVA	Analysis of Variance
APC	APC Microbiome Ireland
APCs	Antigen-presenting cells
Arg	Arginine
ARLD	Alcohol-related liver disease
ASBT	Apical Sodium Dependent Bile Acid Transporter
ASC	Apoptosis associated speck-like containing a CARD domain
Asn	Asparagine
Asp	Aspartic acid
ATCC	American Type Culture Collection
ATG16L1	Autophagy-related 16-like 1 gene
Atoh	Atonal homolog
ATP	Adenosine triphosphate
BA	Bile acid
BA	bile acids
BAAT	Bile acid-CoA:amino acid N-acyltransferase
BACS	Bile acid cholyl-CoA synthetase
Bai	Bile acid inducible
BAR	Bile acid receptor
BAT	Brown adipose tissue
Bcl2	B-cell lymphoma protein 2

BCRP	Breast cancer resistance protein
BMDM	Bone marrow derived macrophages
BMI	Body mass index
BMP	bone morphogenetic protein
Bp	base pair
BSEP/ABCB11	Bile salt export pump/ATP-binding cassette
BSH	Bile salt hydrolase
BSU	Biological services unit
C	degrees Celsius
C-section	Caesarean section
C-section	caesarean section
CA	Cholic acid
CA	Conventional adenoma
CA	cholic acid
CaCl2	Calcium chloride
CAD	Coronary artery disease
cAMP	Cyclic adenosine monophosphate
CAPE	Caffeic acid phenethyl ester
CARD	Caspase-recruitment domain
CBAH	Conjugated bile acid hydrolase
CCL5	Chemokine
CD	Crohn's disease
CD	Clostridia difficile
CD	Crohn's disease
CDCA	Chenodeoxycholic acid
cDNA	Complementary DNA
CE	Cholesterol esters
CF	Cystic fibrosis
CFTR	Cystic fibrosis transmembrane conductance regulator
CFU	Colony forming unit
CGH	Choloylglycine hydrolase
CKD	Chronic kidney disease
CLSI	Clinical & Laboratory Standards Institute
cm	centimetre
CNS	Central nervous system
COX	Cyclooxygenase
CRC	Colorectal cancer
CREB	cAMP-response element-binding protein
CRISPR-Cas	Clustered Regularly Interspaced Short Palindromic Repeats-CRISPR associated protein
CSD	Cysteine sulfinic acid decarboxylase
CSL	CBF1, Suppressor of Hairless, Lag-1
CspC	Cold shock-like protein

CVD	Cardiovascular disease
CVR	Cardiovascular risk
CXC	Chemokine
CYP	Cytochrome P450 enzyme
Cys	Cysteine
D4 CA	Deuterated cholanic acid
D4 CDCA	Deuterated chenodeoxycholic acid
DAMP	Damage-associated molecular pattern
DAMPs	Danger-associated molecular patterns
DC	Dendritic cell
DCA	Deoxycholic acid
DCA	deoxycholic acid
DCs	dendritic cells
DHA	Docasahexaenoic acid
DHCA	Dehydrocholic acid
DIO	Diet induced obesity
DIO-2	Deiodinase 2
DLL	Delta Like Ligand
DMEM	Dulbecco's Modified Eagle's Medium
DNA	Deoxyribonucleic acid
dNTP	Deoxyribonucleotide 5'-triphosphate
DPC	DPC Culture collection Biobank
DPP-4	Dipeptidyl peptidase-4
DR	Direct repeats
DRG	Dorsal root ganglion
dsDNA	Double-stranded DNA
DSS	Dextran Sulfate Sodium
E.coli	Escherichia coli
EB	Elution buffer
EC	Epithelial cadherin
Edg	Endothelial differentiation gene
EDTA	Ethylenediaminetetraacetic acid
EDTA	ethylenediaminetetraacetic acid
EEC	Enteroendocrine cells
EEC	Enteroendocrine cells
EFSA	European Food Safety Authority
EGF	epidermal growth factor
EGFR	Epidermal growth factor receptor
Egr-1	Early growth response protein 1
ELISA	Enzyme linked immunosorbent assay
ENS	Enteric nervous system
EPA	Eicosapentaenoic acid
EPS	Exopolysaccharide

ER	Endoplasmic reticulum
ER-1	Everted repeats
ERBB1	Part of EGFR
ERK1/2	Extracellular signal-regulated kinases
ESPCG	European Society for Primary Care Gastroenterology
EU	European Union
FA	Ferulic acid
FA	Fatty acids
FADR	Fatty acid metabolism regulator protein
FAE	Fatty acid ester
FAO	Food and Agriculture Organization of the United Nations
FAPR	Transcription factor
FBS	Foetal bovine serum
FDA	Food and Drug Administration (US)
FFAR3	Free fatty acid receptor 3
FGF15/19	Fibroblast growth factor 15/19
FGFR4	Fibroblast growth factor receptor 4
FMT	Faecal microbial transplant
Foxp3	Forkhead box protein P3
FXR	Farnesoid X receptor
g	gram(s)
GABA	gamma-Aminobutyric acid
GALT	Gut-associated lymphoid tissue
GC	Guanine and cytosine
GCA	Glycocholic acid
GF	Germ Free
GI	Gastro intestinal
GIs	Genomic Island
GIT	Gastrointestinal tract
GLP-1	Glucagon-like peptide 1
GLUT2	Glucose transporter 2
GNAT	Gcn5-related N-acetyltransferases
GPCRs	G-protein–coupled receptors
GRAS	Generally recognised as safe
GUF	Gene of Unknown Function
GWAS	Genome-Wide Association Study
HC0$_3$-	Bicarbonate
HCA	Hyocholic acid
HDAC	Histidine deacetylases
HDCA	Hyodeoxycholic acid
HDL	High-density lipoproteins
HES	hairy and enhancer of split

HES1	hairy and enhancer of split
HF	High Fat
HFD	High fat diet
HMG-CoA	3-hydroxy-3-methyl-glutaryl-coenzyme A reductase
HMOs	Human milk oligosaccharides
HMP-I	Human Microbiome Project 1
HMP-II	Human Microbiome Project 2
HNF4α	Hepatocyte nuclear factor 4 alpha
HPLC	High-performance liquid chromatography
HSDH	Hydroxysteroid dehydrogenases
HTS	High throughput screening
IBABP	Ileal bile acid binding protein
IBD	Inflammatory bowel disease
IBS	Irritable bowel syndrome
ICAM	Intercellular Adhesion Molecule
ICP	Intrahepatic cholestasis of pregnancy
IELs	intraepithelial lymphocytes
IFN-ϒ	interferon gamma
IgA	Immunoglobulin A
IgE	Immunoglobulin E
IKK	NF-κB regulatory subunit IκB kinase
IL	Interleukin
ILCs	innate lymphoid cells
INFγ	Interferon gamma
IP3	Inositol triphosphate
IPA	International Probiotic Association
IR-1	Inverted repeats
IRAK	IL-1R associated kinases
IRGM	immunity related GTPase family M
IS	Internal standard
ISC	intestinal stem cells
ISCs	intestinal stem cells
IκBα	Nuclear factor of kappa light polypeptide gene enhancer in B-cells inhibitor, alpha
KCl	Potassium chloride
KDa	Kilo daltons
KLF	Krüppel-like factor
KLF4	Krüppel-like factor-4
KO	Knockout
L	litre
LAB	Lactic acid bacteria
LB	Lysogeny Broth (Luria-Bertani)
LCA	lithocholic acid

LCFA	Long chain fatty acids
LDH	lactate dehydrogenase
LDL	Low-density lipoproteins
LDLR	Low density lipoprotein receptor
LFD	Low Fat diet
Lgr5	leucine-rich repeat-containing G-protein coupled receptor
LI	Large intestine
LP	lamina propria
LP	lamina propria
LPA	Lysophosphatidic acid
Lpk	Liver type pyruvate kinase
LPS	Lipopolysaccharide
LPS	lipopolysaccharide
LPS	lipopolysaccharide
LRG5	leucine-rich repeat-containing G-protein coupled receptor 5
LRH-1	Liver receptor homolog-1
LRRs	leucine-rich repeats
LXR	Liver X receptor
M cells	Microfold cells
M3R	Muscarinic receptor 3
MAFG	Maf transcription factor protein G
MAMP	microbe-associated molecular pattern
MAP	Mitogen-activated protein kinase
MCA	Muricholic acid
MCFA	Medium chain fatty acids
MDP	muramyl dipeptide
MDR	Multidrug resistance
MDR2/3	Multi drug resistance tansporter 2/3
MeOH	Methanol
METaHit	Metagenomics of the Human Intestinal Tract
mg	Milligram(s)
mg/kg	Milligram/kilogram
MHC	Class II major histocompatibility complex
MHC	Major histocompatibility complex
MIC	Minimum inhibitory concentration
min	Minutes(s)
ml	Millilitre(s)
MLNs	Mesenteric lymph nodes
MLST	Multilocus sequence typing
mM	millimolar
MOI	multiplicity of infection
mRNA	messenger RNA

MRP2	Multi drug resistance associated protein 2
MRS	Man Rogosa Sharpe
MSD	Meso Scale Discovery
MT-1	Metallothionein-1
MUC2	Mucin-2
Mw	Molecular weight
MYD88	Myeloid differentiation primary response 88
MYD88	myeloid differentiation factor 88
MZ	Mass
N/A	Not applicable
NaCl	Sodium chloride
NAD(P)H	Nicotinamide adenine dinucleotide phosphate
NADH	Nicotinamide adenine dinucleotide
NAFLD	Non-alcoholic fatty liver disease
NaHCO$_3$	Sodium bicarbonate
NASH	Non-alcoholic steatohepatitis
NEUROG3	neurogenein3
NF-κB	Nuclear factor kappa-light-chain-enhancer of activated B cells
NFIL3	Nuclear factor interleukin-3-regulated protein
NGS	Next generation sequencing
NICD	Notch Intracellular Domain
NLR	NOD-like receptor
NLRP3	Nucleotide-binding oligomerization domain, leucine rich repeat and pyrin domain containing 3
NLRs	Nucleotide-binding oligomerisation domain-like receptors
NOD	Nucleotide-binding oligomerisation domain
NOTCH	Notch receptor
NR	Nuclear receptor
NR1H1	Nuclear receptor subfamily 1, group H, member 1
NR1H2	Nuclear receptor subfamily 1, group H, member 2
NR1H3	Nuclear receptor subfamily 1, group H, member 3
NR1H4	Nuclear receptor subfamily 1, group H, member 4
NR1H5	Nuclear receptor subfamily 1, group H, member 5
NR1I1	Nuclear receptor subfamily 1, group I, member 1
nrdB	Ribonucleoside-diphosphate reductase ß chain
NSAID	Non-steroidal anti-inflammatory drugs
NTCP	Na+/Taurocholate Cotransport polypeptide
Ntn	N-terminal nucleophile
OATP1B	Organic anion transporting polypeptide
OCA	Obeticholic acid
OD	Optical density
OH	Hydroxyl

OMV	outer membrane vesicle
Opp	Oligopeptide ABC transporter
ORF	Open reading frame
OSTα	Organic solute transporter alpha
OSTβ	Organic solute transporter beta
OTU	Operational taxonomic unit
PAMP	pathogen associated molecular pattern
PAMPs	Pathogen-associated molecular patterns
parB	Chromosome partitioning protein
PBC	Primary biliary cirrhosis
PBS	Phosphate buffered saline
PCA	Principal components analysis
PCR	Polymerase chain reaction
PDB	Protein Database
Pen/Strep	Penicillin/ Streptomycin
PFGE	Pulsed field gel electrophoresis
pg	picogram(s)
PGC-1α	Peroxisome proliferator-activated receptor gamma coactivator 1-alpha
Ph	Potential of hydrogen
pI	Isoelectric point
pIgR	polyimmunoglobulin receptor
PKA	Protein Kinase A
PKC	Protein Kinase C
pmol	picomoles
PP	Peyer's patches
PPAR	Peroxisome proliferator-activated receptor
ppm	Parts per million
PRR	pathogen recognition receptor
PRRs	pattern recognition receptors
PSC	Primary sclerosing cholangitis
pstB	Phosphate transport, ATP-binding protein
PUFA	Polyunsaturated fatty acids
PVA	Penicillin V acylase
PXR	Pregnane X receptor
QPS	Qualified Presumption of Safety
qRT-PCR	Quantitative reverse transcription polymerase chain reaction
QTOF	Quadrupole time-of-flight
RA	Retanoic acid
RAST	Rapid Annotation using Subsystem Technology
RE	Recognition elements
RegIIIγ	Regenerating islet-derived protein 3 gamma
RFLP	Restriction fragment length polymorphism

RNA	Ribonucleic acid
RORγt	receptor-related orphan receptor γt
ROS	Reactive oxygen species
rpoA	RNA polymerase α chain
rpsB	SSU ribosomal protein S2P
rRNA	ribosomal Ribonucleic acid
RSPO3	R-Spondin 3
RT	Retention time
RXR	Retinoid X receptor
S1P	Sphingosine 1-phosphate
S1PR	Sphingosine 1-phosphate Receptor
SBS	Short bowel syndrome
Scd1	Stearoyl-CoA desaturase-1
SCFA	Short chain fatty acids
SCFA	short chain fatty acids
SD	Standard deviation
SFB	segmented filamentous bacteria
SGF	Simulated gastric fluid
SHP	Small heterodimer partner
SI	Small intestine
SIF	Simulated intestinal fluid
SIGA	RNA polymerase sigma factor SigA
SIgA	secretory IgA
SMAD	mothers against decapentaplegic homologue
SOX9	SRY-box transcription factor 9
SOX9	SRY-box transcription factor 9
spp	species
Src	Proto-oncogene tyrosine-protein kinase
SREBF1	Sterol regulatory element-binding transcription factor 1
SREPB-1c	Sterol regulatory element-binding proteins -1c
ST	Sequence type
STAT	signal transducer and activator of transcription
STAT3	Signal transducer and activator of transcription 3
T2D	Type 2 diabetes
T3	Thyroid hormone
T4	Thyroxine
TA	Toxin-antitoxin
TAE	Tris-acetate-EDTA
TAGs	Triacylglycerides
TaMCA	Tauro-alpha-muricholic acid
TCA	Taurocholic acid
TCA	Tricarboxylic acid cycle

TCDCA	Taurochenodeoxycholic acid
Tcf4	T cell factor 4
TDCA	Taurodeoxycholic acid
TetM	Tetracycline resistance protein
TGF	Tumour growth factor
TGR5	Takeda-G-protein-receptor-5
Th	T helper
Th cell	T helper cell
THCA	Taurohyocholic acid
THDCA	Taurohyodeoxycholic acid
TIR	Toll/IL-1R
TIRAP	TIR domain-containing adapter protein
TJ	Tight junction
TLC	Thin layer chromatography
TLCA	Taurolithocholic acid
TLR	toll-like receptor
TLRs	toll-like receptors
TM	Transmembrane
TMA	Trimethylamine
TMAO	trimethylamine-N-oxide
TMCA	Tauromuricholic acid
TNBS	2,4,6-trinitrobenzene sulfonic acid
TNF-α	tumor necrosis factor alpha
TNFA	Tumor necrosis factor alpha
TNFR	tumour necrosis factor receptor
Treg	T regulatory cells
tRNAs	Transfer RNAs
TUDCA	Tauroursodeoxycholic acid,
UC	Ulcerative colitis
UDCA	Ursodeoxycholic acid
UDP	Uridine triphosphate
UEC	University College Cork Animal Experimentation Ethics Committee
UPLC-MS	Ultra performance liquid chromatography - mass spectrometry
UV	Ultraviolet
v/v	volume/volume
VDR	Vitamin D receptor
VITD	Vitamin D
VLCFA	Very long chain fatty acids
VRE	Vancomycin resistance enterococci
w/v	weight/volume
WAT	White adipose tissue
WHO	World Health Organisation

WNT	Wingless-related integration site
WT	Wild type
x g	G force/Relative Centrifugal Force (RCF)
ZO-1	zona occludens
ZO-1	zona occludens 1
α-MCA	Alpha- muricholic acid
β-MCA	Beta- muricholic acid
μg	microgram(s)
μl	microlitre(s)
μM	micromolar
ω-MCA	Omega- muricholic acid

Abstract

Crohn's disease (CD) is a chronic inflammatory condition of unknown aetiology, with the microbiota thought to be a major contributor to the disease. This thesis aimed to investigate the potential role of the gut microbiota in this context. The approaches taken were to examine CD associated *Bacteroides*. We choose 3 *Bacteroides* species (*B. fragilis*, *B. vulgatus*, *B. thetaiotaomicron*) to examine here, for their ability to impact gut related functions via a range approach from cell culture to metabolite production and in application to relevant animal models. We found subtle, but significant effects in co-cultures with cells via supernatants that could induce changes to gene expression to impact cell proliferation and maturation as well as immune response modulation. The effects were strain dependent, and they were impactful. The work revealed alterations to signalling metabolites, bile acids, again in a strain dependant manner. These effects did not translate to huge changes in metabolites in vivo, in normal mice and in the genetic CD model. However, gender specific changes to inflammation modulation, BAs, the faecal microbiota and in signalling were determined in female mice related to the antibiotic cocktail issued to them and altered in male mice colonized by *B. vulgatus.* The work provides several different impacts towards future direction, this work has also been, in part, published.

Graphical Abstract
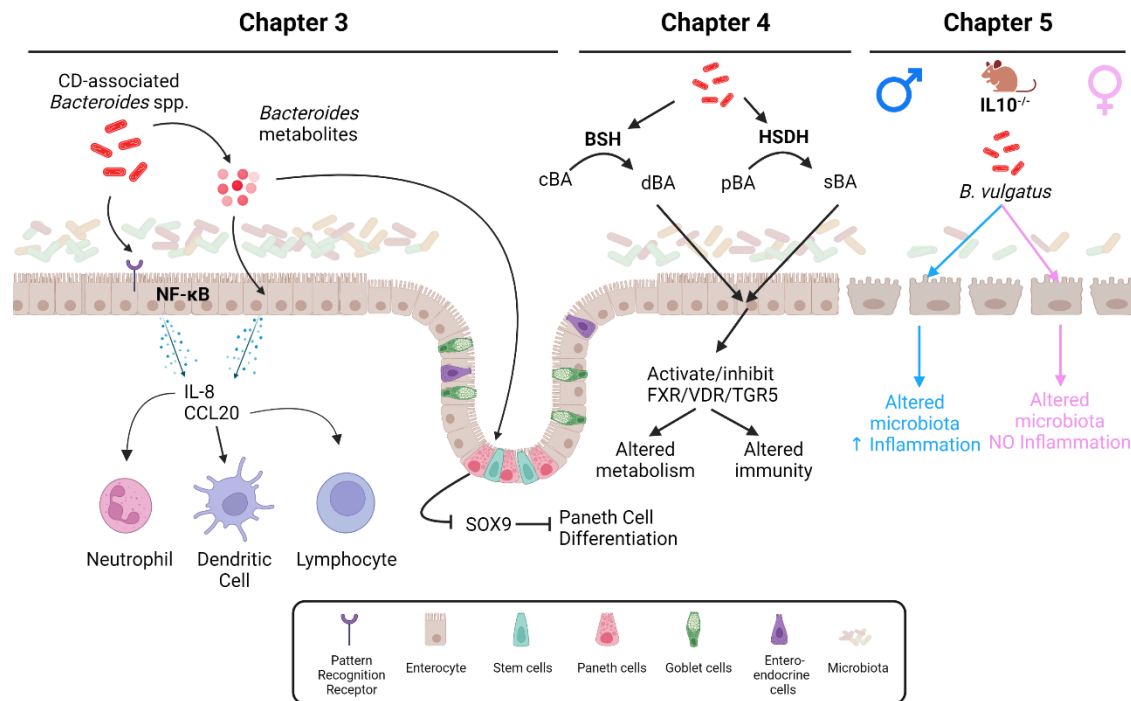
A graphical overview of the research chapters presented in this thesis.

BSH = bile salt hydrolase, HSDH = hydroxysteroid dehydrogenase, cBA = conjugated bile acids, dBA = deconjugated bile acids, pBA = primary bile acids, sBA = secondary bile acids, VDR = vitamin D receptor, FXR = farnesoid X receptor, TGR5 = G protein-coupled bile acid receptor. Created with BioRender.com

Chapter 1 General Introduction

1.1 The gut microbiota

1.1.1 The holobiont

The human gastrointestinal tract (GIT) constitutes the second largest barrier/interface between the external environment and the internal milieu with a surface area of 30 m^2 (Helander and Fändriks, 2014). The GIT forms an ideal environment for rich and diverse microbial growth, it is warm, has a continuously cycling source of nutrients, and possessing both aerobic and anaerobic compartments. Indeed, the human colon contains one of the most densely populated microbial habitats known to us. The number of bacteria inhabiting the human GIT is estimated at 3.8x10^{13} putting them in a near 1:1 ratio with human cells in the body (3x10^{13}) (Sender, Fuchs and Milo, 2016).

While the number of bacterial cells to human cells may be even, the genomic potential between the two is not, with bacteria in the gut estimated to possess 100-150 times the number of genes as the human genome (Gill et al., 2006), prompting researchers to coin the phrase the human "superorganism" or holobiont (Bäckhed et al., 2005; Gill et al., 2006) . These microorganisms colonising the GIT are collectively called the gut microbiota while their genetic content is referred to as the gut microbiome.

The gut microbiota has co-evolved over thousands of years with their human host to form a complex and symbiotic relationship (Neish, 2009). Benefits provided to the host by the presence and metabolic activity of the gut microbiota include maintenance and fortification of the epithelial barrier (Natividad and Verdu, 2013), increased energy harvest (Den Besten et al., 2013), protection from pathogen colonisation (Baümler and Sperandio,

2016), education of the immune system (Gensollen et al., 2016a) and bile acid modification (Ridlon, Kang and Hylemon, 2006; Joyce, MacSharry, et al., 2014a).

Perturbations to an individual's microbiota, known as dysbiosis, have been linked to a wide array of diseases such as inflammatory bowel disease (Sokol et al., 2009), irritable bowel syndrome (Carroll et al., 2012), celiac disease (Schippa et al., 2010), asthma (Abrahamsson et al., 2014), arthritis (Scher et al., 2015), autism (Kang et al., 2013), kidney stones (Zampini et al., 2019), obesity (Turnbaugh et al., 2008), and *Clostridium difficile* infection (Britton and Young, 2014). This variety of diseases and conditions linked to the gut microbiota highlight its crucial role in the promotion and maintenance of human health.

1.1.2 How do we study the microbiota?

Traditionally the study of the gut microbiome was carried out through laborious culture-dependent methods, with relatively few microbes being identified by these methods (Song, Lee and Nam, 2018). A study using early sequencing technology highlighted the insensitivity and bias of these culture-dependent methodologies when 76% of 16S rRNA gene amplicons obtained from a faecal sample belonged to novel and uncharacterised species (Suau et al., 1999).

However, the advent of next-generation sequencing (NGS) technologies in the last 15 years has led to an explosion in gut microbiome research, due to the reduced cost of accessing sequencing technologies, as evidenced by the rapidly increasing number of publications since 2009. These new technologies facilitated several large-scale studies such as the European

Metagenomics of the Human Intestinal Tract (MetaHIT) (Qin et al., 2010) and the Humane Microbiome Project (Methé et al., 2012) which have accumulated large amounts of metagenomic data on the human gut microbiome.

The most prevalent NGS technique used in microbiome studies today is the high-throughput sequencing of the prokaryotic 16S rRNA gene. In prokaryotes, this gene is composed of nine hypervariable (V1-V9) and conserved loci allowing the detection and identification of prokaryotes through the design of universal primers (Fanning et al., 2017). Although the selection of which hypervariable region for microbiome studies still appears to be a matter of debate (Claesson et al., 2010; Rintala et al., 2017). 16S rRNA analysis allows the profiling of a microbial community. While 16S rRNA analysis is fast and cheap, it requires a certain degree of expertise for data analysis and it does not provide data on the functionality of a microbial community, as only a single gene has been sequenced. Also, different bacteria possess different 16S rRNA copy numbers, this may introduce a bias towards bacteria with greater copy numbers (Louca, Doebeli and Parfrey, 2018).

Another NGS technology that is a staple of microbiome research is shotgun DNA sequencing. Contrasting 16S rRNA profiling, this high-throughput technique allows sequencing of the metagenome, the entire genetic content, of a sample (Quince et al., 2017). Shotgun metagenomics not only allows identification of all organisms in a microbial community, to species or strain level, but it also provides functional information on the microbial community as the whole genome of the microbes was sequenced. While

shotgun metagenomics has many advantages over 16S rRNA, it also contains several drawbacks (Hodkinson and Grice, 2015). Shotgun metagenomics is significantly more expensive than 16S rRNA profiling and requires greater expertise to handle and analyse the larger volume of data generated (Hodkinson and Grice, 2015).

Other new technologies have been leveraged to study different aspects of the gut microbiota including metatranscriptomics, to study the activity/expression of host and microbial genes, metaproteomics, investigating expressed proteins, and meta-metabolomics, to identify and quantify metabolites produced and altered by the microbiota and infer physiological activity.

Utilising these new technologies researchers have been able to characterise the human gut microbiota with greater resolution than ever before and identify changes in the gut microbiota associated with health and disease.

1.1.3 Composition of the microbiota

The term gut microbiota collectively describes all the microorganisms resident in the gut and is comprised of bacteria, archaea, fungi, and viruses (Cani, 2018). Traditionally, most microbiome research has been focused on the bacterial microbiome due to a lack of taxonomic tools for the classification of the viral (virome) and fungal (mycobiome) components of the gut microbiome.

As of 2015, there have been 2,172 species of bacteria isolated, at least once, from humans (Hugon et al., 2015). These bacteria were represented in 12 of the 50 known bacterial phyla with 93.5% of them belonging to just

four: Firmicutes, Bacteroidetes, Proteobacteria, and Actinobacteria (Hugon et al., 2015). Of the 12 bacterial phyla identified in humans, three of them contained only one species, including the intestinal bacteria *Akkermansia muciniphilia,* the only known bacteria from the phylum Verrucomicrobia (Hugon et al., 2015).

The gut microbiota is composed primarily of two phyla, Firmicutes and Bacteroidetes, accounting for 90% of observed species (Arumugam et al., 2011). The phylum Firmicutes contains over 200 genera and is represented by the genera *Clostridium, Lactobacillus, Ruminicoccus, Bacillus,* and *Enterococcus* in the gut with *Clostridium* accounting for 95% of this representation (Arumugam et al., 2011). The most prominent members of the Bacteroidetes phylum in the gut are the genera *Bacteroides* and *Prevotella* (Arumugam et al., 2011). While not as abundant as Firmicutes or Bacteroidetes the phylum Actinobacteria is primarily represented by the genus *Bifidobacterium* (Arumugam et al., 2011).

While variation in an individual's microbiota is relatively low, indicating stability over time, there is much greater variation between the microbiotas of individuals (Huttenhower et al., 2012). This inter-individual variation makes the characterisation of a healthy gut microbiota challenging; however, 66 species of bacteria have been identified as core microbiota species (Rajilić-Stojanović and de Vos, 2014). Yet, this core microbiota only represents 2% of observed species and is only present in 50% of the population (Rajilić-Stojanović and de Vos, 2014). Due to this large inter-individual variation Arumugam et al. suggested that human gut microbiomes could be clustered based on enrichment of bacterial genera and function

and separated into three "enterotypes"; *Bacteroides* enterotype, *Prevotella* enterotype, and *Ruminococcus* enterotype (Arumugam *et al.*, 2011). This method of characterising the gut microbiota is still being debated with some researchers demonstrating that it is too simplistic and masks important variations in the data. (Jeffery *et al.*, 2012; Knights *et al.*, 2014).

Even though there is a large variation in microbiota composition between individuals the microbiota does demonstrate a large degree of functional redundancy, producing comparable protein and metabolite profiles (Moya and Ferrer, 2016). In a large study combining 249 newly sequenced samples with the MetaHIT projects previously sequenced 1,018 samples, Li et al were able to establish a catalogue of ~ 10,000,000 genes (Li *et al.*, 2014). Analysis of this gene catalogue demonstrated that microbiota composition differs by country indicating that environmental and external factors are important determinants for microbiota composition as well as host genetics (Li *et al.*, 2014).

1.1.4 Acquisition and development of the gut microbiota in infants

When exactly the GIT becomes colonised with the microbiota is a topic still under debate. Traditionally it was thought that the GIT was sterile *in utero* (Maynard *et al.*, 2012) with microbe colonisation occurring during birth when the infant encounters the vaginal, skin, and faecal microbiotas of the mother (Lee and Polin, 2003). This view has been challenged by the observation that bacteria have been detected in the placenta (Satokari *et al.*, 2009), umbilical cord (Jiménez *et al.*, 2005) and amniotic fluid (DiGiulio *et al.*, 2008) indicating prenatal transfer of microbes from mother to infant. Further,

meconium collected two hours postpartum from healthy neonates was shown to be colonised with *Enterococcus faecalis*, *Staphylococcus epidermis*, and *Escherichia coli* (Jiménez *et al.*, 2008).

Generally, facultative anaerobes, such as *Enterococcus faecalis* and *Enterococcus faecium*, are the first bacteria to colonise the gut after a vaginal birth but are quickly followed by strict anaerobes like *Bacteroides, Clostridium* and *Bifidobacterium* spp. (Adlerberth and Wold, 2009). However, postpartum the infant gut microbiota develops depending on several factors. With infants delivered vaginally, at term, which are breastfed, with no history of antibiotic treatment are considered to develop the most salutogenic gut microbiota (Vandenplas *et al.*, 2020).

1.1.4.1 Gestational period

Whether a neonate is born prematurely or at term can impact how the microbiota will colonise. Compared with at term, the gut microbiota of prematurely delivered neonates is characterised by late colonisation with a limited diversity of the gut microbiota (Rougé *et al.,* 2010). In preterm infants, the colonisation of strict anaerobes is delayed with the abundance of *Bifidobacterium*, *Bacteroides*, and *Atopobium* reduced (Arboleya *et al.*, 2012). Whereas the abundance of potentially pathogenic facultative anaerobes from the *Enterobacteriaceae* family is increased (Arboleya *et al.*, 2012). *Enterobacter*, *Enterococcus*, *Escherichia*, and *Klebsiella* occur in preterm neonates more frequently than at term neonates (Arboleya *et al.*, 2012). In addition to gestational age, the unique environmental conditions that preterm infants are exposed to places different pressures on the infant influencing microbiota composition (Grier *et al.*, 2017). The intensive care

environment and standard clinical practices around the treatment, care and, feeding of preterm neonates contribute to the abnormal development of the gut microbiota (Grier *et al.*, 2017).

1.1.4.2 Delivery mode

Whether an infant has been delivered via vaginal birth or caesarean section (c-section) has been shown to have a significant impact on the neonate's gut microbiota composition (Dominguez-Bello *et al.*, 2010). Following vaginal birth, the neonate's microbiota resembles that of the mother's vaginal microbiota and is dominated by *Lactobacillus*, *Prevotella*, and *Sabathia* (Dominguez-Bello *et al.*, 2010). In contrast, the microbiota of neonates delivered by c-section more closely resemble the mothers skin microbiota with *Staphylococcus*, *Corynebacterium*, and *Propionibacterium* dominating (Dominguez-Bello *et al.*, 2010). Consequently, c-section-delivered neonates showed delayed colonisation with *Bifidobacterium*, *Bacteroides*, and *Parabacteroides* spp. relative to their vaginally delivered counterparts (Shao *et al.*, 2019). While the relative abundance of *Bifidobacterium* in c-section neonates recovers to that of those vaginally delivered quickly the same cannot be said for *Bacteroides* (Shao *et al.*, 2019). This may impact the future health of the neonate as bacteria from the *Bacteroides* genus have been shown to affect the maturity of the immune system (Sjögren *et al.*, 2009). Indeed, infants delivered by c-section have an increased risk of developing different diseases including allergies, asthma, and celiac disease (Renz-Polster et al., 2005; Decker, Hornef and Stockinger, 2011).

1.1.4.3 Diet: breast or formula feeding

Milk is the first form of nutrition an infant will be exposed to, with its source having a profound impact on the development of the gut microbiota (Guaraldi and Salvatori, 2012).

Breast-fed infants exhibit a gut microbiota with higher relative abundances of *Bifidobacterium*, *Lactobacillus*, *Streptococcus*, *Staphylococcus*, and *Prevotella* (Bäckhed *et al.*, 2015; Ho *et al.*, 2018). Breast milk is an important factor in early gut colonisation as it contains its own microbiota with genera such as *Bifidobacterium*, *Lactobacillus*, *Staphylococcus*, *Enterococcus*, and *Bacteroides* frequently found (Zimmermann and Curtis, 2020), although this can change dependent on numerous maternal factors (Moossavi *et al.*, 2019). An important feature of breast milk for early gut colonisation is that it contains human milk oligosaccharides (HMOs). While these HMOs cannot be digested by the infant, they can act as a prebiotic for certain bacteria namely *Bifidobacterium* spp. (Asakuma *et al.*, 2011). Consequently, breastfed infants develop a microbiota rich in *Bifidobacterium* spp. capable of resisting pathogen colonisation (Liu and Newburg, 2013)and supporting the healthy development of the infant (Garrido *et al.*, 2015).

In contrast, infants who were predominantly formula fed showed increased relative abundances of Firmicutes, Bacteroidetes, and Proteobacteria represented by *Clostridium difficile*, *Enterobacter cloacae*, *Bilophila wadsworthia*, *Enterococcus faecalis*, *Lachnospiraceae*, and *Bacteroides* spp. (Ho *et al.*, 2018). Due to an increased presence of pathobionts in formula-fed infants (*Clostridium difficile*), they are at an increased risk of infection than breastfed infants (Tamburini *et al.*, 2016).

Multiple studies have demonstrated the importance of breastfeeding with breastfed infants exhibiting reduced risk for developing a host of chronic conditions and diseases such as allergies, asthma (Dogaru *et al.*, 2014), diabetes (Horta, Loret De Mola and Victora, 2015), obesity (Wang *et al.*, 2017), and Crohn's Disease (CD) (Xu *et al.*, 2017).

1.1.5 Transition from infant to adult and the microbiota in ageing.

In the first year of life, an infant's gut microbiota is unstable, characterised by low diversity and composed primarily of bacteria from the phyla Actinobacteria and Proteobacteria (Rodríguez *et al.*, 2015). As the infant ages, microbiota diversity increases and functional capacity shifts from one of lactate utilisation to plant-derived polysaccharide utilisation and vitamin biosynthesis (Koenig *et al.*, 2011). By three years old a child's microbiota has a similar composition and functional capacity as an adult's and is dominated by the phyla Firmicutes, Bacteroidetes and Actinobacteria (Yatsunenko *et al.*, 2012).

Where the adult microbiota has been shown to be relatively stable throughout adulthood (Huttenhower *et al.*, 2012; Faith *et al.*, 2013) shifts in composition and function have been observed with advancing age. Claesson et al. with their ELDERMET study demonstrated that the microbiotas of elderly people (>65yrs) showed greater inter-individual variation than a younger cohort. They also observed that the elderly microbiota was characterised by a dominance of Bacteroidetes bacteria with a reduction in Firmicutes. A shift from *Clostridium* cluster XIV prominence in young adults to *Clostridium* cluster IV in the elderly was also

observed and decreased abundances of *Bifidobacterium* in the elderly (Claesson *et al.*, 2011). A follow-up study demonstrated that variation in the elderly microbiota could be explained through diet and residential status (Claesson *et al.*, 2012). Elderly people residing in residential care facilities showed the highest proportion of Bacteroidetes whereas those living in the community showed a higher proportion of Firmicutes. The microbiota of individuals living in residential care was less diverse than their community living counterparts with this loss in diversity significantly correlated with increased frailty (Claesson *et al.*, 2012).

1.1.6 The role of diet on microbiota composition

Evidence has demonstrated that diet has the capacity to alter gut microbiota composition and diversity both in the short and long term (David *et al.*, 2013). Much of the research on this topic has focused on the detrimental effects of a Western diet and the beneficial effects of a Mediterranean diet. The Western diet is characterised by foods high in animal protein, animal fats, and refined sugars. Diets high in animal protein have been shown to increase species from the *Bacteroides*, *Alistipes*, and *Bilophila* genera, with decreases in beneficial bacteria such as *Lactobacillus*, *Roseburia*, and *Eubacterium rectale* (Singh *et al.*, 2017). Studies have also shown that a diet high in saturated animal fats can increase levels of trimethylamine-N-oxide (TMAO) and decrease short-chain fatty acid (SCFA) levels (Singh *et al.*, 2017). TMAO has been linked to inflammation and associated with obesity and type-2 diabetes (Schugar *et al.*, 2017). Indeed, western diet is often linked to low-grade inflammation in the gut and is associated with obesity, type-2 diabetes as well as cardiovascular disease,

neurodegenerative diseases, and cancer (Christ, Lauterbach and Latz, 2019). In contrast to the Western diet, the Mediterranean diet is plant-focused, high in fibre, and low in animal protein and saturated fats. Adherence to a Mediterranean diet has been associated with increased *Prevotella* and fibre degrading Firmicutes (De Filippis *et al.*, 2016). Other studies have shown greater abundances of *Bacteroidetes*, *Bifidobacterium* and lower counts of *Escherichia coli* and an increased level of SCFAs (Mitsou *et al.*, 2017; Garcia-Mantrana *et al.*, 2018). The microbiome of an individual adhering to a Mediterranean diet instead of a Western one is more diverse and there is a decrease in pro-inflammatory markers in their gut (Nagpal *et al.*, 2018; Pagliai *et al.*, 2020). One potential mechanism for this decrease in inflammation is the increased production of SCFAs seen from a Mediterranean diet. SCFAs are bacterial metabolites derived from the fermentation of indigestible fibres (Koh *et al.*, 2016). They can promote the secretion of IL-10 and drive differentiation of Treg cells and can also inhibit NF-κB signalling as well as improving barrier function (Al-Lahham *et al.*, 2010; Gonçalves, Araújo and Di Santo, 2018).

1.2 The gastrointestinal system

The gastrointestinal system is comprised of the gastrointestinal tract (GIT) along with its accessory organs. The primary function of this system is to facilitate the mechanical and enzymatic digestion of food and the absorption of nutrients, fluids, and electrolytes along with the excretion of waste. The GIT runs from the mouth to the anus and is comprised of the mouth, pharynx, oesophagus, stomach, small intestine, large intestine, rectum, and anus. Its accessory organs are comprised of salivary glands, liver, gall

bladder, and pancreas. The primary components of the GIT for nutrient and fluid absorption are respectively the small and large intestine. The small intestine is comprised of the duodenum, the jejunum, and the ileum while the large intestine refers to the colon (ascending, transverse, and descending) and the rectum. The overall structure of the large and small intestines is similar with each composed of four layers of tissue; the serosa, the muscularis, the submucosa, and the mucosa. The outermost layer, the serosa is composed of connective tissue and serves to keep the GIT in place. The muscularis layer is comprised of two muscle layers, one running longitudinally along the GIT where the other runs around its circumference, these muscle layers work in tandem to generate the peristaltic movements which propel the GIT contents along its length, with the myenteric plexus located between these two layers. The submucosa is composed of loose connective tissue encompassing blood and lymph vessels along with the submucosal plexus. The mucosa, the most internal layer, is itself composed of three distinct layers; the muscularis mucosae - a thin layer of muscle, the lamina propria - a layer of connective tissue, and the epithelium.

1.2.1 The gastrointestinal epithelium

The gastrointestinal epithelium, whether in the small intestine or colon, is crucial in maintaining homeostasis. Not only through nutrient and fluid absorption but also by constituting a physical barrier to the gut microbiota while facilitating immune responses to it and mediating communication between the gut microbiota and the host. It is comprised of a single layer of columnar epithelial cells and has a surface area of over 30 m^2 representing one of the largest surface areas exposed to the external environment in the

human body, second only to the alveolar surface in the lungs (Helander and Fändriks, 2014). While the overall intestinal structure is similar there are anatomical differences in the epithelium between the small and large intestines reflecting the primary function of each. In the small intestine where nutrient absorption takes place, the epithelium is organised into folds and invaginations called villi and crypts of Lieberkühn where each villus is also folded giving microvilli, this greatly increases the surface area available for nutrient absorption. Whereas in the colon villi are absent as nutrient absorption is no longer paramount and the colonic environment experiences larger mechanical forces due to the movement of solid waste.

The epithelium is composed of several differentiated cell types, broadly divided into two categories: absorptive or secretory, with each performing specialised functions. Absorptive cells including enterocytes (colonocytes in the colon) the most common cell type accounting for ~ 80-90% of all epithelial cells and are involved in nutrient and fluid absorption while Microfold cells (M cells) are involved in antigen sensing of the gut lumen and transfer of antigens to immune cells underlying the epithelium located in Peyer's patches and over solitary lymphoid follicles present along the GIT. Secretory cells include the mucus-secreting goblet cells which lubricate the GIT and provide a physical barrier against bacteria, the chemosensory tuft cells, the Paneth cells, which produce antimicrobial peptides and niche factors for maintaining stem cells, Enteroendocrine cells (EECs) which produce hormones coordinating digestion and related to processes such as satiety and insulin release.

The cells of the epithelium are exposed to one of the harshest environments in mammalian physiology, encountering forces such as extreme pH variations, high mechanical stresses, and colonisation by the trillions of microorganisms of the microbiota. It has been postulated that exposure to this harsh environment is responsible for the rapid turnover of cells seen in the gastrointestinal epithelium (Beumer and Clevers, 2020) with the renewal of the entire epithelium occurring every 3-5 days (Darwich *et al.*, 2014). This swift turnover rate is facilitated by the intestinal stem cells (ISCs) which lie at the base of the crypts of Lieberkühn.

1.2.2 Stem cells and the intestinal crypt niche

Crypts of Lieberkühn are invaginations of the gastrointestinal epithelium surrounded by mesenchymal cells and at the base of which lie the ISCs. The crypts serve the dual role of protecting the ISCs from the harsh luminal environment, and facilitating signalling gradients, due to their architecture, allowing for the compartmentalisation of proliferation and differentiation of the gastrointestinal epithelium. The crypt can be conceptualised as having three distinct zones 1) the stem cell zone, where proliferation occurs, 2) the transit amplifying zone, where lineage committed ISC daughter cells further divide, expand, and differentiate, and 3) the mature zone at the mouth of the crypt, composed of post-mitotic fully differentiated cells.

Stem cells were first hypothesised to reside at the base of the crypts in 1974 by Cheng and Leblond who, using electron microscopy, observed slender cells intercalated with granular Paneth cells at the base of the crypt (Cheng and Leblond, 1974). Following this, the observation that Wingless-related integration site (WNT) signalling was necessary for homeostatic renewal of

colonic epithelium and aberrations in WNT signalling were associated with colon cancer led to the identification of a WNT target gene, the leucine-rich repeat-containing G-protein coupled receptor 5 (Lgr5) (Van de Wetering *et al.*, 2002). In 2007, Barker et al. confirmed that these LGR5^{+} cells were the stem cells hypothesised by Cheng and Leblond and responsible for long-term self-renewal as well as the generation of multiple lineages in the epithelium (Barker *et al.*, 2007).

As mentioned above the stem cell zone at the base of the crypt, containing LGR5^{+} and Paneth cells is the initial site of proliferation and constitutes the stem cell niche. Paneth cells not only produce antimicrobial peptides but also provide WNT ligands, epidermal growth factor (EGF) and Notch stimuli that maintain the stemness of the LGR5^{+} cells and provide nutrient supplementation in the form of lactate and represent a crucial component of the stem cell niche (Sato *et al.*, 2010; Rodríguez-Colman *et al.*, 2017). Indeed, genetic ablation of Paneth cells by diphtheria toxin resulted in a concomitant loss of LGR5^{+} cells (Sato *et al.*, 2010). However, the epithelium demonstrates great plasticity in response to injury, with EECs and tuft cells having been observed to provide alternative sources of Notch stimuli to LGR5^{+} cells following Paneth cell ablation (Van Es *et al.*, 2019), whereas the mesenchyme lying under the crypt can provide enough WNT ligands to maintain homeostasis (Kabiri *et al.*, 2014). While the LGR5^{+} and Paneth cells constitute the stem cell niche, the mesenchyme beneath the crypt also constitutes a niche, supporting stem cell homeostasis by establishing a bone morphogenetic protein (BMP) signalling gradient along the crypt axis (Kosinski *et al.*, 2007). Where at the base of the crypt mesenchymal

trophocytes secrete gremlin 1, a BMP signalling antagonist, while at the mouth of the crypt mesenchymal telocytes activate BMP signalling (Kosinski *et al.*, 2007). These observations highlight how proliferative activity and lineage determination are tightly controlled by several spatially dependent signalling pathways and gradients in the crypt niche including WNT/β-catenin, R-spondin, EGF, Notch, and BMP signalling.

1.2.3 Signalling pathways involved in epithelial proliferation and differentiation

The WNT signalling pathway is closely associated with stem cell maintenance/proliferation and WNT ligands are most concentrated at the base of the crypt and decrease towards the top of the crypt. Here LGR5^{+} cells are interspersed with Paneth cells which produce the ligand WNT3 which acts paracrinally on LGR5^{+} cells to maintain stemness and promote proliferation (Nusse and Clevers, 2017). WNT3 binds to the Frizzled and LRP5/6 receptors forming a heterodimer leading to phosphorylation of the intracellular tail of LRP5/6 (Nusse and Clevers, 2017). This allows the recruitment of the Axin component of the adenomatous polyposis coli (APC) destruction complex inhibiting its continuous destruction of β-catenin and allowing it to accumulate in the cytoplasm (Nusse and Clevers, 2017). β-catenin can then translocate to the nucleus where it binds T cell factors (TCF) and directly regulates gene expression (Nusse and Clevers, 2017). Studies have demonstrated the importance of this pathway in stem cell maintenance and epithelial cell homeostasis, with the deletion of TCF4 in the intestinal epithelium of mice leading to rapid loss of LGR5^{+} cells (van Es *et al.*, 2012), while deletion of the APC destruction complex enhancing WNT

signalling and promoting the growth of large adenomas in mouse intestine (Barker *et al.*, 2009).

R-spondin signalling in the crypt serves to enhance the activity of WNT signalling. When R-spondin binds *lgr5* on LGR5^{+} cells it leads to the recruitment of the transmembrane E3 ubiquitin ligases RNF43 (de Lau *et al.*, 2014). This E3 ubiquitin ligase controls the cycling of the WNT receptor, Frizzled, by facilitating its rapid endocytosis and destruction thereby attenuating WNT signalling. R-spondin binding to *lgr5* reduces the amount of free RNF43, preventing Frizzled destruction and enhancing WNT signalling (de Lau *et al.*, 2014). R-spondin plays a vital role in maintaining intestinal homeostasis with mutations in RSPO3 identified through GWAS as a susceptibility risk for Crohn's disease development (Jostins *et al.*, 2012a).

EGF is produced by Paneth cells and is important in the proliferation of LGR5^{+} cells (Snippert *et al.*, 2014). The EGF receptor, ERBB1, is a receptor tyrosine kinase which is highly expressed on LGR5^{+} cells (Yan *et al.*, 2012). While EGF signalling is important in the proliferative rate of the epithelium it does not seem to have any direct impact on lineage determination as blockade of its signalling only appears to arrest proliferation in organoids (Basak *et al.*, 2017).

Notch signalling in the crypt is exclusively juxtracrine between one cell expressing Notch ligands (i.e., Delta Like Ligand (DLL) 1, DLL4) and another expressing Notch receptors (i.e., NOTCH1) (Sancho, Cremona and Behrens, 2015). Notch signalling is a crucial element in lineage determination and controls cell switching between the absorptive or

secretory progenitors (Sancho, Cremona and Behrens, 2015). When Notch signalling is activated, the Notch Intracellular Domain (NICD) of the receptor is cleaved by γ-secretase and translocated to the nucleus to bind the transcription factor CBF1, Suppressor of Hairless, Lag-1 (CSL) (Sancho, Cremona and Behrens, 2015). The primary downstream effector of Notch signalling is the transcription factor hairy and enhancer of split (HES) 1, which represses the expression of the transcription factor atonal homolog (Atoh) 1, thereby preventing the expression of DLL1 (Sancho, Cremona and Behrens, 2015). Due to the juxtracrine nature of Notch signalling, a strongly activated cell will express HES1 resulting in inhibition of Atoh1 and subsequent repression of Notch ligands. This cell will then express fewer Notch ligands on its surface and weakly activate its neighbouring cells, leading to less HES1 expression allowing induction of Atoh1 and the production of more Notch ligand. This mechanism is known as "lateral cell fate specification", an elegant process to maintain a balance between the binary of absorptive or secretory cells in epithelial lineage determination with absorptive cells expressing HES1 and secretory cells expressing Atoh1 (Sancho, Cremona and Behrens, 2015). While the Notch signalling pathway is important in stem cell maintenance and epithelial lineage determination its overactivation has also been associated with a more severe disease course in Crohn's disease (Rodriguez-Antequera et al., 2019).

In contrast to WNT, BMP signalling is low at the base of the crypt, due to the secretion of BMP antagonists such as noggin by myofibroblasts under the crypt and with increasing BMP signalling higher up the crypt (Zhang and Que, 2020). BMPs are members of the TGF (tumour growth factor) β

superfamily of signalling proteins. The BMP signalling pathway is initiated by the binding of BMP ligands to their type II serine-threonine kinase receptor which then binds and phosphorylates the BMP type I receptor (Zhang and Que, 2020). This allows the recruitment and phosphorylation of mothers against decapentaplegic homologue (SMAD) 1, 5, and 8. Phosphorylated SMAD1/5/8 form a complex with common SMAD (SMAD4) which translocate to the nucleus and regulate gene expression (Zhang and Que, 2020). BMP signalling in the intestine counteracts the stem cell maintenance and proliferative drive of WNT signalling and promotes epithelial differentiation as demonstrated by deletion of type II BMP receptors in mice leading to an expansion of stem cells and the formation of polyps (He *et al.*, 2004). Additionally, repression of the BMP pathway has been shown in Crohn's disease with increased levels of the negative regulator of BMP signalling SMAD7 (Troncone *et al.*, 2021). Indeed, a SMAD 7 antisense oligonucleotide, Mongersen, has demonstrated an ability to induce remission in patients with Crohn's disease (Monteleone *et al.*, 2015). However, no efficacy in treating Crohn's disease was reported in a recent phase 3 trial (Sands *et al.*, 2020). **Figure 1.1** summarises the epithelial cell subtypes, niches and pathways regulating epithelial cell differentiation covered in **section 1.2.3**
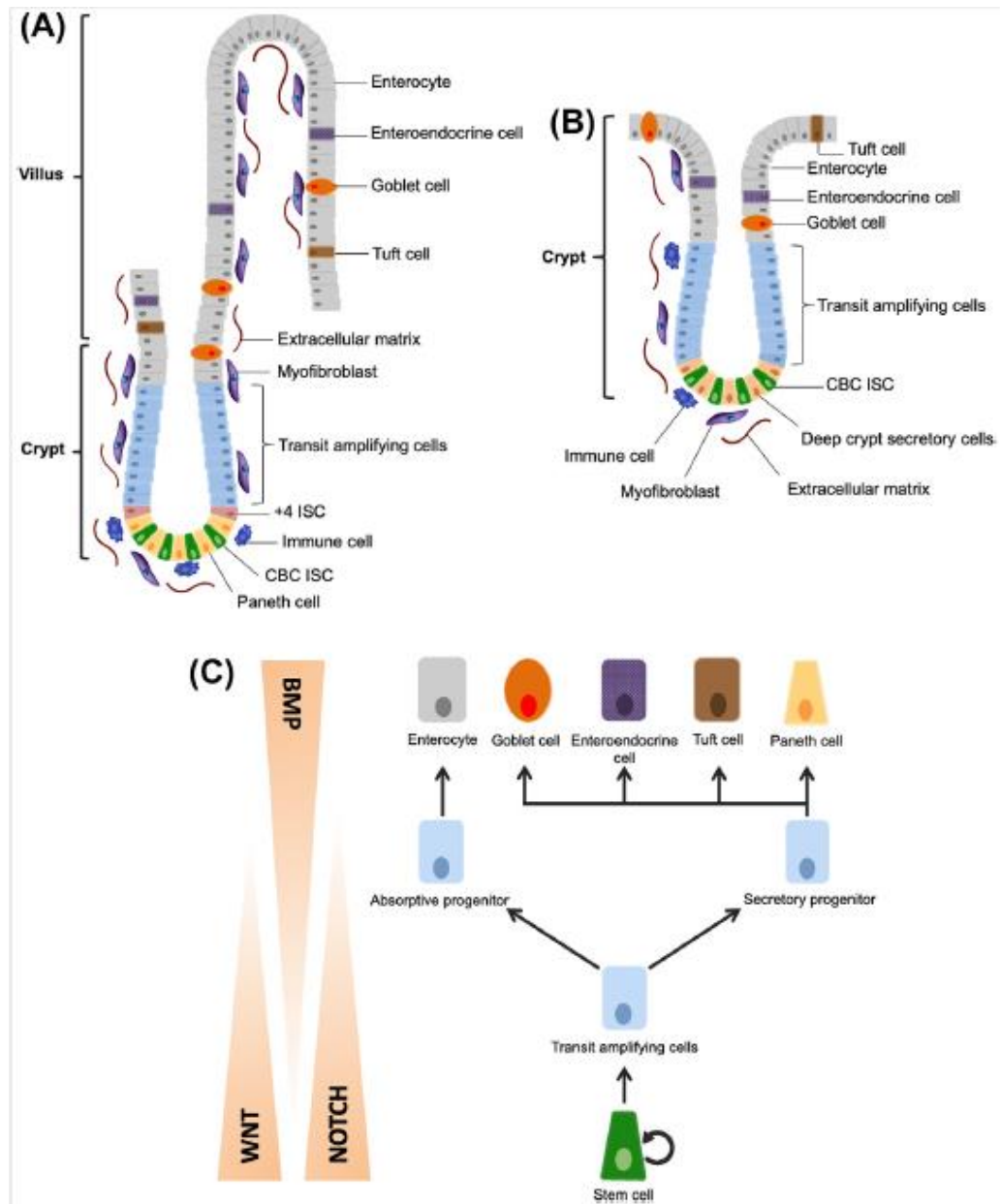
Figure 1.1 Sketch showing the organisation of the intestinal epithelial cell niche and differentiation pathways and cell types. A) Epithelial cell subtypes and niche in the villus and crypt compartment of the small intestine. B) Epithelial cell subtypes and niche in the crypt of the colon. C) Schematic intestinal stem cell lineages and differentiation. Figure adapted from (Calibasi-Kocal et al., 2021)

1.2.4 Cell types and their differentiation pathways and functions

The signalling pathways outlined above coordinate in a tightly controlled

manner epithelial homeostasis through, maintenance of the stem cell niche,

control of stem cell proliferation, epithelial renewal, and epithelial lineage determination. As outlined above Notch signalling mediates the first stage of lineage determination and controls whether the cell enters the absorptive (enterocyte) or secretory lineage (Paneth cell, goblet cell, enteroendocrine cell) (**Figure 1.1**). Once a cell leaves the stem cell niche, complex signalling pathways determine which epithelial cell subtype the cell will ultimately become.

1.2.4.1 Enterocytes

Enterocytes constitute the primary output of the absorptive lineage and are the most abundant cell type in the gastrointestinal epithelium. Their differentiation is characterised by loss of WNT signalling as the cell leaves the base of the crypt while maintaining Notch activation, with HES1 expression and repression of Atoh1. Studies show that WNT inhibition in organoids increased enterocyte numbers (Yin *et al.*, 2014) and that deletion of Atoh1 pushes all differentiating cells into the absorptive lineage whereas its forced expression pushes cells into the secretory lineage (Yang *et al.*, 2001; VanDussen and Samuelson, 2010).

1.2.4.2 Paneth cells

Paneth cells secrete antimicrobial peptides and are responsible for maintaining the stem cell niche and unlike all other lineages migrate to the bottom of the crypt during differentiation. They differentiate in an environment with no Notch activation and in the presence of a high concentration of WNT ligands. This leads to the expression of the WNT target gene SRY-box transcription factor 9 (SOX9) required for Paneth cell development (Mori-Akiyama et al., 2007).

1.2.4.3 Goblet cells

Goblet cells produce mucus and are the most common cell type in the secretory lineage. Progenitor cells differentiate into goblet cells in the presence of a low concentration of WNT ligands and no Notch activation (Van Es *et al.*, 2005; VanDussen and Samuelson, 2010). Goblet cell differentiation also depends on the transcription factor Krüppel-like factor (KLF) 4, which is inhibited by the Notch target HES1 (Ghaleb *et al.*, 2008), and whose deletion results in lower numbers of goblet cells in the colonic epithelium (Katz *et al.*, 2002).

1.2.4.4 Enteroendocrine cells

Enteroendocrine cells are the scarcest cell type in the epithelium accounting for <1% of its cells. They are hormone-secreting cells, producing hormones related to food digestion. Their characterisation is based on the hormone they produce e.g., glucagon-like peptides, cholecystokinin, somatostatin, gastric inhibitory peptide, serotonin, ghrelin, and tachykinin. The mechanisms by which enteroendocrine cell subtypes differentiate are poorly understood however differentiation to their common progenitor is driven by the expression of the transcription factor neurogenein3 (NEUROG3), activated by Atoh1. NEUROG3 knockout leads to the depletion of enteroendocrine cells while its overexpression increases their generation in the gastrointestinal epithelium (Jenny *et al.*, 2002; López-Díaz *et al.*, 2007).

1.3 Mucosal immunity of the Gastrointestinal Tract

The luminal environment of the GIT harbours the trillions of microbes of the microbiota along with potential pathogens and numerous dietary antigens.

Consequently, the GIT contains the largest number and diversity of immune compartments and immune cells (Mörbe *et al.*, 2021). These immune compartments are divided into two categories: inductive sites comprised of mesenteric lymph nodes (MLNs), Peyer's patches, and gut-associated lymphoid tissue (GALT), where cells of the adaptive arm of the immune system are primed and differentiated. Effector sites, constituted by the lamina propria (LP) and epithelium, contain cells from the immune system's innate arm and migrated, primed, and differentiated adaptive immune cells from the inductive sites (Mörbe *et al.*, 2021). The immune cells of these compartments and the epithelium coordinate a delicate balance of pro- and anti-inflammatory signals between the innate and adaptive immunity to prevent the overgrowth of commensals and recognise and attack harmful pathogens.

1.3.1 Innate immunity in the Gastrointestinal Tract

The innate immune system represents the first line of defence, preventing commensal/pathogenic bacteria from entering the body and with the ability to recognise a broad range of antigens. It comprises different components, including physical and chemical barriers and innate leukocytes, such as macrophages, dendritic cells, and neutrophils in the LP (Beutler, 2004).

In the context of the GIT, the first obstacle a bacteria will encounter is the mucus barrier. This barrier is composed of a layer of mucus produced by epithelial goblet cells, and its structure differs between the small intestine and colon, reflecting their physiological function (Johansson and Hansson, 2016a). In the small intestine, where there is relatively low bacterial colonisation, a thin, permeable, single layer of mucus is seen, conversely in

the colon, which is densely colonised, a thick double mucus layer is observed, composed of a dense inner layer with a loose "watery" outer layer lying on top of it (Johansson and Hansson, 2016a). In a healthy GIT, the inner mucus layer is closely associated with the epithelium and is composed of a dense framework preventing the entrance of luminal bacteria. In contrast, the loose outer layer serves as a niche for certain bacteria to colonise, providing an easily accessed source of carbohydrates (Hansson and Johansson, 2010). The loose nature of this outer layer also means that any bacteria encapsulated within are transient and efficiently moved along the GIT and excreted with waste matter. The mucus secreted by the goblet cells is composed of gel-forming, heterogeneous, highly glycosylated proteins called mucins, with Mucin-2 (MUC2) being the main constituent of colonic mucus in both the inner and outer layers (Johansson and Hansson, 2016a). MUC2 is vital for epithelial homeostasis, with MUC2 null mice developing spontaneous colitis (Van der Sluis *et al.*, 2006).

While the mucus layer represents a physical barrier against luminal bacteria, its structure provides a medium for the retention of antimicrobial peptides (AMPs), which establish a chemical barrier, further preventing luminal bacteria from associating with the epithelium. Paneth cells of the epithelium are the primary producers of AMPs, secreting lysozyme, α-defensins, β-defensins, and cathelicidins, effective against a wide array of microorganisms (Ostaff, Stange and Wehkamp, 2013). The production of these AMPs is influenced by luminal bacteria with muramyl dipeptide (MDP), a component of peptidoglycan in bacterial cell walls, sensing by NOD2, leading to the secretion of α-defensins (Kobayashi *et al.*, 2005). The

importance of these AMPs to controlling luminal bacteria is demonstrated in cathelicidin KO mice, where infection with the murine pathogen *Citrobacter rodentium* results in deeper penetration of the pathogen into the mucosa (Iimura *et al.*, 2005), and mice with decreased numbers of Paneth cells were more susceptible to *E. coli* infections (Sherman *et al.*, 2005).

Once luminal bacteria have navigated the mucus and AMP barriers, they will reach the epithelium, the single layer of cells covering the lamina propria. The epithelium is the last barrier to cross before gaining access to the internal environment and is composed of the enterocyte surface (transcellular pathway) and the tight junctions (TJ) (paracellular pathway) formed between them. Passage through the transcellular pathway is mediated by transporters and channels in the apical and basolateral surfaces of the enterocytes (Ivanov, 2012). The more likely route for the entry of luminal bacteria is through the transcellular pathway, which is regulated by the apical junction (AJ) complex, composed of several structures including TJs, adherens junctions, desmosomes, and gap junctions (Su *et al.*, 2011). The AJ complex is supported by a dense actin cytoskeleton network (Madara, 1987). Here the adherens junctions are primarily responsible for holding cells together, with their main component being cadherin proteins, a set of transmembrane proteins that interact with the extracellular component of other cadherins on an adjacent cell (Takeichi, 2014). While adherens junctions do not contribute to paracellular permeability, they are necessary for effective tight junction assembly, where depletion of epithelial cadherin (E-cadherin) interferes with tight junction assembly but not their maintenance (Capaldo and Macara, 2007). Tight

junction proteins are the primary regulator of paracellular permeability (Anderson and Van Itallie, 2009); they are composed of multiple proteins, including claudins (Furuse *et al.*, 1998), tight junction-associated marvel proteins (TAMPs) like occludin (Furuse *et al.*, 1993), junctional adhesion molecules (JAMs) (Martìn-Padura *et al.*, 1998), and intracellular scaffold proteins like the zona occludens (ZO-1) (Ikenouchi *et al.*, 2007) and located on the apical side of epithelial, cells lateral membrane.

Beneath the epithelium lies the LP, where the myeloid cells of the innate immune system are found. During homeostasis, the primary cells of the innate immune system are the monocyte-derived, phagocytic, and antigen-presenting cells (APCs), such as macrophages and dendritic cells (DCs) and, during inflammation, polymorphonuclear phagocytes such as neutrophils (Beutler, 2004). Macrophages primarily phagocytose any bacteria that may make it past the epithelial defences, and this prevents unnecessary mucosal inflammation by limiting the activation of adaptive immunity (Macpherson and Uhr, 2004). They also secrete immune mediators to activate and attract other immune cells to a site of infection (Mowat and Agace, 2014). Dendritic cells are the main APCs of the GIT, found in the LP and GALT, where they continuously sample the intestinal lumen for antigens through intraepithelial dendrites (Stagg, 2018). They serve as a bridge between innate and adaptive immunity by phagocytosing bacteria and displaying antigens on their surface via the class II major histocompatibility complex (MHC) for presentation to T-cells (Beutler, 2004). The LP also harbours the innate lymphoid cells (ILCs), a class of cells that belong to a family of innate immune cells that share phenotypic and

functional similarities with T-lymphocytes of the adaptive immune system (Geremia and Arancibia-Cárcamo, 2017). They are divided into three categories, with group 3 ILCs (ILC3s) being the most relevant for intestinal inflammation. They play a pivotal role in mucosal inflammation, recruiting neutrophils, stimulating AMP production, and bolstering epithelial tight junctions (Spits and Cupedo, 2012).

1.3.2 Bacteria sensing of the innate immune system

A key feature of the innate immune system is an unspecific response to microbial or dietary antigens. This lack of specificity is accomplished by recognising highly conserved microbial moieties called microbial-associated molecular patterns (MAMPs). The innate immune system detects these MAMPs through pattern recognition receptors (PRRs), germline-encoded sensory molecules constitutively expressed in all mammalian cell types representing a vital element of the innate immune system (Akira, Uematsu and Takeuchi, 2006). The two primary PRRs in the GIT are toll-like receptors (TLRs) and nucleotide-binding oligomerisation domain-like receptors (NLRs). Both TLRs and NLRs are constituently expressed on/in intestinal epithelial cells (Furrie *et al.*, 2005), macrophages (Akira, Uematsu and Takeuchi, 2006), dendritic cells (Iwasaki and Medzhitov, 2004) and the T and B cells of the adaptive immune system (Hornung *et al.*, 2002).

1.3.2.1 Toll-like receptors

TLRs are type I integral membrane glycoproteins consisting of three distinct domains (Botos, Segal and Davies, 2011); a variable extracellular MAMP binding domain, dependent on TLR type, of leucine-rich repeats (LRRs); a

transmembrane domain anchoring the receptor in place, and a cytoplasmic domain involved in signal transduction, homologous to the IL-1R and thus dubbed the Toll/IL-1R homology (TIR) domain (Bell *et al.*, 2003). The binding of TLRs by their agonists initiates intracellular signalling cascades leading to the induction of genes related to numerous biological functions, primarily related to antimicrobial defence, such as the production of proinflammatory chemokines and cytokines. The general signalling pathway of TLR activation is outlined here. Upon ligand binding, TLRs will dimerise, homogenously or heterogeneously, in the cell membrane provoking a conformational change in the intracellular domain, which allows the recruitment of TIR domain-containing adapter protein (TIRAP). Once the TIR domain of TIRAP is bound to its counterpart on the TLR receptor, this allows the binding of myeloid differentiation factor 88 (MyD88), an adapter molecule integral to signalling in all TLRs (except TLR3), to TIRAP. This membrane-bound complex of TLR dimer, TIRAP, and MyD88 now recruits IL-1R associated kinases (IRAK) 1 leading to the recruitment and activation of IRAK4, which, once activated, phosphorylates MyD88 associated with IRAK1 and provokes a conformational change allowing it to associate with the ubiquitin ligase tumour necrosis factor receptor (TNFR) associated factor (TRAF) 6. TRAF6 catalyses the phosphorylation of the NF-κB regulatory subunit IκB kinase (IKK) β. IKKβ, in turn, phosphorylates and ubiquitinates IκB, which dissociates from NF-κB and allows it to translocate to the nucleus and induce the expression of genes for proinflammatory chemokines and cytokines (Akira, Uematsu and Takeuchi, 2006).

To date, 13 TLRs have been identified, with each receptor binding to a specific ligand (Kawai and Akira, 2011). Plasma membrane-bound TLR2 detects bacterial lipopeptides and heterodimerises with TLR1 to detect triacylated lipopeptides or TLR6 in sensing diacylated lipopeptides, whereas TLR4 recognises gram-negative bacterial lipopolysaccharide (LPS) (Kang *et al.*, 2009). TLR9 recognises unmethylated double-stranded microbial DNA (Lee *et al.*, 2006). TLR5 is bound by flagellin from flagellated gram-negative bacteria (Gewirtz *et al.*, 2001). While TLR10 was described to be activated by the gram-positive bacteria *Listeria monocytogenes* (Regan *et al.*, 2013). TLRs can also be found intracellularly, including TLR3, which binds double-stranded RNA, and TLRs 7 and 8 which detect single-stranded RNA (Kawai and Akira, 2011), TLRs 11 and 12 are involved in the detection of protozoan parasites (Koblansky *et al.*, 2013), while TLR13 binds bacterial 16S RNA (Oldenburg *et al.*, 2012).

In the GIT epithelium, to regulate immune responses and promote immune hypo-responsiveness to commensal bacteria, TLRs are segregated in subcellular compartments and differentially distributed across the polarised epithelial cells (Gay *et al.*, 2014). For example, TLRs 2-5 are expressed at low levels in the apical membranes of epithelial cells but at a higher level in the basolateral surfaces (Abreu, 2010). This compartmentalisation ensures these TLRs are only stimulated in the presence of invasive bacteria and prevents a sustained immune response, however in times of inflammation, the expression of TLRs 2 and 4 in the apical membrane is increased (Hausmann *et al.*, 2002).

DCs also possess TLRs, which, when stimulated, will direct the maturation of the DCs towards an effector or regulatory subset, provoking them to migrate to Peyer's patches and other GALT to activate naïve T cells of the adaptive immunity to various functional phenotypes (Chang, Ko and Kweon, 2014)

1.3.2.2 Nucleotide-binding oligomerisation domain-like receptors

Nucleotide-binding oligomerisation domain (NOD)-like receptors (NLRs) are intracellular PRRs of innate immunity found on both intestinal epithelial cells and immune cells. The signalling of NODs in epithelial cells will be described next. NOD1 and NOD2 detect MAMP components of peptidoglycan, a vital component of bacterial cell walls (Girardin *et al.*, 2003; Inohara *et al.*, 2003). NOD1 recognises muramyl tripeptides present exclusively in Gram-negative bacteria (Girardin *et al.*, 2003), whereas NOD2 recognises muramyl dipeptide, which is found in the cell walls of Gram-positive and Gram-negative bacteria (Inohara *et al.*, 2003). NLRs are also a vital component of inflammasomes, which play a large role in epithelial immunomodulation and homeostasis by recognising pathogens and tissue damage markers (Zaki, Lamkanfi and Kanneganti, 2011). Inflammasomes are cytoplasmic complexes composed of; an NLR sensor protein (NLRP1, NLRP2, NLRP3, NLRP6, NLRP7, NLRP12, and NLRC4), an adapter protein, apoptosis-associated speck-like protein containing a CARD domain (ASC), and caspase-1 (Schroder and Tschopp, 2010). The inflammasome is activated when the sensor protein detects a PAMP/damage-associated molecular patterns (DAMPs) specific for each NLR (Martinon, Mayor and

Tschopp, 2009). Where NLRP1 is activated by muramyl dipeptide, NLRC4 is activated by flagellin, and NLRP3 is activated by numerous compounds such as bacterial and viral nucleic acids, bacterial lipopolysaccharides (LPS), and DAMPs such as uric acid, amyloid β peptides, and ATP (Martinon, Mayor and Tschopp, 2009). Activating a sensor protein leads to the activation of caspase-1 and subsequently increases the processing and secretion of IL-1β and IL-18, leading to the initiation of pyroptosis in infected/damaged cells (Sahoo *et al.*, 2011).

1.3.3 Adaptive immunity in the Gastrointestinal Tract

Unlike the innate immune system, the adaptive immune system is highly specific, confers long-lasting immunity, and is adaptable due to its specificity for antigens being determined by a complex maturation and development of immune cells. In the context of the gut, the primary components of the adaptive immune system are B and T cells residing in inductive (GALT) or effector sites (epithelium and LP). DCs, macrophages, and epithelial cells of the innate immune system coordinate with the adaptive immune cells to present antigens to naïve cells and induce the maturation of these cells. B cells are responsible for the humoral element of the adaptive immune response in the GIT, whereas naïve T cells (T0) activate and differentiate into different T helper (Th) cells, with the most prominent being Th1, Th2, Th17, and regulatory T cells (Tregs).

1.3.3.1 B cells and IgA

B cells perform several functions in GIT immunity, including antibody production, antigen presentation, and cytokine generation. B cells in the

mucosa are predominantly plasma cells secreting IgA, the most abundant antibody type and vital for mucosal immunity (Cerutti and Rescigno, 2008; Bunker *et al.*, 2017). B cell differentiation into IgA-producing plasma cells is initiated in PP where exposure to the cytokine TGF-β initiates class switching of B cells (Cerutti and Rescigno, 2008). Clonal expansion of these B cells takes place in the presence of interleukin (IL)-4, IL-6, IL-10, TGF-β, and retinoic acid, following which B cells migrate into the LP where they differentiate into IgA secreting plasma cells (Cerutti, 2008). In the LP, IgA can bind to the polyimmunoglobulin receptor (pIgR) on the basolateral side of epithelial cells allowing its secretion to the lumen through the transcellular route (Kaetzel, 2005). The secreted IgA is known as secretory IgA (SIgA) as it takes the extracellular component of the pIgR with it (Kaetzel, 2005). In the lumen, sIgA binds to bacterial antigens, preventing them from associating with the epithelium, and holds them in the mucosa for degradation or elimination without activating an immune response (Corthésy, 2013).

1.3.3.2 T cells

The GIT harbours the largest population of T cells in the body, existing in the GALT, LP, and interspersed throughout the epithelium (so-called intraepithelial lymphocytes (IELs)) (Heel *et al.*, 1997). There are many subtypes of T cells present in the gut where IELs are CD8+, and LP T cells are CD4+ with CD8 αβ and γδ populations also present (Ma, Tao and Zhu, 2019). Herein, we will focus on the CD4+ Th cells of the LP. Th cells represent a varied group of cells, each with specific cytokine and chemokine profiles that alter numerous immunological processes such as the

development of and activity of other leucocytes, macrophage stimulation, and antibody production and type switching in B cells.

Th1 cells protect the body from infectious pathogens by activating macrophages and directing cytotoxic CD8+ T cell effects to eliminate intracellular pathogens (Manetti *et al.*, 1993). Upon exposure to APC secreted IL-12, Th0 cells increase signal transducer and activator of transcription (STAT) 4 signalling leading to the initiation of the transcription factor T-bet and differentiation and expansion of Th1 cells (Thieu *et al.*, 2008). The primary cytokines associated with Th1 cells are IFNγ and TNF, which have long been known to act synergistically to impair barrier function and kill intestinal epithelial cells (Woznicki *et al.*, 2021). Excessive activation of Th1 cells is also a common feature of IBD, especially Crohn's disease (Li *et al.*, 2016).

Th2 cells have traditionally been considered active in anti-parasitic immunity but are also known as effector cells in asthma (Walker and McKenzie, 2018). They differentiate in response to IL-4, which activates STAT6 signalling and induces the transcription factor GATA3 (Walker and McKenzie, 2018). Atypical Th2 cells play an inflammatory role in ulcerative colitis (Li *et al.*, 2016).

Th17 cells primarily maintain commensal bacteria at barrier sites such as the GIT epithelium, but overactivation can also exacerbate disease states (Weaver *et al.*, 2013). Their differentiation is driven by exposure to the cytokines IL-6 and TGF-β and stabilised by IL-23 and IL-1β (Langrish *et al.*, 2005; Bettelli *et al.*, 2006; Chung *et al.*, 2009). IL-6 activates STAT3 signalling, which activates the transcription factor retinoic acid receptor-

related orphan receptor (ROR) γt, promoting Th17 differentiation (Ivanov *et al.*, 2006). The DC-produced cytokine IL-23, whose receptor is induced by IL-6 and TGF-β (Morishima *et al.*, 2009), also enhances Th17 differentiation (McGeachy and Cua, 2008). Th17 cells secrete the cytokines IL-17A and IL-17F, which act on activated T cells and epithelial cells and induce inflammatory cytokines and chemokines in target cells and play an important role in epithelial barrier function (Gaffen, 2015). Th17 cell overactivation is a well-established cornerstone of Crohn's disease pathology.

Tregs act in opposition to the other Th cells discussed and have a suppressive effect on inflammation and are crucial in the maintenance of homeostasis in the GIT by reducing the immune response to the gut microbiota (Yamada *et al.*, 2016). Tregs are characterised by the expression of the transcription factor forkhead box protein P3 (Foxp3) and secretion of anti-inflammatory cytokines such as IL-10 and TGF-β, with the autocrine effect that IL-10 activates STAT3, which induces the proliferation of Tregs (Schmidt, Oberle and Krammer, 2012). The immunosuppressive effects of IL-10 are exerted on various cell types, including macrophages and DCs, reducing their ability to stimulate T cells (Schmidt, Oberle and Krammer, 2012). Likewise, TGF-β reduces inflammatory responses by macrophages and T cells (Neurath, 2014). As mentioned above, TGF-β is also a driver for Th17 differentiation indicating Treg and Th17 differentiation is reciprocal and which subset develops is dependent on the local immune environment (Zenewicz, Antov and Flavell, 2009). The maintenance of this balance is crucial to GIT homeostasis.

1.3.4 Interactions between the immune system and the microbiota

Given that the GIT immune system has coevolved in the presence of the gut microbiota, it is unsurprising that there is a significant interplay between these two (Gensollen *et al.*, 2016b). This relationship was highlighted by early germ-free (GF) mouse studies, where the gut microbiota was shown to be essential for developing a normal functioning immune system (BAUER *et al.*, 1963). At birth, GF mice produce less sIgA, a major component of GIT humoral immunity, a defect that is ameliorated by bacterial colonisation (Hapfelmeier *et al.*, 2010). Th17 cells are also absent in GF mice but are induced following colonisation with segmented filamentous bacteria (SFB) and *Bifidobacterium* species (Ivanov *et al.*, 2009; Tan *et al.*, 2016). Bacterial products such as PSA from the commensal *Bacteroides fragilis* have also demonstrated a capacity to affect the maturation of the developing immune system in mice by correcting T cell deficiencies and Th1/Th2 imbalances (Mazmanian *et al.*, 2005). These studies highlight the importance of immune system/microbiota interaction in developing a functional immune system; however, microbiota signals continue to influence immunity and epithelial function throughout life.

1.4 Bile acids

Bile is a physiological aqueous solution synthesised in the liver, stored in the gall bladder, and secreted to the small intestine. It performs multiple biological functions including emulsification of fats, activation of pancreatic lipase, and facilitating the absorption of fat-soluble vitamins such as A, D,

E, and K (Chiang, 2013a). While bile contains several components, such as cholesterol, lipids, phospholipids, and proteins, it is primarily composed of bile salts. No longer seen as just an adjunct to digestion, bile acids (BAs) have demonstrated a capacity to act as signalling molecules potentially influencing multiple metabolic pathways (Boyer, 2013; Joyce, MacSharry, *et al.*, 2014b; Martinot *et al.*, 2017). The liver synthesises primary BA, which only represents a small portion of BA moieties seen in the BA pool. This increased diversity of BA moieties is due to microbial metabolism of primary BA to secondary BA where the relative composition of this pool depends on the microbiota composition and alterations to this pool can alter host signalling both in the gut and systemically. These processes are summarised in **Figure 1.2**
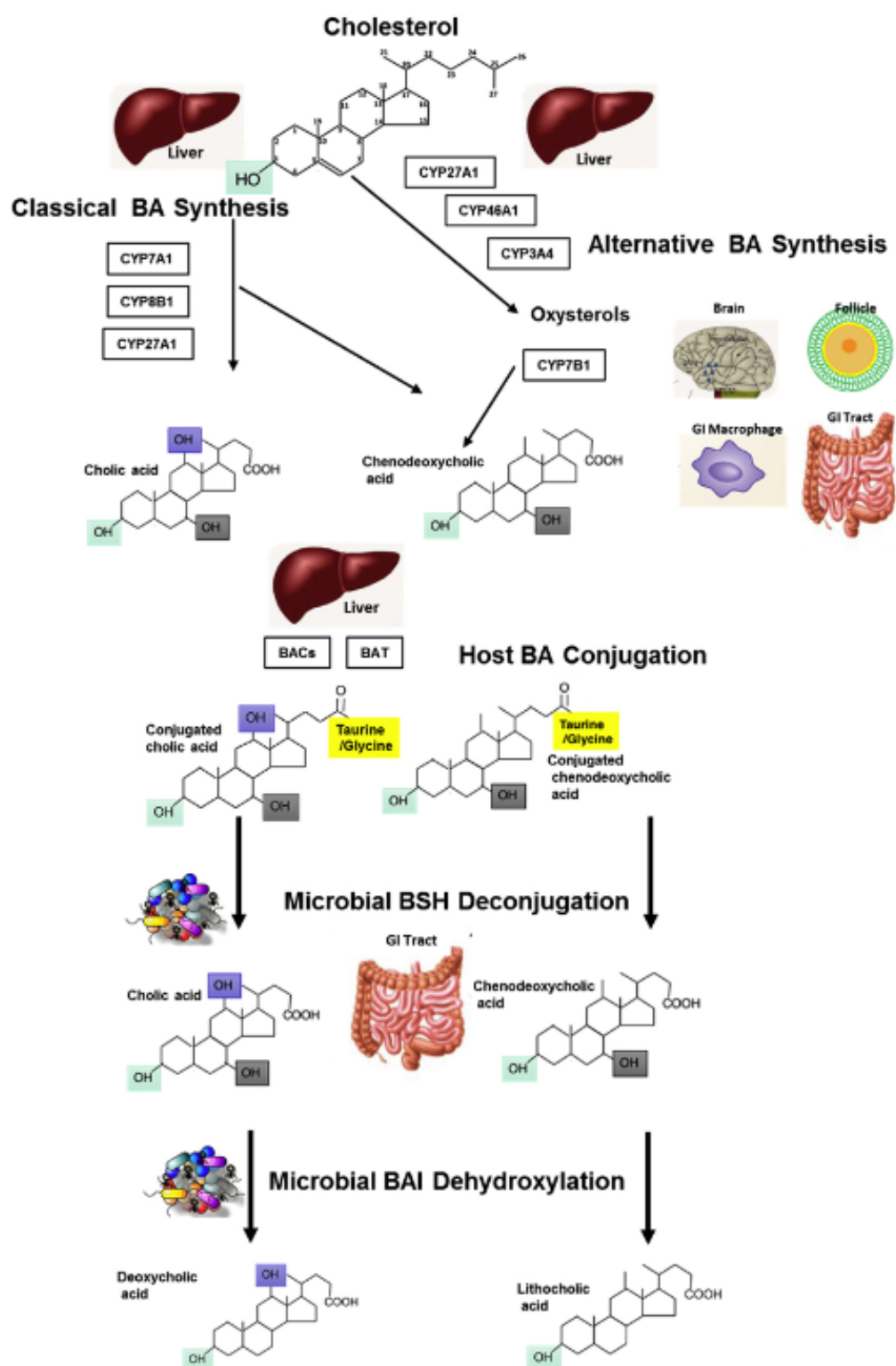
Figure 1.2 Summary of bile acid synthesis, microbial deconjugation and generation of secondary bile acids from (Long, Gahan and Joyce, 2017).

1.4.1 Bile acid synthesis

Bile acids are synthesised in the liver from cholesterol and have a structure with 24-carbon atoms arranged like the cholesterol steroid core with 6-carbon and 5-carbon rings. Many BAs possess hydroxyl and carboxyl groups arranged on one side of the carbon skeleton, giving them amphipathic properties, and conferring their powerful detergent properties (Monte *et al.*, 2009). The synthesis of BAs from cholesterol is by several multistage reactions facilitated by 17 distinct enzymes located in the cytosol, endoplasmic reticulum, microsome, and peroxisome (Long, Gahan and Joyce, 2017). Bile acids are synthesised through two distinct pathways, the classical pathway, and the alternative pathway (extensively reviewed by Li and Chiang) (Li and Chiang, 2014). The cytochrome P450 enzyme (CYP) cholesterol 7α-hydroxylase (CYP7A1) initiates the classical pathway and is considered the rate-limiting step in BA synthesis. The action of CYP7A1 converts cholesterol to 7α-hydroxycholesterol which acts on a 3β-hydroxysteroid dehydroxylase (3β-HSDH) converting it to 7α-hydroxy-4-cholestene-3-one (C4), which is a precursor to primary BAs. C4 undergoes 12α-dehydroxylation by the enzyme CYP8B1 to produce the two principal primary bile acids, cholic acid (CA) and chenodeoxycholic acid (CDCA), where the ratio between CA and CDCA is mediated by CYP8B1 (Martinot *et al.*, 2017). While CA and CDCA are the primary bile acids in humans, in rodents there is little CDCA as it has undergone hydroxylation to form the two primary murine BAs, α-muricholic acid and β-muricholic acid (Long, Gahan and Joyce, 2017). While the classical pathway produces most BA in humans, the alternative pathway accounts for 9-25% of BAs produced and

only synthesises CDCA (De Aguiar Vallim, Tarling and Edwards, 2013). Once synthesised, the BAs are conjugated to an amino acid, typically taurine or glycine, increasing their solubility for secretion in the biliary fluid. Conjugation is mediated by the enzyme bile acid cholyl-CoA synthetase (BAC) through the amidation of C24 to taurine/glycine by bile acid-CoA: amino acid N-acyltransferase (BAT) (Long, Gahan and Joyce, 2017). Once synthesised in the hepatocytes, conjugated BAs are transported to the bile canaliculus via members of the ATP-binding cassette transporters. Here the bile salt export pump (BSEP/ABCB11) transports BAs, while the multi-drug resistance 2/3 (MDR2/3/ABCB4) and ABCG5/ABCG8 transporters secrete phospholipids and cholesterol into the bile canaliculus (Meier and Stieger, 2002). Following secretion from hepatocytes BAs form micelles with the lipids which help protect the epithelium of the canaliculus from the detergent properties of the BAs. Bile acids are then stored in the gall bladder until release which is stimulated by the ingestion of food (Chiang, 2013a; Martinot *et al.*, 2017).

1.4.2 Enterohepatic circulation of bile acids

When cells of the upper intestine detect hydrochloric acid, amino acids, and lipids following ingestion of a meal they will secrete the hormone cholecystokinin. This hormone triggers the contraction of the gall bladder, secreting bile to aid in the digestion of fat and protein. Up to 95% of BAs are reabsorbed as they move from the proximal to the distal ileum, by passive and active transport, with the greatest reabsorption occurring in the distal ileum. Unconjugated BAs, due to their amphipathic nature passively diffuse through the gut epithelium, whereas conjugated BAs require active

transport through the apical sodium-dependent bile acid transporter (ASBT). Upon entering the ileal epithelial cells, BAs are bound by a cytosolic protein, ileal bile acid binding protein (I-BABP), which shuttles the BAs from the apical to the basolateral membrane of the cell. Heterodimeric organic solute transporters (Ostα/Ostβ) are located on the basolateral side of intestinal epithelial cells and these transport the BAs into the portal venous system for return to the liver (Meier and Stieger, 2002; Rao *et al.*, 2008; Chiang, 2013a). Uptake of BAs to hepatocytes from the portal system occurs by a similar route that in the ileum, except that conjugated BAs are transported via the sodium-dependent taurocholate cotransporter polypeptide (NCTP) transporter or sodium-independent organic anion transporting polypeptides (OATP1B1 and OATP1B3) (Trauner and Boyer, 2003). Once returned to the liver, these BAs can be reconjugated and released back to the gall bladder as described in section 1.5.1. The synthesis of BAs is controlled by a negative feedback loop where BAs activate the nuclear farnesoid X receptor (FXR). When BAs, reabsorbed in the ileum by ABST, activate FXR this induces ileal epithelial cell transcription of fibroblast growth factor (FGF) 15/19, which is secreted into the portal system and binds to the FGFR4/β-klotho complex on hepatocytes. This binding leads to downstream inhibition in the rate-limiting enzyme of BA synthesis, CYP7A1, mediated by ERK1/2, leading to decreased BA synthesis (Lin *et al.*, 2007). BAs returning to the liver can also repress BA synthesis through FXR activation, inducing expression of small heterodimer partner (SHP), which in turn inhibits the liver receptor homolog-1 (LRH-1), thereby reducing CYP7A1 expression and BA production

(Goodwin *et al.*, 2000). Using these mechanisms of enterohepatic circulation and BA-induced repression of BA synthesis, only 5% daily of the bile acid pool progresses to the colon, where it can be further metabolised by the gut microbiota to generate secondary bile acids.

1.4.3 Microbial modifications of bile acids

The body only synthesis the primary bile acids CA, CDCA (and muricholic acid in mice), however analysis of the BA acid pool reveals a much more varied composition of BA moieties than just CA (a triol) and CDCA (a diol). Bacteria of the gut microbiota possess enzymes capable of altering the primary BAs and generating secondary, and tertiary, BAs.

1.4.3.1 Bile salt hydrolase

Bile salt hydrolase enzymes (BSH) are found in bacteria and belong to the Ntn-hydrolase superfamily of proteins. BSHs cleave the amide bond on the C24 position between taurine/glycine on a BA moiety in a process called deconjugation (Begley, Hill and Gahan, 2006). Deconjugation is the first step in bacterial modification of bile acids and represents the rate-limiting step and the gateway reaction in this process (Jones *et al.*, 2008a). These BSH enzymes are represented in many bacterial species across nearly all phyla with BSH activity reported in *Lactobacillus*, *Bifidobacterium*, *Enterococcus*, *Clostridium*, and *Bacteroides* spp to name a few (Long, Gahan and Joyce, 2017). Conjugated BAs are toxic to bacteria in the gut, particularly at low pH, and can influence bacterial growth (Islam *et al.*, 2011). As such, for bacteria the ability to deconjugate BA is valuable. Indeed studies show that the presence of BSH is advantageous for bacterial

colonisation (Begley *et al.*, 2005a; Jones *et al.*, 2008a). As BSH confers a competitive advantage for colonisation its presence is often included in the selection criteria of probiotics (Jones *et al.*, 2008a). In addition to the benefits BSH confers to bacteria, BSH activity may also provide benefits to the host. Studies in mice have demonstrated that increased BSH activity in their gut microbiota significantly lowered levels of LDL cholesterol (Begley, Hill and Gahan, 2006; Joyce and Gahan, 2014) with a similar effect seen in a human study (Ooi *et al.*, 2010). Increased BSH activity in mice also led to significantly less weight gain relative to controls, indicating BSH as a potential avenue for treatment of obesity (Joyce, MacSharry, *et al.*, 2014b). These studies underscore the role of BSH in lipid and cholesterol metabolism. However, BSH activity has also demonstrated a capacity to alter epithelial cell homeostasis and local immune function in the gut (Joyce, Shanahan, *et al.*, 2014).

1.4.3.2 Microbial generation of secondary bile acids

Following deconjugation by BSH, the C3, C7, and C12 positions on the BA moiety are accessible for further metabolism by stereospecific bacterial enzymes including hydroxylases, dehydrogenases, and epimerases. A key transformation of BAs by bacteria is dehydroxylation at C7, where 7-dehydroxylation of CA yields the secondary BA deoxycholic acid (DCA), while 7-dehydroxylation of CDCA produces the secondary BA lithocholic acid (LCA). These secondary BAs represent the two most commonly found in the human colon (Hamilton *et al.*, 2007). CDCA can also be converted in a two-step epimerisation reaction where the 7α-hydroxyl group is converted to a 7β-hydroxy group to the tertiary BA UDCA (reviewed by (Long, Gahan

and Joyce, 2017)). While secondary bile acids are generally cytotoxic as a detergent, UDCA is not per se, its main side effect in animals is in inducing hibernation (Kotb, 2012). At the cellular level, it is anti-apoptotic through p53 (Solá *et al.*, 2007), it can modulate gene expression through histone acetylation (Akare *et al.*, 2006) and it can prevent DNA repair (Burnat, Majka and Konturek, 2010). UDCA can also be made from the secondary BA LCA in a two-step reaction where the 7α-hydroxy group is oxidised by 7α-hydroxysteroid dehydrogenase (HSDH) to 7-keto-LCA which is then reduced by 7β-HSDH, this process essentially detoxifies LCA (Lepercq *et al.*, 2004). Bile acids can also undergo epimerisation at the C3 hydroxyl group to generate 3β-hydroxy BAs also known as "iso" BAs. IsoCDCA, IsoDCA, and isoLCA are found in the colon however when recirculated to the liver they are re-epimerised back to their 3α hydroxy forms (Devlin and Fischbach, 2015). More recently these latter but minor BAs species have been assigned roles in modulating Th and Treg cell development (Campbell *et al.*, 2020a). Therefore, without microbial activity the range and diversity of BAs would be limited, it is the microbial interactions that create a range of interkingdom signalling molecules of diverse functions.

1.4.4 Bile acids as receptor ligands

In recent years BAs have been recognised as signalling molecules capable of interacting with both nuclear receptors (NRs) and G-protein coupled receptors (GPCRs) (reviewed by (Li and Chiang, 2014). All the nuclear receptors function similarly, once activated by a ligand, here BAs hetero-dimerise with the retinoic acid receptor, (RXR) to function as transcription factors to induce the expression of a range of different genes. The first BA

receptor described was the farnesoid X receptor (FXR) which is now recognised as the main regulator of BA synthesis as well as ileal BA-induced endocrine signalling (Makishima *et al.*, 1999), it also functions to induce BA transport in the terminal ileum and to induce hormone fgf15/19 from the gut, together these feedback to the liver to shut off BA synthesis (T. Fu *et al.*, 2016). Not only that but FXR can direct FA metabolism and glucose metabolism through both small heterodimeric protein (SHP) and sterol regulatory element–binding protein (SREBP) in the liver, it can also influence the glucose metabolism through GLP-1 induction and improve insulin sensitivity (Prawitt *et al.*, 2011). Interestingly, FXR interplays with a range of NRs and GCPRs including GBAR1 (TGR5) (Abdelkarim *et al.*, 2010). In recent years BA receptor, the GPCR Takeda G-protein receptor 5 (TGR5 or GPBAR1), has been identified (Duboc, Taché and Hofmann, 2014). While FXR and TGR5 are considered dedicated BA receptors with high affinity for BAs, other nuclear receptors such as retinoid X receptor (RXR), liver X receptor (LXR), pregnane X receptor (PXR) and vitamin D receptor (VDR) constitute more promiscuous receptors capable of being activated by BAs. Activation of these receptors by BA can influence multiple metabolic pathways, where FXR, PXR, LXR, VDR, and TGR5 have been detected in myeloid cells (Fiorucci *et al.*, 2018). For BA receptors different microbially altered BAs act as their agonist and antagonists. Again, the differential here is the level of microbial functionality in terms of BSH activity and the presence of microbes capable of producing the different suites of BAs that can interact with them. Hence, if microbial gut populations are adjusted then BAs signatures will be adjusted, and receptor responses

altered. Indeed, such alterations are associated with a myriad of conditions including, metabolic syndrome, colorectal cancer, non-alcoholic fatty liver diseases and IBD (reviewed by (Joyce and Gahan, 2016). Indeed, the turnover and modification of BA by host microbes is now recognised as a factor in the effectiveness of different poorly water-soluble drugs (Enright *et al.*, 2016). Together this implicates the importance of these receptors and BAs not just in metabolism but also in determining effective treatments where BAs converge in disease states.

1.5 Inflammatory Bowel Disease

Inflammatory bowel disease (IBD) is an incurable, chronic, relapsing inflammatory disease of the gastrointestinal tract. IBD drastically impacts the quality of life of patients as well as confers a significant financial burden to global health care services. The incidence of IBD is highest in the Western world and was rising over the last two decades but this has plateaued in developed countries. However, due to the low mortality of IBD, these countries are now experiencing compounding prevalence (Windsor and Kaplan, 2019) where IBD affects 1 in 200 people (Ng *et al.*, 2017). In contrast, developing countries are still seeing an increase in IBD incidence and prevalence (Singh, Ananthakrishnan and Ahuja, 2017).

IBD is a hypernym for many conditions the two most prevalent being Crohn's disease and ulcerative colitis. While these are both inflammatory disorders affecting the gastrointestinal tract, they have distinct mechanisms of pathology and differ in symptoms, complications, and treatment. Crohn's disease exhibits transmural "patch-wise" inflammation which predominantly affects the distal ileum but can affect anywhere from the mouth to the anus.

Whereas ulcerative colitis displays continuous mucosal inflammation which starts at the rectum and travels up the colon. As the emphasis of this project was on Crohn's disease, this will be the focus of this text. **Figure 1.2** summarise factors associated with Crohn's disease pathogenesis.
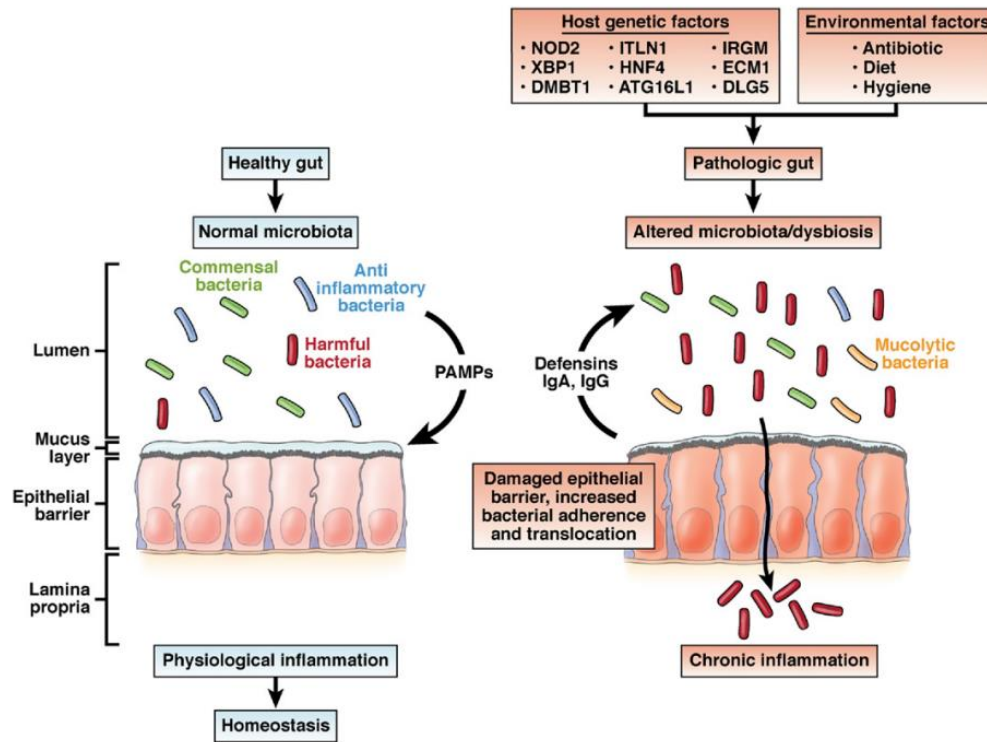
Figure 1.3 Factors affecting Crohn's disease pathogenesis include genetic, environmental, and microbial factors and a dysregulated inflammatory response. Adapted from (Chassaing and Darfeuillemichaud, 2011)

1.5.1 Crohn's Disease Overview

Crohn's disease is one of the most prevalent forms of IBD, characterised by discontinuous "patch-wise" inflammation of the whole gut wall. While Crohn's disease can be diagnosed at any age it is most common in the 20-30-year-old demographic, however, there are paediatric cases (very early onset Crohn's disease) and a slight rise in incidence in the 50-70 years old

demographic (Johnston and Logan, 2008). Crohn's disease can present at any part of the GIT but >50% of the cases are observed in the distal ileum and proximal colon with 30% involving only the small intestine and 20% involving only the colon (Cheifetz, 2013).

The classification of Crohn's disease is (further) complicated by the behaviour of the disease which is divided into 3 phenotypes: inflammatory, stricturing, and fistulising (Cheifetz, 2013). The inflammatory phenotype is classified by transmural inflammation with an absence of stricturing and fistula. However, chronic inflammation may eventually cause fibrosis and narrowing of the lumen, patients are then classified as having stricturing disease with surgical intervention often required to prevent obstruction of the bowel. In fistulising Crohn's disease, the chronic transmural inflammation may lead to the formation of a fistulous tract leading to a fistula developing between the bowel and any adjoining organs. In addition, patients with any of these three phenotypes may also develop perianal disease. To aid in the characterisation of Crohn's disease, the Vienna (Gasche *et al.*, 2000) or Montreal (Satsangi *et al.*, 2006) classification systems are used. These factor in age at diagnosis, disease location and phenotype, with the presence/absence of perianal disease.

Like Crohn's disease, symptoms can be variable and often correspond with disease phenotype. Abdominal pain and diarrhoea are the most common symptoms. Systemic symptoms such as weight loss, fatigue, and low fevers may also be present. Additionally, 43% of patients with Crohn's disease also exhibit extra intestinal manifestations (EIM) (Vavricka *et al.*, 2011) which may affect the joints, liver, skin, eyes, and kidneys with arthritis being the

most common EIM affecting 25% of Crohn's disease patients (Harbord *et al.*, 2016). Primary sclerosing cholangitis is another EIM that is more common in ulcerative colitis but can be present in Crohn's disease patients as well (Halliday *et al.*, 2012).

Due to the variable nature of Crohn's disease, treatment must be adapted depending on several factors including disease severity, location, anatomical involvement, and complications. As there is no cure for Crohn's disease the overarching strategy is to induce and maintain remission with a focus on reducing gastrointestinal inflammation and promoting mucosal healing. For mild to moderate Crohn's disease, induction of remission is achieved by the administration of systemic corticosteroids (budesonide or prednisolone) (Faubion *et al.*, 2001). Once remission is induced corticosteroids are not recommended for maintenance as long-term use is linked to an increased risk of infection and mortality (Lichtenstein *et al.*, 2006). Steroid-free maintenance of remission is achieved with the use of immunomodulator drugs such as thiopurines (mercaptopurine and azathioprine) and methotrexate. For treatment of moderate to severe Crohn's disease more modern pharmaceuticals are employed, biologics. Monoclonal antibodies directed against the proinflammatory cytokine tumour necrosis factor (TNF), such as Infliximab, are potent at induction and maintenance of remission (Hanauer *et al.*, 2002). Other monoclonal antibody treatments presenting alternative treatments to anti-TNFs and targeting different targets are Vedolizumab, which targets integrins (Sandborn *et al.*, 2013), and Ustekinumab, targeting the p40 subunit of IL-12 (Feagan *et al.*, 2016).

1.5.2 Crohn's Disease Epidemiology

Traditionally regarded as a disease of the western world, IBD (and Crohn's disease) has demonstrated that it is an emergent global disease (Molodecky *et al.*, 2012; Ng *et al.*, 2017). In 2012 Molodecky and colleagues conducted the first global comprehensive systematic review of population-based studies from 1930-2010, showing that the highest global incidence rates were in western countries; North America (Canada 20.2 per 100,000), Northern Europe (United Kingdom 10.6 per 100,000) and Australia (23.9 per 100,000). Correspondingly prevalence rates were greatest in North America (Canada 319 per 100,000) and Europe (Italy 322 per 100,000) (Molodecky *et al.*, 2012).

Molodecky and colleagues also identified that 75% of all Crohn's disease studies showed a significant increase in incidence rates, from 1930-1980, which fell to 56% showing an increase in incidence since 1980 with no studies demonstrating a decrease in Crohn's disease incidence (Molodecky *et al.*, 2012). This suggests that global incident rates are either rising or stable, in every region with available data. This was confirmed in an updated report by Ng and co-workers in which they demonstrated that incidence rates were either stable or decreasing in 72.7% of Crohn's disease studies from North America and Europe since 1990 (Ng *et al.*, 2017).

This later study by Ng and colleagues also confirmed that Crohn's disease is increasing in newly industrialised countries in Africa, South America, and Asia (Ng *et al.*, 2017). Historically Crohn's disease has been rare in developing countries but as these countries become increasingly

industrialised or "westernised" the incidence of Crohn's disease is increasing (Kaplan, 2015).

Variation in the incidence rate of Crohn's disease is high in China with the highest incidence rates being observed in regions with the most urbanisation and greatest economic advancement (Windsor and Kaplan, 2019). This urbanisation correlates to changes in diet with increased antibiotic usage, microbial exposure, and pollution (Ananthakrishnan *et al.*, 2018). This indicates that there is a strong association between environmental factors and Crohn's disease onset in a population. This is further compounded by the observation that first-generation children of immigrants, from countries with low IBD prevalence, who emigrated to countries with high IBD prevalence take on the same risk of IBD development as the native population (Kaplan, 2015).

Even though incidence rates are stabilizing in western countries IBD still represents a rapidly growing burden to global health services, owing to compound prevalence. The nature of IBD (having no non-surgical cure, often being diagnosed at an early age and low mortality) means that prevalence can rise rapidly, as demonstrated in Olmstead County in Minnesota (Kaplan and Ng, 2017). This sentiment is equally true for developing countries where IBD is emergent and is showing similar patterns in incidence/prevalence seen in western countries 50 years ago (Kaplan and Ng, 2017). These epidemiological trends indicate that environmental factors confer a significant risk of developing Crohn's disease.

1.5.3 Environmental risk factors and Crohn's disease

The risk of developing Crohn's disease in western countries appears to correlate with several environmental exposures such as smoking status, childhood antibiotic use, use of non-steroidal anti-inflammatory drugs (NSAIDs), and diet.

Cigarette smoking has been thoroughly studied and consistently identified as a risk factor for Crohn's disease. Current smokers have a two-fold increase in the risk of developing Crohn's disease (Birrenbach and Böcker, 2004; Lakatos, Szamosi and Lakatos, 2007; Higuchi *et al.*, 2012). Current smokers also demonstrate a more severe disease course with more flairs and a need for surgery with greater resurgence after surgery (Mahid *et al.*, 2006) with this risk lasting for several years post smoking cessation (Higuchi *et al.*, 2012). Smoking status in Crohn's disease also appears to have a gender component with females more predisposed to the adverse effects of smoking on Crohn's disease than males (Cosnes *et al.*, 2004).

Exposure to antibiotics in childhood perturbs the development of the gut microbiota and may increase the risk of Crohn's disease development. In a nested case-control analysis by Shaw and colleagues, it was demonstrated that 58% of children who received a dose of antibiotics in their first year of life developed Crohn's disease compared with only 39% of controls (Shaw, Blanchard and Bernstein, 2010). This effect is less if the antibiotics are received after the first year of life and a greater risk of Crohn's disease development was conferred with repeated exposure to antibiotics (Kronman *et al.*, 2012). This increase in risk also appears to depend on what antibiotics

are used with the greatest risk for Crohn's disease development seen with metronidazole and fluoroquinolones (Ungaro *et al.*, 2014).

Perturbations to the gut wall have long been known to be an adverse effect of NSAID use. However, this disruption to the gastrointestinal barrier may also increase the risk of developing Crohn's disease. In a study focusing on aspirin use, Chan and co-workers demonstrated a 6-fold increase in the risk of developing Crohn's disease (Chan *et al.,* 2011). Conversely, Ananthakrishnan and colleagues showed aspirin did not increase the risk of Crohn's disease development but other NSAIDs did and that this was in a dose and duration dependent manner. (Ananthakrishnan *et al.*, 2012).

Diet also appears to modify the risk of Crohn's disease development. Epidemiological observations indicate that Crohn's disease is increasing in developing nations (Ng *et al.*, 2017) with this development paralleled with the westernisation of dietary habits (Lewis and Abreu, 2017). A western diet is characterised by decreased fibre and increased animal protein consumption with an increase in foods with high-fat content and processed foods containing dietary additives such as emulsifiers. This diet is also associated with a decrease in microbiota diversity (Gupta, Paul and Dutta, 2017), increased abundances of *Bacteroides* and *Enterobacteriaceae*, with a lowered abundance of *Firmicutes* (David *et al.*, 2014). Indeed, diets high in saturated fats and sugars with lower consumption of fibre increased the risk of developing Crohn's disease (Basson, 2012). The effects of carbohydrates proteins and fats are reviewed by Schreiner et al (Schreiner *et al.*, 2020). Interestingly a higher consumption of fibre (24.3g/d) has been shown to decrease the risk of Crohn's disease by up to 40%, with the

greatest risk reduction coming from fibre derived from fruit sources (Ananthakrishnan *et al.*, 2013).

1.5.4 Crohn's disease Aetiology

The precise pathogenesis of Crohn's disease is still unknown, but it is understood to result from exposure to environmental triggers in a genetically susceptible individual initiating a dysregulated immune response against luminal antigens and leading to chronic inflammation of the gut.

1.5.4.1 Genetics of Crohn's disease

Over the last two decades, genome-wide association studies (GWAS) have identified a significant genetic component in developing Crohn's disease. Identification of the genes involved in Crohn's disease also lends great insights into its aetiology by understanding the function of these genes.

The first clue that genetics played a causative role in Crohn's disease development came from observations in monozygotic twins, where there was a 58.3% concordance rate of Crohn's disease (Tysk *et al.*, 1988). While siblings of Crohn's disease patients had a 15 to 35-fold increased risk of Crohn's disease development (Tysk *et al.*, 1988), and an eight-fold increase in risk for first-generation relatives (Moller *et al.*, 2015).

To date, GWAS have identified over 200 risk loci associated with IBD (Jostins *et al.*, 2012b; Liu *et al.*, 2015) with 70% of these genes conferring increased risk for both Crohn's disease and ulcerative colitis (Bianco, Girardelli and Tommasini, 2015), with mutations in NOD2, ATG16L1 and IRGM being the major specific risk determinants of Crohn's disease.

In 2001, the nucleotide-binding oligomerisation domain 2 (NOD2) gene was identified as the first susceptibility locus which confers the greatest risk for Crohn's disease development (Hugot *et al.*, 2001). The presence of one NOD2 risk allele increases the risk of Crohn's disease development by 2 to-4 fold, while the presence of two risk alleles increases the risk of Crohn's disease development by 20 to 40-fold (Caruso *et al.*, 2014; Negroni *et al.*, 2018). NOD2 is an intracellular protein expressed in APCs as well as epithelial cells (particularly Paneth cells) (Sidiq *et al.*, 2016; Negroni *et al.*, 2018), responding to the bacterial component muramyl dipeptide found in gram-positive and negative bacteria (Negroni *et al.*, 2018). When activated by muramyl dipeptide NOD2 induces the expression of proinflammatory and anti-microbial molecules IL-1β, TNF-α, IL-6, IL-8 and α-defensins via the activation of NF-κB and leads to immune cell recruitment and differentiation (Negroni *et al.*, 2018). NOD2 impairment has also been shown to affect bacterial recognition in Paneth cells leading to a decrease in α-defensin secretion and infiltration of bacteria into the mucosa (Caruso *et al.*, 2014). Additionally, NOD2 is crucial for the initiation of autophagy by recruiting autophagy-related 16-like 1 (ATG16L1), mutations in which also confers a high risk of Crohn's disease development (Negroni *et al.*, 2018).

Autophagy has been demonstrated to play an important role in the regulation of intestinal microbiota and mutations in genes regulating it confer an increased risk of Crohn's disease development (Chu *et al.*, 2016a). ATG16L1 mutations conferred a 2-fold increased risk for Crohn's disease which increased to 7-fold in smokers (Fowler *et al.*, 2008). Biopsies from Crohn's disease patients with ATG16L1 mutations have shown

increased abundances of *Bacteroides fragilis, Fusobacteria* and *E. coli* indicating that ATG16L1 is necessary to maintain immune homeostasis in the gut (Sadabad *et al.*, 2015). The autophagy-associated, immunity-related GTPase family M (IRGM) gene has also been strongly associated with Crohn's disease development (Parkes *et al.*, 2007; Prescott *et al.*, 2010). IRGM codes an autophagy protein that aids in the innate immune clearance of Crohn's disease associated bacteria *Salmonella typhimurium* and *adherent invasive E. coli* (AIEC) (McCarroll *et al.*, 2008; Lapaquette *et al.*, 2010).

There are also mutations in other genes which increase the risk of developing IBD but not Crohn's disease specifically. Gain of function mutations in the IL-23 receptor (IL-23R) have been linked to IBD development (both Crohn's disease and ulcerative colitis) (Duerr *et al.*, 2006). IL-23 is important in generating and maintaining T-cell-mediated immunity and is primarily secreted by macrophages and dendritic cells after bacterial recognition (McGovern and Powrie, 2007). IL-23 is a known mediator of the chronic inflammation seen in IBD with high levels detected in the mucosa of IBD patients (Liu *et al.*, 2011). IL-23R is expressed on dendritic cells, macrophages and Th17 cells. Th17 cells are differentiated by the exposure of naïve T cells to TGFβ and IL-6 which also upregulate the expression of IL23R making them susceptible to IL-23 stimulation (McGovern and Powrie, 2007). Gain of function on IL-23R leads to maintenance of a disproportionate Th17 inflammatory response to luminal microbes characterised by excessive IL-17 production (McGovern and Powrie, 2007). Whereas in dendritic cells and macrophages, it stimulates

continuous production of inflammatory cytokines IL-12, IL-17, IFNγ TNFα and IL-23 driving chronic inflammation (Liu *et al.*, 2011).

Loss of function mutations in IL-10 and IL-10 receptor (IL-10R) have been demonstrated as risk factors for very early onset Crohn's disease (Kotlarz *et al.*, 2012; Uhlig *et al.*, 2014; Lin *et al.*, 2017). IL-10 is an anti-inflammatory cytokine secreted by several immune cells including APCs, macrophages, and lymphocytes (Saraiva and O'Garra, 2010). IL-10 attenuates inflammatory responses and is an important mediator of immune tolerance against luminal bacteria (Saraiva and O'Garra, 2010). Loss of function of IL-10 leads to an excessive immune response characterised by increased TNFα and IL-12 production which would usually be attenuated by IL-10 (Glocker *et al.*, 2009a).

The cadherin 1 (CDH1) gene, related to epithelial barrier integrity, is also a known risk loci for early-onset Crohn's disease (Muise *et al.*, 2009a; Moran *et al.*, 2015). The product of the CDH1 gene is E-cadherin a membrane-associated protein important in the regulation of epithelial tight junctions (Muise *et al.*, 2009a). Mutations in CDH1 lead to E-Cadherin being trafficked to the cytosol instead of the cell membrane and lead to "leaky" epithelial tight junctions allowing the infiltration of luminal bacteria into the mucosa (Muise *et al.*, 2009a).

While the aetiology of Crohn's disease is still not understood completely identification of these genetic risk loci in Crohn's disease development have given insights into how these biological process' are important for the prevention of chronic inflammation in the gut. These risk loci implicate

bacterial recognition, bacterial clearance, a dysregulated immune response, and a defective epithelial barrier in the development of Crohn's disease.

1.5.4.2 Microbiota dysbiosis in Crohn's Disease

Given that mutations in genes related to bacterial handling in the GIT confer the largest risk for Crohn's disease development, it follows that the microbiota would play an integral role in its pathogenesis. Early evidence for the involvement of the gut microbiota was seen where surgical diversion of the faecal stream decreased or eliminated inflammation in patients with Crohn's disease (Rutgeerts *et al.*, 1991). In addition, recurrence of inflammation after surgical resection was dependent on exposure to luminal contents (D'Haens *et al.*, 1998). Further evidence for microbial involvement in Crohn's disease comes from animal models where transfer of faecal microbiota from mice with colitis will initiate inflammation in healthy mice (Schaubeck *et al.*, 2016). Moreover, colitis-susceptible mice with TCR mutations will develop colitis when colonised with a conventional microbiota but not when raised in germ-free conditions (Dianda *et al.*, 1997).

Many studies have reported changes in the microbiota of patients with IBD patients, however, these have not identified a consistent change in microbial composition. A potential reason for this is the great variation in studies characterising the microbiota in IBD patients due to confounding variables such as disease duration, differences in treatment, sampling location, and variation in analysis. However, it is very well characterised that dysbiosis is present in IBD patients with this being more pronounced in Crohn's disease than ulcerative colitis, with a more altered and unstable microbiota composition in the former (Dalal and Chang, 2014; Pascal *et al.*,

2017). A number of studies have demonstrated that the microbiota of patients with Crohn's disease possesses a reduced richness of species with decreases in *Faecalibacterium prausnitzii*, *Bacteroides*, *Blautia*, *Ruminococcus*, *Roseburia*, *Coprococcus*, and Lachnospiraceae and with increases in *Enterobacteriaceae*, *Fusobacteriaceae*, and *Streptococcaceae* (Eun *et al.*, 2016; Rehman *et al.*, 2016). Among bacteria commonly associated with Crohn's disease are adherent-invasive E. coli (AIEC), with a prevalence of 30-40% in patients with Crohn's with ileal lesions. AIEC lack classical pathogenicity genes but can persist in macrophages without inducing cell death as well as adhere and invade epithelial cells thus affecting the integrity of the epithelial barrier (Rolhion and Darfeuille-Michaud, 2007). Recent studies in animal models associate the impaired autophagy-mediated clearance of AIEC with enhanced inflammation further supporting the role of certain microbial species in IBD (Larabi, Barnich and Nguyen, 2020).

An open question in this field is whether the dysbiosis seen in Crohn's disease precedes inflammation or whether dysbiosis is a result of inflammatory processes. An interesting study investigating the microbiota of paediatric, treatment naïve Crohn's disease patients using mucosal tissue biopsies and faecal samples revealed increased abundances of Veillonellaceae, Paturellaceae, Neisseriaceae, *Fusobacteriaceae* species, *E. coli* species. While there were decreased abundances of Clostridiales, *Bacteroides*, *Faecalibacterium* species, *Roseburia* species, *Blautia* species, *Ruminococcus* species, and Lachnospiraceae (Gevers *et al.*, 2014). As this study investigated a newly diagnosed population it suggests that microbiota

changes occur early and may precede clinical disease. Indeed, a recent study using a genetic model of Crohn's disease (deficient in two Crohn's disease susceptibility genes NOD2 and phagocyte NADPH oxidase) demonstrated an increase in pathobiont species prior to the onset of colitis (Caruso *et al.*, 2019). These observations suggest that dysbiosis in Crohn's disease can be present before inflammation implicating microbiota composition in Crohn's disease pathogenesis.

1.5.4.3 Dysregulated immune responses in Crohn's Disease

The chronic inflammation seen in Crohn's disease is inherently due to a dysregulated immune response to enteric bacteria. Indeed, the GIT immune system in Crohn's disease exhibits defects in both arms of immunity. Mutations in genes related to maintenance of the epithelial barrier confer a significant risk for Crohn's disease development as seen above in **section 1.5.4.1**. Further to this, Crohn's disease is also associated with defects in the chemical barrier of the epithelium where expression of mucins is decreased in Crohn's disease patients (Buisine *et al.*, 1999) as well as a reduction in the AMP α defensin (Wehkamp *et al.*, 2005). Innate sensing of the microbiota may also be dysregulated in Crohn's disease, where DAMPs, increased in Crohn's disease, are known to activate TLR4 signalling and thus NF-κB signalling (Testro and Visvanathan, 2009; Boyapati *et al.*, 2016). Further dysregulation of innate bacterial sensing is seen where NOD2 mutations can reduce TLR2 inhibition leading to exacerbated inflammation and excessive Th1 responses (Watanabe *et al.*, 2004). Dysfunction in innate immune cells has also been observed in Crohn's disease. Dendritic cells which are APCs and capable of activating multiple lineages of T cells

are accumulated in inflamed tissue in Crohn's disease (te Velde *et al.*, 2003). Mouse models of colitis show an increase in activated DCs in the LP and mesenteric lymph nodes and where blockade of CD134L prevented T cell activation and prevented the development of colitis (Malmström *et al.*, 2001; Krajina *et al.*, 2003). Macrophages are also associated with Crohn's disease where large numbers of CD14^{+} macrophages are seen in the inflamed mucosa, producing excessive IL-23, TNF, and IL-6 (Kamada *et al.*, 2008).

The cytokine TNF-α plays a pivotal role in CD pathology, as evidenced that its blockade by the monoclonal antibody infliximab is one of the primary therapies for induction of remission (Hanauer *et al.*, 2002). TNF-α is a pleiotropic cytokine influencing a range of cells and pathways including gut epithelial cells and the NF-κB pathway. This pathway activates the transcription of a variety of both pro and anti-inflammatory mediators and is composed of several transcription factor subunits including p50/p105, p52/p100, p65, RelB and c-Rel (Oeckinghaus and Ghosh, 2009). When there is no inflammatory stimulus present these transcription factor subunits are bound to inhibitor of κB (IκB) in the cytosol preventing nuclear translocation of NF-κB and induction of gene transcription. The NF-κB pathway is activated in response to a range of pro-inflammatory stimuli derived from both the host and the gut microbiota which bind to host receptors including TNF-α receptor, TLRs, NOD1/2, and IL-1 receptor (IL-1R), to name a few. Signalling cascades from these receptors result in the phosphorylation of residues on the IκB kinase (IKK) complex, which is composed of two kinase subunits, IKKα and IKKβ with a regulatory subunit

IKKγ. Activation of the NF-κB pathway leads to phosphorylation of the IKKβ subunit with downstream phosphorylation, ubiquitination, and degradation of IκB. With IκB no longer binding the NF-κB subunits they are free to translocate to the nucleus and induce gene expression of numerous inflammatory chemokines including IL-8 and chemokine (C-C motif) ligand 20 (CCL20). IL-8 and CCL20 have demonstrated elevated levels in the colonic mucosa of patients with CD (Daig *et al.*, 1996; Kaser *et al.*, 2004). IL-8 is a potent chemoattractant for neutrophils initiating bone marrow egression, extravasation, and mucosal migration along with aiding in respiratory burst and neutrophil degranulation (Cotton *et al.*, 2016). CCL20 has been identified as a susceptibility gene for CD development (Liu *et al.*, 2015). CCL20 exclusively binds to chemokine receptor 6 (CCR6), which is expressed on dendritic cells, B cells, Tregs and Th17 cells (Skovdahl *et al.*, 2015). As such CCL20 is involved in the chemotaxis of these cells to the gut mucosa (Skovdahl *et al.*, 2015).

While dysregulation in the innate immune system will have profound effects on the activation of the adaptive immune system, inflammation in Crohn's disease is primarily thought to be driven by excessive activation of the effector Th1 and Th17 cells (Annunziato *et al.*, 2007). T helper 1 cells primarily produce the cytokines IFNγ and TNF, and their numbers and activity are increased in Crohn's disease mucosa (Breese *et al.*, 1993) in the initiation of disease and decreases as the disease progress (Kugathasan *et al.*, 2007). IFN-γ is a cytokine which is highly upregulated in CD (Neurath, 2014), with mutations in the IFNG gene (encoding IFN-γ), leading to its overexpression, increasing the severity of CD as well as

increased resistance to anti-TNF treatment, highlighting the cytokine's importance in Crohn's disease pathology (Gonsky *et al.*, 2014). Although IFNγ abrogation severely reduced colitis in the adoptive T cell transfer model (Neurath *et al.*, 2002), treatment with the IFNγ blocker fontolizumab failed to produce a strong clinical response in patients with CD in a clinical trial (Reinisch *et al.*, 2010). IFN-γ mediates many inflammatory and immunomodulatory processes including induction of epithelial chemokine gene expression through IFN receptors (IFNR) and Janus kinase/signal transducer and activator of transcription (JAK/STAT) signal transduction, in both of which mutations have been associated with CD development (Barrett *et al.*, 2008). Briefly, the JAK/STAT pathway is activated by the binding of IFN-γ to an IFNR, which has associated JAK proteins, leading to dimerisation of IFNR and allowing JAK proteins to trans/auto phosphorylate with them, subsequently phosphorylating intracellular tyrosine residues on the IFNR. These phosphotyrosines on the intracellular IFNR can act as binding sites for STAT proteins and initiate JAK-mediated tyrosine phosphorylation of STAT proteins. The active STAT proteins can now dissociate from the receptor, hetero/homo dimerise, and translocate to the nucleus to induce/repress the expression of a plethora of genes including chemokines such as chemokine C-X-C motif ligand 10 (CXCL10/IP-10) and CCL5 (RANTES). Both chemokines are increased in patients with CD (Mazzucchelli *et al.*, 1996; Ansari *et al.*, 2006; Østvik *et al.*, 2013; Singh *et al.*, 2016). CXCL10 production is induced by IFN-γ in intestinal epithelial cells and binds to C-X-C motif chemokine receptor (CXCR) 3 (Dwinell *et al.*, 2001), which is expressed on Th1 cells and facilitates their migration to the

gut (Wadwa *et al.*, 2016). CCL5 expression in colonic epithelial cells is induced by IFN-γ (Lee *et al.*, 2008) and like CXCL10 is involved in the chemotaxis of Th1 cells to the gut (Oki *et al.*, 2005).

T helper 17 cells are found abundantly in the LP and submucosa of Crohn's disease patients along with increased levels of IL-23, which drives differentiation of Th17 cells, and proinflammatory IL-17A (Fujino *et al.*, 2003; Kobayashi *et al.*, 2008). Additionally, increased IL-17 production is seen in IL10$^{-/-}$ mice (Lytle *et al.*, 2005). Further to this, supplementation of IL-23 to mouse models of colitis drives Th17 differentiation and cytokine production exacerbating colitis whereas an anti-IL-23 antibody mitigates inflammation (Yen *et al.*, 2006; Elson *et al.*, 2007). During homeostasis, Treg cells control inflammation through the anti-inflammatory cytokines IL-10 and TGF-β. In Crohn's disease, there is, paradoxically, an increase in Treg cells in the inflamed colon (Hardenberg, Steiner and Levings, 2011). A potential explanation for this contradiction can be seen in the observation that Treg cells isolated from the inflamed colon retain their contact-dependent, cytokine-independent suppressive capabilities *in vitro* (Saruta *et al.*, 2007), however, effector T cells from Crohn's disease colons display resistance to suppression mediated by Treg cells (Fantini *et al.*, 2009). Effector T cells in Crohn's disease are known to overexpress the TGF-β signalling inhibitor Smad7 (Fantini *et al.*, 2009). This overexpression may make the effector T cells unresponsive to Treg cell suppression. Indeed, the Smad7 antisense oligonucleotide named Mongersen had demonstrated positive results in phase 1 clinical trials for the treatment of Crohn's disease (Monteleone *et*

al., 2015), however, a recent phase 3 trial demonstrated no efficacy for treating Crohn's disease (Sands *et al.*, 2020).

Taken together these observations highlight dysfunctional immune pathways, in both arms of the immune system, and in the pathology of Crohn's disease.

1.5.5 Bile acids in Crohn's disease

As outlined above, compositional changes in the gut microbiota are a contributing factor in driving the inflammation seen in Crohn's disease. It follows that any alteration in gut bacteria will consequently alter the bacterially generated metabolite landscape of the gut. These bacterial metabolites, including BAs, have been shown to impact many host processes including host metabolism, epithelial barrier integrity, and both innate and adaptive immune responses (Lavelle and Sokol, 2020). Indeed, early observations of BAs in Crohn's disease showed that a reduced BA pool was associated with Crohn's disease but not ulcerative colitis, indicating a role for their involvement in Crohn's disease pathology (Vantrappen *et al.*, 1977). A more recent study revealed impaired BA metabolism featuring decreased BA deconjugation with a concomitant reduction in secondary bile acids in IBD patients with active disease (Duboc *et al.*, 2013a). Compounding these observations recent multi-omics studies have demonstrated increased primary BAs such as CA and CDCA, including their conjugated forms, and reduced secondary BA, such as LCA and DCA in Crohn's disease patients and these changes correlated with the presence of dysbiosis (Franzosa *et al.*, 2019; Lloyd-Price *et al.*, 2019; Wang *et al.*, 2021). These alterations in the bile acid pool are associated with a

decrease in bacterial genera containing BSH and 7α-dehydroxylation enzymes (Wang *et al.*, 2021). These studies underpin the role of dysregulated BA metabolism in Crohn's disease pathology. Incidentally, changes in the BA pool have been suggested as an indicator for therapeutic response, where patients with increased serum levels of DCA responded better to infliximab whereas patients with elevated serum levels of unconjugated CA and CDCA did not respond (Ding *et al.*, 2020). There is a growing body of evidence that suggests that BAs through bile acid receptors (BARs), expressed on epithelial cells, DC, ILC3, macrophages, and Th17 cells can influence immune processes (Biagioli *et al.*, 2021).

Mutations in FXR, the master regulator of BA synthesis, have been associated with IBD (Attinkara *et al.*, 2012). In epithelial cells and macrophages, FXR can exert an anti-inflammatory effect by modulating signalling pathways, such as NF-κB, and inhibiting targets of TNF-α, IL-1, and IL-6 (Ding *et al.*, 2015). Recent experiments in FXR[null] mice demonstrated BA synthesis was increased and there was bacterial overgrowth and reduced epithelial barrier function with this phenotype being ameliorated by addition of FGF19 (Gadaleta *et al.*, 2020). This study also corroborated that FGF-19 levels were reduced in patients with Crohn's disease relative to healthy controls (Gadaleta *et al.*, 2020). FXR activation on dendritic cells by isoDCA was recently shown to induce the differentiation of Treg cells illustrating a potential anti-inflammatory role of BAs (Campbell *et al.*, 2020a).

TGR5 activation by BA is associated with anti-inflammatory properties. Mice treated with a TGR5 agonist had decreased expression of proinflammatory

cytokines and chemokines such as IL-1β, IL-6, IFNγ TNFα and CCL2 with induced expression in the anti-inflammatory cytokine IL-10 (Biagioli *et al.*, 2017). The anti-inflammatory effects of TGR5 activation were further demonstrated where mice with chemically induced colitis treated with the TGR5 agonist LCA, had reduced expression of proinflammatory cytokines. This was dependent on TGR5 expression in immune cells and not epithelial cells (Sinha *et al.*, 2020). However, TGR5 activation in the epithelium is associated with intestinal stem cell renewal and regeneration after injury (Sorrentino *et al.*, 2020).

VDR activation is also associated with anti-inflammatory effects. It can induce Treg cell differentiation, however, this is only when exposed to specific combinations of primary and secondary BAs (Song *et al.*, 2020). This underscores how small deviations in the BA pool may have larger reaching implications than previously envisioned. Complementary to this, VDR activation can also inhibit the differentiation of Th1 cells leading to decreased IFNγ and TNFα production (Pols *et al.*, 2017). Interestingly 3-oxo-LCA and isoLCA also inhibited Th17 differentiation in a VDR-independent manner by directly inhibiting RORγt and bacteria that possess the 3α-HSDH to produce these LCA metabolites are significantly decreased in IBD patients (Paik *et al.*, 2021).

These observations demonstrate that BAs are altered in Crohn's disease and can influence several pathways and immune cells implicated in Crohn's disease pathology.

1.5.6 Preclinical models of Inflammatory Bowel Disease

The heterogeneity seen in IBD patients makes it difficult for clinicians to study its pathology and aetiology. Animal models have proved invaluable for studying pathophysiological mechanisms of intestinal inflammation. Since the development of the first animal model of intestinal inflammation in 1957, using rabbits sensitised to crystalline egg albumin with a formalin enema, over 60 models have been developed to study IBD (Kirsner, 1958; Mizoguchi, 2012). While none of these models can fully recapitulate the complexity of IBD in humans and cannot replace studies using patient samples, they do offer an avenue for targeted investigation of pathophysiological mechanisms in a controlled and reproducible manner while avoiding the heterogeneity often seen in clinical studies. Animal models of IBD can broadly be characterised into; chemically induced, adoptive T cell transfer, genetically engineered, and spontaneous models.

1.5.6.1 Chemical Induced Model: Dextran Sodium Sulphate

Among the chemically induced, Dextran sodium sulphate (DSS) is one of the most used models in research. DSS is a polymer which dissolves readily in water. This provides an easy mode of delivery, with a 3-5% DSS solution in drinking water administered for 4-7 days inducing acute inflammation in the colon while additional treatment cycles can induce chronic inflammation (Okayasu *et al.*, 1990; Melgar, Karlsson and Michaëlsson, 2005; Kawada, Arihiro and Mizoguchi, 2007). Its mechanism of action is thought to be due to direct epithelial toxicity which compromises the epithelial barrier allowing penetration of luminal bacteria to the submucosa (Westbrook, Szakmary

and Schiestl, 2016). Dextran sodium sulphate induced inflammation is associated with diarrhoea, bleeding, ulceration, and granulocyte infiltration of the mucosa (Perše and Cerar, 2012). This model is frequently used in studying innate immune responses in IBD onset and epithelial barrier restoration (Wirtz *et al.*, 2017).

1.5.6.2 Adoptive T cell Transfer Model: CD4+ CD45RBhi

Transfer models induce inflammation by transferring immune cells into animals with impaired immune systems such as RAG$^{-/-}$ or severe combined immunodeficiency (SCID) mice. In this model transfer of naïve T cells (CD4+ CD45RBhi) into immune-deficient mice will induce colitis in 5-10 weeks after transfer (Jurjus, Khoury and Reimund, 2004). Inflammation in this model is more chronic in nature and is characterised by inflammation and hyperplasia in the colon (Elson *et al.*, 1995). A Th1 cell response, with a lack of Treg cells, drives inflammation in this model (Westbrook, Szakmary and Schiestl, 2016). This model allows the investigation of early immunological events in IBD (Ostanin *et al.*, 2009), however, it requires the utilisation of a cell sorter and expert intravenous inject skills to implement.

1.5.6.3 Genetically Engineered Model: IL10$^{-/-}$ Mice

Mutations in the IL-10 receptor are associated with early onset familial Crohn's disease (Glocker *et al.*, 2009b). As such mice with targeted deletion of IL-10 will spontaneously develop colitis at around three months of age (Keubler *et al.*, 2015). This inflammation is characterised by discontinuous, transmural lesions with infiltration of lymphocytes, macrophages, and neutrophils in the LP (Kühn *et al.*, 1993a). Similar to Crohn's disease this inflammation is initially driven by Th1 cells, however, like Crohn's disease,

the production of IFNγ decreases over time (Berg *et al.*, 1996a; Spencer *et al.*, 2002). Colitis development in IL10-/- mice is dependent on several factors including the 1) genetic background of the mouse, where mice from a C3H/HeJBir background will develop severe colitis while mice from a C57BL/J6 background are relatively resistant to colitis (Berg *et al.*, 1996a), 2) presence of a complex microbiota, since germ-free IL10-/- mice do not develop colitis and treatment with antibiotics will prevent its development in IL10-/- mice (Sellon *et al.*, 1998a; Madsen *et al.*, 2000a), and 3) the microbe status of the housing facility (Sellon *et al.*, 1998a).

1.5.6.4 Spontaneous Model: C3H/HeJBir Mice

Mice of the C3H/HeJ strain exhibit soft, light-coloured faeces, histological evidence of colitis, and intermittent presence of perianal ulceration while lacking the presence of any pathogens (Sundberg *et al.*, 1994). As such researchers reasoned that this strain of mice possessed a genetic predilection towards IBD development and used them to develop a sub strain, C3H/HeJBir, which exhibits a high incidence of spontaneous colitis (Sundberg *et al.*, 1994). Inflammation begins at 3-4 weeks of age and can last up to 10-12 weeks old, affecting the ileocecal region, and presenting similar characteristics to Crohn's disease (Cong *et al.*, 1998).

1.6 Motivation for this study

Crohn's disease is a chronic lifelong disease of the bowel that severely impacts a person's quality of life and requires lifelong treatment. While the cause of Crohn's disease has not yet been elucidated, a cardinal feature of it is a dysregulated immune response to dysbiotic gut microbiota. To date,

no individual member of the microbiota has been recognized as a causative agent. Results from studies investigating microbiota composition in Crohn's disease are often contradictory due to the heterogeneity of study designs. Recent findings from our group showed significant enrichment of *Bacteroides fragilis* in inflamed mucosal biopsies from patients with Crohn's disease vs healthy controls (Ryan *et al.*, 2020). This study also noted an increased abundance of *Bacteroides vulgatus* in a cluster associated with decreased diversity but no disease state. The literature demonstrates no consensus on the abundance of *Bacteroides* species in Crohn's disease, with some reporting increased and others reporting decreased abundance, as highlighted by a recent systematic review (Aldars-García, Chaparro and Gisbert, 2021). This project was conceived to dissect the role of *Bacteroides* spp in the pathology of Crohn's disease. For this we targeted our analyses on 1) the colonic epithelium as it represents the first barrier to the microbiota and acts as a central coordinator of immune responses in the gut 2) the capability of *Bacteroides* in altering bile acid metabolism 3) using a preclinical model (IL10$^{-/-}$ mice), we assessed the impact of *Bacteroides vulgatus* colonisation on the microbiota and bile acid composition in a longitudinally study and on the host response.

Thus, the main objective of this research was to gain a deeper insight into mechanisms regulated by *Bacteroides* spp and their relevance to Crohn's disease pathogenesis. The research work is presented in three chapters with the following aims.

The aim of the work presented in **Chapter 3** was to explore the inflammatory potential of *Bacteroides fragilis* and *Bacteroides vulgatus* using *in vitro*

epithelial cell systems and to investigate if they could elicit inflammation in a genetically intact host *in-vivo*.

The aim of the work presented in **Chapter 4** was to assess the capability of *Bacteroides* species to modify bile acids *in vitro* and to examine if this functionality was retained *in vivo* in a genetically intact host.

The aim of the work presented in **Chapter 5** was to evaluate the effect of proinflammatory *Bacteroides vulgatus* on the microbiota and metabolic landscape during colitis development in IL10$^{-/-}$ mice. This model was chosen as it displays a similar inflammatory profile as Crohn's disease, with similar immune cell involvement. Further to this a cardinal feature of the inflammation seen in IL10$^{-/-}$ mice is that it is in response to the gut microbiota. This is conducive to the targeted study of bacteria associated with Crohn's disease.

Chapter 2 Materials and Methods

2.1 Bacteria, media, and culture conditions

The bacterial species used in this project are listed in **Table 2.1**. The three *Bacteroides* species, *Bacteroides vulgatus, Bacteroides fragilis* and *Bacteroides thetaiotaomicron* were sourced from DR David J. Clarke and they were grown in Brain Heart Infusion (BHI, Oxid, UK) agar and broth supplemented with 5 mg/L hemin (Sigma, China), 400 µg/L cysteine (Sigma, China), 8 ml/L of 20% $NaHCO_3$ (Sigma, USA) and 200 µl/L of gentamycin (Sigma, Israel). *Lactobacillus rhamnosus* GG was grown in de Man, Rogosa, and Sharpe (MRS, Sigma, Switzerland) agar and broth. *Salmonella typhimurium* was grown in lysogeny broth (LB Oxoid, UK) and agar. *Bacteroides* species and *L. rhamnosus* GG were incubated anaerobically at 37 °C, using an anaerobic jar and an Anaerocult® A pack (Merck, Germany) to generate an anaerobic environment with 18.5% CO_2, for 24-48 hours. *S. typhimurium* was incubated aerobically at 37 °C with no shaking for 24 hours. Bacteria were stored as frozen stocks in 20% (v/v) glycerol at -80°C.

Table 2.1 List of bacteria used in the project

Bacteria	Source
Bacteroides fragilis	NCTC-9343
Bacteroides vulgatus	ATCC-8482
Bacteroides thetaiotaomicron	University of Michigan
Lactobacillus rhamnoses GG	Culturelle Probiotics
Salmonella typhimurium	Quadram Institute

2.2 Preparation of bacterial cell-free supernatant, conditioned media

Bacteria were streaked onto agar plates from frozen stocks and incubated at 37 °C until colonies formed, 24-48 hours. From these plates, individual colonies were transferred to 5 mL of their respective broth to grow overnight using the conditions outlined in **Section 2.1**. Following this, OD_{600} values were measured using a BioPhotometer (Eppendorf), used to calculate the volume of overnight to give an OD_{600} of 0.05 for *Bacteroides*, 0.1 for *S. typhimurium* and *L. rhamnoses* GG in 50 mL of broth. The strains were then incubated until either the exponential or stationary phase of growth was reached as indicated by the respective bacteria's growth curves. Following incubation, for the relevant time, the culture was removed and the OD_{600} read, to confirm growth phase status against a growth curve, and centrifuged at 10,000 rpm for 15 minutes. The supernatant was decanted to a fresh tube and filter sterilised using a 0.2μm filter (Millipore). The supernatant was filter sterilised a second time and aliquoted into 1.5 mL tubes and stored at -20 °C until needed.

2.3 Preparation of *Bacteroides* for animal inoculation

In preparation for oral gavage of *Bacteroides vulgatus* and *Bacteroides fragilis* to mice (**sections 2.10 and 2.11**), fresh agar plates were streaked from frozen stocks and incubated for 24-48 hours. Single colonies were selected for overnight growth in 5 mL of media (section 2.1). The OD_{600} of these overnight cultures were read and used to calculate the volume of the overnight culture required to give an OD_{600} of 0.05 in 5 mL of broth which was again cultured overnight. On the morning of the oral gavage, this

overnight culture was centrifuged for 10 minutes at 3,000 g, the supernatant was decanted, and the pellet was resuspended in phosphate-buffered saline (PBS, Sigma, UK). This process was repeated two more times and the OD_{600} was read to calculate the final volume of $5x10^9$ cfu/ml, or $1x10^9$ cfu/200µl to be used for animal inoculation.

2.4 *Bacteroides*/bile acid co-incubation assays

2.4.1 Porcine bile co-incubation

A co-incubation assay was performed to assess the *Bacteroides* species' potential for bile acid metabolising, establish their substrate specificity and detect which bile acid moieties they have the potential to produce. Three individual colonies from each of the three *Bacteroides* strains were taken from freshly streaked plates for overnight culture in 10 mL BHI broth. Following this, each culture was normalised to 1 OD_{600} and centrifuged at max speed for 5 minutes to pellet the bacteria and washed twice with PBS. The pellet was resuspended in 10 mL BHI with 0.5% porcine bile spiked with tauro/glyco cholic acid, tauro α-muricholic acid, tauro β-muricholic acid, tauro ω-muricholic acid and tauro/glyco deoxycholic acid to a final concentration of 1µg/ml. The co-incubation reaction was incubated anaerobically at 37 °C for 3 hours. Deuterated internal standards of both cholic acid (CA d_4) and chenodeoxycholic acid (CDCA d_4) were added to a final concentration of 1 µg/ml. This mixture was vortexed and centrifuged for 10 minutes at 10,000 g and the supernatant was removed and extracted in one volume of 100% methanol split between two tubes and placed at -20 °C for 30 minutes before being centrifuged again for 10 minutes at 10,000g. The extract was then vacuum dried under nitrogen and reextracted using

acetonitrile with 5% formic acid and dried as outlined above. The extract was resuspended in 150 µl of ice-cold 50% methanol and centrifuged for 10 minutes at 10,000g after which the supernatant was transferred to glass vials (Waters Ltd.) for mass spectrometry application. A control reaction was conducted where extracts were taken from BHI, with spiked porcine bile, lacking bacteria.

2.4.2 Primary bile acid co-incubation

This experiment and bile acid extraction was carried out as outlined above (**section 2.4.1**) with minor alterations to the starting parameters. The bacteria were normalised to 2 OD_{600} and incubated in BHI, spiked with 10 µM each of the primary bile acids Cholic acid (CA) and chenodeoxycholic acid (CDCA) for 2 hours. The extraction protocol continued as outlined above.

2.5 Epithelial cell culture

2.5.1 C2BBe1 cells

The human colonic epithelial cell line C2BBe1 was used for all cell work in this project as they represent more differentiated enterocytes in comparison to other cell lines and have demonstrated responses to bacteria. C2BBe1 cells (CRL-2102; ATTC, UK) were grown in high glucose (4,500 mg/L) Dulbecco's Modified Eagles Medium (DMEM Sigma, UK). This basal medium was supplemented with 10% foetal bovine serum (FBS Sigma, Non-USA origin), 100µg/ml penicillin (Sigma, Israel), 100U/ml streptomycin (Sigma, Israel) and 0.01mg/ml of transferrin (Sigma, UK). The cells were incubated at 37 °C with 5% CO_2 with constant humidity, and the media was

replaced every 2-3 days. Cells used in all experiments described in this thesis were between passages 52 and 60.

2.5.2 C2BBe1 Passage

C2BBe1s were sub-cultured once they reached ≥ 70% confluency. The spent medium was removed, and the cells were washed 3 times with warmed PBS to remove any FBS, to ensure it did not interfere with trypsin activity. Following washing, C2BBe1s were exposed to a 0.5% trypsin/EDTA solution and incubated at 37 °C for 5 – 10 minutes or until the cells had fully detached from the flask bottom. The trypsin was deactivated by the addition of DMEM with 10% FBS and the cell suspension was transferred to a 15 mL falcon and pelleted by centrifuging at 800 g for 3 minutes. The pellet was resuspended in 10 mL of fresh medium which was used to seed a fresh T175 culture flask (Greiner, Germany). T175 flasks were seeded with 2 mL of the above cell suspension to give 70% confluence in 3-5 days.

2.5.3 Freezing/thawing C2BBe1

Fresh media was applied to C2BBe1 cells 24 hours before freezing. The protocol for freezing the cells is described in **section 2.5.2** except after centrifuging cells post-trypsination, the cell pellet is resuspended in cryopreservation media [90% FBS and 10% dimethyl sulphoxide (DMSO Sigma, UK)] and transferred to cryo-vials, at a density of 2×10^6 per vial. The cryo-vials were placed in a "Mr Frosty" freezing container at -80 °C overnight followed by transfer to liquid nitrogen storage until needed. The Mr Frosty container surrounds the cryo-vials with isopropanol which cools

at a fixed rate of 1°C per minute preventing the formation of ice crystals and thus cell lysis.

DMSO is toxic to cells above 4°C so rapid thawing of the cells is necessary. Cryo-vials were thawed in a 37°C water bath and contents were immediately transferred to 5 mL of pre-warmed supplemented DMEM. Cells were centrifuged at 800rpm for 3 minutes and the supernatant was decanted. The pellet was resuspended in fresh warm supplemented DMEM and transferred to a T25 flask (Greiner, Germany) to incubate at 37°C, 5% CO_2 and constant humidity. Once confluent the cells were passaged to a T75 (Greiner, Germany) or T175 flask for stock maintenance.

2.5.4 C2BBe1 cell counting and viability

For cell counting and viability assessment, the Countess™ cell counter (Thermo Fisher Scientific) was used. To count cells the procedure was similar to passaging cells (**Section 2.5.2**). 25 µl of cell suspension was mixed with 25 µl of trypan blue (Sigma, UK), with 10 µl of this mix transferred to each chamber of a Countess™ cell counting chamber slide. This slide was inserted into the Countess™ cell counter to calculate the number of cells per mL, this was repeated for both chambers on the slide and an average was taken as the final cell count. The Countess™ also calculated cell viability with the expected value of a viable culture being $\geq 85\%$.

2.5.5 Seeding cell culture plates for co-culture experiments

For experimental work, C2BBe1 cells were seeded in 24-well cell culture plates (Corning, USA) at a density of 1×10^5 cells per well. The cells were

grown to > 90% confluency over 5-6 days with the medium replaced every 2-3 days.

2.5.6 C2BBe1 cells co-incubation with *Bacteroides* conditioned media

To investigate the inflammatory potential of bacterial metabolic products from IBD-associated *Bacteroides* species, cell-free conditioned media from *Bacteroides* species were co-incubated with C2BBe1 cells. C2BBe1 cells were seeded in 24-well plates (**section 2.5.5**) and grown to over 90% confluency. To ensure C2BBe1 cells were in the same phase of growth, basal DMEM was replaced with serum-free DMEM 16 hours prior to the start of the experiment. Serum-free DMEM was removed and C2BBe1 cells were exposed to bacterial conditioned media in a 1:1 ratio with supplemented DMEM and incubated for 24 hours at 37 °C with 5% CO_2. The supernatant was subsequently harvested and stored at -80 °C for cyto/chemokine quantification by ELISA and LDH cytotoxicity analysis. The C2BBe1 cells were harvested for RNA isolation (**section 2.6.1**) and gene expression analysis by RT-qPCR (**section 2.6.4**). Growth of conditioned media for the selected IBD-associated *B. fragilis* and *B. vulgatus* and the colitis protective *B. thetaiotaomicron* strains; the gut pathogen *Salmonella typhimurium* (served as a positive control for gut inflammation) and the known commensal *Lactobacillus rhamnoses* GG (served as a negative control for gut inflammation) was performed as **outlined in section 2.1**.

2.5.7 C2BBe1 co-incubation with whole *Bacteroides* cells

A schematic representation in **Figure 2.1** demonstrates the experimental design to elucidate the impact of host-microbe interaction on gut

inflammation and epithelial homeostasis of IBD-associated *Bacteroides* species. After passage, C2BBe1 cells were seeded into 24-well plates (**Section 2.5.5**) and grown to >90% confluency. Basal DMEM was replaced with serum-free DMEM 16 hours before the co-incubation experiment started. Before bacteria were applied to C2BBe1 cells, two wells were trypsinised and CBBe1 cells counted (**Section 2.5.5**), which was used to calculate the volume required to give a 10:1 multiplicity of bacterial infection (MOI) to C2BBe1 cells. Live whole *Bacteroides (B. fragilis*, *B. thetaiotaomicron* and *B. vulgatus*) along with *S. typhimurium* (positive control) and *L. rhamnoses* GG (negative control) were grown to the stationary growth phase (**Section 2.1**), and prior to the co-incubation step, they were centrifuged at 10,000g for 5 minutes, washed with PBS twice, resuspended in serum-free DMEM to 10:1 MOI followed by co-incubation with C2BBe1 cells for 3 hours. Following this, the medium was removed, and cells were washed x3 with PBS and antibiotics (40 mg/L metronidazole for *Bacteroides* and 100 µg/ml penicillin 100U/ml streptomycin for *S. typhi* and LGG). C2BBe1 cells were further incubated for a further 5 hours, in supplemented DMEM medium, to allow stimulated responses to develop. The experiment ended 8 hours after bacterial application and supernatants were harvested for ELISA and LDH assays and cells were harvested for RNA isolation and gene expression analysis.
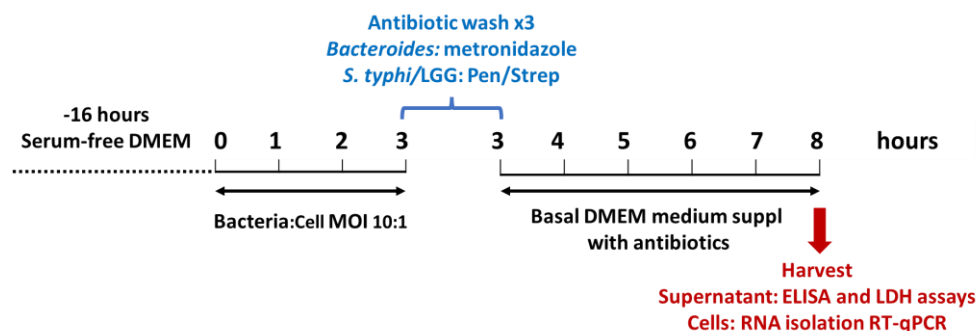
Figure 2.1 Schematic of a co-incubation experiment with Bacteroides and C2BBe1 cells

2.6 RNA isolation and RT-qPCR

2.6.1 RNA Isolation

All RNA isolation was carried out using the RNeasy Mini Kit (Qiagen, Germany). For mouse tissue samples, 30 mg was weighed out and placed in a MagNA lyser tube containing 1.4mm ceramic beads (Roche, Germany) and 400 µl RLT buffer containing 10 µl/mL β-mercaptoethanol (β-ME) (Sigma, Germany). The samples were placed in a MagNA lyser instrument (Roche), centrifuged at 4,000 rpm for 30 seconds, stored on an ice disk for 1 minute, and the procedure was repeated one more time with 5 minutes of centrifugation at max speed (~20,000 g) to pellet any cellular debris. Lysate supernatants were removed to a new 1.5 mL tube and stored at -80° C until use.

For cell lines, RLT buffer with 10 µl/ml β-ME was applied directly to the well (350 µl/well in a 24-well plate), aspirated 10 times and the solution was removed to a 1.5 mL tube and frozen at -80° C until needed.

To the homogenised tissue and cell lysates 1 volume of 70% ethanol (Sigma, Hungary) was added and thoroughly mixed by pipetting. Seven hundred µL of the lysates were transferred to a RNeasy spin column

(Qiagen, Germany) and centrifuged at 10,000g for 30 seconds. The flow-through was discarded and 700 µL of RW1 buffer (Qiagen, Germany) was added to the column and centrifuged at 10,000g for 30 seconds. This flow through was discarded and 500µl of RPE buffer (Qiagen, Germany) was added to the spin column and centrifuged at 10,000g for 30 seconds, with the flow-through discarded. 500 µL of RPE buffer was added to the spin column and centrifuged at 10,000g for 2 minutes, the spin column was moved to a clean 2 mL collecting tube and centrifuged at max speed for 1 minute to ensure the membrane is dry and no RPE is carried forward to the subsequent steps. The dried spin column was placed in a clean 1.5 mL tube and 30 µL of RNAse-free water (Qiagen, Germany) was applied directly to the membrane, followed by centrifugation at 10,000g for 1 minute to elute the RNA. For maximum yield, the elute was reapplied to the membrane and centrifuged at 10,000g for 1 minute.

RNA concentration and quality of the elute were assessed using a NanoDrop™ spectrophotometer (Thermo Fisher Scientific). The NanoDrop™ takes absorbance readings at 230nm, 260nm, and 280nm. High-quality RNA is indicated by an A260/A280 value of between 1.8 - 2.1 and an A260/A230 value of between 2.0 - 2.2 (Imbeaud *et al.*, 2005). Low A260/A230 values can indicate contamination with salt or protein but most commonly guanidine thiocyanate, a salt found in the RNeasy kit lysis buffer (Imbeaud *et al.*, 2005).

2.6.2 DNase treatment

Genomic DNA and reagent removal were performed using the TURBO DNA-*free*™ Kit (Invitrogen, USA). In brief, 0.1 volume of 10X TURBO

DNase buffer and 1 µL of TURBO DNase was added to up to 5 µg of RNA (in 40µL of RNA-free water (Qiagen, Germany)) and mixed gently. Samples were incubated at 37 °C for 25 minutes followed by the addition of 0.1 volume of resuspended DNase Inactivation Reagent and incubation at room temperature for 5 minutes, mixing every minute. Next, samples were centrifuged at 10,000g for 1.5 minutes to pellet the Inactivation Reagent and RNA was removed to a new 1.5 mL tube. RNA purity and concentration were assessed as in **section 2.6.1** and RNA was stored at -80 °C until needed.

2.6.3 cDNA generation

cDNA was synthesised from 500 ng of RNA using Transcriptor Reverse Transcriptase (Roche, Germany), Protector RNase Inhibitor (Roche, Germany), PCR nucleotide mix (Roche, Germany) and random primers (Roche, Germany). A PTC-200 thermal cycler (MJ Research) was used to generate cDNA in four steps. Step 1 – 25 °C for 5 minutes, step 2 – 55 °C for 30 minutes, step 3 – 85 °C for five minutes and then cooled to 4 °C where the volume was brought to 100 µL with the addition of RNase-free water. The cDNA was stored at -20 °C until needed.

2.6.4 qPCR

qPCR was carried out using SensiFAST™ Probe No-ROX (Meridian Bioscience, UK). Primer pairs and probes (outlined in Tables 2.2 (mouse) and 2.3 (human)) were designed using Universal Probe Library (UPL Roche, Germany). All samples were run at least in duplicates, with positive and negative controls for each run, on a LightCycler 480 (Roche). Gene

expression values were calculated using the $2^{-\Delta\Delta Ct}$ method with β-actin as a housekeeper gene (Livak and Schmittgen, 2001). This allows for the calculation of gene expression relative to a stable housekeeper gene. During qPCR, the LC480 measures fluorescence, as more DNA is synthesised by the primers the fluorescent probe is intercalated between the DNA and a higher fluorescence signal is read. This fluorescence must exceed a certain number of cycles to be considered a positive reaction, this is known as the cycle threshold (Ct) and is inversely proportional to the concentration of cDNA in the sample.

Table 2.2 Mouse primers used in this study

Gene Name	Primer R Sequence	Primer L Sequence	Probe No	Function/Marker
B-actin	gtggtacgaccagaggcatac	aaggccaaccgtgaaaa	56	Housekeeper
Cxcl2	ctttggttcttccgttgagg	aaaatcatccaaaagatactgaacaa	26	Inflammatory marker
Ccl20	gtccaattccatcccaaaa	aactgggtgaaaagggctgt	73	Inflammatory marker
Lyz	tctctcaccaccctctttgc	ggcaaaaccccaagatctaa	46	Paneth cells
Chga	aagctgctgtgttgctgct	tcaagacctggctctccaag	3	Chomogranin A
Muc2	agtcacagtcaccgccagt	aaagtgtgccacagcaagct	15	Goblet cells
Vil-1	cagggagatcctctacagacttgt	gagccagattgctgacgag	11	Enterocytes
Zo-1	agcatcagtttcgggtttc	tttgagagcaagccttctgc	4	Tight junction
Lgr5	cagccagctaccaaataggtg	cctcactcggtgcagtgct	60	CBC stem cells
Axin2	tgccagacatcctgtgac	tggagggatgtccagtgc	6	Wnt Signalling
Tcf4	tcgggttcagattcctttctc	agctcctgattctccaccag	43	Wnt Signalling
Smad5	gtactggtgacgtcctgtcg	tgagctcaccaagatgtgtacc	32	BMP Signalling
Smad4	cacagacgggcatagatcac	gagaacattggatggacgact	83	BMP Signalling
Ccnd1	gcgggaagacctcctctt	catccatgcggaaaatcg	68	Proliferation
Hes1	cgcctcttctccatgatagg	acaccggacaaaccaaagac	99	Absorptive cells
Atoh	tctcttctgcaaggtctgatttt	tgcgatctccgagtgagag	69	Secretory cells
Sox9	ctcctccacgaagggtctct	gtacccgcatctgcacaac	66	Paneth cells
Inos	ggctggacttttcactctgc	ggagcctttagacctcaacaga	3	Inflammatory marker
Il-6	ttcatgtactccaggtagctatcg	tgatggtgcaccaaactcg	78	Inflammatory marker
Ifn-y	ttcaagacttcaaaagagtctgagg	atctggaggaactggcaaaa	21	Inflammatory marker
Il-17a	cattgtggagggcagacaat	gattttcagcaaggaatgtgg	34	Inflammatory marker
Stat1	tctgtacgggatcttctgga	gcagcacaacatacg	90	JAK/STAT pathway
Foxp3	tctgaaggcagagtcaggaga	tcaggagcccaccagtaca	78	Treg
Fxr	tccttgatgtattgtctgtctgg	aaagtgttggagaactcaaaatga	63	Bile acid receptor
Vdr	ccccacctggaactttatga	gtggcagccaagactacaaat	1	Bile acid receptor
Rxra	cclgatgagcttgaagaaga	gcgtactgcaaacacaagtac	1	Bile acid receptor
Ostx	ttgaagaaggcgtactggaaa	gctgcccacctctcatactt	3	Bile acid transporter
Ostb	tgcaggtcttctggtgtttct	atcctggcaaacagaaatcg	5	Bile acid transporter
Mrp3	aacagtgtcaacaggccaatta	ttgaactagglagcatcagc	13	Bile acid transporter
Akt7	acctggtgtcagtctcagagg	tcgtgtggcaggatgtgtat	45	Organoid phenotype
Psen7	ggaaggaagctgcagaagtc	tttcctgtgtcctcagctaaca	109	Organoid phenotype
Rxra	cclgatgagcttgaagaaga	gcgtactgcaaacacaagtac	1	Organoid phenotype

Table 2.3 Human primers used in this study

Gene Name	Primer R Sequence	Primer L Sequence	Probe No	Function/Marker
B-ACTIN	cctccatgatgctgcttac	ccagcagagaatggaaagt	11	Housekeeper
IL-8	gagcactccataaggcacaaa	atggttccttccggtggt	72	Inflammatory marker
CCL20	tcaaagttgcttgctgcttc	Gctgctttgatgtcactgct	39	Inflammatory marker
IL-1β	tctttgggtaattttttgggat	tacctgtcctgcgtgtgaa	76	Inflammatory marker
P50	ctcagcaaatcctccaccac	atctgtaccagacgcccttg	47	NF-κB subunit
P65	gatgcgctgactgatagcc	accgctgcatccacagtt	39	NF-κB subunit
IKKα	gccttaaaggtaccgttacc	ccttggaattcggaaact		NF-κB Signalling
CCL5	ctttcgggtgacaaagacg	tgcccacatcaaggagtattt	59	Inflammatory marker
CXCL10	aagaatttgggcccccttg	aaaaggtatgcaatcaaatctgc	26	Inflammatory marker
STAT1	ggattgaaagcatcctagaactca	gatgaagcccatgatgcac	32	JAK/STAT pathway
STAT3	cccttggattgagagtcaaga	aagcggctatactgctggtc	14	JAK/STAT pathway
JAK1	aatggctgtcatggttccaat	tacatcccctcctcgcttc	147	JAK/STAT pathway
JAK2	caggaacaagatgtgaactgtttc	cccatgcagagtctttttcag	52	JAK/STAT pathway
VILLIN	gtcctggccaatccagtagt	actgctacatcatcctggcctatc	71	Enterocytes
KLF4	actttttatgctctggaattataggaa	gcaatcccagtctctccaaa	52	Proliferation/differentiation
AXIN2	gatatccagtgatgcgctga	actgcccacacgataaggag	56	Wnt Signalling
TCF4	cgcgcgggataactatggaaag	ccgacacttctttggagtatttg	35	Wnt Signalling

2.7 ELISA / Meso Scale Discovery

2.7.1 Faecal Calprotectin and chemokine ELISA

Faecal calprotectin levels were assessed in faecal samples collected from wild-type (WT) and IL10-/- mice longitudinally to monitor colitis development by ELISA (R&D Systems). Protein extraction was carried out by resuspending faeces in a PBS/0.1% Tween20 (Sigma, USA) buffer at a concentration of 100 mg/mL and vortexed at max speed for 20 minutes followed by centrifugation at 15,000g for 10 minutes at 4 °C. Clear supernatant was transferred to a sterile 1.5 mL tube and stored at -20 °C until needed. The secretion of the human chemokines IL-8, CCL20, and CXCL10 were performed on supernatants collected from C2BBe1 cells co-cultured with whole bacteria and bacteria conditioned media by using DuoSet ELISA kits (R&D Systems, USA). The ELISA was carried out according to the manufacturer's protocol. In brief, to prepare the ELISA a high-binding 96-well plate (Merk, Germany) was coated with 50 µL of

capture antibody diluted in PBS sealed and left to incubate overnight at room temperature. After incubation, the plate was washed with a PBS/0.05% Tween20 wash buffer 3 times using a plate washer (BioTEK ELx50). Next, the plates were blocked using 150 µL of Reagent Diluent for 2 hours followed by 3 washes with PBS/0.05% Tween20 wash buffer. A 2,000 pg/ml standard was made and a series of 1:1 dilutions were performed to generate a seven point-standard curve (lowest concentration 31.3 pg/mL). Fifty µL of each standard concentration and test samples were added to the plate and incubated for 2 hours at room temperature. The faecal samples were diluted with reagent diluent to 1:4 (due to the high sensitivity of the assay) and supernatant samples were diluted at 1:1. The plates were again washed as described above and 50 µL of the detection antibody (DA, diluted in Reagent Diluent) was added and the plate was incubated for 2 hours at room temperature. Following 3x wash series, 50 µL of Streptavidin-HRP was added to the plates and incubated at room temperature for 20 minutes. A final 3x wash series was performed and 50µl of substrate reagent was added to the plate, the reaction proceeds at room temperature until the standards were developed and quenched using 25 µL of stop solution. The optical density of the samples was determined using a plate reader (BioTEK Synergy2 Gen5 v1.08) set at 450nm.

2.7.2 Meso Scale Discovery Multiplex Assays

A custom 96-well plate assay (Meso Scale Discovery, MSD) containing antibodies for murine IL-1β, IL-6, and mKC was prepared according to the manufacturer's protocols. Briefly, as this is a multiplexed assay, each biotinylated capture antibody must be coupled with a unique linker which

will associate it to a defined spot on the plate. The biotinylated capture antibody for each cyto/chemokine (200 µL) listed above were each individually mixed with their assigned linker (300 µL). These were pooled, diluted up to 6 mL with the stop solution provided by the kit and used to coat the MSD plate (50 µL/well) overnight at 4 °C. The protocol proceeds similarly to the ELISA protocol outlined above (2.7.1) with samples diluted 1:4 with Diluent 41 and analysed in duplicates. Plates were read using an MSD Sector Imager 6000 (Meso Scale Discovery) to assess cytokine and standard concentrations. Range of standards were for IL-1β: 5-20,000 pg/mL, IL-6: 3-10,000 pg/mL, and mKC: 1-22,000pg/mL.

2.8 Small intestinal organoids

The last decade has seen a major jump in our understanding of intestinal stem cells and the advent of intestinal organoids (Sato and Clevers, 2013a). These organoids permit the targeted investigation of signalling pathways that regulate the renewal and lineage determination of the gastrointestinal epithelium.

2.8.1 Crypt Isolation

To generate organoids, crypts were isolated according to Sato et al, with some modifications (Sato and Clevers, 2013a). Briefly, the murine small intestine was dissected, and the distal half (ileum) was placed in a petri dish with ice-cold PBS. The Ileum was cleaned of any mesentery and cut into 4 segments, each flushed with PBS using a 1000 µL pipette. The ileal segments were pinned down and opened longitudinally. A cell scraper (Sarstedt, Germany) was used to gently scrape the tissue to remove mucus

and as many villi as possible. Tissue segments were cut into 5 mm^2 pieces and transferred to a 50 mL Falcon containing 25 mL of ice-cold PBS. The tube containing the intestinal pieces was shaken vigorously for approximately 1 minute, to further clean the tissue and detach the villi and mucosa. Tissue pieces were transferred to a Falcon containing 25 mL of ice-cold PBS and the process was repeated three more times, or until the supernatant remains clear after shaking. Following this, the tissue segments were transferred to a 15 mL Falcon containing 10 mL of Gentle Cell Dissociation Solution (STEMCELL Technologies, UK) and incubated on rollers at room temperature for 15 minutes. The tissue was transferred to 10 mL of ice-cold PBS and shaken gently for 30 seconds, and the supernatant was poured through a 70 µm filter into a Falcon. This process was repeated 3 times with tissue yielding 4 fractions. A 10 µl solution was taken from each fraction and assessed for crypt numbers and minimal tissue debris under a microscope (Olympus CKX31). The fraction with the least number of debris and most crypt enrichment was selected for organoid culture.

2.8.2 Organoid culture

The culture of organoids was performed according to Sato et al, with some modifications (Sato and Clevers, 2013b). Briefly, to develop into 3D organoids, crypts are cultured in a basement membrane extract, BME-2 (Basement membrane extract reduced growth factor, Amsbio, USA). The required volume of the selected crypt fraction (**section 2.8.1**) to be seeded into plates at 500 crypts per well was taken and centrifuged at 200g for 5 minutes at 4 °C. The supernatant was removed and BME-2, 50 µL per well, was added to the tube and the pellet was gently resuspended to avoid air

bubbles. This crypt suspension was added to a prewarmed 24-well plate at 50 μL per well carefully, so it formed a dome. The plate was transferred gently, not to disturb the dome, to a 37 °C incubator for 5 minutes to polymerise the BME-2 and 500μL of Intesticult (Stemcell Technologies, Canada) supplemented with 100 μg/ml penicillin; 100 U/mL streptomycin was added to each well. The crypts were incubated under constant humidity at 37 °C with 5% CO_2 with the medium changed every 3 days and passaged every 7-10 days.

2.8.3 Organoid passage

Organoids reach "maturity" after 7 days following which the lumen starts to fill with dead cells and they require passage (Sato and Clevers, 2013b). To passage mature organoids, the medium was removed from the plates and domes and washed with 500 μL of ice-cold PBS. Plates were placed on ice for 30 minutes, to allow the BME-2 to depolymerise. The domes were then mechanically disrupted using a 1000 μL pipette tip followed by vigorous pipetting with a 200 μL pipette to facilitate sheer forces for mechanical disruption. The remains of the domes were transferred to a 1.5 mL tube and centrifuged at 4 °C for 5 minutes at 500 g. The supernatant was discarded, and the pellet was washed with 500 μL of cold PBS and centrifuged. This step aided in removing as much BME-2 as possible. The crypts are counted, centrifuged, and resuspended in the appropriate amount of BME-2. Depending on the quality of the culture, each well can be split in a 1:2-1:4 ratio according to the seeding protocol in **section 2.8.2**

2.8.4 Organoid fluorescence immunocytochemistry (ICC)

To validate the epithelial cell composition of the small intestinal organoids, immunofluorescence staining was performed. Antibodies used in the study include synaptophysin (enteroendocrine cells), MUC2 (goblet cells) and the tight junction protein Occludin and the adherence junction E-cadherin (details of antibodies are outlined in **Table 2.4**).

Table 2.4 Primary and secondary antibodies used in immunofluorescent cytochemistry of organoids

Antibody	Cell marker	Dilution	Species	Reactivity	Antibody	Dilution	Species	Reactivity
			Primary				Secondary	
Occludin	Apical tight junction	1:50	Conjugated monoclonal antibody	Anti-mouse	-	-	-	-
E-Cadherin	Adherens junction	1:200	Goat	Anti-mouse	AF488	1:1,000	Donkey	Anti-goat
Synaptophysin	Enteroendocrine cells	1:300	Rabbit	Anti-mouse	AF488	1:1,000	Goat	Anti-rabbit
Muc2	Goblet cells	1:300	Rabbit	Anti-mouse	AF488	1:1,000	Goat	Anti-rabbit

The medium was removed from the plates and organoids were fixed in 1 mL of a 4 % paraformaldehyde (Sigma, USA) solution per well for 15 minutes. Fixed organoids were removed to a 1.5 mL tube and centrifuged at 300 g for 5 minutes after which the supernatant was removed, and fixed organoids were washed in PBS, with the wash repeated 4 more times. The fixed organoids were permeabilised in 500 µL 0.2 % Triton-100 solution for 15 minutes, centrifuged at 600g for 5 minutes and washed 5 times with Tris-buffered saline with 0.1% Tween® 20 detergent (TBST, **recipe in table 2.5**).

Table 2.5 TBST recipe

Tris-buffered saline with 0.1% Tween 20 (500ml)	
Tris base	1.21g
NaCl	4.39g
H20	up to 500ml
Tween 20	0.5ml

The fixed organoids were blocked in 500 µL TBST supplemented with 20% FBS for 1 hour, followed by centrifugation and washed in TBST 5 times. Organoids were transferred to 1.5 mL tubes and centrifuged at 300 g for 5 minutes. The supernatant was removed, and primary antibodies (**Table 2.4**) were applied in 20 µL of blocking solution (20% FBS in TBST) and incubated overnight in darkness at 4 °C. The next day, the organoids were centrifuged at 300 g for 5 minutes and washed 5 times with TBST and the supernatant was removed. Secondary antibodies (**Table 2.4**) were applied in 20µL of blocking solution and incubated at room temperature in darkness for 2 hours. Next, the organoids were centrifuged at 300g for 5 minutes and washed 5 times with TSBT. The stained organoids were resuspended in 10

μL of water, to prevent salt crystal formation, and embedded in a drop of mounting medium containing DAPI (nuclear staining) (Invitrogen, USA) on a glass slide (VWR, China). A cover slip (Marienfeld, Germany) was applied, and the slides were left to dry in darkness for 2 hours after which clear varnish was applied to the edges of the coverslip to seal them. The slides were stored at -20 °C until examination under the microscope. An Olympus BX51 WI microscope was used for imaging.

2.8.5 Exposure of developing organoids to *Bacteroides* conditioned media

Intestinal crypts were isolated (**Section 2.8.1**) and seeded into a 24-well plate at a density of 500 crypts per well and allowed to acclimatise to *in vitro* conditions for 24 hours. Fresh media containing a 1:100 and 1:500 dilution of *Bacteroides* conditioned media was applied and removed and replaced every two days. The organoid cultures were visually evaluated by microscopy (EVOS FL) every two days to monitor their growth and viability throughout the experiment. After five days of growth in *Bacteroides* conditioned media the organoids were harvested, as per passage protocol **section 2.8.3**, for RNA isolation and RT-qPCR (**sections 2.6.1 and 2.6.4**)

2.8.6 Developed organoids challenged with *B. vulgatus* conditioned media

Organoids were cultured in Intesticult as per **section 2.8.2** with *B. vulgatus* conditioned media applied in a 1:20 dilution acutely twenty-four hours before the end of the experiment i.e., on day 6. Harvesting of cells for RNA isolation and RT-qPCR was performed as above.

2.9 Mice

IL-10$^{-/-}$ mice (B6.129P2-Il10tm1Cgn/J) were ordered from Charles River Laboratories, UK and bred as homozygotes at the Biosciences unit Annex at University College Cork. Male C57BL/6OlaHsD mice (22-25 g) acquired from Envigo (UK) and were acclimatised for at least two weeks before entering the study. All animals were housed in individually ventilated cages (IVCs), (OptiMICE) and given food and water *ad libitum*. Mice were sacrificed by cervical dislocation. Animal husbandry and experimental procedures were approved by the University College Cork ethics committee (AEEC2015-016) and Health Product Regulatory Authority (HPRA, project nr AE19130/P054).

2.10 Initial characterisation of disease progression in IL-10$^{-/-}$ mice

To assess the disease progression and inflammatory profile of the IL10$^{-/-}$ colony recently established in our animal facility, a longitudinal study was designed. Mice were divided into six groups, five IL10$^{-/-}$ mouse groups and one group of wild-type mice. Mice were housed under standard conditions and culled at various ages to assess the progression of colitis in the IL10$^{-/-}$ mice. Group 1: mice at 6 weeks old (n = 8), Group 2: mice at 9-10 weeks old (n = 8), Group 3: mice at 13 weeks (n = 10), Group 4: mice at 16 weeks (n = 8), and Group 5: mice at 19 weeks (n = 7). Group 6 was comprised of wild-type mice, aged 9-13 weeks, (n=6), and were used as a control. On the cull days, mice were weighed and scored for disease activity, faeces were also collected and scored, and tissues were harvested as in **section 2.13** for downstream processing.

2.11 IBD-associated *Bacteroides* species colonisation in C57BL/6 wild-type mice

To assess the impact of oral gavage with Crohn's disease associated *Bacteroides* species in wild-type mice, a study was designed as outlined in **Figure 2.2**. C57BL/6 mice were divided into four groups; Group 1 Control, Group 2 Antibiotic treated, Group 3 Antibiotic treated with *B. vulgatus* oral gavage, Group 4 Antibiotic treated with *B. fragilis* oral gavage and housed in IVCs. n = 10 mice per group in all groups except Group 1, n=5.
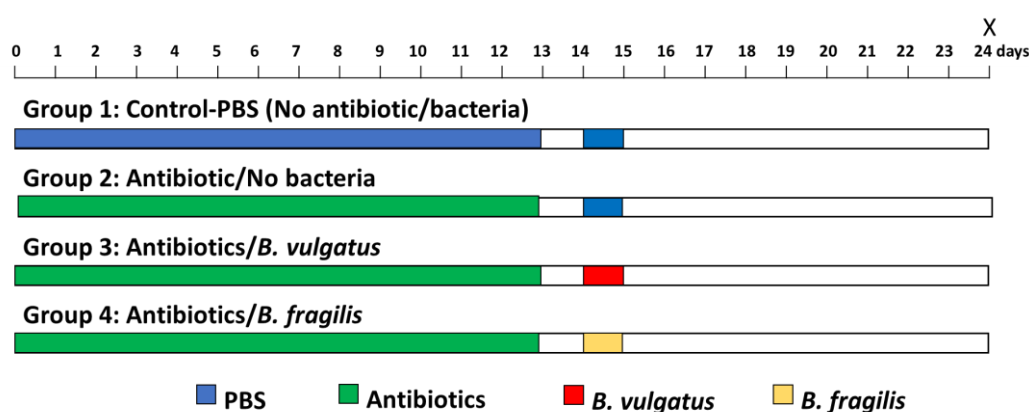
Figure 2.2 Schematic of study design in C57BL/6 wild type mice, to determine the metabolome and inflammatory modulating potential of the CD associated strains Bacteroides fragilis and Bacteroides vulgatus. Mice were treated with an antibiotic cocktail (metronidazole 10mg/ml, vancomycin 5mg/ml, neomycin 5mg/ml and amphotericin B 0.1mg/ml), or vehicle (PBS), for 13 days via oral gavage and by ampicillin (1,000mg/L) added to their drinking water followed by oral gavage of $1x10^9$ cfu/200µl of B. fragilis or B. vulgatus, or vehicle, for 2 consecutive days. Group 1 received no antibiotics or bacteria but received sham PBS oral gavage; Group 2 received antibiotics for 13 days followed by sham PBS oral gavage in lieu of Bacteroides spp; Group 3 received antibiotics for 13 days followed by oral gavage of B. fragilis; Group 4 received antibiotics for 13 days followed by oral gavage of B. vulgatus. During antibiotic treatment mice weights were recorded every 4 days. Animals were euthanised at day 24 post start and fluids, faecal, caecal, and intestinal samples collected.

To clear a niche for *Bacteroides* colonisation, Groups 2-4 were administered an antibiotic cocktail (**Table 2.6**) by oral gavage and in drinking water (Ampicillin) for 13 days. On day 0, Groups 2-4 received the antibiotic cocktail whereas the control Group 1 received PBS as vehicle control. Oral gavage

was performed without anaesthesia, using hand restraint. A ball-tipped, 20-gauge, gastric feeding needle was inserted through the mouth into the stomach where 100 µL of PBS/antibiotic cocktail was administered to the mice. Body weight was assessed every four days throughout antibiotic treatment to monitor for adverse effects of the antibiotics.

Table 2.6 Antibiotic cocktail used to reduce bacteria abundance in mice

Antibiotic Cocktail	Concentration / Mode of delivery/daily
Ampicillin	1000mg/L In drinking water
Metronidazole	10mg/ml oral gavage
Vancomycin	5mg/ml oral gavage
Neomycin	5mg/ml oral gavage
Amphotericin B	0.1mg/ml oral gavage

Following 13 days of PBS/antibiotic cocktail, the mice were rested for a day to allow the antibiotics to clear from their system. On days 14 and 15, mice in Groups 1 and 2 received PBS gavage while Groups 3 and 4 received oral gavage with *B. vulgatus* and *B. fragilis,* respectively. The trial continued for another nine days, and the mice were culled on day 24 of the trial. On the day of culling, faeces were collected for bile acid analysis and tissues were collected as in **section 2.13** for downstream analysis.

2.12 Colonisation of *Bacteroides vulgatus* to IL-10$^{-/-}$ mice and disease progression

To assess the effect of *B. vulgatus* on colitis progression, microbiota, and bile acid composition in IL10$^{-/-}$ mice a study was designed as illustrated in **Figure 2.3**.
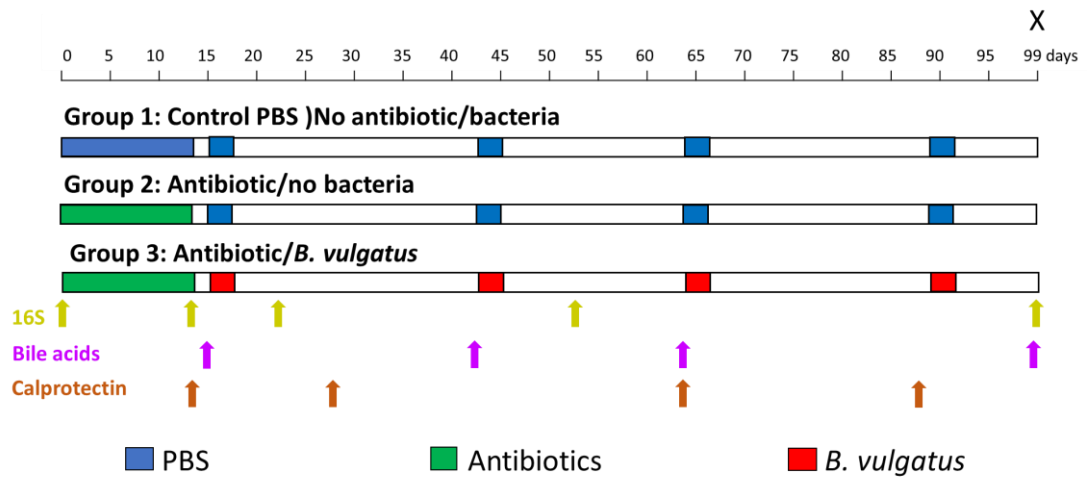
Figure 2.3 Schematic design of IL10^{-/-} mice depleted of microbiota by full spectrum antibiotic treatment followed by colonisation of the IBD associated Bacteroides vulgatus to determine its microbial, metabolome and inflammatory modulating potential. IL10^{-/-} mice were treated with an antibiotic cocktail or vehicle (PBS) as described in Figure 2.2, or vehicle (PBS), for 13 days via oral gavage followed by oral gavage of $1x10^9$ cfu/200µl B. vulgatus, or vehicle (PBS), for 3 consecutive days, Oral gavage of B. vulgatus and PBS was repeated 3 times every 3-4 weeks (at days 15, 42, 64, 87). Group 1 received no antibiotics or bacteria but received sham PBS oral gavage. Group 2 received antibiotics for 13 days followed by sham PBS oral gavage in lieu of B. vulgatus. Group 3 received antibiotics for 13 days followed by oral gavage of B. vulgatus. During antibiotic treatment mouse weights were recorded every 4 days and every second day following that. Arrows indicate faeces collection for 16S analysis (gold arrows), bile acid analysis (purple arrow) and Calprotectin analysis (brown arrow). Animals were euthanised at day 99 post start and fluids, faecal, caecal and intestinal samples collected.

Thirty male IL10^{-/-} mice, aged between 9-11 weeks at the start of the study, were randomised into three groups, control (PBS), antibiotic cocktail and B. vulgatus. Mice received an antibiotic cocktail (metronidazole 10mg/ml, vancomycin 5mg/ml, neomycin 5mg/ml and amphotericin B 0.1mg/ml) for 13 days via oral gavage and in drinking water (ampicillin 1g/L) followed by oral gavage of $1x10^9$ cfu/200µl *B. vulgatus*, or vehicle (PBS), for 3 consecutive days, followed by three days gavage of PBS/*B. vulgatus* every 3-4 weeks (at days 15, 42, 64, 87). Group 1 sham PBS oral gavage; Group 2 received antibiotics for 13 days followed by sham PBS oral gavage in lieu of *B. vulgatus* and Group 3 received antibiotics for 13 days followed by oral gavage of *B. vulgatus*. During antibiotic treatment, mouse weights were

recorded every 4 days and every second day following that. Each group consisted of 5 males and 5 females. During the study, faeces were collected for 16S rRNA analysis, bile acid analysis and Calprotectin. Animals were euthanised at day 99 post start and fluids, faecal, caecal, and intestinal samples were collected and stored at -80°C.

2.13 Dissection and collection of tissue and fluids

At the end of the trials (day 24 – wild type and day 99 – IL10$^{-/-}$), animals were sacrificed by concussion followed by cervical dislocation. Colons were removed from the anus to the caecum and opened longitudinally. The colon was washed in cold PBS, length recorded, divided in the proximal and distal colon and weights recorded. A 0.5 cm piece was removed from the proximal colon and stored in RNAlater at +4°C for 24 hours followed by freezing and storage at -80 °C for further RNA isolation and RT-qPCR. The remaining proximal colon was trimmed to 3 cm in length and divided into two sections longitudinally. One section was rolled (Swizz roll), embedded in optimum cutting temperature (OCT) compound and snap frozen in liquid nitrogen for histological analysis. The other section was snap frozen in a 1.5 mL tube for protein analysis by ELISA and MSD (see **section 2.7**). The caecum and spleen were removed and weighed, and faeces were collected for bile acid analysis, calprotectin ELISA, and 16S rRNA gene analysis. Gall bladders were also carefully dissected using a string loop and snap frozen in liquid nitrogen. Following all tissue collecting snap frozen samples were transferred to -80 °C for storage until needed. The colon segment retained for MSD analysis was weighed and placed into a green-capped MagnaLyser tube (Roche) containing beads. 500μl homogenisation solution

was added to each tube. Each sample was subject to 3 rounds of homogenisation using a MagnaLyser at 6,000rpm for 15 seconds, and placed on ice for 30 seconds between each round followed by centrifugation at 10,000g for 10 minutes at 4˚C. Transfer over the supernatants/homogenates (with no tissue pieces) and aliquot into fresh 1.5ml tubes and store at -80˚C until use.

2.14 Sample preparation for bile acids

To extract bile acids from the gall bladder 2 µL of bile was pipetted into a 1.5 mL tube. To this 15 µL of deuterated standards, cholic acid D4 (d_4 CA) and chenodeoxycholic acid D4 (d_4 CDCA) (CDN Isotopes, Canada), were added with a final concentration of 5 ng/ml. Next, 200 µL ice-cold 50% methanol was added, and the tube was mixed by vortexing for 1 minute and incubated at -20 °C for 30 minutes and centrifuged at 10,000 g for 10 minutes. The supernatant was transferred to a 1.5 mL tube for further processing.

For extracting bile acids from murine faeces, 25 mg of the sample was weighed out and added to MagNA lyser tubes containing 900 µL ice-cold 50% methanol and 15 µL deuterated standards (final concentration 5 ng/ml) and placed in the MagNA lyser. Samples were run at 6,000 rpm for 30 seconds after which the samples were removed to an ice disk to cool for 1 minute, a process repeated another 2 times. The samples were centrifuged at 10,000 g for 10 minutes and the supernatant was transferred to a 1.5 mL tube for further processing.

The supernatants from both gall bladder and faeces were vacuum-dried under nitrogen at 45 °C for 3 hours. Next, 1 mL of ice-cold 5% formic acid

was added and vortexed for 1 minute followed by gentle agitation in a vortex for 1 hour at room temperature. The samples were centrifuged at 10,000g for 10 minutes, and the supernatant was transferred to 1.5 mL tubes and dried under vacuum for 3 hours. The sample extracts were then reconstituted in 150 µL ice-cold 50% methanol and centrifuged at 10,000 g for 5 minutes. The supernatants, containing the extracted bile acids, were transferred to glass vials (Waters Ltd.) ready for Ultra Performance Liquid Chromatography Mass Spectrometry (UPLC-MS) analysis.

2.14.1 Preparation of bile acids for standard curve generation

A standard bile acid stock was prepared as a 1 mg/ml solution and diluted in 50% methanol to give 10 standard solutions with a final volume of 150 µL for each standard. The standard curve generated from these stocks allowed for measuring extraction efficiency and normalisation of samples.

2.14.2 Ultra-Performance Liquid Chromatography-Tandem Mass Spectrometry (UPLC -TMS) for bile acid quantification

UPLC -TMS was performed to measure bile acid concentration in faecal and gall bladder samples using a protocol from (Joyce, MacSharry, *et al.*, 2014b) with samples being injected in triplicates. In brief, 5µL of bile acid extract was injected onto a 50mm T3 Acquity column (Waters Corp.) and eluted using a 20-min gradient of 100% A to 100% B (A, water, 0.1% formic acid; B, methanol, 0.1% formic acid) at a flow rate of 400 µL/min and column temperature of 50 °C. Samples were analysed using an Acquity UPLC system (Waters Ltd.) coupled online to an LCT Premier mass spectrometer (Waters MS Technologies Ltd.) in negative electrospray mode with a scan

range of 50–1,000 m/z. Bile acids ionise strongly in negative mode, producing a prominent [M-H]- ion. The capillary voltage was 2.4 kV, sampling cone 35 V, desolvation temperature 350 °C, source temperature 120°C and desolvation gas flow was 900L/h. MassLynx and TargetLynx™ software were used for the processing and quantitation of bile acids. Standard curves were generated and used to identify, quantify, and normalise analytes based on their properties of mass and retention time. TargetLynx™ (Waters Ltd.) software was used for all sample data processing and quantitation of analytes against the standard curve.

2.15 Isolation of bacterial DNA from faeces

To investigate how the murine microbiota changes over time post *Bacteroides* gavage, faecal samples were collected at different time points throughout the trial (**Figure 2.3**), bacterial DNA was isolated and 16S rRNA sequencing was performed for microbiota composition.

Bacterial DNA was isolated using the QIAamp Fast DNA Stool Mini Kit (QIAGEN, Germany) according to the manufacturer's specification except for using a bead-beater instead of a vortex for faecal homogenisation, outlined in brief below. Fifty mg of faeces was weighed and placed in a sterile 2 mL tube containing one 5 mm glass bead, a small spatula spoon of 1mm zirconium beads and 0.1mm glass beads. To lyse bacteria in the faeces, 1ml of InhibitEX (Qiagen, Germany) buffer was added and the tubes were subjected to bead beating for 30 seconds, followed by 1 minute on ice, with the procedure repeated 2-3 times. To aid in the lysis of Gram-positive bacteria the suspension was heated to 95 °C for 5 minutes, vortexed for 15 seconds and centrifuged at 16,000 g for 1 minute. Fifteen µL of proteinase

K was pipetted to 200 μL of supernatant and 200 μL of AL buffer (Qiagen, Germany) and vortex for 15 seconds. The tubes were incubated at 70 °C for 10 minutes, 200 μL 96-100% ethanol was added, and tubes were mixed by inverting. The lysate was transferred to a QIAamp spin column (Qiagen, Germany) and centrifuged at 16,100 g for 1 minute. The column was placed in a collecting tube and 500 μL of AW1 buffer was added and centrifuged at 16,100 g for 1 minute. This process was repeated once using AW2 buffer and the spin column was transferred to a sterile 1.5 mL tube. Following this, 200 μL of ATE buffer was pipetted onto the spin column membrane and incubated at room temperature for 7 minutes followed by centrifugation at 16,100g for 1 minute. The concentration and quality of the DNA was assessed using a Qubit Fluorometric Quantification (Thermo Fischer Scientific).

2.16 16S rRNA gene sequencing

The 16S rRNA gene sequencing was conducted by Dr Fiona Crispie at Teagasc Food Research Centre as previously described in (Ryan *et al.*, 2020)

2.17 16S rRNA gene analysis

Data were analysed similarly to those previously described (Ryan *et al.*, 2020). Briefly, for all sequence data, the quality of the raw reads was visualized with FastQC v0.11.3 followed by read trimming and filtering with Trimmomatic v0.36 to ensure at least an average quality of 25 and a minimum length of 50 bases after adapter removal, with the reads for 16S rRNA being further filtered following merging of forward and reverse reads.

The reads were then imported into R v4.1.0 for analysis with the DADA2 package v1.10.1. Quality filtering and trimming were performed on both forward and reverse reads with reads only retained when both were of sufficient quality. DADA2 error correction was carried out on each forward and reverse reads separately and subsequently merged before chimaeras were removed from the retained high-quality merged reads of at least 340 nucleotides. The resulting unique (as opposed to reads clustered into operational taxonomic units) and error-corrected ribosomal sequence variants (RSVs) were exported, and further chimaera filtered using a reference-based chimaera filtering implemented in USEARCH v8.1.1861 with the Chimera-Slayer gold database v20110519. The non-chimeric RSVs were subsequently assigned in Mothur v.1.39.5 with the SILVA database v132 with a bootstrap cut-off of 80% to species level wherever possible. 69.74% of the reads survived, and 2 samples had to be excluded due to low read numbers with 48550 ± 7256 reads per sample on average. After removing unclassified eukaryota, chloroplasts and mitochondria 7077 ASVs remained. Multivariate testing for differences in composition was performed via HMP using the *HMP_2.0.1* package in R. Alpha diversity and Bray-Curtis distances was generated using *phyloseq v1.16.2* with statistical significance calculated using Kruskal-Wallis and Mann-Whitney U tests used for alpha diversity. Principal coordinate analysis on Bray-Curtis distances were calculated on all ASVs present in at least 5% of samples using the *vegan* package in R. Beta-diversity significance testing was carried out using PERMANOVA. Differential taxonomic abundances were calculated using the *ALDEx3* package in R, where an effect size of absolute 1 and an

adjusted p value of 0.05 were deemed significantly differentially abundant genera. All statistical analysis was carried out in R v4.1.0. Reported p-values throughout were subjected to Benjamini–Hochberg correction for multiple testing.

2.18 Statistical analysis

Excluding analysis in **section 2.17**, statistical analysis was carried out using GraphPad Priam for Windows (V8.0; GraphPad Software, San Diego, CA). Data are plotted as means with standard deviation (SD). Differences between two groups were assessed using an unpaired Students *t*-test (two-tailed). Differences between three or more groups were calculated using one-way analysis of variance (ANOVA with Dunnett's post-hoc test unless otherwise stated. Results were considered statistically significant when $p < 0.05$. Where, ns = no significance, * = $p < 0.05$, ** = $p < 0.01$, *** = $p < 0.001$, and **** = $p < 0.0001$.

Chapter 3 Effect of *Bacteroides* species on inflammation and homeostasis in gastrointestinal epithelium, *in vitro and in vivo*

3.1 Abstract

Crohn's disease (CD) is a chronic inflammatory condition of unknown aetiology, although the microbiota appears to be a major contributor to the disease. In a recently published study (Ryan et al.) we showed an increased abundance of *Bacteroides fragilis* in inflamed colon biopsies from patients with CD, from an Irish IBD-cohort. *Bacteroides vulgatus* was also seen enriched in biopsies from participants associated with lower microbiota diversity. This study aims to identify mechanisms regulated by *Bacteroides* species and their relevance to CD-pathogenesis. Human colon epithelial cells (C2BBe1) are exposed to whole *Bacteroides* cells and conditioned media followed by viability (LDH), gene expression (RT-qPCR) and cytokine analysis (ELISA). Murine intestinal organoids were differentiated in media supplemented with *Bacteroides* conditioned media followed by an analysis of epithelial differentiation genes, Wnt/β-catenin and BMP pathways. Antibiotic-depleted-microbiota wild-type mice were orally gavaged with *B. fragilis* and *B. vulgatus* and colon samples were collected 2 weeks later for gene expression analysis. Culturing of C2BBe1 cells with whole Bacteroides species and their conditioned media resulted in the induction of pro-inflammatory chemokines (IL-8, CCL20, CXCL10) and genes belonging to the NF-kB and JAK/STAT pathways. *B. vulgatus* presented the most pro-inflammatory potential. Bacteroides conditioned media had a low impact on organoid development and on pro-inflammatory chemokine gene expression. Bacteroides conditioned media altered the expression of genes associated with the BMP-pathway (Smad4 and 5), Wnt/β-catenin pathway (Axin2) and Paneth cells (lysozyme and SOX9), potentially affecting

epithelial cell proliferation and maturation. Colonisation of wild-type mice with *B. vulgatus* or *B. fragilis* mildly increased the colon weight but did not significantly change gene expression of cytokines, epithelial cell subsets and BMP- Wnt/β-catenin pathways. In summary, our data indicate that Bacteroides spp and their metabolites has a significant impact on epithelial cells' inflammatory response, cell proliferation and differentiation, which was not corroborated in Bacteroides' colonised wild-type mice. Collectively, these data indicate the potential of certain Bacteroides species in driving inflammation under specific conditions.

3.2 Introduction

Crohn's disease (CD) is a chronic inflammatory bowel disease characterised by patch-wise transmural ileocolonic inflammation with unknown aetiology. In the last 15 years, genome-wide association studies have identified that defects in genes related to luminal environment sensing (NOD2) and host response to microbes (ATG16L1) convey the largest risk pathogenesis. Indeed, the gut microbiota of patients with CD displays decreased diversity and greater instability than a healthy gut (Sartor, 2008; Sokol and Seksik, 2010). In CD, the gut microbiota shows a decrease in the phyla *Firmicutes* and *Bacteroidetes* with a concomitant increase in the phylum *Proteobacteria* representing a decrease in beneficial bacteria and an expansion of pathobionts (Sokol and Seksik, 2010). This decrease in beneficial bacteria and increase in pathobionts, termed dysbiosis, is a key component in inducing/maintaining gut inflammation. The inflammation seen in CD is often characterised by the presence of the pro-inflammatory cytokines TNF, IFNγ, IL-1β, IL-6, and IL-17a (De Souza and Fiocchi, 2015). The NF-κB pathway, described in **section 1.5.4.3**, is a key regulator of inflammatory responses in the gut, with its over-activation associated with greater epithelial damage in CD (Han *et al.*, 2017). A large range of stimuli can activate NF-κB signalling, including responses to bacterial antigens through PRRs, TNFRs, and TCRs (Liu *et al.*, 2017). NF-κB signalling regulates the expression of a large array of inflammatory chemokines, including epithelial chemokines IL-8/CXCL10 (Lee *et al.*, 2005), a potent chemoattractant for neutrophils initiating bone marrow egression, extravasation, and mucosal migration and aiding respiratory burst and

neutrophil degranulation (Cotton *et al.*, 2016) and chemokine (C-C motif) ligand 20 (CCL20)/MIP3a (Fujiie *et al.*, 2001), a susceptibility gene for CD development (Skovdahl *et al.*, 2015) and a ligand for the chemokine receptor 6 (CCR6), which is expressed on dendritic (DCs), B-, Treg- and Th17 cells (Skovdahl *et al.*, 2015) and thus a chemoattractant for these cells. Both these chemokines are elevated in CD (Daig *et al.*, 1996; Kaser *et al.*, 2004). Another cytokine produced by epithelial cells due to TLR-activation is IL-1β, which is a key mediator of the inflammatory response in CD and can also be regulated by the NF-kB pathway (Ligumsky, 1990; Coccia *et al.*, 2012).

The JAK/STAT pathway, described in **section 1.5.4.3,** has been identified as a viable target in the treatment of CD (Salas *et al.*, 2020). Cytokines and growth factors predominantly activate JAK/STAT signalling, but recent evidence suggests it can also be activated by LPS indicating a role for Gram-negative bacteria in JAK/STAT signalling (L. Fu *et al.*, 2016). Activation of this pathway induces/represses the expression of a plethora of genes, including epithelial chemokines such as chemokine C-X-C motif ligand 10 (CXCL10/IP-10) and CCL5/RANTES. Both chemokines are induced by IFN-γ after binding to their receptor, CXCL10-CXCR3 and CCL5-CCR1,-3,-5, are chemoattractants of Th1 cells to the gut (Dwinell *et al.*, 2001) (Wadwa *et al.*, 2016) (Lee *et al.*, 2008) (Oki *et al.*, 2005) and are increased in patients with CD (Mazzucchelli *et al.*, 1996; Ansari *et al.*, 2006; Østvik *et al.*, 2013; Singh *et al.*, 2016).

In addition to possessing a dysbiotic gut microbiota and a dysregulated immune response to gut luminal antigens, CD patients also exhibit a

disrupted gastrointestinal epithelial barrier (Ma, 1997). The cytokines TNF-α and IFN-γ have been shown to disrupt the epithelial barrier by altering tight junction (TJ) proteins (Li *et al.*, 2008). This barrier disruption leads to increased penetration of luminal bacteria to the mucosa and activation/exacerbation of inflammation. Indeed, disruption of proteins involved in epithelial barrier maintenance is common in CD and intestinal inflammation. The pore-forming protein Claudin-2, responsible for increasing barrier permeability, displays increased expression in active CD (Zeissig *et al.*, 2007). E-cadherin, coded for by the CDH1 gene, a protein found in adherens junctions, plays a pivotal role in cell-cell adhesion in the gut epithelium and is vital in the regulation of the epithelial barrier (Schnoor, 2015). Mutations in the CDH1 gene were identified as a risk factor for developing CD (Muise *et al.*, 2009b). Occludin, a TJ-associated protein, and zona occludens (ZO)1, a TJ-scaffold protein, are vital in forming apical tight junctions, with impaired phosphorylation of these proteins leading to the development of spontaneous colitis in mice (Resta-Lenert, Smitham and Barrett, 2005).

Further to acting as a physical barrier, the gut epithelium comprises multiple cell types (i.e., enterocytes, goblet cells, enteroendocrine cells, Paneth cells, tuft cells, and M cells), which constantly self-renew and shed into the lumen. These cells are responsible for nutrient absorption, mucus production, hormone secretion, anti-microbial peptide secretion and coordination of innate and adaptive immune responses to the gut microbiota. The last decade has seen a major increase in our understanding of intestinal stem cells and the advent of intestinal organoids (Sato and

Clevers, 2013a). These organoids permit the targeted investigation of signalling pathways that regulate the renewal and lineage determination of the GIT epithelium. The intestinal epithelium has a very high "turn-over" rate, with the entire epithelium being replaced every 3-5 days. This high replication rate is accomplished via stem cells that reside at the base of the intestinal crypt and this proliferation is coordinated through the Wnt/β-catenin pathway. Two relevant proteins regulated by the Wnt/β-catenin pathway are Axin2 and T cell factor family 4 (Tcf4). Axin 2 is a component of the destruction complex that breaks down β-catenin and prevents its translocation to the nucleus and activation of downstream genes (Jho *et al.*, 2002). T cell factor family 4 (Tcf4) is a DNA binding protein that is one of the primary downstream effectors of the Wnt pathway. Previously thought to only be involved in embryogenesis it has been identified as essential in intestinal epithelial homeostasis (van Es *et al.*, 2012).

As previously stated, the gut microbiota of patients with CD is broadly characterised by a decrease in the phyla *Firmicutes* and *Bacteroidetes*, with an increase in *Proteobacteria*. Species from the genus *Bacteroides* constitute 50-80% of the *Bacteroidetes* component of the gut microbiome, and consensus in the literature is lacking regarding the involvement of *Bacteroides* in CD pathology, as highlighted recently in a systematic review (Aldars-García, Chaparro and Gisbert, 2021). A meta-analysis by Zhou and co-authors identified that, in general, lower levels of *Bacteroides* are associated with CD (Zhou and Zhi, 2016a). However, they observed disparate results depending on the technique used to quantify bacteria levels. Studies utilising RT-qPCR demonstrated lower levels of *Bacteroides*

in CD vs healthy controls, while studies using conventional culture methods and Fluorescence *in-situ* hybridisation (FISH) identified higher levels of *Bacteroides* in CD vs healthy controls. However, Zhou et al. ascribed this disparity to different ethnicities in the studies. Recently published data from our group (Ryan *et al.*, 2020) reporting the colonic microbiota from matched inflamed and non-inflamed mucosa of an Irish IBD cohort identified higher abundances of *Bacteroides* in IBD. The study revealed that *Bacteroides fragilis* was more abundant in inflamed CD mucosa vs healthy controls and that *Bacteroides vulgatus* was in high abundance in a cluster of predominantly IBD patients and was associated with lower diversity and inflammation.

In this chapter, we hypothesized that *B. fragilis* and *B. vulgatus* strains harbour a pro-inflammatory potential relevant to the pathogenesis of Crohn's disease and assessed their impact on epithelial homeostasis and inflammatory potential in *in vitro* cell systems and *in vivo*. To accomplish this, we investigated gene expression in a human (C2BBe1) colonic cell line following exposure to bacterial metabolites or whole live bacteria and assayed for genes related to inflammation and epithelial homeostasis along with measuring cytokine production. To confirm the findings from the cell line, a primary cell system, i.e., a small intestinal organoid model was utilised. This allowed targeted investigation of the pathways involved in epithelial maintenance and lineage determination in an *ex-vivo* physiologically relevant epithelial cell model. Finally, we investigated the impact of *Bacteroides* colonisation on healthy wild-type mice and their impact on inflammation and epithelial homeostasis.

3.3 Results

3.3.1 Determination of optimal bacterial growth phase

The literature points to two phases of secretion for bacteria where activity and metabolite production is differentially represented during the exponential phase and the stationary phase (Tashiro *et al*., 2010). Therefore, growth timepoints to best represent bacterial secretion, including both primary and secondary metabolites and proteins, were first determined by examining the growth and the relative OD_{600} over time. Bacterial strains were cultured from single colonies in their respective media (**Section 2.1**) and their growth dynamics were monitored with OD_{600} over time. Optimal culture periods were determined as between 8-10 hours for representative *Bacteroides* species/strains associated with CD, at 7 hours post inoculation for the gut pathogen *Salmonella enterica* serovar Typhimurium (*S. typhimurium*) and 10 hours for the commensal and probiotic strain, *Lactobacillus rhamnosus* GG (*L. rhamnosus* GG) (**Figure 3.1 a-e**). These time frames were applied to generate bacteria conditioned media in both, late exponential and stationary phases of growth reported in **Table 3.1**. Twenty hours post inoculation was taken along with media controls for harvest to represent stationary phase conditioned media and stored at -20°C before use.
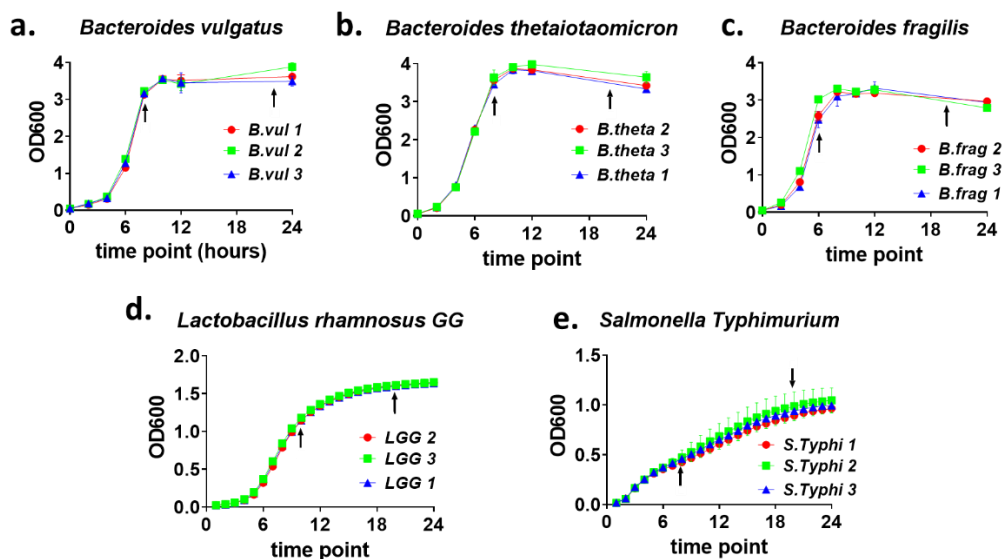
Figure 3.1 Bacterial growth curves. Bacterial growth assessed over 24 hours for (a) Bacteroides vulgatus (B. vul), (b) Bacteroides thetaiotaomicron (B. theta), (c) Bacteroides fragilis (B. frag), (d) Lactobacillus rhamnosus GG (LGG), (e) Salmonella enterica serovar Typhimurium (S. typhi). Arrows indicate late exponential and stationary phases of growth for bacteria conditioned media harvest Error bars represent the mean ± standard deviation (SD) from the mean in triplicate experiments from three independent experiments.

Table 3.1 Table of bacterial OD600 values for supernatant harvest at exponential and stationary phases of growth.

Bacteria	OD600	
	Exponential	Stationary
Bacteroides thetaiotaomicron	3.0	3.3
Bacteroides fragilis	2.5	3.0
Bacteroides vulgatus	3.0	3.5
Lactobacillus rhamnosus GG	3.0	6.0
Salmonella enterica serovar Typhimurium 4/74	0.5	0.9

3.3.2 *Bacteroides* species bacteria conditioned media reduces the viability of human epithelial cells

To evaluate whether bacteria conditioned media from *Bacteroides* species and control species collected from stationary and exponential phase of growth affected the viability of C2BBe1 cells an LDH cytotoxicity assay was carried out (**Figure 3.2 a**). This demonstrated that bacteria conditioned media, from the stationary phase of growth, in all *Bacteroides* species significantly decreased C2BBe1 viability by ~10% relative to medium control and *B. thetaiotaomicron* at exponential phase. *S. typhimurium* conditioned media did not alter cell viability while *L. rhamnosus* GG conditioned media from both growth phases significantly increased cell viability relative to medium control (**Figure 3.2 b**).
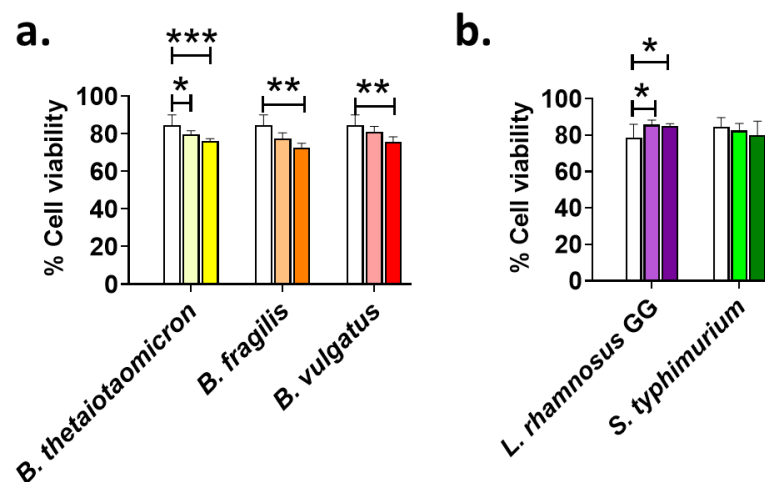

Figure 3.2 Assessment of bacterial conditioned media impact on C2BBe1 cell viability. Cell viability was calculated using an LDH cytotoxicity assay and subtracting this value from 100 and expressed as % viability. (a) C2BBe1 cells co-cultured with Bacteroides spp conditioned media. (b)C2BBe1 cells co-cultured with control bacteria species conditioned media. The light colour of the column designates the bacteria conditioned media collected at the exponential growth phase, the solid colour denotes the bacteria conditioned media collected at the stationary growth phase and the white colour denotes the medium control. Data presented as mean ± SD, n = 3 individual experiments from pooled triplicates. Statistical significance was calculated for each individual bacteria species by one-way ANOVA with Dunnett post-hoc test, with media control as the control column. *, ** and *** denote p < 0.05, 0.01 and 0.001, respectively.

3.3.3 Strain-dependent impact on homeostatic and inflammatory markers provoked by conditioned media derived from CD-associated Bacteroides species

Colonic C2BBe1 cells are reported as responsive to commensals, pathobionts, and their metabolites/products (Groman, 2009). To determine the influence of microbially secreted components, from different growth phases, C2BBe1 cells were exposed independently to conditioned media and media controls following the growth of Bacteroides species (*B. vulgatus, B. thetaiotaomicron* and *B. fragilis*) (**Section 2.5.6**) and control bacteria (the commensal *L. rhamnosus* GG and the enteric *pathogen S. typhimurium*). In brief, cell exposure to conditioned media (1:1 ratio, conditioned media: cell culture medium) was for 24 hours, followed by RNA isolation for gene expression analysis by qPCR (**Section 2.6.1 and 2.6.4**). Of particular interest were epithelial-derived inflammatory cytokines/chemokines and their associated pathways associated with CD-pathology including IL-8/CCL20/IL-1β and NF-κB pathway (p50, p65, IKKa); CXCL10/CCL5 and JAK/STAT pathway (STAT1, STAT3, JAK1 and JAK2), as well as genes related to epithelial homeostasis (E-cadherin-CDH1, villin and Klf4), all assessed via RT-qPCR (**Table 2.4, Section 2.6.4**). C2BBe1 cell supernatant was also harvested with and without respective bacterial conditioned media and media controls to assess cytokine/chemokine production via ELISA. The data, summarised in **Table 3.2**, and described below, represents species-dependent, media-independent differences supporting differential responses by these colonic epithelial cells in terms of gut health.

Table 3.2 Summary table of genes significantly altered upon co-culture of C2BBe1 cells with conditioned media of Bacteroides, and control bacteria species, collected from the exponential and stationary phases of growth

	Gene	B. thetaiotaomicron		B. fragilis		B. vulgatus		L. rhamnosus GG		S. typhimurium	
		Exponential	Stationary	Exponential	Stationary	Exponential	Stationary	Exponential	Stationary	Exponential	Stationary
Inflammatory	p50	-	-	↓*	-	-	-	-	-	-	-
	p65	-	-	-	↑*	-	↑**	-	-	-	-
	IKKα	-	-	-	-	-	↑***	-	-	-	-
	IL-8	-	↑**	↑*	-	-	↑*	-	-	↑*	-
	CCL20	-	-	-	↑*	-	↑**	-	-	↑*	-
	IL-1β	-	↑**	-	-	-	↑***	↓***	↓**	-	-
	STAT1	-	-	-	-	-	-	-	-	-	-
	STAT3	-	-	-	↑**	-	-	-	-	-	↑*
	JAK1	-	-	-	↑**	-	↑**	-	-	-	↑*
	JAK2	-	-	-	↑*	-	-	-	-	-	-
	CCL5	-	-	-	-	↑*	-	-	-	-	-
	CXCL10	↑*	↑*	↑*	-	-	-	-	-	↑***	↑***
Homeostasis	CDH1	-	-	-	-	-	-	-	-	-	-
	Villin	-	-	-	↑*	-	-	-	-	-	-
	Tcf4	-	-	-	↑*	-	↑*	-	-	-	-
	Axin2	-	↓*	-	-	-	-	-	-	-	-
	Klf4	-	-	-	-	-	↑**	-	-	-	-

*The arrow direction indicates significant change (increased or reduced) relative to relevant medium controls. Statistical significance was calculated by one-way ANOVA with Dunnett's post-hoc test with medium control as the control column. * = p<0.05, ** = p<0.01, *** = p<0.001, and - =not significant. n = 2-3 individual experiments from pooled triplicates*

3.3.3.1 Stationary phase conditionate media from *Bacteroides* species increased the expression and production of chemokines regulated by the NF-κB pathway

From the summary in Table 3.2, the conditioned media collected at the stationary phase of growth from *Bacteroides* regulated the expression of genes associated with the NF-kB pathway which will be discussed more in detail in this section. The gene expression of the neutrophile chemotactic IL-8 was significantly increased in C2BBe1 cells relative to control treatments, by the addition of conditioned media generated from all 3 *Bacteroides* species (**Figure 3.3**). Furthermore, this increase was observed in a species and growth phase dependant manner. Here, stationary phase conditioned media of *B. thetaiotaomicron* and *B. vulgatus* (**Figure 3.3 a**), significantly increased IL-8 expression, with *B. vulgatus* stationary phase conditioned media eliciting the highest induction in IL-8 expression in C2BBe1 cells (**Figure 3.3 a**). In contrast, *B. fragilis* conditioned media from the stationary phase of growth did not alter the expression of IL-8, while conditioned media from the exponential phase of growth did induce a significant increase in IL-8 expression (**Table 3.2**). Similarly, the conditioned media from the stationary phase of the pathogen *S. typhimurium* increased IL-8 expression significantly (up to 5-fold) (**Figure 3.3 c**), an effect not seen with exponential phase conditioned media from this strain (**Table 3.2**). As expected, *L. rhamnosus* GG conditioned media, from either phase of growth, did not alter IL-8 gene expression (**Table 3.1, Figure 3.3 c**).
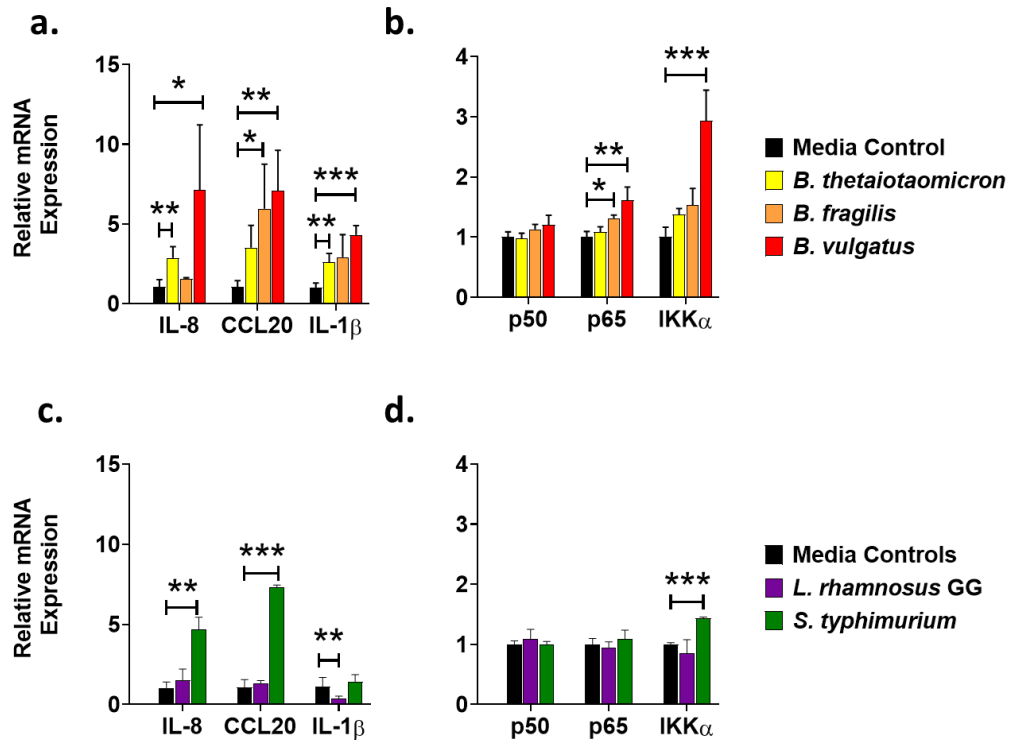
Figure 3.3 : Assessment of the expression of genes associated with the NF-κB pathway after coculture of stationary phase conditioned media of Bacteroides species in C2BBe1 cells. Genes assayed included the IL-8, CCL20, IL-1β and NF-κB pathway components p50, p65 and IKKα following co-culture with (a-b) Bacteroides conditioned media or (c-d) control species. Data presented as mean ± SD, n = 2-3 individual experiments from pooled triplicates. Statistical significance was calculated by one-way ANOVA with Dunnett post-hoc test, with media control as the control column. *, ** and *** denote p < 0.05, 0.01 and 0.001 respectively.

The mRNA expression of CCL20, a potent chemoattractant for lymphocytes and dendritic cells, was also significantly increased by *B. fragilis* and *B. vulgatus* stationary phase conditioned media compared to control (**Figure 3.3 a**). *B. thetaiotaomicron* conditioned media, from either phase of growth, did not alter CCL20 mRNA levels significantly (**Table 3.2, Figure 3.3 a**). In line with IL-8 mRNA levels, *S. typhimurium* conditioned media from the stationary phase only, significantly increased the expression of CCL20, (**Figure 3.3 c**). As expected, probiotic strain *L rhamnosus* GG conditioned

media did not alter the relative transcription of CCL20, from either phase of growth (**Table 3.2, Fig 3.3 c**).

We next evaluated IL-1β expression whose mRNA levels were significantly increased, albeit to a lesser degree than IL-8 and CCL20, in C2BBe1 cells exposed to *B. thetaiotaomicron* and *B. vulgatus* stationary phase conditioned media (**Figure 3.3 a**) but not for *B. fragilis* (**Table 3.2**). Interestingly conditioned media from both the exponential and stationary phases of growth from *L. rhamnosus* GG significantly lowered IL-1β expression with conditioned media from the exponential phase resulting in the greatest decrease in IL-1β expression (**Table 3.2, Figure 3.3 c**). *S. typhimurium* conditioned media from either phase of growth had no impact on IL-1β gene expression (**Table 3.2, Figure 3.3 c**).

Whilst gene expression through mRNA and transcription analysis is a good indicator of potential protein production, it does not account for post-transcriptional and other modifications, which may impede the development of mature protein. To confirm that the induction in inflammatory gene expression seen above reflected an increase in the production of inflammatory mediators at the protein level, ELISA for IL-8 and CCL20 was performed on C2BBe1 cell supernatant following 24 hr co-incubation with bacterial conditioned media.

B. thetaiotaomicron conditioned media from both phases of growth induced IL-8 production with conditioned media in the stationary phase of growth eliciting the largest increase (**Figure 3.4 a**). Whereas *B. fragilis* conditioned media from either phase of growth did not increase the production of IL-8 (**Figure 3.4 a**). *B. vulgatus* conditioned media from exponential, but not

stationary, phase of growth significantly increased production of IL-8, relative to medium control, in C2BBe1 cells (**Figure 3.4 a**). *L. rhamnosus* GG supernatant did not affectIL-8 production while *S. typhimurium* significantly increased IL-8 production from conditioned media in both phases of growth (**Figure 3.4 b**).
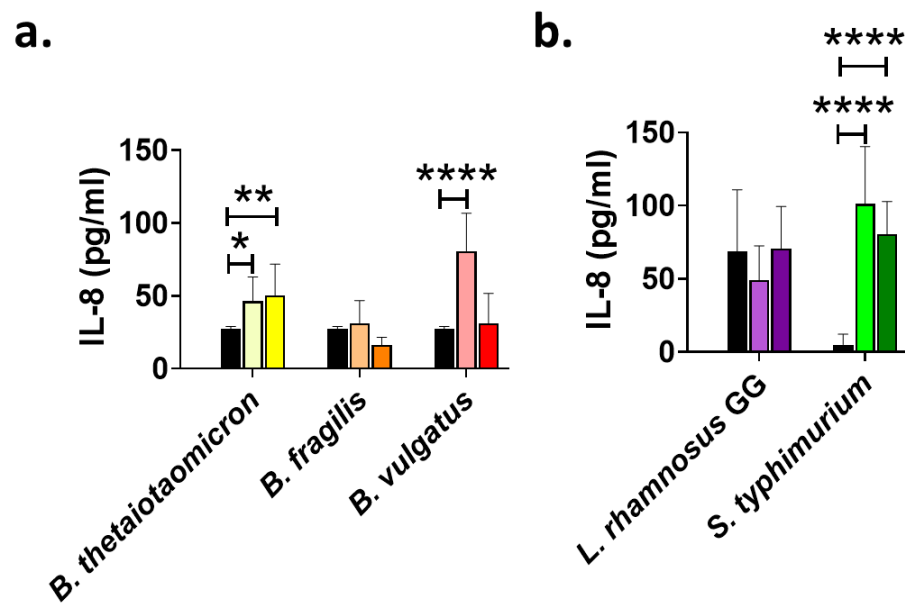

Figure 3.4 Assessment of IL-8 secretion after coculture of exponential and stationary phase conditioned media of Bacteroides species in C2BBe1 cells. (a) IL-8 production was quantified by ELISA from C2BBe1 cells cocultured with conditioned media for Bacteroides and (b) control bacterial species. Black colour indicates media controls, a light colour designates conditioned media collected from the exponential phase, and a solid colour denotes conditioned media collected from the stationary phase. Data presented as mean ± SD, n = 2-3 individual experiments from pooled triplicates. Statistical significance was calculated by one-way ANOVA with Dunnett post-hoc test, with media control as the control column. *, **, and * denote p < 0.05, 0.01, and 0.0001, respectively.***

Conditioned media from the stationary phase of all *Bacteroides* species significantly increased the production of CCL20 (**Figure 3.5 a**), with *B. vulgatus* exponential phase conditioned media also increasing CCL20 production (**Figure 3.5 a**). Conditioned media from both phases of growth of the pathogen *S. typhimurium*, induced a significant increase in CCL20

production, while no secretion of CCL20 was observed from *L. rhamnosus* GG conditioned media from both phases of growth (**Figure 3.5 b**). These analyses have demonstrated that the increase in IL-8 and CCL20 gene expression induced by conditioned media from CD-associated *Bacteroides* species corresponds to a significant increase in chemokine production from epithelial cells.
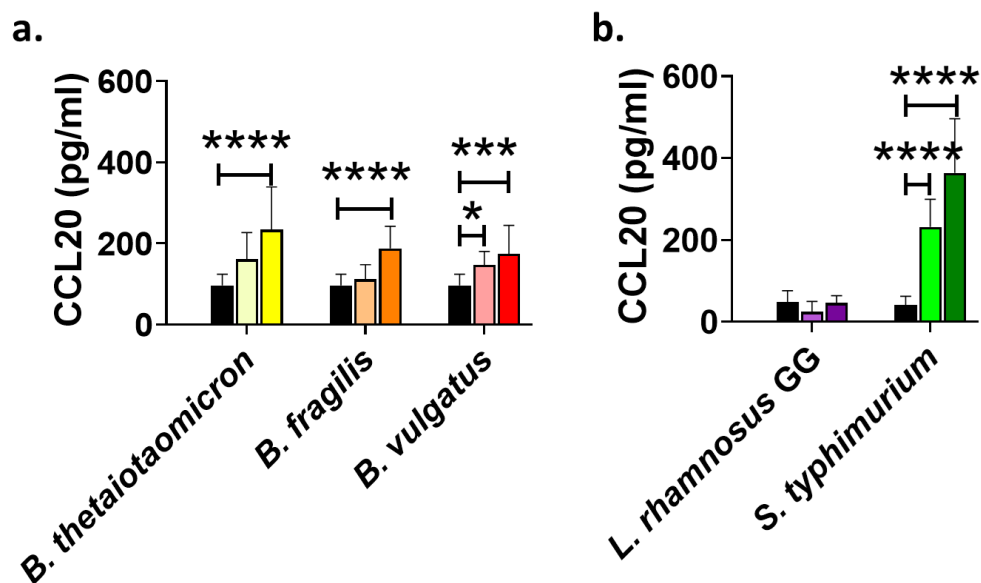

Figure 3.5 Assessment of CCL20 secretion after coculture of exponential and stationary phase conditioned media of Bacteroides species in C2BBe1 cells. (a) CCL20 production was quantified by ELISA from C2BBe1 cells cocultured with conditioned media for Bacteroides and (b) control bacterial species. Black colour indicates media controls, a light colour designates conditioned media collected from the exponential phase, and a solid colour denotes conditioned media collected from the stationary phase. Data presented as mean ± SD, n = 2-3 individual experiments from pooled triplicates. Statistical significance was calculated by one-way ANOVA with Dunnett post-hoc test, with media control as the control column. *, **, and **** denote p < 0.05, 0.01, and 0.0001, respectively.

Next, we assayed the gene expression of the NF-kB subunits provoked by *Bacteroides*. *B. thetaiotaomicron* and *B. vulgatus* conditioned media from any phase of growth did not significantly alter C2BBe1 expression of the NF-κB subunit p50 (NF-κB1) relative to control assessment (**Figure 3.3 b**). However, a significant decrease in expression was observed from the

exponential growth phase conditioned media of *B. fragilis* (**Table 3.2**). Conditioned media of both *L. rhamnosus* GG and *S. typhimurium* from both phases of growth did not alter the expression of p50 in C2BBe1 cells (**Figure 3.3 d**).

Overall, only stationary phase conditioned media from both *B. fragilis* and *B. vulgatus* showed the capacity to significantly alter gene expression of the other family members of this transcription factor, specifically subunits p65 and IKKα when assessed at the level of transcription (**Figure 3.3 b**). None of the conditioned media from *B. thetaiotaomicron, L. rhamnosus* GG *or S. typhimurium* from either phase of growth affected the expression of any of these subunits (**Table 3.2, Figure 3.3 b, d**).

Taken together, these data demonstrate that the conditioned media from CD-associated *Bacteroides* species can activate the NF-κB pathway to induce inflammatory chemokine gene expression and functional chemokine production, while other commensal bacteria do not. This inflammatory potential was observed in a species and supernatant growth phase dependant manner with *B. vulgatus* being the most potent inducer of inflammatory chemokine expression and production and NF-κB subunit expression.

3.3.3.2 Conditioned media from *Bacteroides* species increased the gene expression of members of the JAK/STAT pathway and effector chemokines but not chemokine secretion

From the summary results in Table 2, we noticed that *Bacteroides* species can activate the JAK/STAT pathway in a strain and growth phase specific manner. Specifically, the T cell chemoattractant CCL5had its expression in C2BBe1 cells altered by conditioned media from CD-associated *Bacteroides* strains (**Table 3.2**). Conditioned media collected from the exponential phase but not from the stationary phase from *B. vulgatus* significantly increased CCL5 expression (**Table 3.2**). Neither *B. thetaiotaomicron*, *B. fragilis* or *L. rhamnosus* GG conditioned media in any phase of growth altered CCL5 gene expression (**Table 3.2, Figure 3.6 a, c**). In contrast, conditioned media from the pathogen *S. typhimurium*, from both phases of growth, increased CCL5 expression by 4-fold, without reaching significance (**Table 3.2, Figure 3.6 c**).
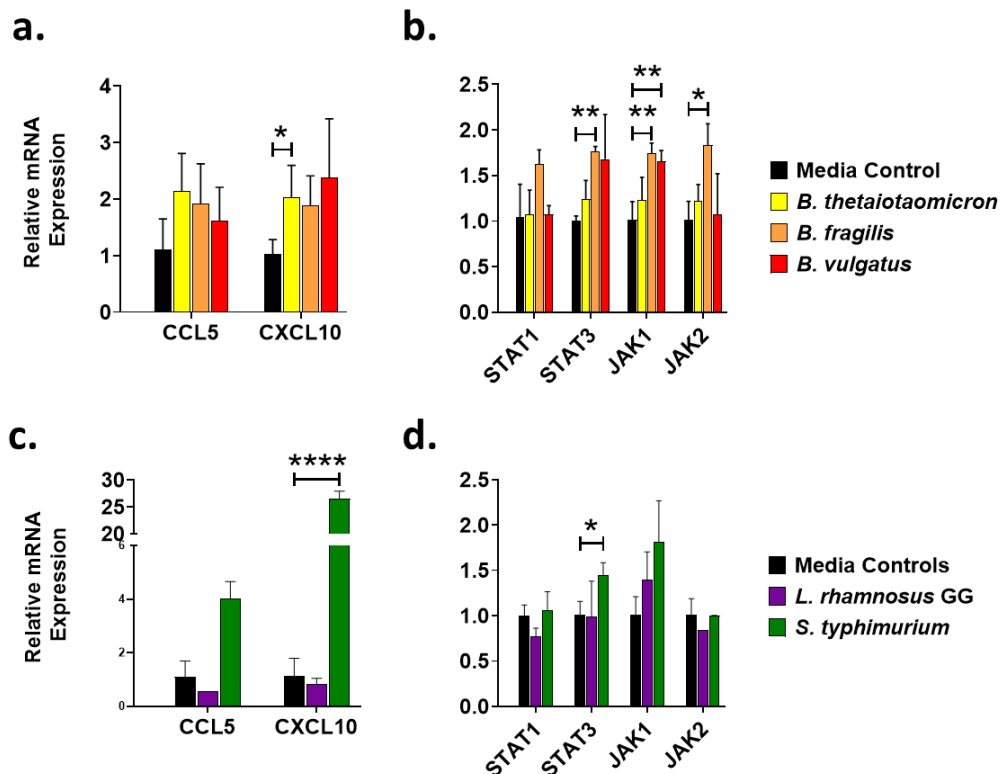
Figure 3.6 Assessment of the expression of genes associated with the JAK/STAT pathway after coculture of stationary phase conditioned media of Bacteroides species in C2BBe1 cells. Genes assayed included the inflammatory chemokines CCL5 and CXCL10 and STAT1, STAT3, JAK1, and JAK2 following co-culture with (a-b) Bacteroides supernatants, or (c-d) control bacterial species. Data presented as mean ± SD. n = 2-3 individual experiments from pooled triplicates. Statistical significance was calculated by one-way ANOVA with Dunnett post-hoc test, with media control as the control column. *, ** and **** denote p < 0.05, 0.01 and 0.0001, respectively.

Expression of another T cell and macrophage chemoattractant CXCL10 was increased in the presence of conditioned media from *Bacteroides* species (**Figure 3.6 a**). Media collected from both phases of growth from *B. thetaiotaomicron* and *B. vulgatus* increased CXCL10 expression, although this was only significant for *B. thetaiotaomicron*, relative to control (**Table 3.2, Figure 3.6 a**). Conditioned media of *B. fragilis* in the exponential but not the stationary phase of growth significantly increased CXCL10

152

expression relative to control (**Table 3.2**). Conditioned media from the exponential and stationary phases of growth from *S. typhimurium* significantly increased CXCL10 expression (20-fold) while conditioned media from *L. rhamnosus* GG elicited no change in CXCL10 expression (**Table 3.2, Figure 3.6 c**).

To investigate if *Bacteroides* conditioned media induced CXCL10 expression led to functional chemokine production an ELISA was performed on supernatants collected from C2BBe1-cultures. This demonstrated that conditioned media from either of the three *Bacteroides* species and any phase of growth did not significantly alter CXCL10 secretion from C2BBe1 cells (**Figure 3.7 a**). In contrast, conditioned media from the stationary phase of growth from *S. typhimurium* significantly increased CXCL10 production while conditionate media from *L. rhamnosus* GG did not alter CXCL10 production (**Figure 3.7 b**) This data showed that the increased expression of CXCL10 seen earlier did not transfer into increased CXCL10 production.
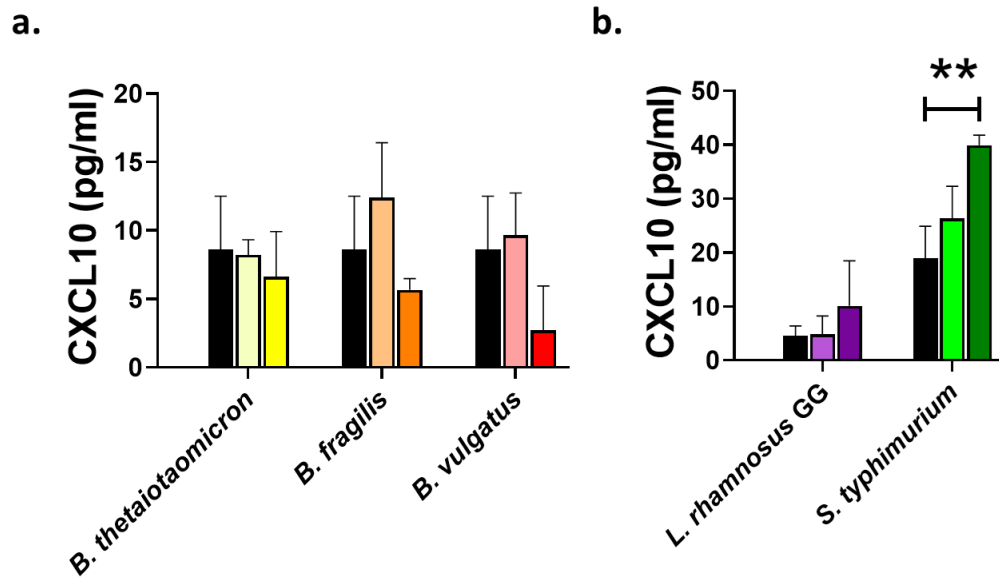
Figure 3.7 Assessment of CXCL10 secretion after coculture of exponential and stationary phase conditioned media of Bacteroides species in C2BBe1 cells. CXCL10 production was quantified by ELISA from C2BBe1 cells cocultured with conditioned media for (a) Bacteroides and (b) control bacterial species. Black colour indicates media controls, a light colour designates conditioned media collected from the exponential phase, and a solid colour denotes conditioned media collected from the stationary phase. Data presented as mean ± SD, n = 2-3 individual experiments from pooled triplicates. Statistical significance was calculated by one-way ANOVA with Dunnett post-hoc test, with media control as the control column. *, **, and **** denote p < 0.05, 0.01, and 0.0001, respectively.

Transcriptional readouts indicated that all bacterial conditioned media (both *Bacteroides* and controls) from both phases of growth, did not significantly alter the gene expression of STAT1 in C2BBe1 cells (**Table 3.2, Figure 3.6 b, d**). Conditioned media from *B. thetaiotaomicron*, in either growth phase, also did not affect the gene expression of STAT3, JAK1 or JAK2 (**Table 3.1 Figure 3.6 b**), whereas conditioned media from the stationary growth phase from *B. fragilis* significantly increased the expression of STAT3, JAK1 and JAK2 relative to medium control (**Figure 3.6 b**). Conditioned media from the stationary phase of growth from *B. vulgatus* significantly increased JAK1 gene expression relative to control (**Figure 3.6 b**). Conditioned media from

the probiotic *L. rhamnosus* GG had no impact on any of the genes associated with JAK/STAT signalling (**Figure 3.6 d**), while conditioned media from the stationary phase from the pathogen *S. typhimurium* significantly increased the gene expression of STAT3 and JAK1 (**Figure 3.6 d**). These data indicate that metabolic/cellular products from CD-associated *Bacteroides* species have the potential to alter signalling in the JAK/STAT pathway as well as its downstream target chemokines.

3.3.3.3 Conditioned media from *Bacteroides* species altered the expression of genes related to epithelial homeostasis and proliferation

Following the observation that conditioned media from *Bacteroides* species had the capacity to induce an inflammatory response, we hypothesised that they may also be capable of influencing gene expression related to epithelial homeostasis and proliferation. This is an important consideration in the context of CD pathogenesis as the epithelium lies at the junction of the lumen and internal environment, maintaining a physical barrier to luminal contents while coordinating immune responses, any perturbation to its normal functioning can lead to bacterial invasion of the mucosa or a dysregulated immune response, both features of CD (Coskun, 2014). To further explore this hypothesis, the expression of genes related to barrier function, enterocyte homeostasis and proliferation was investigated.

Conditioned media from all bacteria, i.e., *Bacteroides* and controls, did not induce any changes in the gene expression of the adherens junction protein CDH1 (**Figure 3.8 a**).
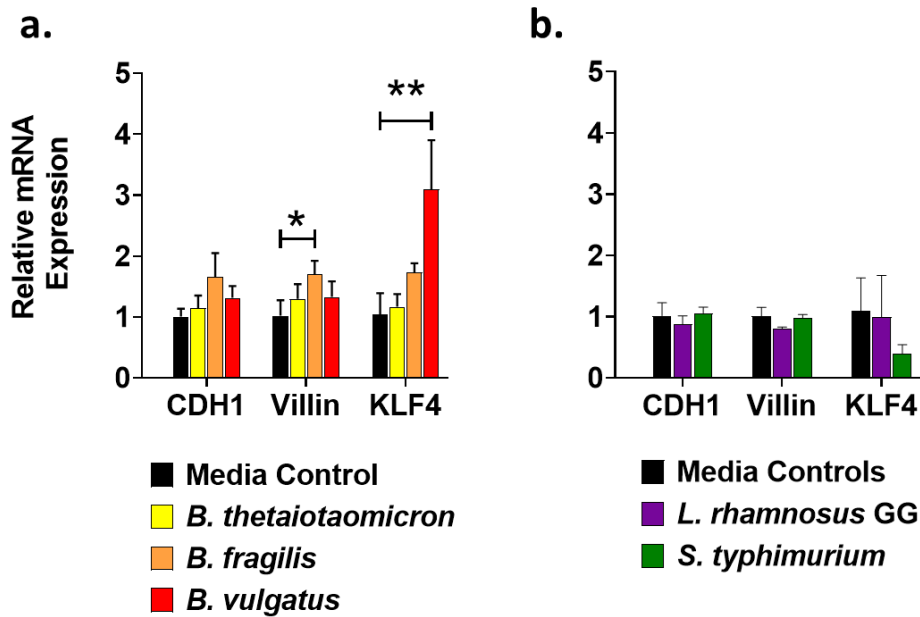
a.

b.

Figure 3.8 Assessment of the expression of genes associated with epithelial barrier and homeostasis after coculture of stationary phase conditioned media of Bacteroides species in C2BBe1 cells. Genes assayed included CDH1 (E-cadherin), Vil-1 (villin), and KLF4 following co-culture with (a) Bacteroides, or (b) control bacterial species conditioned media. Data presented as mean ± SD, n = 2-3 individual experiments from pooled triplicates. Statistical significance was calculated by one-way ANOVA with Dunnett post-hoc test, with media control as the control column. *, ** denote p < 0.05, 0.01, respectively.

Villin is crucial to the normal functioning of enterocytes, it is found in the brush border of the microvilli and is a regulator of apoptosis in the villi (Wang *et al.*, 2008). Gene expression of villin was increased, relative to control, in C2BBe1 cells exposed to conditioned media from the stationary phase of growth from *B. fragilis* (**Figure 3.8 a**), with neither of the other *Bacteroides* species or control bacteria affected villin expression (**Figure 3.8 a**).

The impact of *Bacteroides* conditioned media on epithelial proliferation was assessed by studying the expression of the KLF4 gene (Ghaleb *et al.*, 2011; Yu *et al.*, 2012). Only the conditioned media from the stationary phase of growth from *B. vulgatus* and *B. fragilis* significantly increased KLF4 gene

expression while the other bacterial media did not affect KLF4 gene expression in C2BBe1 cells relative to medium controls (**Figure 3.8 a**).

Taken together these data suggests that only conditioned media from *Bacteroides* stationary phase appear to impact epithelial homeostasis with *B. fragilis* altering villin expression and *B. vulgatus* increasing KLF4 expression, indicating an increase in epithelial cell proliferation and differentiation by the conditioned media from these two strains.

3.3.3.4 Conditioned media from *Bacteroides* species altered Wnt/β-Catenin pathway gene expression

With the observation that conditioned media from *Bacteroides* species altered expression of the proliferation-related gene KLF4, we asked whether this altered epithelial gene expression was regulated by members of the Wnt/β-catenin pathway (Teo and Kahn, 2010).

For this purpose, we evaluated the expression of two genes regulated by the Wnt/β-catenin pathway namely Axin2 and Tcf4. Conditioned media from *B. thetaiotaomicron* in the stationary phase of growth significantly reduced the gene expression of Axin2 (**Figure 3.9 a**), while neither of the other bacteria media, from both phases of growth, significantly changed Axin2 gene expression (**Figure 3.9 a, b**).
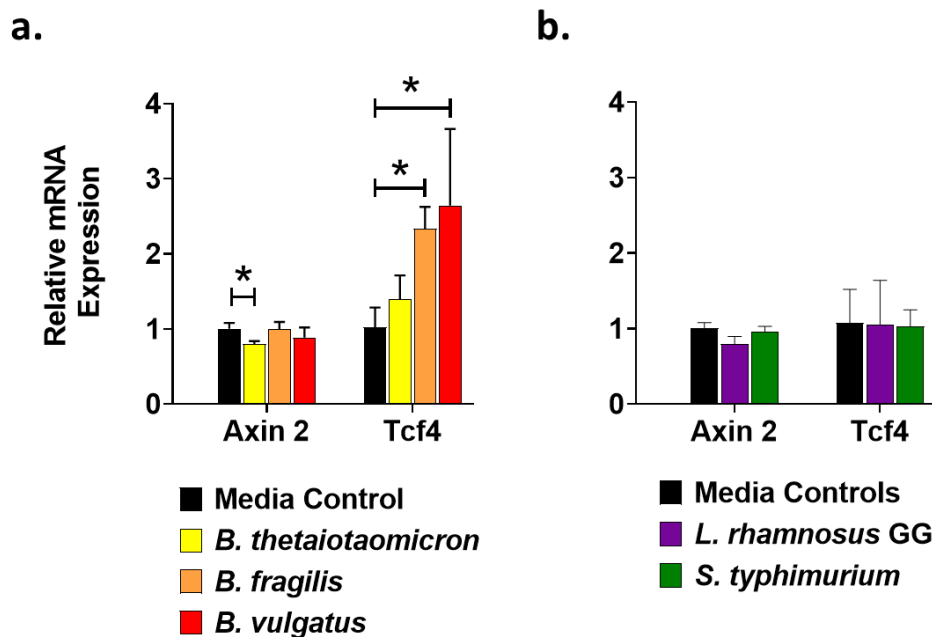
Figure 3.9 Assessment of the expression of genes associated with Wnt/β-catenin pathway after coculture of stationary phase conditioned media of Bacteroides species in C2BBe1 cells. Genes assayed included Axin2 and Tcf4 following co-culture with (a) Bacteroides, or (b) control bacterial species. Data presented as mean ± SD, n = 2-3 individual experiments from pooled triplicates. Statistical significance was calculated by one-way ANOVA with Dunnett post-hoc test, with media control as the control column. * denotes p < 0.05.

Complementary to Axin2, Tcf4 expression in C2BBe1 cells was increased in the presence of conditioned media from *B. vulgatus* and *B. fragilis* in the stationary phase of growth (**Figure 3.9 a**), but not affected by the conditioned media collected from any phase of growth from any of the other bacteria tested (**Figure 3.9 a, b**).

These data indicate that supernatant from *Bacteroides* species, especially *B. fragilis* and *B. vulgatus*, alter the Wnt/β-catenin pathway which controls proliferation in the intestinal epithelium. This result will be further validated in **section 3.2.5.3** using a more sophisticated primary cell *ex-vivo* model of small intestinal organoids.

3.3.4 Co-culture of live CD-associated *Bacteroides* strains affects the inflammatory response and epithelial homeostasis profile of colonic epithelial cells

We observed that conditioned media from CD-associated *Bacteroides* species, altered inflammatory and epithelial homeostatic gene expression in a growth phase dependent manner in C2Bbe1 cells. To further investigate whether a direct application of whole live *Bacteroides* species (from the stationary phase of growth) could similarly alter gene expression in C2Bbe1 cells, bacterial cells were applied to C2Bbe1 cells at an MOI of 10:1 (**Section 2.5.7**). Since the *Bacteroides* species investigated here are anaerobic but display some aerotolerance they were manipulated on the bench (Groman, 2009). However, to avoid a stunted response in the presence of oxygen, bacterial cells were grown anaerobically and similarly manipulated in advance of treatment.

3.3.4.1 Co-culture of live *Bacteroides vulgatus* altered epithelial gene expression and production of chemokines regulated by the NF-κB pathway

Changes in gene expression provoked by *Bacteroides* spp. co-culture with C2Bbe1 cells is summarised in **Table 3.3**. Increased gene expression of the chemokines IL-8 and CCL20, under control of the NF-κB pathway, was observed in a species-dependant manner. Whole *B. thetaiotaomicron and B. vulgatus*, but not *B. fragilis* significantly increased IL-8 expression by 3.5 and 2.5-fold respectively, relative to control (**Figure 3.10 a**). As expected, the commensal bacteria *L. rhamnosus* GG showed no impact on IL-8 expression, while the pathogen *S. typhimurium* did drastically increase its expression by up to 15-fold (**Figure 3.10 c**). A similar pattern of induction

was evident with the expression of CCL20 significantly increased in the whole *B. vulgatus* co-culture (**Figure 3.10 a**). Although CCL20 expression was elevated when co-cultured with the other *Bacteroides* species, it did not reach significance. Similarly, to the IL-8-response by *L. rhamnosus* LGG and *S. typhimurium* no effect and a fivefold increase in CCL20 gene expression, respectively, were observed, confirming the validity of the findings (**Figure 3.10 c**). IL-1β expression was not altered by any whole *Bacteroides* species nor *L. rhamnosus* GG but was significantly increased by *S. typhimurium* co-culture (**Figure 3.10 a, b**). Interestingly, *Bacteroides* species did not alter gene expression of the assayed NF-κB dependant genes; p50, p65 and IKKα (**Figure 3.10 b**), while *S. typhimurium* significantly increased p65 and IKKα expression by 0.5 to 1.5-fold, respectively (**Figure 3.10 d**)

Table 3.3 Summary table of genes significantly altered by co-culture with whole live Bacteroides and control species in C2BBe1 cells.

	Gene	*B. thetaiotaomicron*	*B. fragilis*	*B. vulgatus*	*L. rhamnosus* GG	*S. typhimurium*
Inflammatory	p50	-	-	-	-	-
	p65	-	-	-	-	↑*
	IKKα	-	-	-	-	↑**
	IL-8	-	-	↑**	-	↑***
	CCL20	-	-	↑***	-	↑***
	IL-1β	-	-	-	-	↑*
	STAT1	-	-	-	-	-
	STAT3	-	-	-	-	-
	JAK1	-	-	-	-	-
	JAK2	-	-	-	-	-
	CCL5	-	-	-	-	-
	CXCL10	↑***	-	↑***	-	↑**
Homeostasis	CDH1	-	-	-	-	-
	Villin	-	-	-	-	-
	Tcf4	-	-	-	-	-
	Axin2	-	-	-	-	-
	Klf4	-	-	-	-	-

*The arrow direction indicates significant change (increased) relative to medium controls. Statistical significance was calculated by one-way ANOVA with Dunnett's post-hoc test with untreated cells as the control column. * = $p<0.05$, ** = $p<0.01$, *** = $p<0.001$, and - =not significant. n= 3 individual experiments from pooled triplicates*
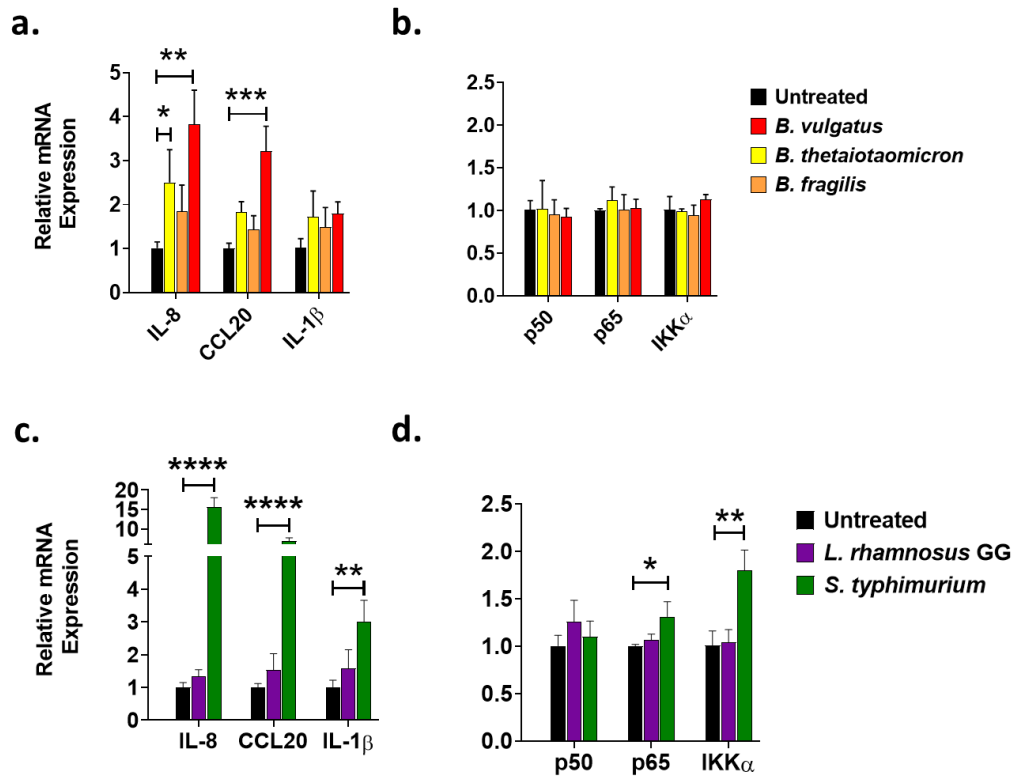
Figure 3.10 Assessment of the expression of genes associated with the NF-κB pathway after coculture of live whole cell Bacteroides species in C2BBe1 cells. Genes assayed included IL-8, CCL20 and IL-1β and NF-κB p50, p65 and IKKα following co-culture with live whole (a-b) Bacteroides cells, or (c-d) control bacterial cells. Data presented as mean ± SD, n = 2-3 individual experiments from pooled triplicates. Statistical significance was calculated by one-way ANOVA with Dunnett post-hoc test, with media control as the control column. *, **, and **** denote p < 0.05, 0.01, and 0.0001, respectively.

Figure 3.11 Assessment of IL-8 and CCL20 secretion of live whole cell Bacteroides species in C2BBe1 cells. Each dot represents one biological experiment made in duplicates or triplicates. Control bacterial species were Lactobacillus rhamnosus GG (LGG) and adherent and invasive E. coli (AIEC) HM605. Two-sided Student's t test analysis of variance was used to calculate the statistical significance. * P < 0.05; ** P <0.01; *** P ≤0.001; ns – not significant. Modified from (Ryan et al., 2020).

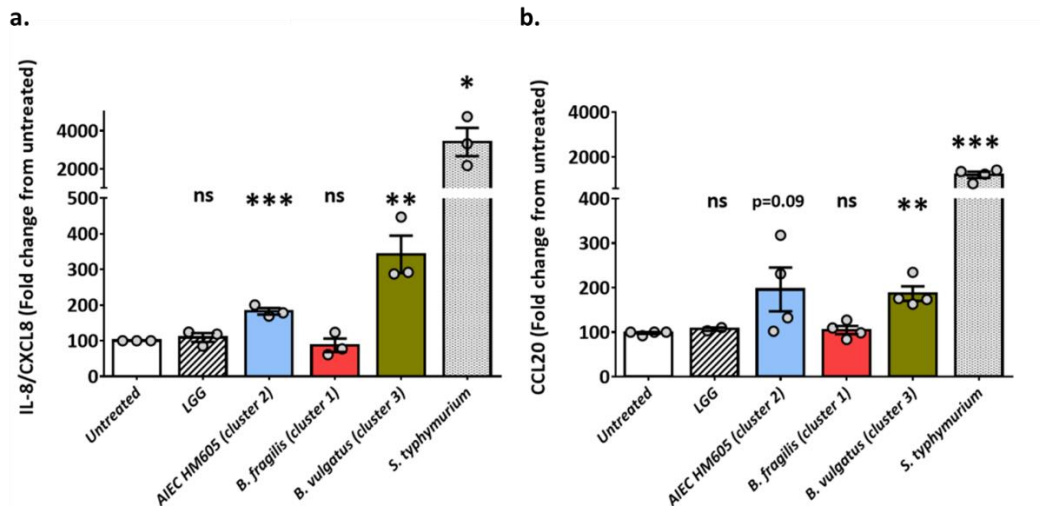### 3.3.4.2 Co-culture of live *Bacteroides* species induced CXCL10 expression but did not significantly alter gene expression of members of the JAK/STAT pathway or chemokine secretion

A species-specific activation profile on the JAK/STAT pathway was detected from conditioned media from *Bacteroides* species (**Figure 3.6**). Again, whole bacteria species co-cultured with C2Bbe1 cells demonstrated a capacity to induce the JAK/STAT regulated chemokine CXCL10. Here, CXCL10 expression was significantly increased, relative to untreated cells, by both *B. vulgatus* and *B. thetaiotaomicron* but not by *B. fragilis*, although it did increase its expression by 2.5-fold. (**Figure 3.12 a**). Genes for other members of the JAK/STAT pathway were assessed, including CCL5, STAT1, STAT3, JAK1 and JAK2, but *Bacteroides* co-culture had no impact on their expression levels **(Figure 3.12 a, b)**. As expected, *L. rhamnosus* GG did not affect any of the JAK/STAT-associated genes while *S.*

typhimurium significantly increased the expression of CXCL10 (50-fold) (**Figure 3.12 c**) and STAT3 and JAK1 (0.5-fold), although it did not reach significance (**Figure 3.12 d**). These data indicate that co-culture with *Bacteroides* species can induce the expression of chemokines controlled by the JAK/STAT pathway and this induction is in a species-dependent manner.

Figure 3.12 Assessment of the expression of genes associated with the JAK/STAT pathway after coculture of live whole cell Bacteroides species in C2BBe1 cells. Genes assayed include the inflammatory chemokines CCL5 and CXCL10 and STAT1, STAT3, JAK1, and JAK2 following co-culture with live whole (a-b) Bacteroides cells or (c-d) control bacterial species. Data presented as mean ± SD, n = 2-3 individual experiments from pooled triplicates. Statistical significance was calculated by one-way ANOVA with Dunnett post-hoc test, with media control as the control column. *, **, and * denote p < 0.05, 0.01, and 0.0001, respectively.***

3.3.4.3 Co-culture of live *Bacteroides* species did not affect the expression of genes related to epithelial cell homeostasis, proliferation, and stem cell niche signalling

As observed in the previous sections (**3.2.3.4, 3.2.3.5**) conditioned media from *Bacteroides* species altered the expression of genes related to epithelial homeostasis (villin), proliferation (KLF4), and stem cell signalling (Axin2, Tcf4). Here, we demonstrate that this effect was specific to conditioned media/bacterial metabolites and not observed when using live, whole bacteria cells in co-culture with C2BBe1 cells. Indeed, no significant changes in the five epithelial genes tested were detected following incubation with whole *Bacteroides* species or with control bacteria **(Fig 3.13 a, b, Fig 3.14 a, b).**
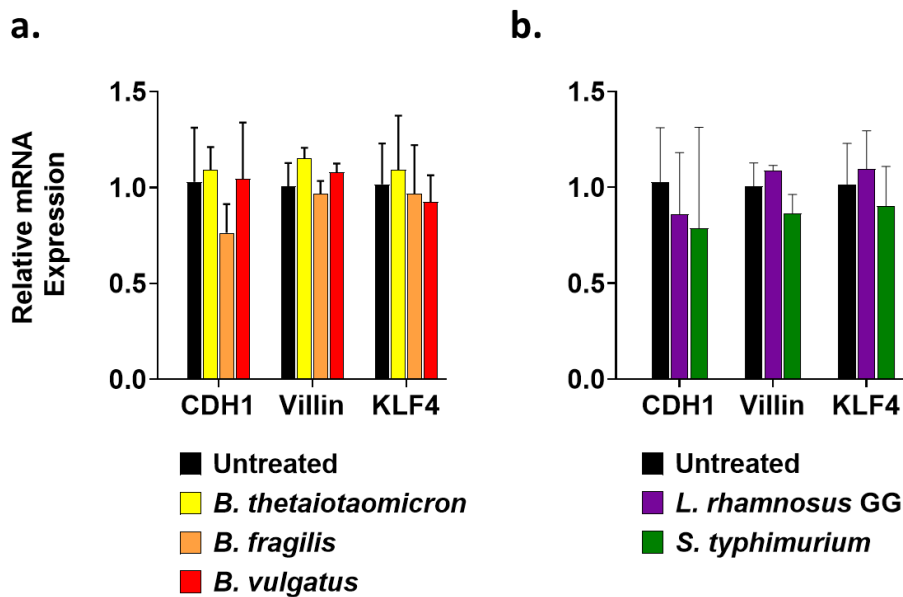
Figure 3.13 Assessment of the expression of genes associated with epithelial barrier and homeostasis after coculture of live whole cell Bacteroides species in C2BBe1 cells. Genes assayed included CDH1 (E-cadherin), Vil-1 (villin), and KLF4 following co-culture with live whole (a) Bacteroides cells or (b) control bacterial species). Data presented as mean ± SD, n = 2-3 individual experiments from pooled triplicates. Statistical significance was calculated by one-way ANOVA with Dunnett post-hoc test, with media control as the control column. *, **, and * denote p < 0.05, 0.01, and 0.0001, respectively.***
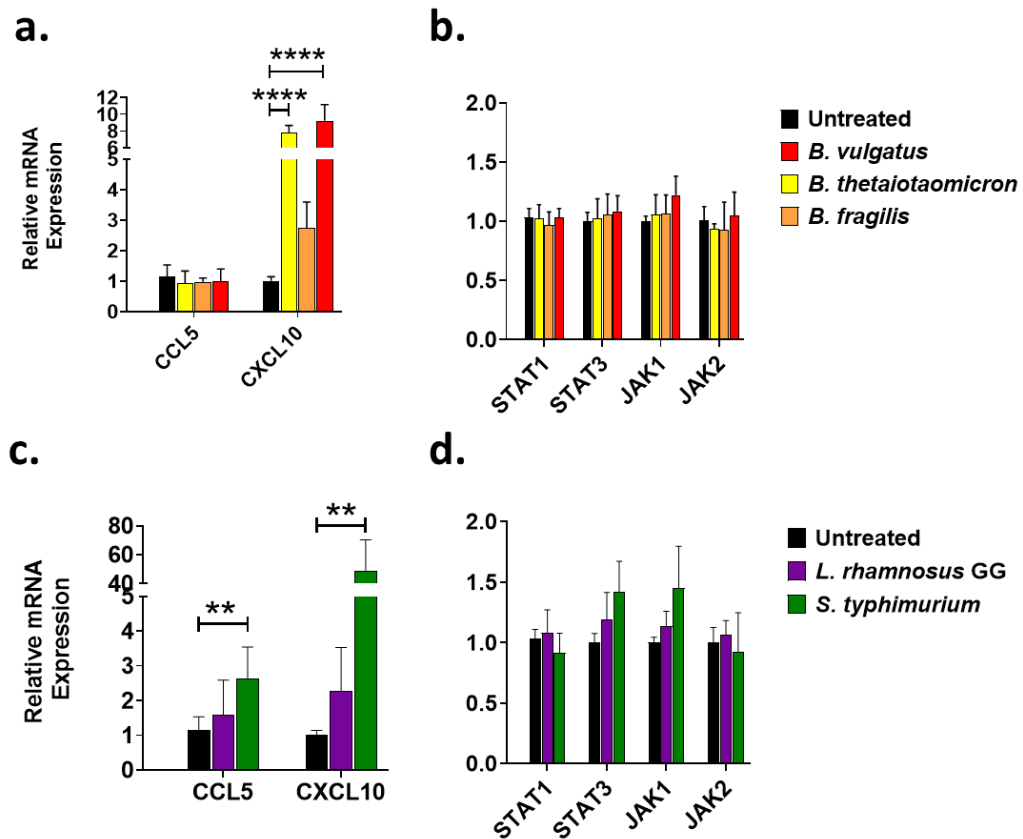
a.

b.
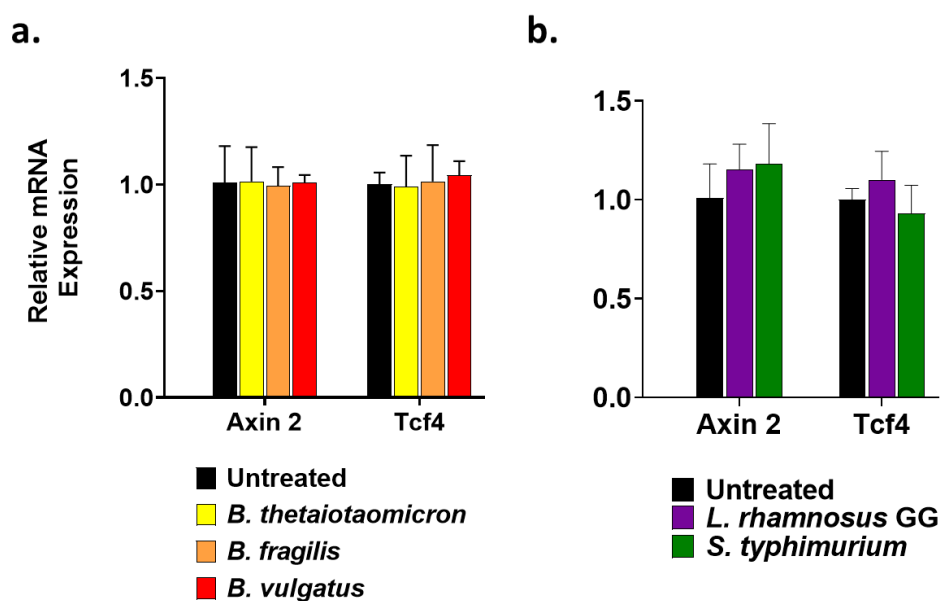
*Figure 3.14 Assessment of the expression of genes associated with Wnt/β-catenin pathway after coculture of live whole Bacteroides species in C2BBe1 cells. Genes assayed include Axin2 and Tcf4 following co-culture with live whole (a) Bacteroides cells or (b) control bacterial cells. Data presented as mean ± SD, n = 2-3 individual experiments from pooled triplicates. Statistical significance was calculated by one-way ANOVA with Dunnett post-hoc test, with media control as the control column. *, **, and **** denote p < 0.05, 0.01, and 0.0001, respectively.*

3.3.5 Effect of conditioned media from *Bacteroides* species in a primary *ex-vivo* small intestinal organoid model

Our work above documented that conditioned media from CD-associated *B. vulgatus and B. fragilis* altered the expression of genes related to inflammation, NF-κB and JAK/STAT pathway, and epithelial homeostasis, differentiation, and proliferation, in a human colonic epithelial cell line. To examine the relevance of these findings in a more physiologically relevant model, a murine primary epithelial *ex-vivo* organoid model was established and validated. In contrast to 2-dimensional cell cultures, intestinal organoids are self-organising, self-renewing, three-dimensional structures composed entirely of epithelial cells, including intestinal stem cells (Lgr5$^+$ cells) and all

166

subsequent epithelial cell sub-types, recapitulating *in vivo* epithelial physiology, constituting a novel platform for the study of epithelial function and host-microbe interactions (Sato and Clevers, 2013b). In this section, we sought to investigate 1) the effect of conditioned media from *Bacteroides* on both the development and differentiation of epithelial cell subpopulations in the organoids; and 2) the acute impact of *Bacteroides* conditioned media on the mature intestinal organoids.

3.3.5.1 Optimisation of organoid development, passage, and validation of epithelial cell subpopulation in matured small intestinal organoids

Organoids were established according to previous protocols (Sato and Clevers, 2013b) with some modifications as described in **sections 2.8.1 and 2.8.2**. In brief, crypts were isolated from the distal small intestine and embedded in a dome of basement membrane extract (Matrigel/BME) and submerged in medium. Organoids were then grown until mature (~7 days), (**Figure 3.15**), and passaged via mechanical disruption of the dome, and organoids split in a 1:3 ratio. The literature reports that organoids maintain their genetic integrity over many passages (Sato and Clevers, 2013b).
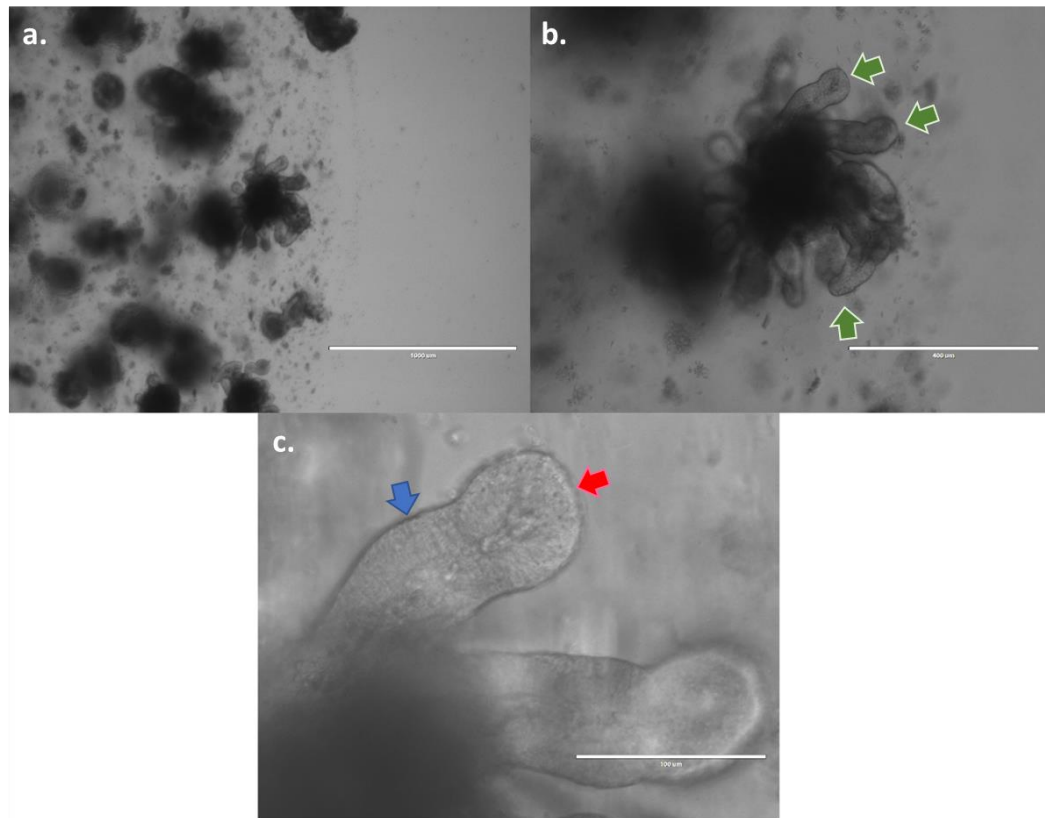
Figure 3.15 Brightfield images of matured murine small intestinal organoids after 7 days in culture. (a) Multiple organoids embedded in Matrigel. (b) An individual organoid displaying multiple crypt domains (green arrow) visibly budding from the central body. (c) An individual crypt domain where the columnar epithelial cells (blue arrow) are evident along the crypt with granular cells (red arrow) visible at the base of the crypt. Bar = 1,000mm (a), 400mm (b), and 100mm (c).

To ascertain if there were differences between organoids grown from crypts or passaged RNA was isolated from a dissociated crypt suspension, organoids grown from crypts (P0) and organoids grown from passage (P1) and RT-qPCR was performed for genes related to epithelial differentiation, stem-cell niche, apoptosis, junction proteins and inflammatory markers (**Figure 3.16**) A full list of genes with their functions can be found in **Section 2.6.4 and Table 2.2.**
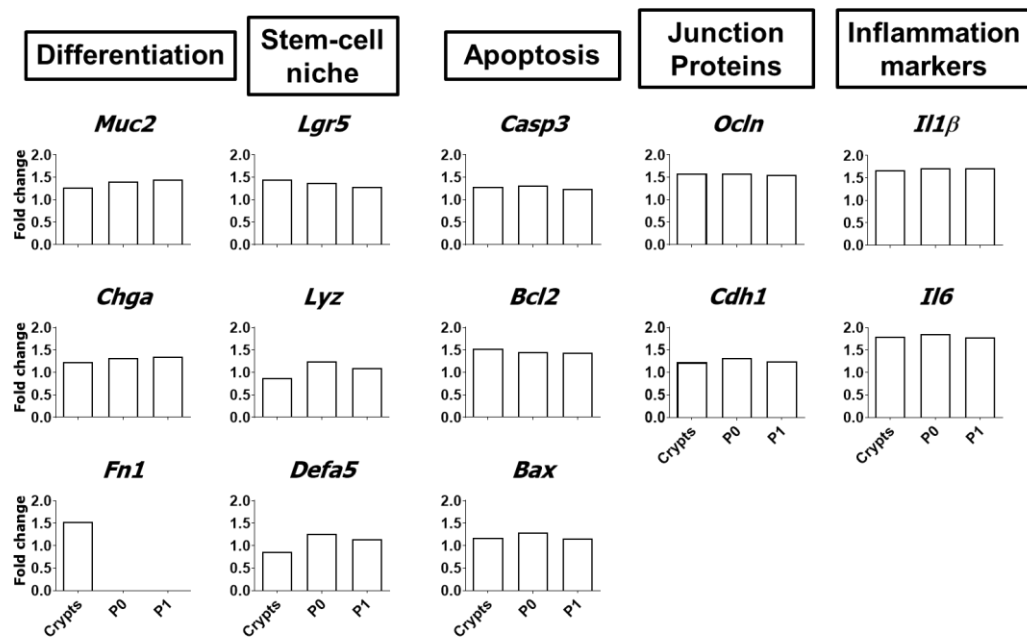
Figure 3.16 Gene expression profile of crypts and matured small intestinal organoids. The expression of genes associated with differentiation, stem cell niche, apoptosis, junction proteins, and inflammatory markers were characterised between three fractions: recent isolated crypts, organoids grown for 7 days (P0) and organoids grown for 7 days after first passage (P1). RNA was extracted from the different fractions and RT-qPCR was used to assay for gene expression. Data representative of one experiment.

No change in expression of epithelial cell sub-type markers assayed between crypts suspension, P0, and P1 was observed at all time points, except for fibronectin **(Figure 3.16)**. Fibronectin, a marker of endothelial cells, was expressed in crypts suspension i.e., directly after crypt isolation, but not at P0 or P1 indicating that after 7 days and after passage organoids consisted of a pure epithelial cell culture. To further validate that the organoids recapitulated the properties of an *in vivo* intestinal epithelial structure, immunofluorescence was performed on mature organoids at the P0 time point (**Figure 3.17**) Organoids were stained for E-cadherin (**Figure 3.17 a**), showing the presence of adherens junctions; MUC2 (**Figure 3.17 b**) to visualise mucus production and presence of goblet cells;

synaptophysin (**Figure 3.17 c**) to highlight the presence of hormone-producing enteroendocrine cells and occludin to indicate the presence of an apical tight junction, which sustains barrier function (**Figure 3.17 d**). These fluorescent stains indicated the integrity of the organoid population and their development to mature IECs, which agrees with previous publications (Sato and Clevers, 2013b) and therefore our established protocol was deemed sufficient for further experiments.
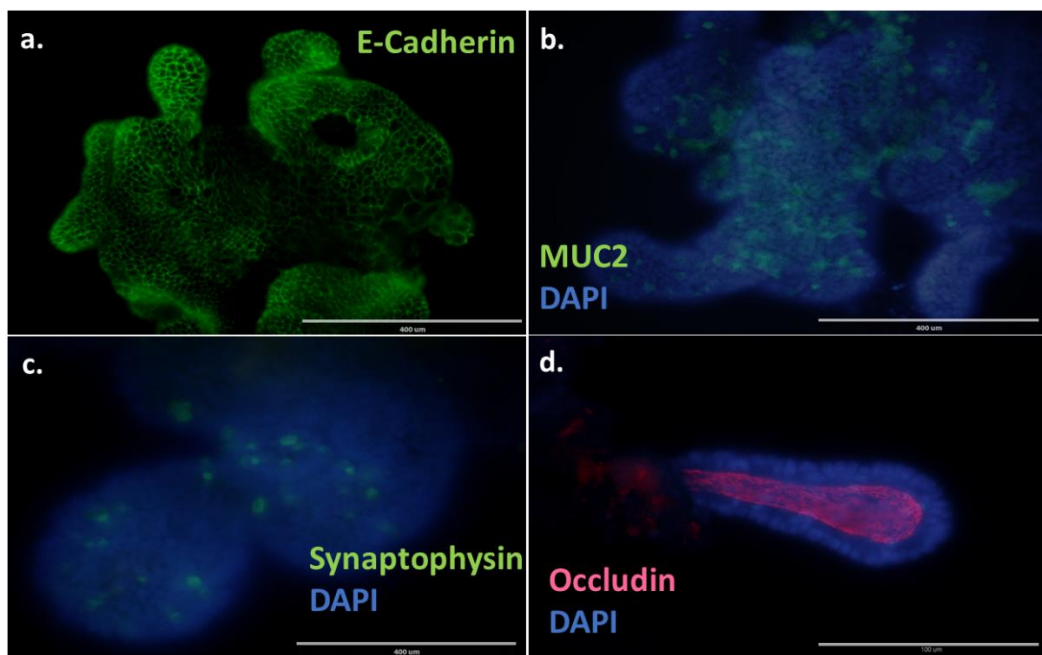
Figure 3.17 Fluorescent immunocytochemistry of mature murine small intestinal organoids. Organoids were grown in Intesticult for 7 days i.e., full differentiation and stained for: (a) E-Cadherin, a marker for adherence junctions demonstrating the presence of epithelial junctions. (b) MUC2, a mucin marker representing the presence of goblet cells. (c) Synaptophysin, a marker for enteroendocrine cells indicating the presence of hormone producing cells in the organoids. (d) Occludin, an apical tight junction marker (d). Representative images from 3 independent experiments. (a-c). 40x magnification, scalebar 400µm, (d.) 60x magnification scalebar 100µm

3.3.5.2 Optimisation of conditioned media concentration from *Bacteroides* for co-culture experiments with small intestinal organoids

We, and others (Lukonin *et al.*, 2020), (Hanrahan et al, unpublished), have previously noted that organoids, as primary cells, are not as robust as cell lines such as C2BBe1 cells when exposed to exogenous stimuli including bacterial conditioned media. We, therefore, determined sensitivity from robustness in terms of serially diluted conditioned media application from *Bacteroides* on organoid development and maturation. Based on findings on C2Bbee1 cells, conditioned media from the stationary phase of growth from *B. vulgatus* and *B. fragilis* (**Figure 3.9/Table 3.3**) was selected for organoid experiments. In brief, isolated crypts were embedded in Matrigel and left to grow for 24 hrs in Intesticult medium before being exposed to BHI medium at 1:100 or *B. vulgatus/B. fragilis* conditioned media at 1:100 or 1:500 for a further 6 days until the organoids were fully developed and matured. After 7 days organoids were visually inspected for morphological abnormalities or death (**Figure 3.18 a-f**). While organoid death did not occur under any of the tested conditions, an increased ratio of spheroids to organoids, in all conditions was evident (**Figure 3.18 g**), indicating that *Bacteroides* conditioned media is not toxic to the organoids but may be impacting their development.
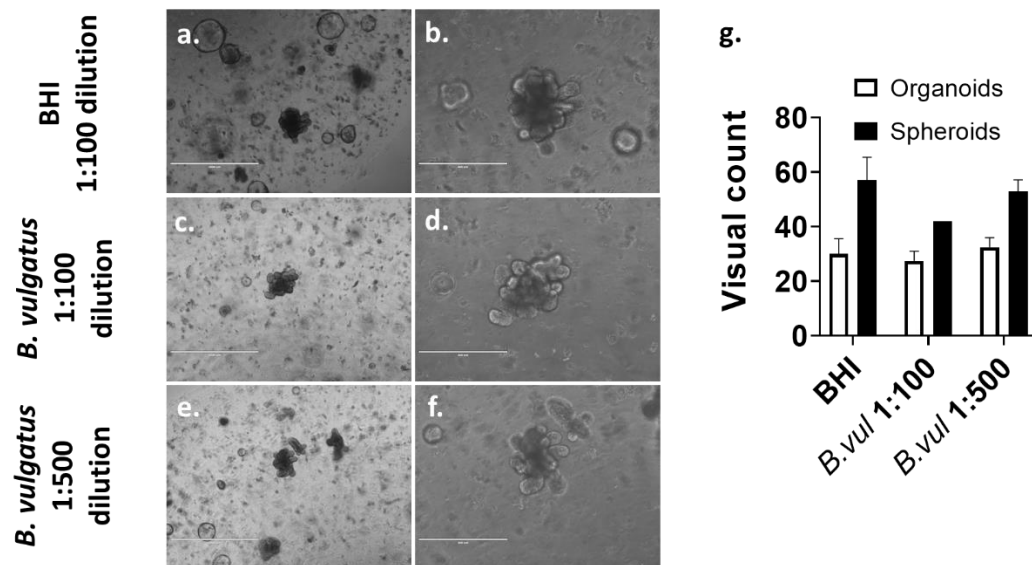
Figure 3.18 Optimisation of tolerance of organoid generation to Bacteroides conditioned media. Organoids were grown in the presence of (a-b) bacterial medium BHI at 1:100 dilution, (c-d) Bacteroides vulgatus conditioned media at 1:100 dilution and (e-f) 1:500 dilution and bright field imaged at day 7. (g) The ratio of organoids to spheroids was counted in duplicate wells for each condition. Data presented as mean ± SD, from one representative experiment. (a, c, and e) Bar = 1,000µm, (b, d, and e) 400µm

.

Lukonin *et al.,* recently described how organoids do not only develop into mature organoids but can also display other dysfunctional phenotypes including enterocysts, Paneth cell hyperplasia and regenerative phenotype. Based on the increased number of spheroids to organoids ratio detected after culture in BHI, the expression of three specific genes identified by Lukonin *et al.,* to represent the dysfunctional phenotypes was examined including *Akt1* representing the 'enterocyst' phenotype, *Psen1* representing the 'Paneth cell hyperplasia' phenotype, and *Rxra* representing the 'regenerative' phenotype', across 3 independent studies (Study A-C) (**Figure 3.19**). Differential phenotype development between studies would be indicated by differential expression of these 'phenotype' genes both

within and between studies. While no differences within a study were seen (**Figure 3.19**), large differences between studies B and C were seen relative to study A (**Figure 3.19**) suggesting that variation between individual studies is not due to the development of dysfunctional phenotypes but minor differences in the culture technique. Based on these optimisation studies, we choose 1:100 dilution for *B. vulgatus and B. fragilis* conditioned media for further experimentation. This dilution exhibited little effect on the development or maturation of the organoids (**Figure 3.20**).
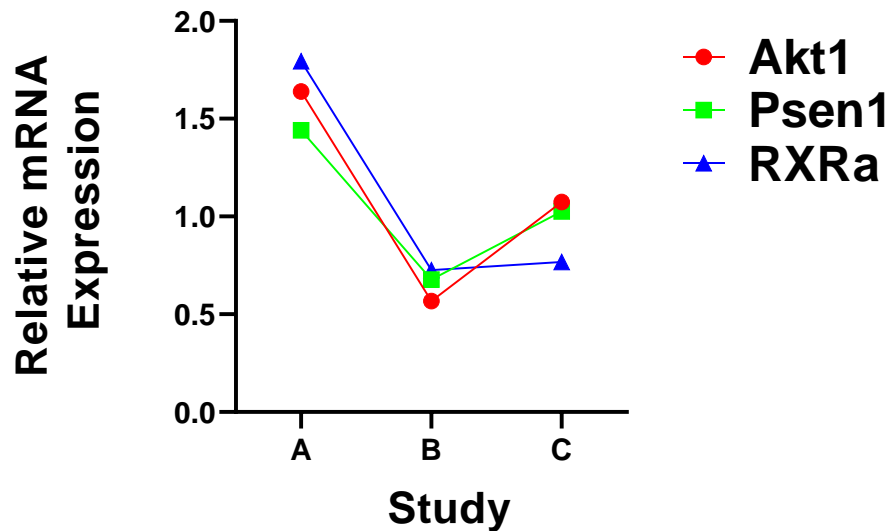
Figure 3.19 Examining the potential presence of dysfunctional organoid phenotypes in organoids cocultured with bacterial medium BHI. Organoids were grown in the presence of bacterial medium BHI for 7 days andthree genes related to dysfunctional organoid phenotypes were assayed by RT-qPCR: Akt1, representing enterocyst formation; Psen1, representing Paneth cell hyperplasia; and RXRa, representing a regenerative phenotype. Each study (A-C) contained one mouse. RT-qPCR for each gene was done in duplicates for each mouse. b-actin was used as housekeeping gene.

3.3.5.3 Exposure of developing organoids to *Bacteroides vulgatus* supernatant altered expression of genes related to proliferation

Based on findings in **section 3.3.3.3**, we noted that conditioned media of the stationary phase of *B. vulgatus* and *B. fragilis* affected the gene expression of differentiation and proliferation markers in human colonic epithelial cells. Therefore, to assess the impact of *Bacteroides* secreted products on inflammation and organoid development, the optimised concentration of *Bacteroides* conditioned media (1:100) was applied to organoids 24 hrs post crypt isolation and subsequently exchanged every second day until fully differentiation of the organoid (day 7). **Figure 3.20** shows representative images of organoid development taken on days 3, 5 and 7 post *B. vulgatus* and *B. fragilis* conditioned media application. RT-qPCR was performed for genes related to inflammation, epithelial cell sub-type markers and epithelial crypt signalling (**Table 2.3**).
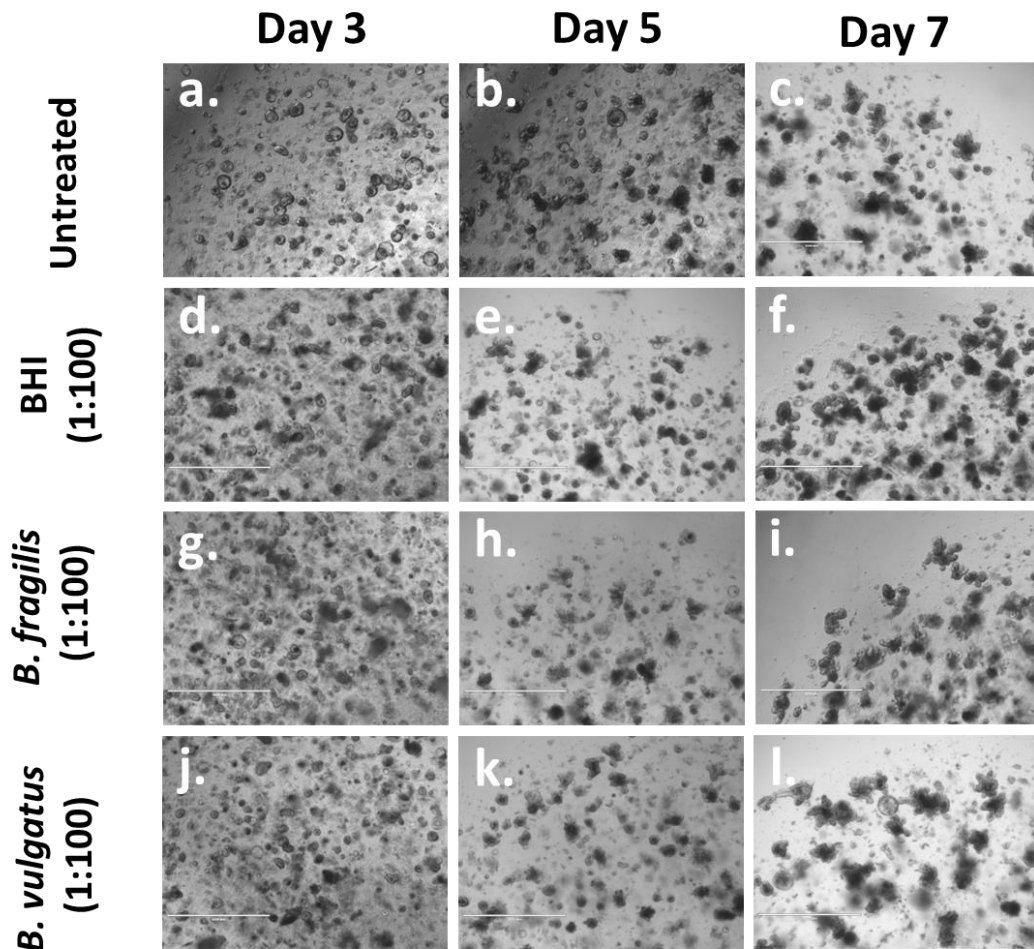
Figure 3.20 : Effect of CD associated Bacteroides fragilis and B. vulgatus stationary phase conditioned media on the development and maturation of murine small intestinal organoids. Organoids were grown to maturation over seven days with their growth assessed at days 3, 5, and 7 for (a-c) untreated organoids, (d-f) organoids grown in the presence of BHI, (g-i) Bacteroides fragilis conditioned media, and (j-l) Bacteroides vulgatus conditioned media, all at 1:100 dilution. Bar = 1,000µm. Pictures are representative of three independent studies

Based on the chemokine profile provoked by *B. vulgatus* and *B. fragilis* in C2BBe1 cells, we choose *Cxcl2* (murine homolog of IL-8) and *Ccl20* to examine whether the culture of organoids in the presence of *Bacteroides* conditioned media during development affects their inflammatory response. Indeed, no significant difference in the gene expression of these two chemokines was detected in fully differentiated organoids grown under the influence of the two *Bacteroides* supernatants (**Figure 3.21 a, b**),

suggesting that, the consistent culture of organoids in conditioned media from *B. vulgatus* and *B. fragilis* do not induce an inflammatory response.
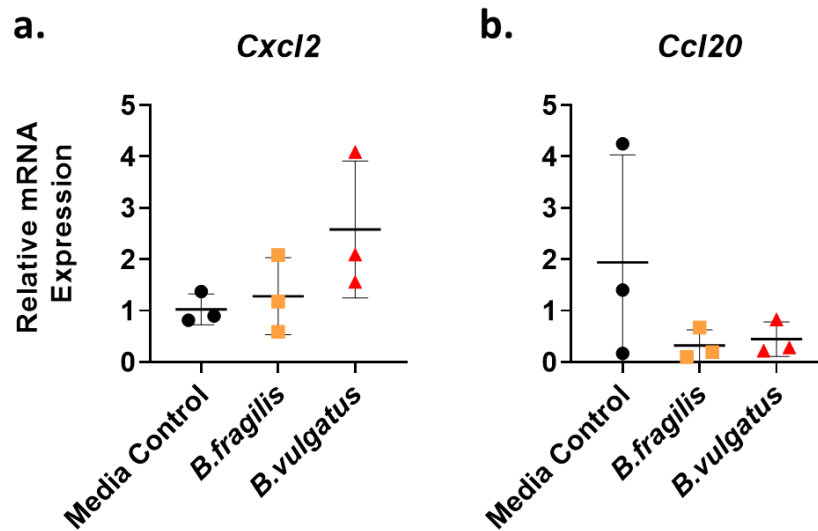
Figure 3.21 Alterations in gene expression of inflammatory markers in organoids grown under Bacteroides species conditioned media. Small intestinal organoids were grown for 7 days in conditioned media from the stationary phase of Bacteroides species. Gene expression for (a) Cxcl2 and (b) Ccl20 was analysed by qRT-PCR. Data presented as mean ± SD, from three independent experiments. Statistical significance was calculated using one-way ANOVA with Dunnett's post-hoc test with media control (BHI) as the control column.

Next, we investigated whether conditioned media from *Bacteroides* species can alter epithelial cell lineage by assaying for the lineage determination genes associated with the different epithelial cell sub-types including *Lgr5* (stem cells), *Lysozyme* (Paneth cells), *Chromogranin A* (enteroendocrine cells), *Muc2* (goblet cells), *villin* (Vil-1, enterocytes) and their transcription factors *Hes1* (absorptive cells), *Atoh1* (secretory cells) and *Sox9* (Paneth cells). In addition, *Zo-1* was used as a marker for tight apical junctions and barrier stability of the organoids and cyclin D1 (*Ccnd1*) was used as a marker of the cell cycle. On day 7, no significant change in the gene expression of these markers was observed in *Bacteroides* conditional

media compared to BHI-control (**Figure 3.22 a-e**). A reduction in *Lysozyme* and *Sox9* expression, markers for Paneth cells, was observed in the *Bacteroides* conditioned media grown organoids, without reaching significance due to the variability encountered in the 3 biological replicates (**Figure 3.22 a, Figure 3.23 i**). The collected data suggest that, under these conditions, conditioned media from both *Bacteroides* species had no major impact on epithelial cell lineage, except for a potential reduction in Paneth cell development.

Figure 3.22 Gene expression analysis of epithelial cell lineage in organoids grown under Bacteroides species conditioned media. Small intestinal organoids were grown for 7 days in conditioned media from the stationary phase of Bacteroides species and the expression of genes related to epithelial cell lineage was assayed by RT-qPCR. Markers of (a) Paneth cells - Lysozyme, (b) enteroendocrine cells – Chromogranin A, goblet cells – (c) Muc2, enterocytes – (d) Villin (Vil-1), and (e) apical tight junctions – Zo-1. Data presented as mean ± SD, from three independent experiments. Statistical significance was calculated using one-way ANOVA with Dunnett's post-hoc test with media control (BHI) as the control column.

Previous observations in C2BBe1 cells revealed that conditioned media from *B. fragilis* and *B. vulgatus* altered the expression of the Wnt/β-catenin pathway as demonstrated by an increased expression of one of its major downstream effectors Tcf4. Therefore, we assayed for the expression of Axin2 and Tcf4 in organoids exposed to the *Bacteroides* conditioned media during their development. In contrast to the findings in the undifferentiated C2BBe1 cells, conditioned media from both *Bacteroides* species significantly decreased the expression of *Axin2* (**Figure 3.23 b**), while no significant difference was detected in *Tcf4*, although a potential reduction in *Tcf4* by *B. vulgatus* conditioned media was observed (**Figure 3.23 c**). Next, we assayed for the expression of genes involved in BMP signalling as the small intestinal organoid model excellently recapitulates the structural and signalling gradients exhibited *in-vivo*, unlike a cell culture system. The components of the BMP pathway, *Smad4* and *Smad5*, were assayed, showing that *Bacteroides* species conditioned media significantly decreased the expression of smad5 relative to control media (**Figure 3.23 d**). These observations indicate that either microbially produced products from *Bacteroides* species or by conversion of media containing factors can induce a proliferative state during the development of small intestinal organoids.
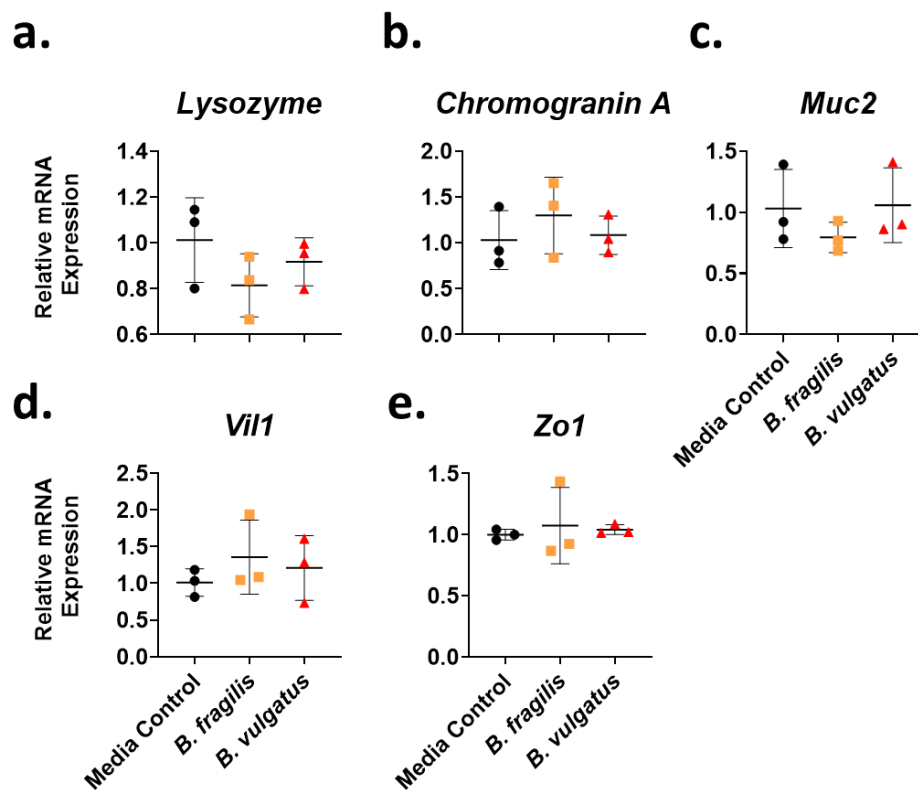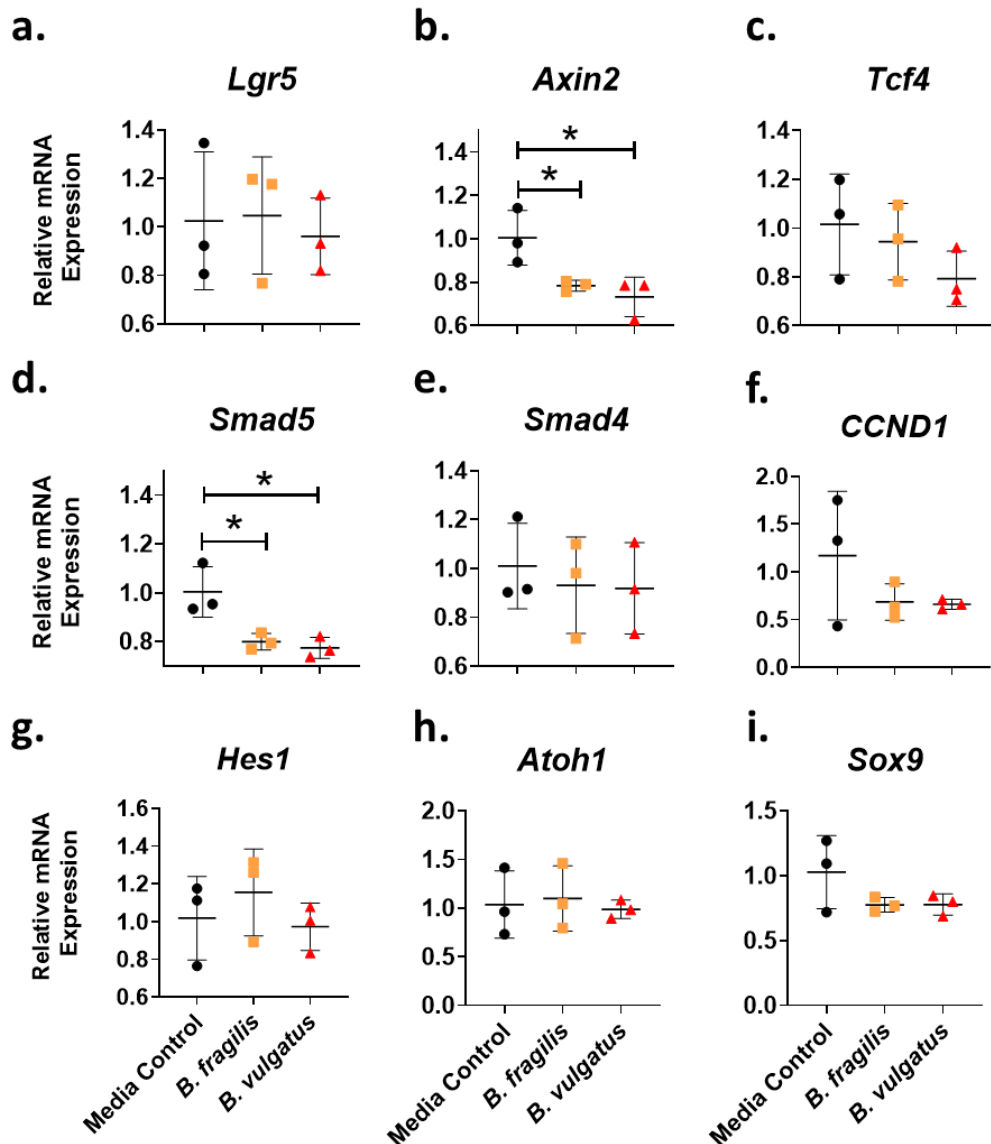
Figure 3.23 Gene expression analysis of epithelial stem cell niche signalling in organoids grown under Bacteroides species conditioned media. Small intestinal organoids were grown for 7 days in conditioned media from the stationary phase of Bacteroides species and genes assayed by qRT-PCR. Markers of (a) crypt-based stem cells – Lgr5, (b-c) Wnt/β-catenin signalling – Axin2 and Tcf4, (d-e) BMP signalling – Smad5 and Smad4, (f) cell cycle -Ccnd1, and (g-i) epithelial cell lineage determination – Hes-1 (absorptive lineage), Atoh-1 (secretory lineage) and Sox9 (Paneth cells differentiation). Data presented as mean ± SD, from three independent experiments Statistical significance was calculated using one-way ANOVA with Dunnett's post-hoc test with media control as the control column. * denotes p < 0.05.

These data indicate that exposure of developing organoids to *Bacteroides*

conditioned media had a low impact on growth or lineage determination.

However, long-term exposure to these media altered signalling in the Wnt/β-

Catenin and BMP pathways, potentially affecting the proliferation and differentiation of epithelial cells.

3.3.5.4 Application of *B. vulgatus* conditioned to differentiated and mature organoids resulted in altered expression of genes related to inflammation and proliferation

We have shown that *B. vulgatus* conditioned media, from the stationary phase of growth, applied for 24 hrs to undifferentiated C2BBe1 cells resulted in an increased expression of inflammatory genes mediated by the NF-κB pathway, along with altering expression of genes related to proliferation. Here, as *B. vulgatus* conditioned media elicited the greatest response, we sought to examine whether *B. vulgatus* conditioned media provoked any effect on almost matured organoids which will reflect a more physiologically encounter of metabolites with the mature epithelium. Organoids were grown, as in **section 2.8.5**, and monitored until they reach an almost mature state on day 6 **(Figure 3.24 a-i)** at which point they were exposed to *B. vulgatus* conditioned media, from the stationary phase of growth, in a ratio of 1:20 (supernatant: Intesticult) for 24 hrs before harvesting for gene expression analysis as in the previous section i.e., genes associated with inflammation, epithelial cell markers and stem-cell niche signalling.
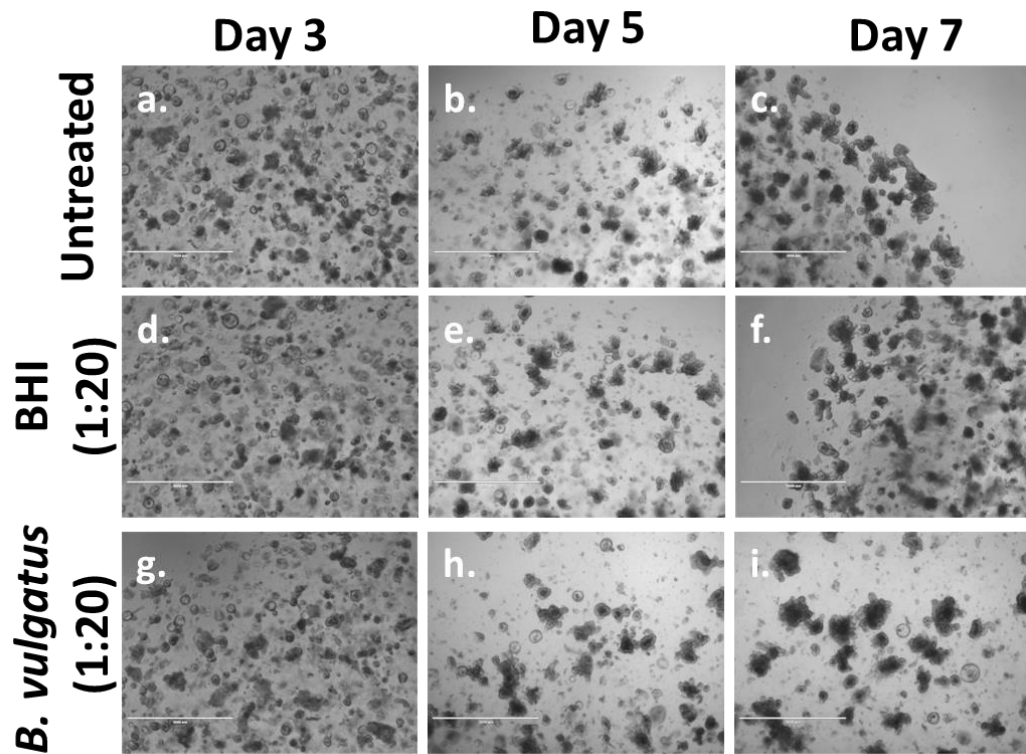
Figure 3.24 Figure 3.24: Acute effect of CD associated Bacteroides species conditioned media on mature small intestinal organoids. Organoids were grown to maturation over six days in basal medium (Intesticult) with their growth assessed visually at days 3 (a, d, g) and 5 (b, e, h). On the sixth day basal medium, bacterial medium (BHI) or Bacteroides vulgatus conditioned media was added (1:20 dilution) for 24 hours with organoids assessed visually on day 7 (c, f, I, respectively). Scalebar = 1,000μm. Representative pictures from three individual experiments.

Cxcl2 gene expression following acute *B. vulgatus* conditioned media stimulation was increased, however, due to variability in the data, it did not reach significance (p = 0.06) (**Figure 3.25 a**). Contrary to previous observations in the cell line, *B. vulgatus* conditioned media significantly reduced *Ccl20* gene expression almost eliminating its expression (**Figure 3.25 b**).

181
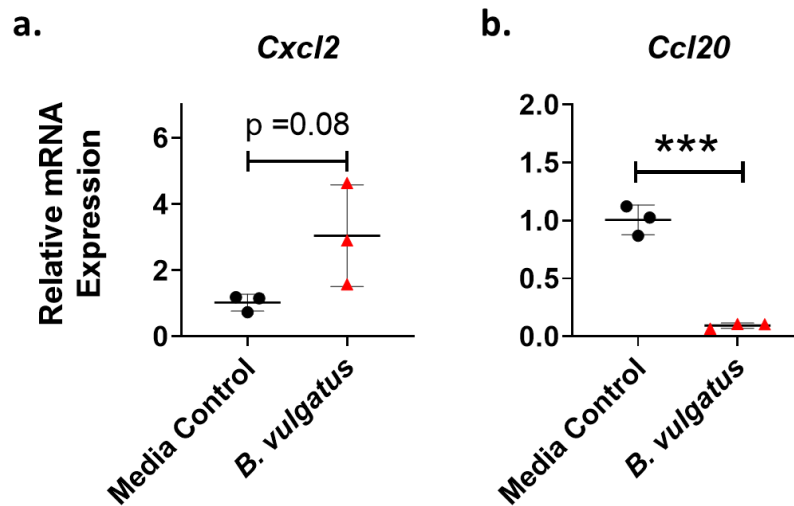
Figure 3.25 Acute effect of Bacteroides vulgatus conditioned media on the gene expression of inflammatory markers in mature small intestinal organoids. At day 6 of organoid development, nearly matured organoids were cocultured with stationary phase B. vulgatus conditioned media for 24 hrs, followed by gene expression analysed by RT-qPCR for (a) Cxcl2 and (b) Ccl20. Data presented as mean ± SD, from three independent experiments. Statistical significance was calculated using a 2-tailed student t-test. *** denotes p < .001.

Unlike the long-term exposure to *B. vulgatus* conditioned media during organoid development, the lysozyme expression was significantly decreased in almost mature organoids exposed to *B. vulgatus* conditioned media (**Figure 3.26 a**). Indicating the potential of *B. vulgatus* metabolites to alter lineage determination and crypt niche signalling. No other epithelial subtype markers were significantly altered (**Figure 3.26 b-c**).

*Figure 3.26 Acute effect of Bacteroides vulgatus conditioned media on the gene expression of epithelial cell lineage in mature small intestinal organoids. At day 6 of organoid development, nearly matured organoids were cocultured with stationary phase B. vulgatus conditioned media for 24 hrs, followed by assessment by RT-qPCR of markers for (a) Paneth cells - Lysozyme, (b) apical tight junctions – Zo1, (c) goblet cells – Muc2 and (d) enterocytes – Vil1. Data presented as mean ± SD, from three independent experiments. Statistical significance was calculated using a 2-tailed student t-test. * denotes p < 0.05.*

Previous observations in both human colonic cells and murine organoids demonstrated an ability of *B. vulgatus* conditioned media to alter the gene expression of components in the Wnt/β-catenin pathway, this however was not seen in almost matured organoids treated acutely with conditioned media (**Figure 3.27 a-b**). Potential alterations in the expression of *Axin2* and *Tcf4* were not significant due to the high variability of expression in the controls. In agreement with previous findings in the developing organoids,

Smad5 but also smad4, both components in the BMP pathway, exhibited significantly decreased expression upon *B. vulgatus* conditioned media treatment, as did *Ccnd1*, a proliferative marker where decreased expression is important for differentiation (**Figure 3.27 c-e**) (Nishi *et al.*, 2009). Taken together these observations suggest that acute treatment of almost mature organoids with *B. vulgatus* conditioned media may push the almost mature organoids into a proliferative state.

The transcription factors *Hes1 and Atoh1* expression were unchanged following acute exposure to *B. vulgatus* conditioned media but Sox9, responsible for Paneth cell differentiation, expression was reduced (P = 0.055) relative to control (**Figure 3.27 f-h**). This implies that Paneth cell differentiation may have been impacted by acute exposure to *B. vulgatus* conditioned media and, as Paneth cells have a pivotal role in both proliferation and epithelial cell lineage determination, this may have a subtle impact on intestinal epithelium homeostasis.
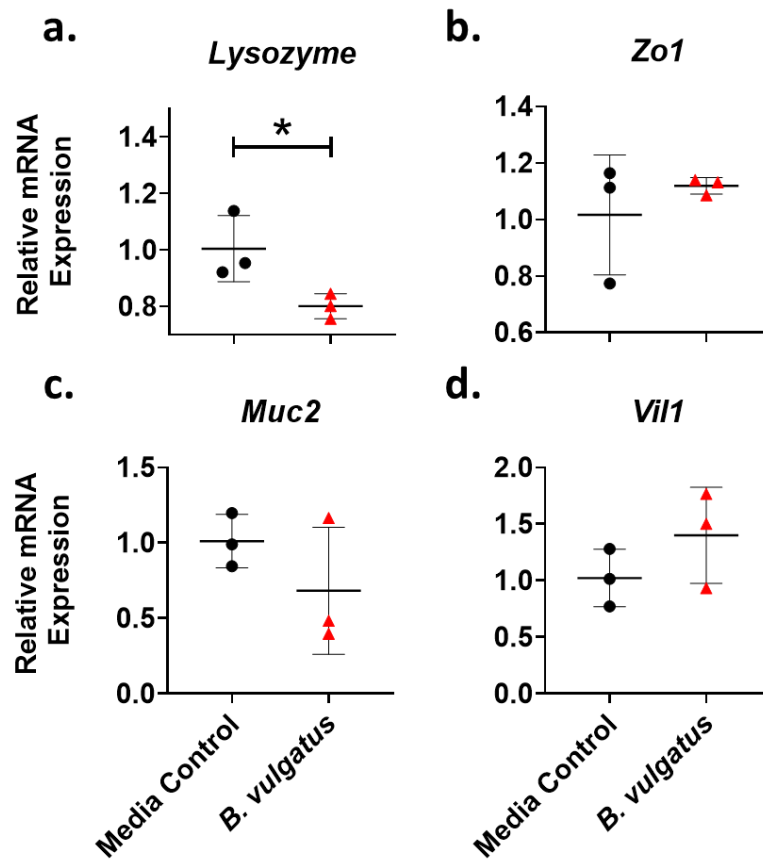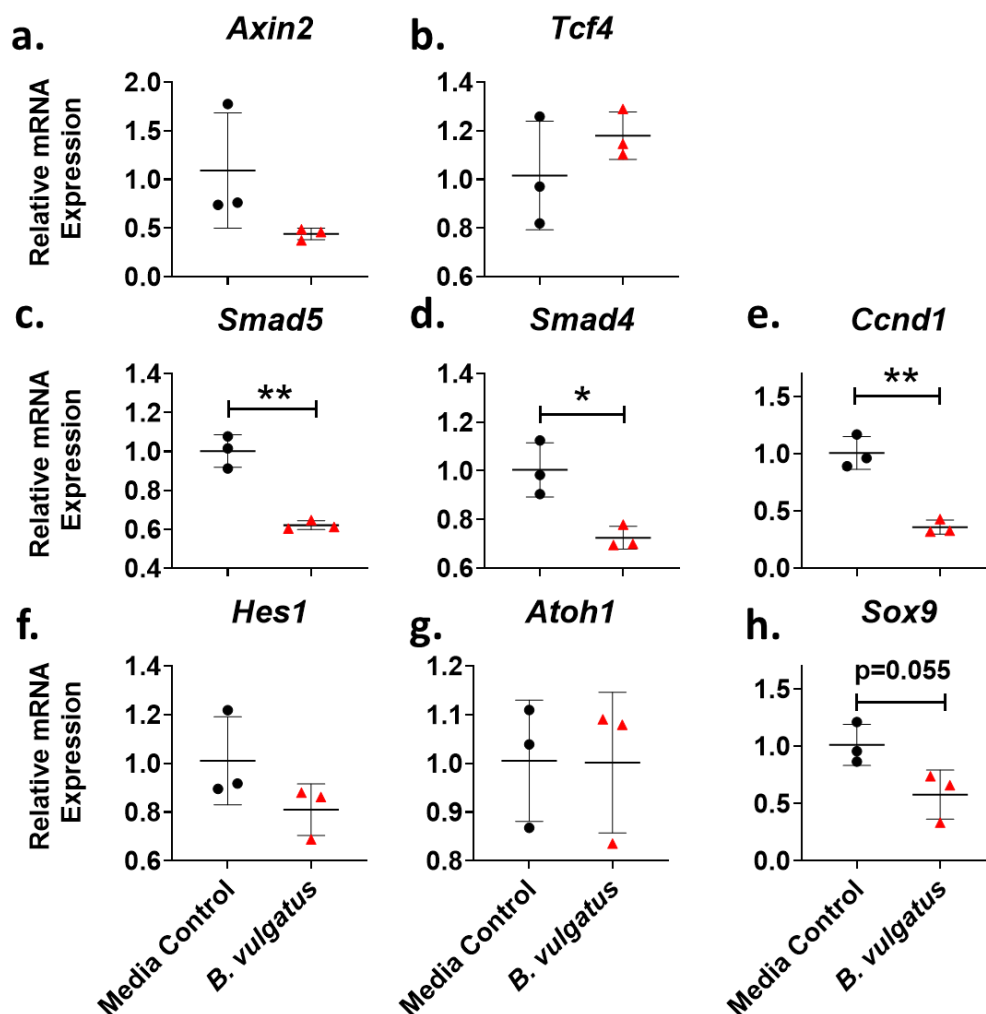
Figure 3.27 Acute effect of Bacteroides vulgatus conditioned media on the gene expression of stem cell niche signalling markers in mature small intestinal organoids. At day 6 of organoid development, nearly matured organoids were cocultured with stationary phase B. vulgatus conditioned media for 24 hrs, followed by assessment by qRT-PCR of markers of (a-b) the Wnt/β-catenin signalling – Axin2 and Tcf4, (c-d) BMP signalling – Smad5 and Smad4, (e) cell cycle – Ccnd1, and (f-h) epithelial cell lineage determination Hes-1 (absorptive lineage), Atoh-1 (secretory lineage) and Sox9 (Paneth cells differentiation). Data presented as mean ± SD, from three independent experiments. Statistical significance was calculated using a 2-tailed student t-test. * and ** denote p < 0.05 and 0.01 respectively.

3.3.6 *In-vivo* impact of proinflammatory *Bacteroides* species in wild-type C57B/6 mice

In-vitro and *ex-vivo* studies described in the previous sections demonstrated that *Bacteroides* species and/or their secreted products/metabolites influenced the expression of genes related to inflammation and epithelial homeostasis in human colonic cells and murine intestinal organoids. While these models can give insight into the mechanisms regulated by specific stimuli such as specific bacteria strains/metabolites, they are simple models lacking the complexity present in the gastrointestinal tract characterised by the interaction between the host's own cells and the full microbiota.

To fully assess the impact of CD-associated *Bacteroides* species on gut inflammation and homeostasis in a whole animal i.e., wild-type mice, *B. vulgatus* and *B. fragilis* were chosen, as these were demonstrated as the most proinflammatory species in the colonic cell line and organoids. *Bacteroides* species have shown poor ability to "supercolonise" mice if other *Bacteroides* are already occupying their niche (Lee *et al.*, 2013). To mitigate this and ensure colonisation with our species of interest an antibiotic cocktail was administered at the beginning of the experiment to deplete gut microbiota. Mice were treated with an antibiotic cocktail for 13 days followed by oral gavage for two days with either PBS or 10^9 cfu of *B. vulgatus* or *B. fragilis* and subsequent colonisation for 9 days before culling and harvesting of tissue for RNA isolation and RT-qPCR (**Figure 3.28**).
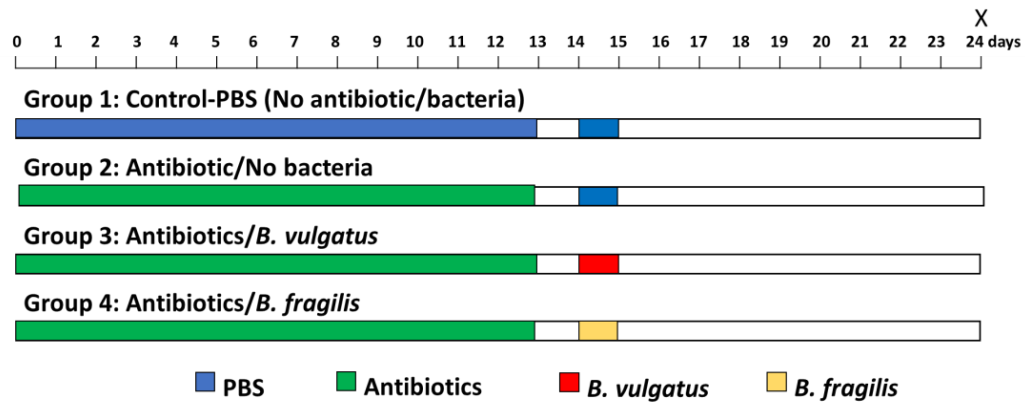
Figure 3.28 Schematic of study design in C57BL/6 wild type mice, to determine the metabolome and inflammatory modulating potential of the CD associated strains Bacteroides fragilis and Bacteroides vulgatus. Male mice were treated with an antibiotic cocktail (metronidazole 10mg/ml, vancomycin 5mg/ml, neomycin 5mg/ml and amphotericin B 0.1mg/ml), or vehicle (PBS), for 13 days via oral gavage and by ampicillin (1,000 mg/L) added to their drinking water followed by oral gavage of $1x10^9$ cfu/200µl of B. fragilis or B. vulgatus, or vehicle, for 2 consecutive days. Group 1 received no antibiotics or bacteria but received sham PBS oral gavage (n=5). Group 2 received antibiotics for 13 days followed by sham PBS oral gavage in lieu of Bacteroides spp (n=10). Group 3 received antibiotics for 13 days followed by oral gavage of B. fragilis (n=10). Group 4 received antibiotics for 13 days followed by oral gavage of B. vulgatus (n=10). During antibiotic treatment mice weights were recorded every 4 days. Animals were euthanized at day 24 post start and fluids, fecal, cecal and intestinal samples collected.

During antibiotic treatment, mice lose up to 5-8% body weight compared to control mice (**Figure 3.29**), which is in line with previous studies in the laboratory (Rossini et al., manuscript in preparation).
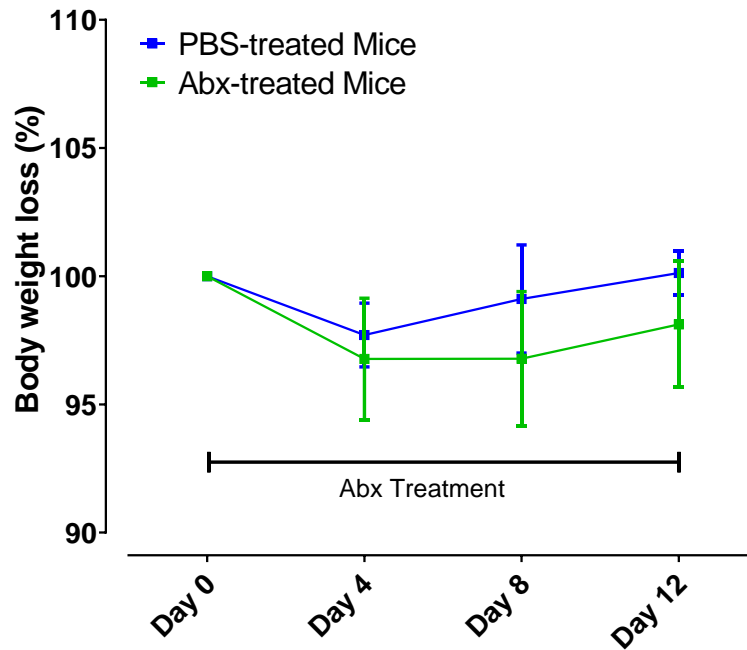
Figure 3.29 Body weight monitoring during 13-day antibiotic treatment of C57BL/6 mice. Male mice were orally gavaged for 13 days with a full spectrum antibiotic cocktail consisting of 10 mg/mL metronidazole, 5 mg/mL vancomycin, 5 mg/mL neomycin, and 0.1 mg/mL amphotericin B and 1,000 mg/L ampicillin, added to drinking water. Body weight was recorded every 4th day. Data presented as mean ± SD, n=5-10 mice per group.

At the end of the experiment colon, cecum and spleen weight were assessed for evidence of inflammation. No difference in body weight change, cecum or spleen weight between the groups was observed at the end of the study (day 24, **Figure 3.30 a, c, d, and e**). The relative weight of the distal colon was not significantly affected by *Bacteroides* gavage while the proximal colon weight was significantly increased in mice gavaged with *B. fragilis* versus antibiotic control indicating the presence of inflammation **(Figure 3.30 b)**. With this observation, we focused on the exploration of gene expression in the proximal colon.

a.

b. **c.**

d. **e.**
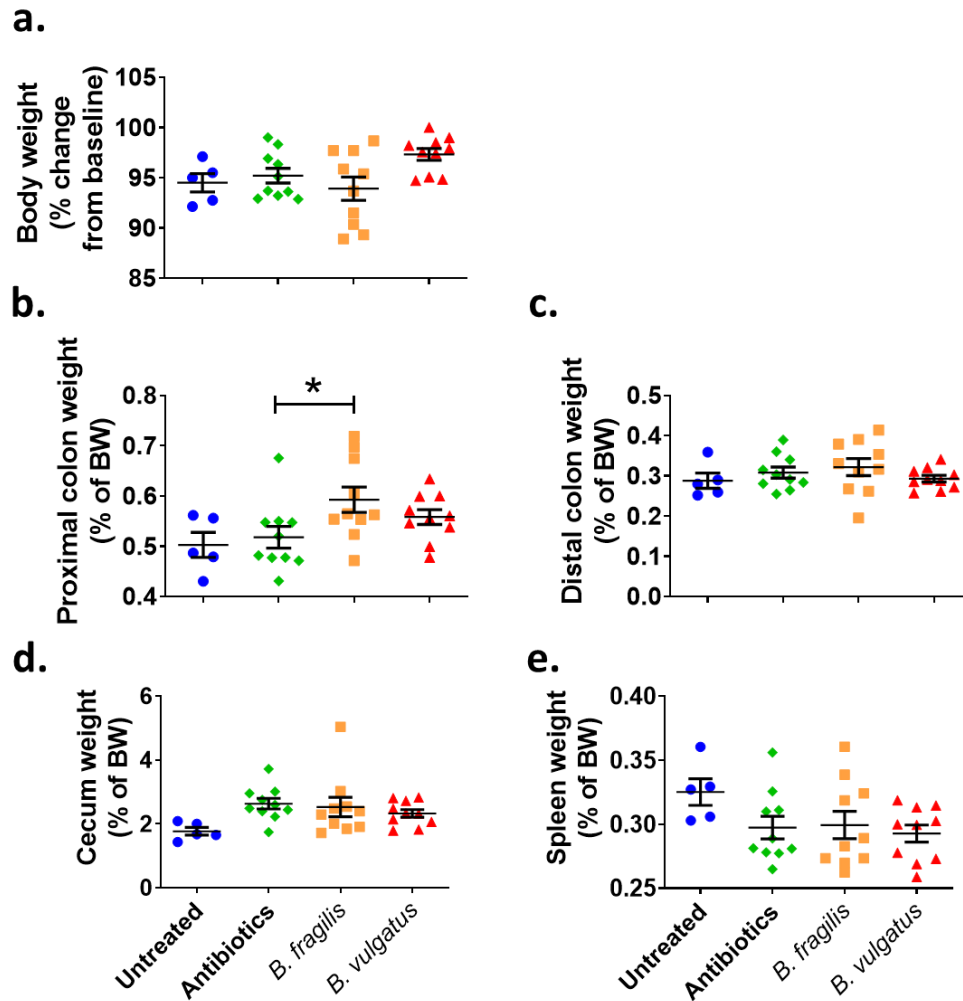
Figure 3.30 Physiological parameters of wild type mice following inoculation with Bacteroides fragilis and Bacteroides vulgatus. Male mice were orally gavaged for 13 days with a full spectrum antibiotic cocktail consisting of 10 mg/mL metronidazole, 5 mg/mL vancomycin, 5 mg/mL neomycin, and 0.1 mg/mL amphotericin B and 1,000 mg/L ampicillin, added to drinking water followed by oral gavage with B. fragilis and B. vulgatus (10^9 cfu) for 2 consecutive days. On day 24, the following parameters were assessed, (a) % Body weight loss (b) relative weights of proximal colon, (c) distal colon, (d) cecum, and (e) spleen. Data presented as mean ± SD, n= 5-10 mice per group. Statistical significance was calculated using one-way ANOVA with Dunnett's post-hoc test. * denotes p < 0.05.

To evaluate the effects of colonisation with *Bacteroides* species on colonic tissue we assayed for genes related to inflammation (*Inos, Cxcl2, Cccl20, Ifnγ, Il-6*, and *IL-17a*) and representative of innate and adaptive immune cell response **(Figure 3.31 a-f)**, epithelial cell-type markers including *Lysozyme* (Paneth cells), *Chromogranin A* (CHGA, enteroendocrine cells), *Muc2*

189

(Goblet cells), *Vil1* (enterocytes), *Zo-1* (tight junction protein) and *Klf4* (proliferation) **(Figure 3.32 a-f)** and stem-cell niche signalling genes including *Lrg5, Axin2* and *Smad5* **(Figure 3.33 a-c)**. For all these genes analysed, there was no significant change provoked by either of the *Bacteroides* strains when compared to the antibiotic control. While *in-vitro* and *ex-vivo* studies demonstrated that both *B. vulgatus* and *B. fragilis* altered gene expression related to inflammation and epithelial homeostasis this was not reproduced in wild-type mice colonised for 2 weeks with these bacteria.
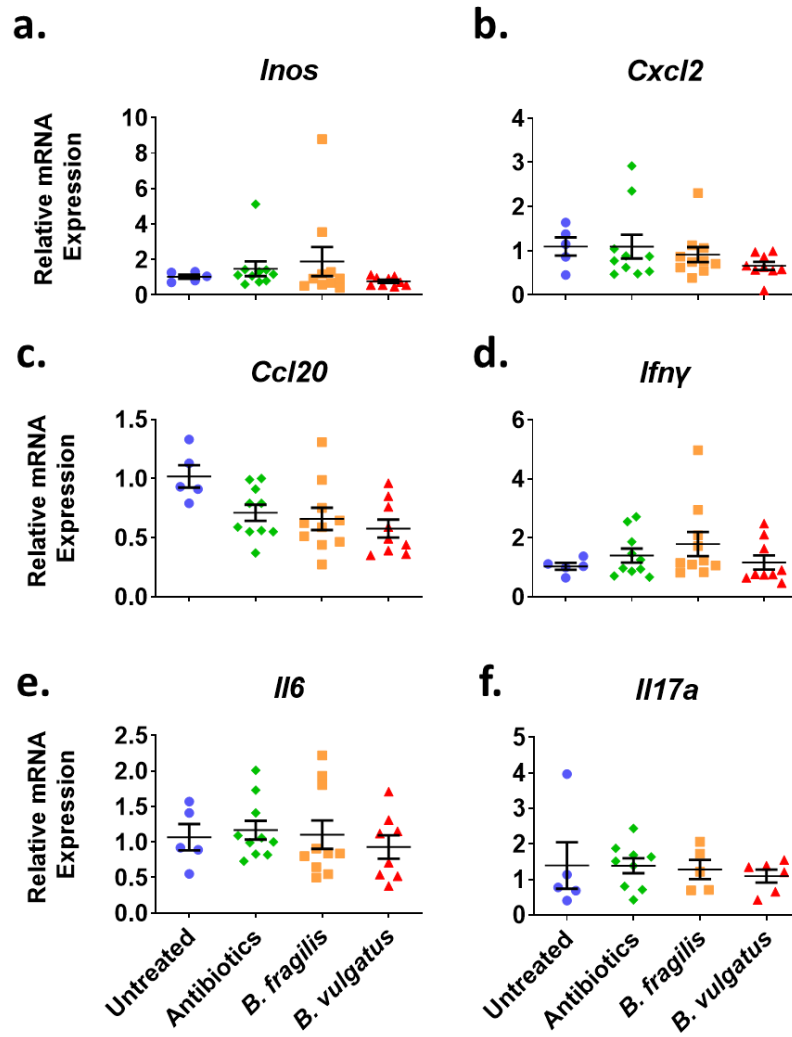
Figure 3.31 Gene expression analysis of colonic inflammatory markers of wild type mice colonised with Bacteroides species. Male mice were orally gavaged for 13 days with a full spectrum antibiotic cocktail consisting of 10 mg/mL metronidazole, 5 mg/mL vancomycin, 5 mg/mL neomycin, and 0.1 mg/mL amphotericin B and 1,000 mg/L ampicillin added to drinking water followed by oral gavage with B. fragilis and B. vulgatus (10^9 cfu) for 2 consecutive days. On day 24 colons were collected and assayed for the expression of (a) Inos, (b) Cxcl2, (c) Ccl20, (d) Ifnγ, (e) Il6, and (f) Il17a by RT-qPCR Data presented as mean ± SD, n=5-10 per group. Statistical significance was calculated using one-way ANOVA with Dunnett's post-hoc test.
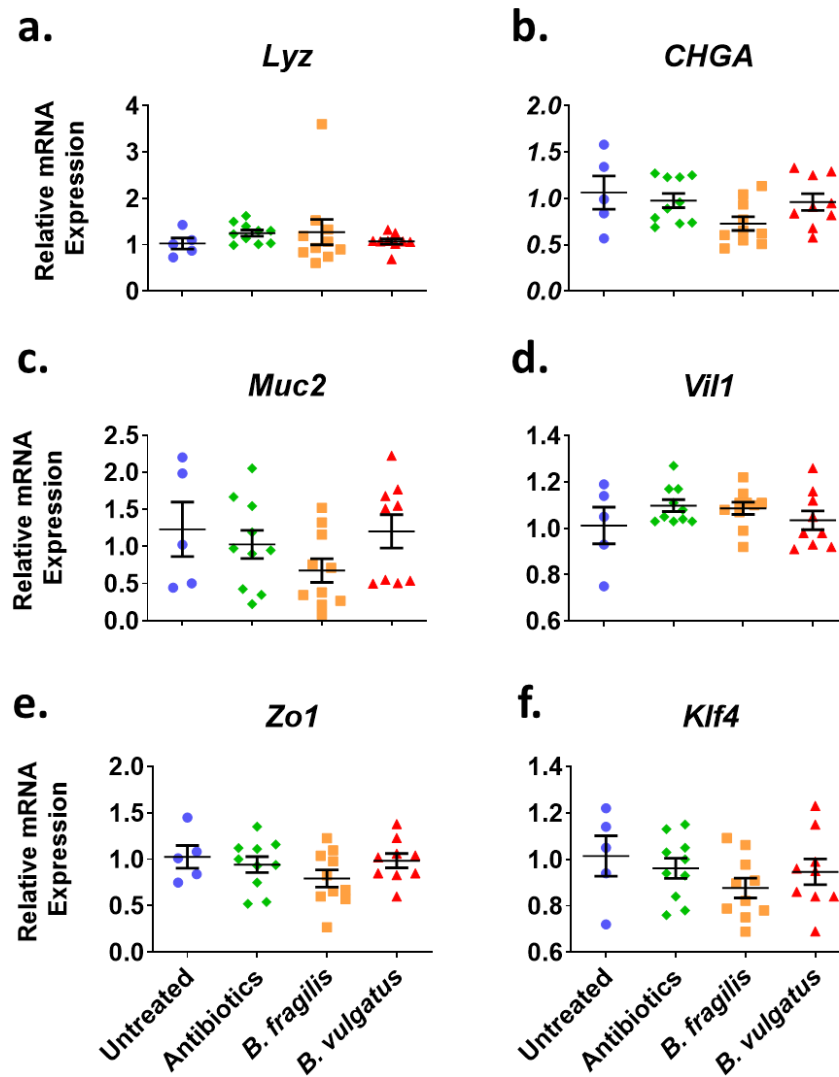
Figure 3.32 Gene expression analysis of colonic epithelial cell lineage of wild type mice colonised with Bacteroides species. Male mice were orally gavaged for 13 days with a full spectrum antibiotic cocktail consisting of 10 mg/mL metronidazole, 5 mg/mL vancomycin, 5 mg/mL neomycin, and 0.1 mg/mL amphotericin B and 1,000 mg/L ampicillin added to drinking water followed by oral gavage with B. fragilis and B. vulgatus (10^9 cfu) for 2 consecutive days. On day 24 colons were collected and assayed for the expression of (a) Lysozyme (Lyz, Paneth cells); (b) Chromogranin A (Chga, enteroendocrine cells; (c) Muc2 (goblet cells); (d) Villin1 (Vil1, enterocytes); (e) Zo-1 (tight junction protein); (f) Klf4 (proliferation marker) by RT-qPCR. Data presented as mean ± SD, n=5-10 mice per group. Statistical significance was calculated using one-way ANOVA with Dunnett's post-hoc test.
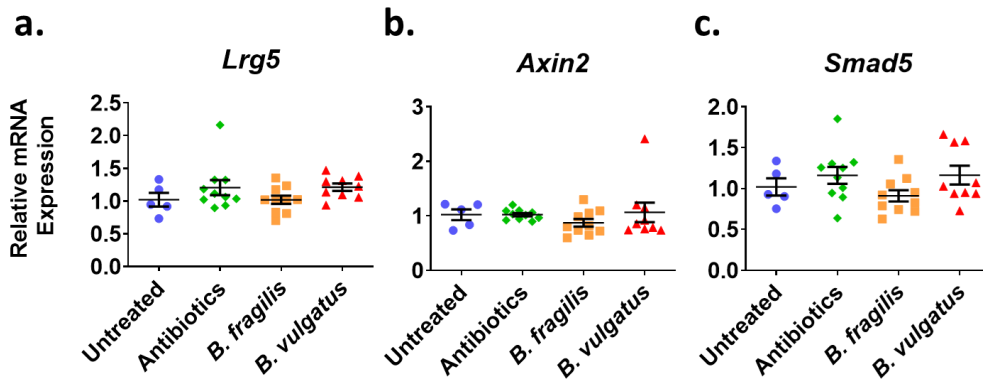
Figure 3.33 Gene expression analysis of colonic epithelial stem cell niche signalling of wild type mice colonised with Bacteroides species. Male mice were orally gavaged for 13 days with a full spectrum antibiotic cocktail consisting of 10 mg/mL metronidazole, 5 mg/mL vancomycin, 5 mg/mL neomycin, and 0.1 mg/mL amphotericin B and 1,000 mg/L ampicillin added to drinking water followed by oral gavage with B. fragilis and B. vulgatus (10^9 cfu) for 2 consecutive days. On day 24 colons were collected and assayed for the expression of (a) Lrg5 (stem cells); (b) Axin2 (Wnt/β-catenin signalling) and (c) Smad5 (BMP-signalling). Data presented as mean ± SD, n = 5-10 mice per group. Statistical significance was calculated using one-way ANOVA with Dunnett's post-hoc test.

3.4 Discussion

In this chapter, we hypothesise that our recent findings on the increased abundance of mucosal-associated *Bacteroides* species (*B. fragilis* and *B. vulgatus*) in patients with active CD have pro-inflammatory traits relevant to the pathophysiology of CD. We demonstrate that whole *Bacteroides* species, and their metabolites can induce host gene expression for inflammatory genes associated with NF-κB-activity with a concomitant increase in chemokine production. This seems to happen while the species are also altering the expression of genes related to epithelial homeostasis including members of the Wnt/β-catenin and BMP-pathways in a human colon cell line and murine organoids. However, these effects were not replicated in wild-type mice colonised with *B. fragilis* or *B. vulgatus* for 2 weeks.

While the literature is highly conflicted on the potential role of *Bacteroides* species in CD pathology our recent publication on an Irish IBD cohort indicated a potential involvement of *B. fragilis* and *B. vulgatus* in CD pathogenesis (Ryan *et al.*, 2020). Much of the focus on the role of *B. fragilis* in CD has been on its enterotoxin-producing strain. However, recent research has demonstrated that only 11.4% of *B. fragilis* strains in active CD possessed this virulence factor with no significant difference when compared to healthy controls (Becker *et al.*, 2021). The potential role of *B. vulgatus* in CD has been previously demonstrated in a study showing that deletion of NOD2, a CD susceptibility gene, results in the expansion of *B. vulgatus* resulting in inflammation and abnormalities in the intestinal

epithelium (Ramanan *et al.*, 2014a). In contrast, the literature is in much closer agreement that *B. thetaiotaomicron* has an ameliorating effect on GIT inflammation hence its inclusion as a negative *Bacteroides* control in this study (Delday *et al.*, 2019a).

During homeostasis, the presence of an intact mucus layer prevents the direct association of the gut microbiota with the epithelium. However, bacterially generated metabolites are free to diffuse through the mucus layer to interact with the epithelium. Also, Gram-negative bacteria, including *Bacteroides* species, are known producers of outer membrane vesicles (OMVs, nano-sized particles which can diffuse through the mucus to interact with the epithelium) that are increasingly recognised as a key mode of communication between bacteria and the host (Kulp and Kuehn, 2010).

In determining the inflammatory potential of CD-associated *Bacteroides* species we investigated the impact of both *Bacteroides*-derived metabolites and direct bacteria-host interactions through the application of cell-free bacterial conditioned media and co-culture with live bacterial cells to a C2BBe1 cell line respectively. These studies demonstrated that *Bacteroides* species metabolites induced expression of proinflammatory chemokines and that this was in a species and growth phase dependent manner.

Our data show that conditioned media from *B. vulgatus* in the stationary phase of growth preferentially increased gene expression of subunits in the NF-κB inflammatory pathway. This contradicts previous observations where *B. vulgatus* conditioned media was shown to inhibit activation of the NF-κB pathway (Blottière *et al.*, 2011). This study looked at the effects of conditioned media from commensals in two NF-κB-SEAP reporter cell lines,

HT-29 and CaCo2. They observed no effect on NF-κB activation in the HT-29 reporter cells but *B. vulgatus* conditioned media inhibited NF-κB activation in the CaCo2 reporter cell line upon TNF-activation. The discrepancies in published findings and our results on *B. vulgatus* conditioned media may be due to fundamental differences in the cell lines and culture conditions utilised i.e., we used C2BBe1 cells with a 1:1 dilution compared to CaCo2 cells and 10% v/v of conditioned media. A more recent study with late-stage stationary phase conditioned media from *B. vulgatus* activated the NF-κB pathway and secretion of IL-8 and CXCL10 in the HT-29 reporter cell line, which is partly in agreement with our data (Ó Cuív *et al.*, 2017). This increase in NF-κB activation and IL-8 expression was postulated to be due to the increased presence of a highly conserved *Bacteroides* permease in late stationary phase conditioned media (Ó Cuív *et al.*, 2017). Our gene expression data agree with this assumption, but our protein data disagrees as increased IL-8 secretion was only detected on *B. vulgatus* conditioned media from the exponential phase of growth. Our observation that *B. vulgatus* conditioned media can induce gene expression and production of the chemokine CCL20 appears to constitute a novel observation and could be relevant for Th17 migration associated with CD (Li *et al.*, 2013). A possible mechanism for the impact of conditioned media on NF-κB activation is the presence of OMVs. There is a lack of research on *B. vulgatus* OMVs with only one paper reporting OMV-mediated immune silencing in DCs (Maerz *et al.*, 2018). However, *B. vulgatus* OMVs likely contain LPS, which recently was shown to activate NF-κB and stimulate IL-8 production (Di Lorenzo *et al.*, 2020).

Co-culture of epithelial cells with whole, live *B. vulgatus* did not induce expression of any subunits in the NF-κB pathway, although an increase in the gene expression of the chemokines IL-8 and CCL20 with a concomitant chemokine production was observed, suggesting NFkB activation has happened. This discrepancy in NF-κB gene expression between conditioned media and whole bacteria co-culture may be explained by the type of stimulation each represents and culture time (24 vs 8 hrs, respectively). The conditioned media constitutes a complex and broad stimulation being composed of numerous unidentified compounds with unknown immunogenicity, which may be eliciting differing effects in multiple pathways. Whereas co-culture with live *B. vulgatus* is a more direct stimulation resulting from the recognition of the bacteria by PRRs. Indeed, research from our group has shown that increased IL-8 gene expression in response to live Adherent and Invasive *Escherichia coli* (AIEC) occurs rapidly with the response diminishing over time (Saiz-Gonzalo *et al.*, 2021). Our observation that *B. vulgatus* co-culture with epithelial cells increases IL-8 expression and production contrasts with the literature. Haller and colleagues demonstrated that *B. vulgatus* did not alter basal IL-8 secretion in HT-29/MTX cells, reflective of mucus-producing cells and enterocytes (Haller *et al.*, 2004), with a more recent study confirming the same observation in HT-29 cells (Pathmanathan *et al.*, 2020). As discussed above Lakhdari et al. demonstrated that HT-29 cells were unresponsive to conditioned media from *B. vulgatus,* but CaCo2 cells were responsive. Differences seen in the literature may be due to the heterogeneity seen among epithelial cell lines e.g., CaCO2 and C2BBe1 cells can form a

polarized monolayer comparable to that of the human intestine (Peterson and Mooseker, 1992; Verhoeckx *et al.*, 2015); HT-29/MTX cells are reflective of mucus-producing cells and enterocytes and HT-29 cells are considered as a pluripotent undifferentiated cell line (Martínez-Maqueda, Miralles and Recio, 2015). Due to the undifferentiated status, HT-29 cells may lack the cellular machinery to detect *B. vulgatus* or its excreted metabolites whereas C2BBe1 cells do. Similarly, to *B. vulgatus* conditioned media, co-culture with whole *B. vulgatus* cells also induced expression and production of CCL20 in C2BBe1 cells, which is contrary to one previous study (Sierro *et al.*, 2001). Our observation that *B. vulgatus* conditioned media increased expression of the Wnt target gene Tcf4 indicated the potential of *B. vulgatus* excreted products to alter proliferation and epithelial lineage determination and warranted further investigation. In line with this assumption, small intestinal organoids grown in the presence of *B. vulgatus* conditioned media showed a decrease in Axin2, a member of the β-catenin destruction complex, and Smad5, a component in the BMP pathway indicating a shift towards proliferation with less differentiation. To the best of our knowledge, these observations are novel, in the context of *Bacteroides* and suggest that excreted metabolites, which may cross the intestinal barrier may impact signalling pathways crucial in the renewal and composition of the epithelium. To expand on this, an acute application of a higher concentration of *B. vulgatus* conditioned media also resulted in a significant decrease in Smad4, Smad5, and Cyclin D1 expression, indicating impaired differentiation and increased proliferation in the epithelium. Indeed, it appeared that acute application of *B. vulgatus*

conditioned media impaired the differentiation of Paneth cells as seen by the reduction in the expression of its cell marker lysozyme as well as the lineage determination gene Sox9 with Paneth cell dysfunction being linked to paediatric CD (Perminow *et al.*, 2010).

As previously stated, much of the research on *B. fragilis* research has been conducted using enterotoxin-producing strains and while increased abundances of *B. fragilis* are associated with CD flares the presence of this virulence factor does not correlate with exacerbation of CD (Becker *et al.*, 2021). There is much work showing the deleterious effects of *B. fragilis* enterotoxin (BFT) *in vitro*, as such, we utilised a non-BFT (NBFT) strain to investigate the inflammatory potential of *B. fragilis*, and its metabolites, in a more CD-relevant context. *B. fragilis* conditioned media increased expression of subunits in the JAK/STAT pathway without induction of associated chemokines CXCL10 and CCL5, while the whole cell co-culture of *B. fragilis* did not alter any of these genes. While BFT *B. fragilis* has been observed to increase activation of STAT3 (Wick *et al.*, 2014), we believe that our result of NBFT *B. fragilis* inducing expression of JAK/STAT subunits to be novel. This suggests that, while excreted products from *B. fragilis* do not alter the expression of chemokines in the JAK/STAT pathway they may play a role in modulating its signalling which may have implications during times of inflammation such as CD exacerbations. Unlike *B. vulgatus* much research has been conducted on *B. fragilis* OMVs, a major component being polysaccharide A (PSA). *B. fragilis* OMVs containing PSA have demonstrated immunomodulatory properties in epithelial cells where low concentrations decrease TLR4 transcription while higher concentrations

increase it (Badi *et al.*, 2019). *B. fragilis* PSA has also shown it can increase the production of the anti-inflammatory cytokine IL-10 (Rubtsov *et al.*, 2008), suggesting that the increased expression in inflammatory pathway components may be immunomodulatory and not pro-inflammatory.

Similar to *B. vulgatus, B. fragilis* conditioned media also demonstrated an ability to increase expression of the downstream effector of the Wnt/β-catenin pathway, Tcf4 and we obtained similar results with *B. fragilis* conditioned media on small intestinal organoids. Overall, this suggests that the ability of *Bacteroides* conditioned media to alter the expression of components in proliferation/differentiation pathways may not be species-specific and represents a broader ability of the *Bacteroides* genus to communicate with the host and influence epithelial proliferation and differentiation.

When we wanted to translate the *in vitro* and *ex vivo* findings of the Bacteroides strains to an in-*vivo,* setting, neither *B. fragilis* nor *B. vulgatus* induce expression of inflammatory or epithelial homeostatic genes. This result is in line with a previous study demonstrating that *B. vulgatus* does not induce colitis in a genetically intact host but did in an IL10r2KO mouse (Bloom *et al.*, 2011a). Furthermore, in a germ-free rabbit model *B. vulgatus* induced inflammation in the appendix (Shanmugam *et al.*, 2005) and *B. vulgatus* induced inflammation in an IL10KO mouse with disrupted barrier function (Sydora *et al.*, 2007). While the anti-inflammatory effects of *B. fragilis* PSA are mediated by the CD risk-associated genes ATG16L1 and NOD2, this anti-inflammatory effect was disrupted by the deletion of these genes (Chu *et al.*, 2016b). These observations suggest that in a genetically

intact host with a functional epithelial barrier CD-associated *Bacteroides* species function as commensals, while only in a genetically compromised host these *Bacteroides* species can induce inflammation.

In summary, our data demonstrate that certain *Bacteroides* species and their metabolites can induce the production of CD-associated chemokines and influence the renewal and homeostatic functioning of the gastrointestinal epithelium. These properties may represent an immunomodulatory role in a genetically sound individual where these *Bacteroides* species act as commensals. However, in a genetically susceptible individual, such as a CD patient or a patient predisposed to intestinal inflammation, these properties may play a role in driving or exacerbating inflammation.

Chapter 4 Bile acid modification is selective for *Bacteroides* species, *in vivo* and *in vitro*

4.1 Abstract

Numerous lines of evidence have pointed to differential colonization and associations with Bacteroidetes in the incidence of diseases including obesity and IBD. There is a myriad of literature to associate bile acid (BA) changes with IBD outcomes and indeed flare-ups in recent years. In silico analysis has identified certain bile acid metabolizing enzymes including bile salt hydrolases (BSHs) and hydroxysteroid dehydrogenases (HSDHs). At the time this work was initiated, only early protein purification of one BSH from one *Bacteroides* species had been characterized. This chapter aimed to understand the BA metabolizing ability of three strains of *Bacteroides*, with a focus on the BSH enzymes that they carry. In contrast to existing work, we identified conserved residues in the predicted BSH proteins from all 3 species. We verified their activity and tested whole-cell activity against individual liberated bile acids to examine modifications downstream from BSH. We show that two strains *B. fragilis* and *B. thetaiotaomicron* show identical BA modifying ability in contrast to *B. vulgatus,* which was selective for conjugated BA substrates and for modifications to single freed BA. In introducing *B. vulgatus* to wild-type mice, subtle effects on BA metabolism were evident. Indeed, it is not clear that these effects are simply related to the strain. Instead, we saw a dominant effect by antibiotic cocktail usage, which may also have translated to *B. vulgatus* colonization, or which may have provided other opportunities for microbial dysrepresentation or outgrowth in the gastrointestinal tract.

4.2 Introduction

In the previous chapter, we showed that phylum Bacteroidetes representatives, and their associated exudates could impact gut epithelial functions in a growth phase dependant and strain-dependent manner. However, there is a range of other properties associated to Bacteroidetes. Bacteroidetes are recognised as important early life colonizers and influencers in gut development and gut barrier function maintenance (Wrzosek *et al.*, 2013) They are capable of producing a myriad of metabolites to influence gut homeostasis and colonization including glycan synthesis (Coyne *et al.*, 2008) and its degradation (Rinninella *et al.*, 2019) to aid mucin interactions (Marcobal *et al.*, 2013), outer membrane vesicle (OMV) production as signalling entities that provide nutrition, they communicate extrachromosomal DNA, inform for biofilm development that protects from antimicrobial onslaught (Jones *et al.*, 2020). Although second-line gut colonizers, members of the genus *Bacteroides* are particularly prevalent in children and indeed *B. ovatus*, *B. fragilis, B. thetaiotaomicron* and, *B. xylanisolvens* appear dominant representations of *Bacteroides* in childhood (Zhong *et al.*, 2019). Interestingly, a larger prevalence of *Bacteroides* spp. appears in the gut of children once facultative anaerobes have established the first line of succession and established an oxygen gradient. These strict anaerobes are depleted in children living with autism (Dan *et al.*, 2020). In fact, males enriched for *Bacteroides* at 12 months (n=206) of age were reported as elevated in cognition, language, motor skills and general development (Canadian Healthy Infant Longitudinal Development (CHILD) Cohort study (Tamana *et al.*, 2021)).

While *B. thetaiotaomicron* is considered the dominant species of *Bacteroides* in infants, along with *B. fragilis,* and *B. vulgatus* they are common representatives in the adult gut and their levels can be modulated by diet (Conlon and Bird, 2014). Amongst the range of metabolites associated with *Bacteroides* are various lipid-derived species including signalling sphingolipids (Gareau *et al.*, 2011), SCFAs, propionate, (Jakobsson *et al.*, 2014) and butyrate (Wrzosek *et al.*, 2013) implicated in influencing cell development (Willemsen *et al.*, 2003), barrier function (Gaudier *et al.*, 2004) and HDACs (Wilson *et al.*, 2010), they are also associated with the production of a range of vitamins and essential co-factors (Carlson *et al.*, 2018).

Indeed, in a meta-analysis study (n=9 relevant studies from 63), (Zhou and Zhi, 2016b) recognised a deficiency in the representation of *Bacteroides* in IBDs, where their representation was reported as even lower, in cases with flare-ups for both UC and CD. At the same time, UC sufferers were reportedly enriched for *B. fragilis* species (Zamani *et al.*, 2017) while in the DSS animal model of colitis *Bacteroides thetaiotaomicron* was shown to dampen inflammation, an effect that authors attributed to a PLP, a pyrin-like protein which they purified and applied to activated cell lines to reduce NF KB levels (Delday *et al.*, 2019b). The latter incited debate, on metabolites and cross signalling that may be attributed to *Bacteroides* in a strain-specific manner, that might be beneficial in the disease context including in the context of IBDs.

At the time of the inception of this work, we were interested in the functional metabolites that could be produced by members of the *Bacteroides* genus. To this point we were aware that a differential in IBDs interrogation of the Human Microbiome Project and the MetaHit consortium determined a lower representation of bile acid metabolizing enzymes bile salt hydrolases (BSHs), dehydroxylation enzymes (they termed ADHs) and in hydroxysteroid dehydrogenases (HSDH) including those from *Bacteroides*, to discriminate UC from CD (Labbé *et al.*, 2014). Interestingly, in examining the modifications to bile acids (BAs) they documented that a range of intermediate BAs en route to full secondary BAs could be enriched from BSH amino acid freed CDCA towards LCA (Lepercq *et al.*, 2004) and from amino acid freed CA towards DCA (Staley *et al.*, 2017). Interestingly, BAs, while lipid emulsifiers, can be assigned a range of moiety-dependent roles, to influence metabolism, gut colonization and colonization resistance and indeed gut homeostasis and immune status ((Joyce, MacSharry, *et al.*, 2014c); (Sayin *et al.*, 2013); (Begley *et al.*, 2005b); reviewed by (Quadrilatero and Hoffman-Goetz, 2003)). In fact, the latter authors suggested a link for secondary BAs (LCA and DCA) to colorectal cancer, a condition associated with colitis as colitis-associated cancer (CAC).

In our interrogations of *Bacteroides* spp, at this time, we found no evidence of a classical and complete *bai* operon (Kang *et al.*, 2008) to produce mature secondary BAs amongst members. Indeed, instead, we found evidence of BA intermediate (oxo, allo and keto, iso, uro forms of BAs) formation that could be attributed to *Bacteroides* spp. among others, including for *B.*

intestinalis species (Fukiya *et al.*, 2009). Indeed, 7α-HSDH activity is associated with *B. fragilis* and *B. thetaiotaomicron* (Sherrod and Hylemon, 1977; Bennett, McKnight and Coleman, 2003). Furthermore, (Duboc *et al.*, 2013b) first reported actual BA dysmetabolism in IBD, they reported reduced conversions to secondary BAs as a feature of IBD. Indeed, more recently through *in silico* analysis, (Heinken *et al.*, 2019), implicated BA reduced amide deconjugation (via BSHs,) accompanied by reduced secondary BAs, predicting that reduced levels of 12-dehydrocholate would feature in an IBD context. Among 223 AGORA microbial genomes (773 in total) interrogated by these authors, *Bacteroides* conversions were limited to BSH activity and 7α-HSDH and 12 α-HSDH activity, this would limit BA moieties here to just 7-Keto CA/CDCA and 12-dehydroCA/CDCA. The potential for synteny, among microbes for BA conversions, here was noted.

The importance and recognition of BAs as central to metabolism, central to signalling functions, engaged in circadian rhythms, and controlled, in part by them, was being recognised when this study began. Furthermore, given the suggested roles of BAs in early colonization and cell differentiation events including apoptosis and apoptosis resistance, and the possible link to inflammation through MYD88 (Duparc *et al.*, 2017), the ability of BAs to interact with receptors central to inflammation (reviewed by (Alatshan and Benkő, 2021) as well as deficiencies in conversions of BAs predicted and associated to IBDs, exploration of actual BA modification and metabolism by key *Bacteroides* species associated with IBDs was undertaken.

We hypothesized that *Bacteroides* species, differentially abundant in IBDs, could alter BAs at the species levels for different moiety specificity and hence signalling outcomes. In this chapter, we aimed to identify species-specific substrates and conversions with the aim to examine whether these conversions could alter gut functions *in vitro* and translate *in vivo*. When this work was initiated, and to the present day, *Bacteroides* BA modifications were neither experimentally verified *en mass*, nor explored sufficiently at a species level. In fact, specificity was reported for *B. vulgatus* to select Tauro conjugates, specifically, taurochenodeoxycholic acid (TCDCA human) and tauro beta muricholic acid (TβMCA murine) (Chikai, Nakao and Uchida, 1987; Kawamoto, Horibe and Uchida, 1989).

4.3 Results

4.3.1 Comparative analysis of the structure and composition of BSH from *Bacteroides* indicates conservation of critical functional residues among active *Bacteroides* BSHs.

BSH (EC 3.5.1.24) is represented across the gut phyla (Jones *et al.*, 2008b) and in diverse environments including food fermentations (Prete *et al.*, 2020). We compared B. *vulgatus* ATCC 8482 and *B. fragilis* NCTC9343 BSH sequence, protein, and specificity relative to well classified and crystal structure elucidated *Lactobacillus salivarius* LGM14476, *Bifidobacteria longum* SBT2928 and *Clostridia perfringens* 13, listed in **Table 4.1 and 4.2** below according to sequence accession number and to their representative protein.

Table 4.1 Table of crystal structure established BSH proteins selected for relative comparison with Bacteroides fragilis BSH.

Strain	Substrate specificity	Nucleotide sequence Accession number	Amino Acid sequence Accession number
Phocaeicola vulgatus ATCC 8482	CDCA core preference	NC_009614.1:3441021-3442100	WP_032944961.1
Bacteroides fragilis NCTC 9343	Nonselective	NC_003228.3:1766014-1767093	WP_005797284.1
L. salivarius LGM14476	Taurine and Glycine deconjugation	FJ591082.1	ACL98204.1
B. longum SBT2928	Glycine deconjugation	AF148138	AAF67801.1
C. perfringens 13	Taurine deconjugation	U20191.1:69-1058	AAC43454.1

The amino acid sequence accession number is given as is the corresponding nucleotide sequence

Table 4.2 Comparative BSH amino acid sequence homology crystal structure established BSH proteins.

% homology	B. vulgatus ATCC 8482	B. fragilis NCTC 9343	L. salivarius LGM14476	B. longum SBT2928	C. perfringens 13
B. vulgatus ATCC 8482	100	52.81	26.25	28.12	31.48
B. fragilis NCTC 9343	52.81	100	24.14	25.32	31.89
L. salivarius LGM14476	26.25	24.14	100	37.70	34.15
B. longum SBT2928	28.12	25.32	37.70	100	35.33
C. perfringens 13	31.48	31.89	34.15	35.33	100

The % homology of amino acid sequences calculated using BLASTp

In comparison, both *Bacteroides* species appeared similar to each other based on amino acid sequence but only at 52% identity. Relatedness to established sequences was lower but varied between 24-25% and 26-28% in comparisons between lactic acid bacteria representations, and *B. fragilis* and *B. vulgatus* representative BSHs respectively. Increased homology was evident with Clostridium perfringens Although homology was low at the level of amino acid sequence in comparisons with LAB and with *Clostridia perfringens*, no comparative analysis to identify critical residues that may be related to activity has been applied for BSHs gram-negative bacteria carrying BSHs. Furthermore, the crystal structure of BSH from *Bacteroides* members has not been elucidated therefore we began our analysis using *Bacteroides* carrying single BSHs, where activity had been assigned,

although not thoroughly investigated for substrate specificity. To examine active *Bacteroides* BSHs, critical residues have been identified and predicted to conserve BSH enzymes activity between distantly related LAB species *Bifidobacterium longum* (Kumar *et al.*, 2006) and most recently *Lactobacillus salivarius* (Xu *et al.*, 2016) and *Clostridium perfringens* (Rossocha *et al.*, 2005)*,* had been compared and identified by (Lambert *et al.*, 2008)). They were established based on actual crystal structure and residue substitutions as well motifs and structural predictions and they are listed in **Table 4.3**.

Table 4.3 Catalytic and binding-pocket residues common to BSH family members

Residue	*Bif. longum*	*C. perfringens*	Bsh1, *Lb. plantarum*	Most common residue in family	Remarks
Catalytic					
2 (2)	C	C	C	C	Conserved
18 (18)	R	R	R	R	Conserved
21 (21)	D	D	D	D	Conserved
82 (82)	N	N	N	N	*Lb. gasseri*: S
177 (176)	N	N	N	N	Conserved
229 (229)	R	R	R	R	Conserved
Binding pocket: loop 1					
20 (20)	L	M	F	L, F	All very hydrophobic
22 (22)	W	I	Y	Y, L, W	All hydrophobic
24 (24)	F	Y	I	I, F	Mostly hydrophobic, but variable
26 (26)	Y	F	Y	Y, F	All hydrophobic
Binding pocket: loop 2					
58 (58)	G	G	T	G, A, S	Neutral to hydrophobic
59 (59)	V	T	A	A, V, I	All hydrophobic
61 (61)	M	F	V	M, V	Mostly hydrophobic, but variable
66 (66)	M	T	L	L	Mostly hydrophobic
68 (68)	F	A	Y	F, Y	All hydrophobic
103 (103)	F	Y	F	F, Y	All hydrophobic
Binding pocket: loop 3					
133 (133)	Deletion	I	F	F, I	All hydrophobic
137 (137)	Q	I	L	L	All hydrophobic
140 (140)	S	T	S	S, A	Neutral to hydrophobic
142 (142)	L	L	L	L	Conserved; very hydrophobic

Table from (Lambert *et al.*, 2008)

In comparisons of the amino acid residue positioning and sequence, interestingly 6 of 7 critical residues, Arg18 (R), Asp21 (D), Asn82 (N), Asn176 (N) and Arg229 (R) deemed essential for activity were conserved between *Bacteroides* BSHs examined, in line with crystal structure-based

predictions for LAB species and *C. perfringens* (**Figure 4.1**). Interestingly, Cys2, cysteine, an essential nucleophile for catalytic activity, was substituted with alanine (A), noting also that Arg18 and Asp21 normally arrange themselves through hydrogen binding to Cys2. The structure supports that Asn82 and Asn175 form the putative oxyanion hole and that Arg228 helps to stabilise the protein structure. There is a precedent for alanine and cysteine substitutions maintaining an active catalytic site even though the sulphur part of cysteine is not contained in alanine. (Kuiper, Klootwijk and Visser, 2002) described a similar catalytic sit substitution (C to A) in type II iodothyronine deiodinase, where active catalytic function remained unaltered. This substitution could therefore lack impact on *Bacteroides* BSH.
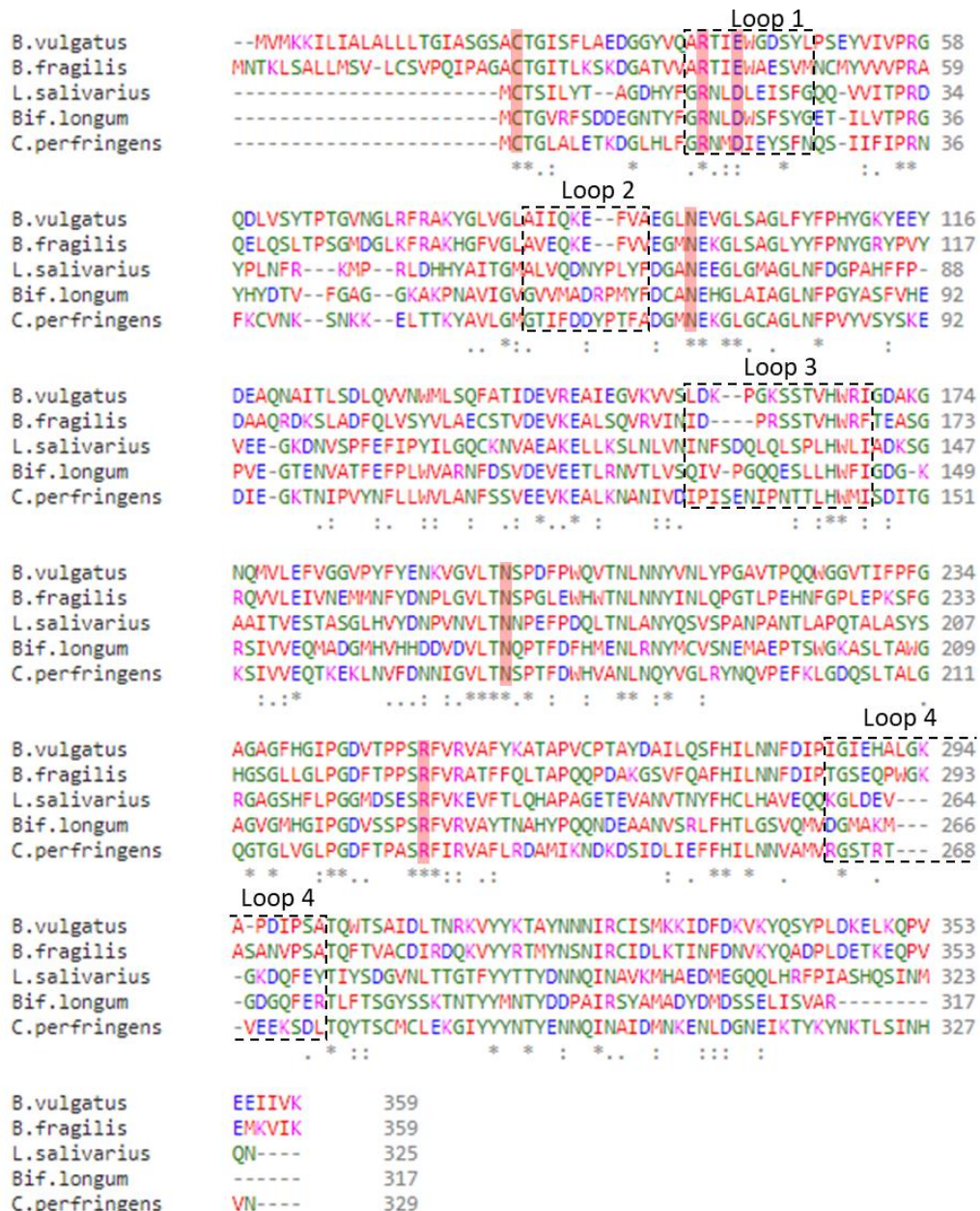
Figure 4.1 Alignment of 3 distinct BSH amino acid sequences where crystal structure is established with single Bacteroides BSHs from B. fragilis and B. vulgatus. Multiple sequence alignment was carried out using Clustal omega (Li et al., 2015).

Both analysed BSHs from *C. perfringens* and *B. longum* can form tetramers while that of *L. salivarius* is mainly dimeric. They each differ in their binding pockets- loop1 and loop2- amino acid sequence (Xu *et al.*, 2016) predicted to determine interaction and associated substrate specificity. These loops differ from these residues in *Bacteroides* BSHs examined, Binding loop 1

ideal motif: is LDFSYGEE, while Loop2: LIN—LSFSEQLPLAGL is a recognised sequence – both are believed to provide depth and orientation for glyco-BA substrate binding. Although residues in Loop1 but not in Loop 2 are conserved, the lack of conservation may indicate restricted substrate binding, monomeric or alternative structure and therefore subsequent activity. Although Loop 3 and Loop 4 are indicated, only Loop 3 histidine (H) and tryptophan (W) appear highly conserved among the different BSHs. Other regions of strong similarity between the different active BSHs were observed, between loop3 and loop 4 amino acids 180-220 and between amino acids 241-247. These conserved or charge-conserving substituted amino acids may have, yet unknown importance relating to BSH activity and may represent potential targets for mutation to uncover actual functionality and interactions (**Figure 4.1**).

Three-dimensional modelling of the different BSH protein sequences (**Figure 4.2 to 4.4**) was performed. There appears commonality of predicted structure between the *Bacteroides* BSHs, and the established crystal structures. Some helical organisation representing Loops 3 and 4 (**Figure 4.1**) and the α-helix structure in the top loop of the arrangement (which may play a crucial part in the activity of this enzyme appear altered here. The high degree of conservation of key residues and indeed, predicted structural overlap, among these highly distinct but active BSHs confirms their established activity and points to both other conserved residues and divergent pockets for possible further BSH mechanistic studies.
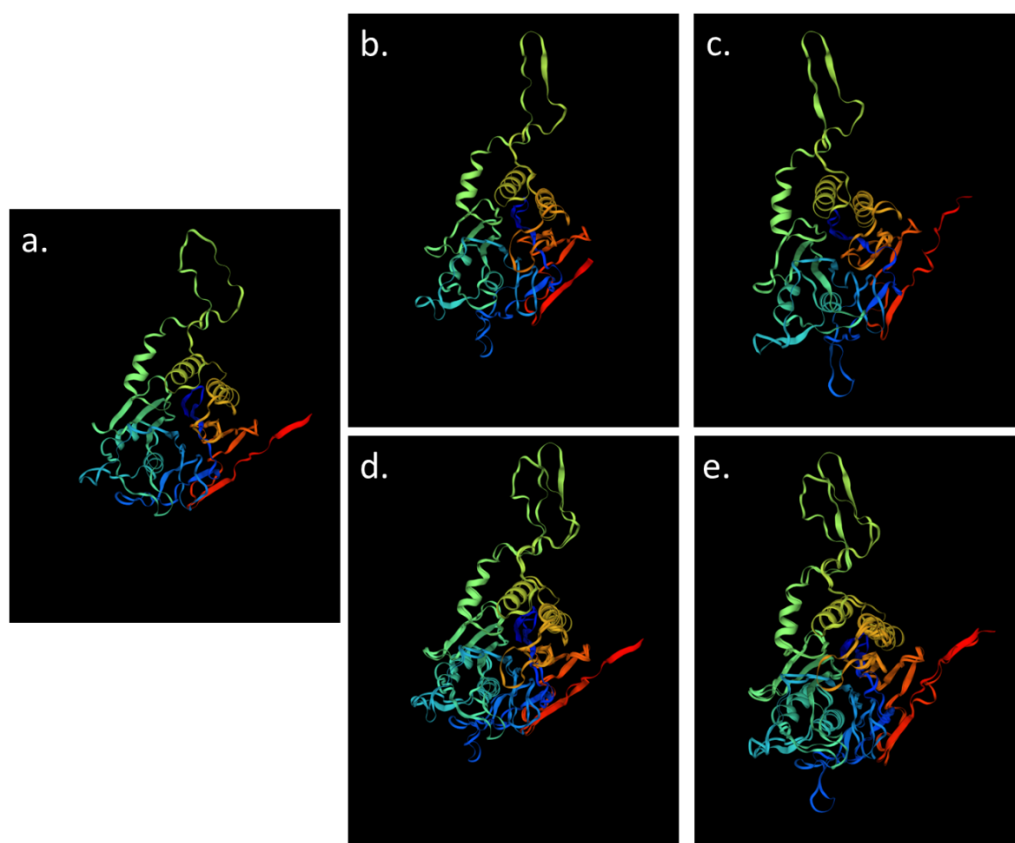
Figure 4.2 Three dimensional predictive models BSH enzymes: from (a) L. salivarius LGM14476, (b) B. fragilis NCTC 9343, and (c) B. vulgatus ATCC 8482. (d) superimposition of L. salivarius and predicted B. fragilis BSH. (e) superimposition of L. salivarius and predicted B. vulgatus BSH. The beta strands/sheets are represented in red while alpha helices are represented in green.
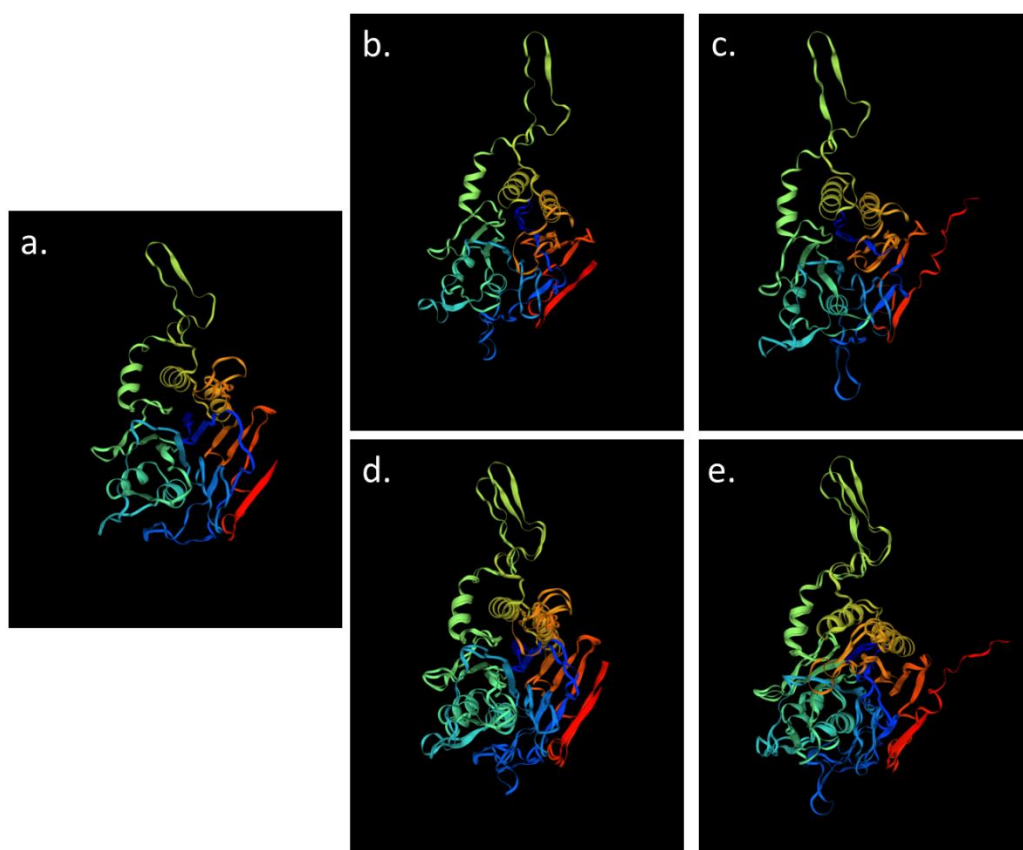
Figure 4.3 Three dimensional predictive models BSH enzymes: from (a) B. longum SBT2928, (b) B. fragilis NCTC 9343, and (c) B. vulgatus ATCC 8482. (d) superimposition of B. longum and predicted B. fragilis BSH. (e) superimposition of B. longum and predicted B vulgatus BSH. The beta strands/sheets are represented in red while alpha helices are represented in green.
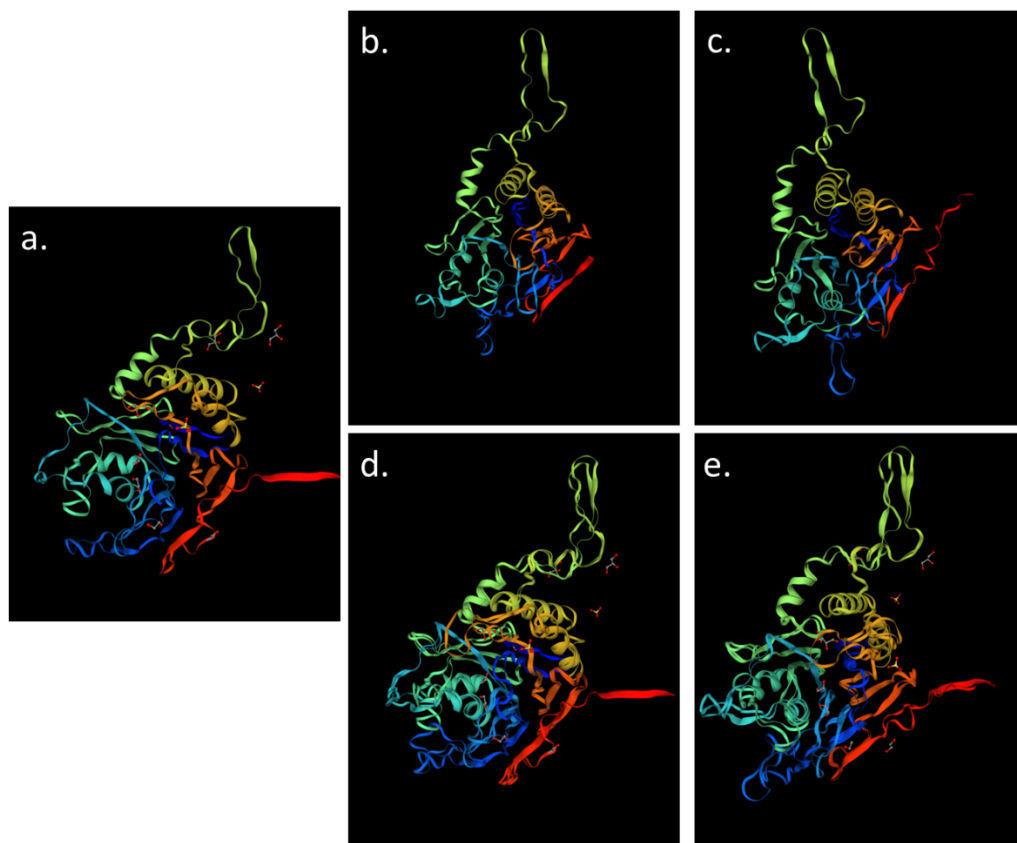
Figure 4.4 Three dimensional predictive models BSH enzymes: from (a) C. perfringens 13, (b) B. fragilis NCTC 9343, and (c) B. vulgatus ATCC 8482. (d) superimposition of C. perfringens and predicted B. fragilis BSH. (e) superimposition of C. perfringens and predicted B vulgatus BSH The beta strands/sheets are represented in red while alpha helices are represented in green.

4.3.2 *Bacteroides* species display differential bile salt hydrolase activity and substrate specificity *in vitro*

To determine specific BA metabolism by *Bacteroides* species co-incubation assays (n=3) with bacteria ($1OD_{600}$) in BHI media containing 0.5% porcine bile spiked with 1μg/ml of each of TCA, GCA, TMCA (α, β, ω), TDCA, and GDCA, those BAs that are normally absent from porcine BA. Incubations were performed for 90 minutes at 37°C under anaerobic conditions. Bile acids were normalised against internal standards (deuterated bile acids) and quantified using standard curves for each moiety using Waters® Targetlynx software. The control was incubated BA alone and served as a baseline for individual moieties. From **Figure 4.5 (a-d)** below clear BSH activity is associated with both *Bacteroides* species *B. vulgatus* and *B. fragilis* are detected. in their ability to deconjugate amino acids from both tauro and glycol conjugated bile acids collectively.
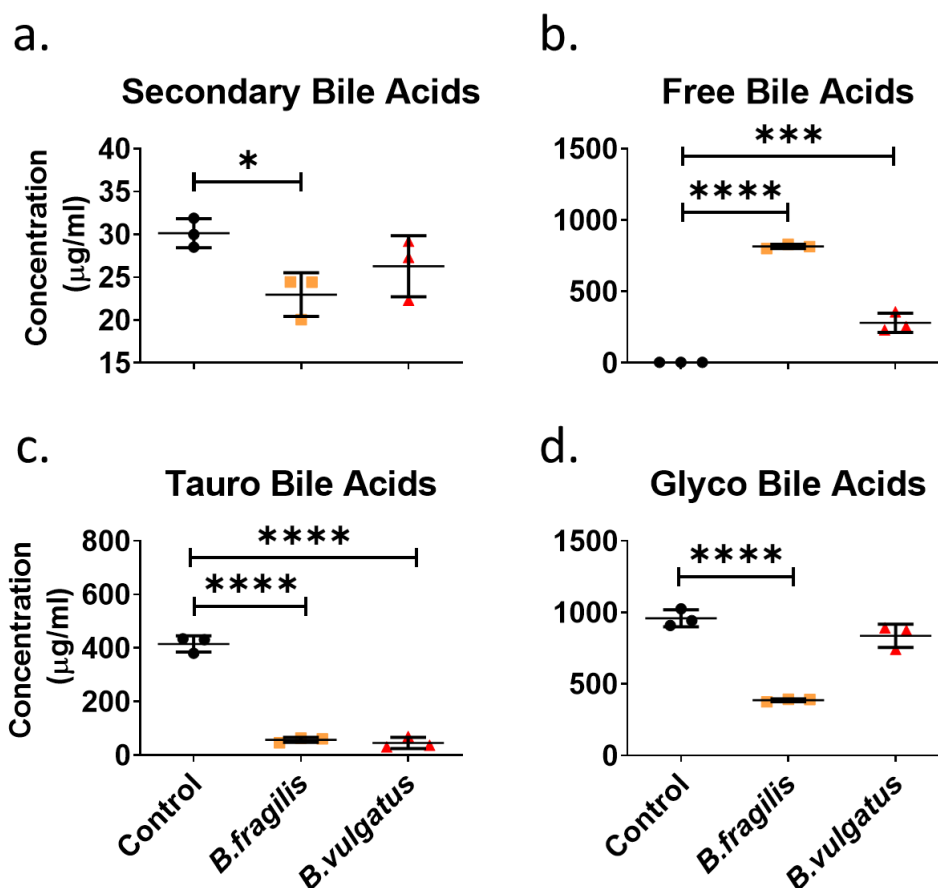
Figure 4.5 Assessment of Bacteroides species overall deconjugation ability: (a)
Secondary bile acids (b) Freed bile acid (c) Tauro conjugated bile acid (d) glyco
conjugated bile acid concentrations were detected and quantified. Bile acid
concentrations were determined after incubation of B. fragilis NCTC 9343, and B.
vulgatus ATCC 8482 with 0.5% porcine bile spiked with 1µg/ml of TCA, GCA, TMCA
(α, β, ω), TDCA, and GDCA. Bile acids were normalised against internal standards
and quantified using standard curves for each moiety using Waters® Targetlynx
software. Data is presented as mean ± SD. n = 3 individual experiments from pooled
triplicates. Statistical significance was calculated using one-way ANOVA with
*Dunnett's post-hoc test with the control column as control. * = p<0.05, ** = p<0.01,*
**** = p<0.001, and **** = p<0.0001.*

Free unconjugated BAs accumulate in *Bacteroides* treated samples with

levels two-fold higher detected in co-incubations with *B. fragilis* relative to

B. *vulgatus* (**Figure 4.5 b**).   Since co-incubations are performed with

conjugated BAs bacteria-free controls were negative for accumulation of

free BAs as expected. The rise in levels of free BAs was accompanied by

a concomitant decrease in tauro conjugated BAs, the activity and substrate

appear similar for both strains (**Figure 4.5 c**). In contrast, there was a clear preference for Glyco-conjugated BAs by *B. fragilis* BSH (**Figure 4.5 d**). These data confirm BSH activity and a differential for substrates that are species dependent. Strikingly, although in a closed system the levels of secondary BAs (conjugated and non-conjugates) were altered significantly (**Figure 4.5 a**) by *B. fragilis* indicating that either specific secondary BA conjugates or subsequent other modifications could be occurring in these assays.

We explored specific moiety interaction as a function of BSH. Again, all co-incubation assay data is quantitative (**Figure 4.6 a-i**). Here a clear distinction in moiety preference and utilization towards deconjugation is evident. We outline the BA families according to the parent moiety/BA (**Figure 4.6 a**). The CA family is slightly and significantly reduced (by up to 30%) in co-incubations with *B. fragilis*, an effect that is not evident and does not reach significance in co-incubation with *B. vulgatus* (**Figure 4.6 b**). Indeed, free CA levels are significantly elevated while both glyco and tauro conjugated CA are significantly reduced by *B. fragilis* an effect that is not shared by *B. vulgatus* (**Figure 4.6 d, e, f**). In contrast, the CDCA family is lower in the presence of *B. fragilis* (**Figure 4.6 c**) a possible indication of further alteration to freed CDCA and its corresponding moieties since both tauro and glyco CDCA were reduced to zero in these incubations (**Figure 4.6 h, i**). *B. vulgatus* elevated CDCA levels four-fold relative to *B. fragilis*, preferentially and significantly utilizing Tauro conjugated CDCA over glyco conjugated CDCA (**Figure 4.6 g-i**). Taken together these data indicate

selective substrate selection among these species and the potential, at least for *B. fragilis* to perform further downstream modifications to freed BAs, an activity that appears less represented in *B. vulgatus.*
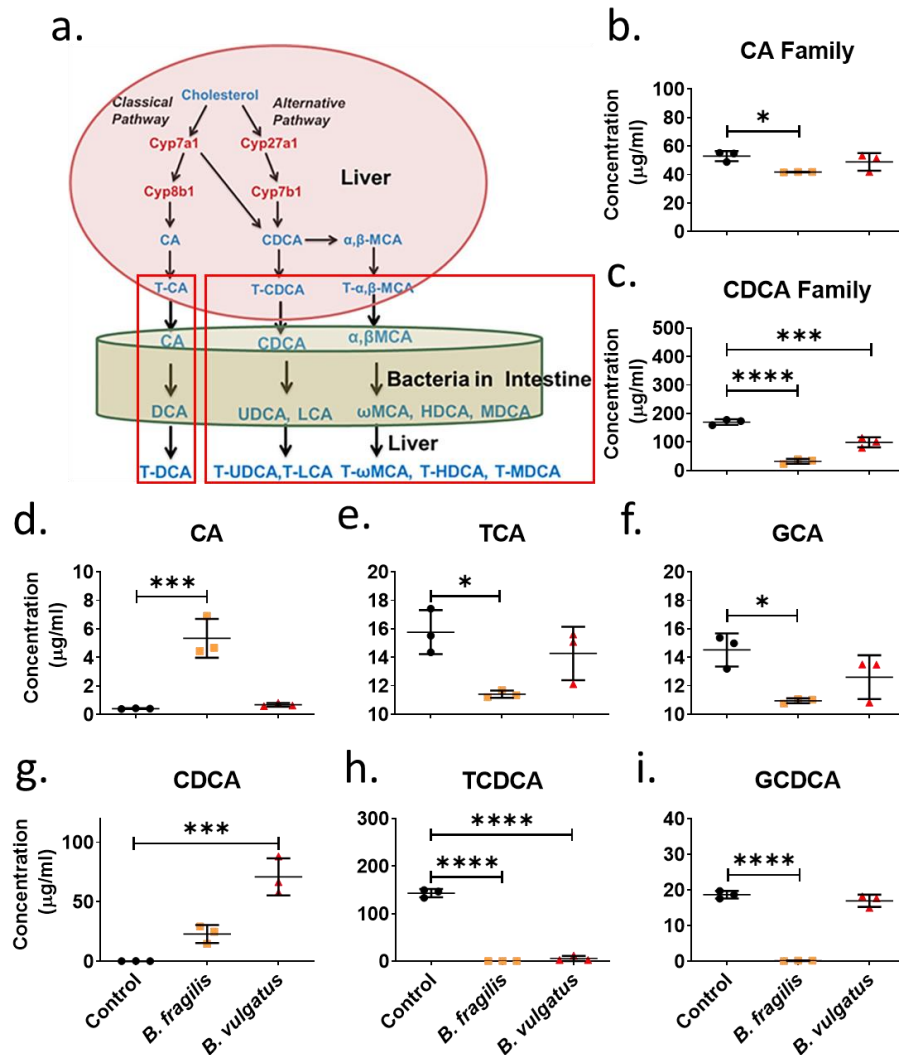
Figure 4.6 Assessment of Bacteroides species family and moiety specificity for deconjugation: (a) Schematic representation of possible BA modification and families of moieties based on parent BA, by gut bacteria B. fragilis NCTC 9343, and B. vulgatus ATCC 8482. (b) CA family concentrations. (c) CDCA family concentration. (d) CA and (g) CDCA with (e, f, h, i) their tauro and glyco conjugates. Bile acid concentrations were determined after incubation of bacteria with 0.5% porcine bile spiked with 1µg/ml of TCA, GCA, TMCA (α, β, ω), TDCA, and GDCA. Bile acids were normalised against internal standards and quantified using standard curves for each moiety using Waters® Targetlynx software. Data is presented as mean ± SD. n = 3 individual experiments from pooled triplicates. Statistical significance was calculated using one-way ANOVA with Dunnett's post-hoc test with the control column as control. * = p<0.05, ** = p<0.01, *** = p<0.001, and **** = p<0.0001. n = 3 individual experiments from pooled triplicates. CA; Cholic acid, CDCA; Chenodeoxycholic acid, T and G indicated tauro and glyco conjugated moieties respectively.

Attention returned to the secondary BA cohort. This cohort includes UDCA and LCA both descendants through microbial BA modification from CDCA and DCA from CA but represented in the spiked porcine bile. It also includes their conjugates to taurine and glycine. Although UDCA accumulates as a result of deconjugation of both tauro and glyco conjugated UDCA, the levels of free UDCA varied significantly relative to species (**Figure 4.7 a-c**) with *B. vulgatus* associated with very low levels of UDCA. *B. vulgatus* did not alter conjugated DCA in any form while *B. fragilis* was very active in converting these moieties to the freed DCA (**Figure 4.7 d-f**). In contrast, LCA accumulated to the same level irrespective of species with a clear equal ability of both to deconjugate tauro conjugated LCA, although *B. vulgatus* was less adapted to glyco-conjugated LCA deconjugation (**Figure 4.7 g-i**)*.*

Figure 4.7 Assessment of Bacteroides species family and moiety specificity for deconjugation. BA modification and families of moieties based on parent BA, by gut bacteria B. fragilis NCTC 9343, and B. vulgatus ATCC 8482. Concentrations of Secondary bile acids (a) UDCA, (d) DCA, and (g) LCA along with their conjugates (b-c, e-f, and h-i respectively). Bile acid concentrations determined after incubation of bacteria with 0.5% porcine bile spiked with 1µg/ml of TCA, GCA, TMCA (α, β, ω), TDCA, and GDCA. Bile acids were normalised against internal standards and quantified using standard curves for each moiety using Waters® Targetlynx software. Data is presented as mean ± SD. Statistical significance was calculated using one-way ANOVA with Dunnett's post-hoc test with the control column as control. * = p<0.05, ** = p<0.01, *** = p<0.001, and **** = p<0.0001. n = 3 individual experiments from pooled triplicates. UDCA; Ursodeoxycholic acid, DCA; Deoxycholic acid, LCA; Lithocholic acid, T and G indicated tauro and glyco conjugated moieties respectively.

Differential substrate affinity and activity were also evident with other conjugated BAs. Again, *B. fragilis* was more efficient in deconjugating glyco-conjugated HDCA and HCA, but less efficient in the case of tauro conjugated HCA muricholic acid (**Figure 4.8 a-i**). For these tauro conjugates to muricholic acid, to HCA, to HDCA (**Figure 4.8 c, e, h**) *B. vulgatus* was

efficient in deconjugation ability. The generation of CDCA at a lower level by *B. fragilis*, although there was efficient substrate deconjugation, the high levels of UDCA were of concern. Therefore, we examined the CDCA downstream intermediate BA 7 Keto LCA, a bile acid generated en route to LCA. Here *B. fragilis* alone was responsible for the huge abundance of this BA moiety in co-incubation assays (**Figure 4.8 k**). A summary of all levels of BAs, their classifications and significance as well as directionality is presented in Table S4.1 Appendix IV.
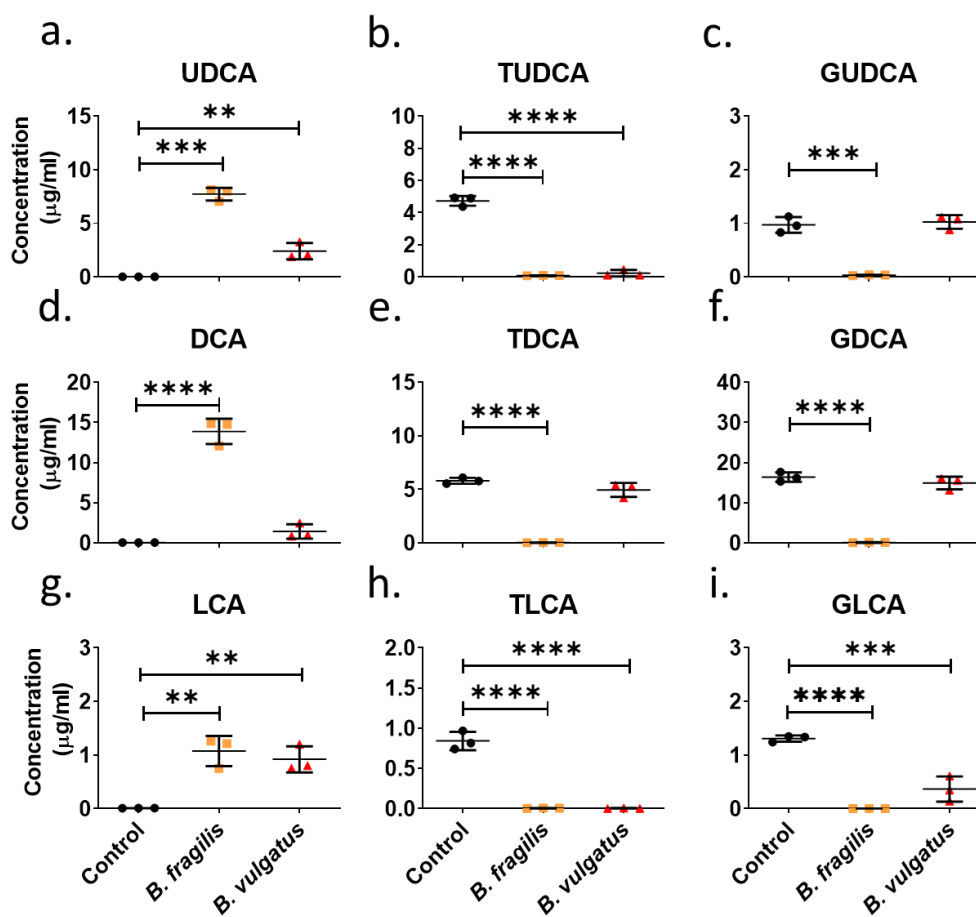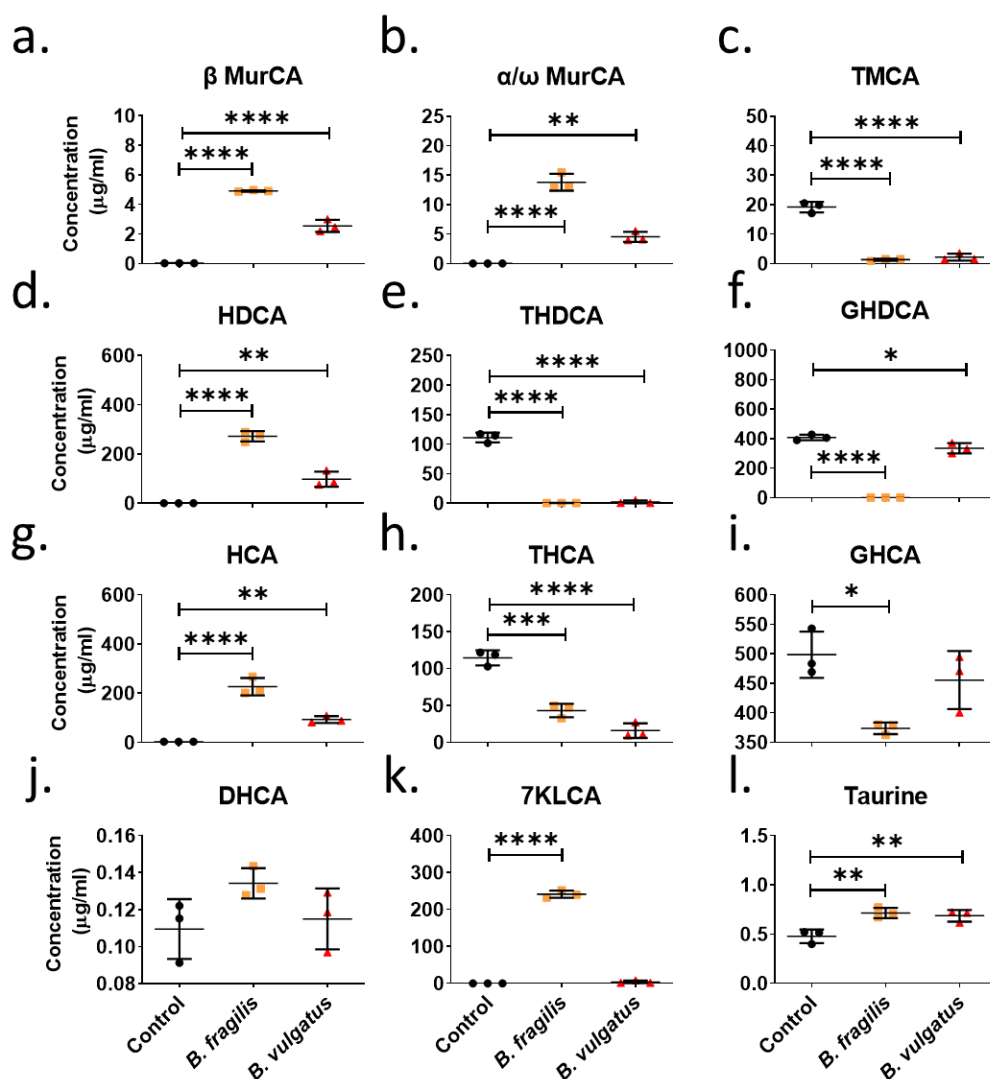
Figure 4.8 Assessment of Bacteroides species family and moiety specificity for deconjugation. *BA modification and families of moieties based on parent BA, by gut bacteria B. fragilis NCTC 9343, and B. vulgatus ATCC 8482. Concentrations of (a-c) muricholic BAs and their tauro conjugate, (d-f) hyodeoxycholic acid and its conjugates, (g-i) hyocholic acid and its conjugates, (j) dehydrocholic acid, and 7-ketolithocholic acid (k). Bile acid concentrations determined after incubation of bacteria with 0.5% porcine bile spiked with 1μg/ml of TCA, GCA, TMCA (α, β, ω), TDCA, and GDCA. Bile acids were normalised against internal standards and quantified using standard curves for each moiety using Waters® Targetlynx software. Data is presented as mean ± SD. n = 3 individual experiments from pooled triplicates. Statistical significance was calculated using one-way ANOVA with Dunnett's post-hoc test with the control column as control. * = p<0.05, ** = p<0.01, *** = p<0.001, and **** = p<0.0001.*

We therefore, conclude that species-specific and BA substrate-specific modifications relate to *Bacteroides in vitro* assays under controlled conditions reveal substrate specificity for both species tested (summarized

225

in **Table 4.4** below) indicating a wide range of activities and potency of BSH associated with *B. fragilis* NCTC 9343. Intriguing is the possible propensity to accumulate intermediate BAs by selected strains only.

Table 4.4 Summary of data generated in Section 4.3.2 highlighting substrate specificity is a feature of Bacteroides and associated BSHs

Species	Glyco substrates	Tauro substrates	BA accumulated
B. fragilis	GCA, GCDCA, GDCA, GLCA, GUDCA, GHDCA, GHCA	TCA, TCDCA, TDCA, TLCA, TUDCA, TMCA, THDCA, THCA	CA, DCA, LCA, UDCA, β-MCA, α/ω-MCA, HDCA, HCA, 7-KLCA
B. vulgatus	GLCA, GHDCA	TCDCA, TLCA, TUDCA, TMCA, THDCA, THCA	CDCA, LCA, UDCA, β-MCA, α/ω-MCA, HDCA, HCA

4.3.3 *Bacteroides* species display differential receptor activation potential *in vitro*

The discriminatory nature of *B. fragilis* NCTC 9343, and *B. vulgatus* ATCC 8482 to modify and metabolize BAs, implicated differential BA signalling potential as a function of each strain. Bile acid moieties are known to act as key agonists and antagonists for receptors – both nuclear receptors and G protein-coupled receptors that are central to metabolism and immune functions as well as to xenobiotic clearance. We examined *in vitro* assay modifications in order of the potential for each *Bacteroides* species for activation of these receptors. The potential for activation of the nuclear receptor Farnesoid X receptor, (the FXR), and G protein-coupled receptor GBAR1 (TGR5) both receptors associated with metabolism and immune system modulation were significantly elevated in *B. vulgatus* co-incubation and BA moiety generation over *B. fragilis* in co-incubation assays (**Figure 4.9**). In contrast, *B. fragilis* enriched for the FXR antagonists (4-fold), LXR agonists (0.25-fold), vitamin D agonists (10-fold) and PXR activation (4-fold)

over *B. vulgatus* in co-incubation assays (**Figure 4.9**). These levels indicate species-specific potential to produce moieties that may impact signalling mechanisms within the host environment both locally and indeed systemically.
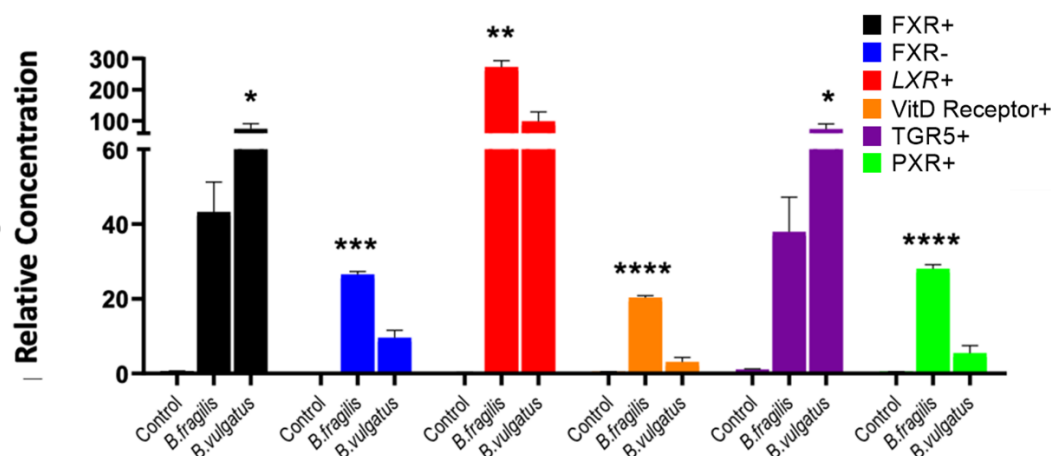
Figure 4.9 The potential of Bacteroides produced BAs to activate nuclear and G-protein coupled receptors is strain dependant. Bile acids conversions by B. fragilis NCTC 9343, and B. vulgatus ATCC 8482 were assessed for levels of those moieties that could collectively impact the Farnesoid X receptor (FXR), the liver X receptor (LX), Vitamin D Receptor (VitD), the Pregnane X receptor (PXR), G protein coupled receptor GBAR1 or alternatively named TGR5. Data is presented as means ± SD. n = 3 individual experiments from pooled triplicates. Significance was calculated using a student t-test between B. fragilis and B, vulgatus. * = p<0.05, ** = p<0.01, *** = p<0.001, and **** = p<0.0001.

4.3.4 *Bacteroides* species reveal overlap and differential potential hydroxysteroid dehydrogenase (HSDH) activity *in vitro*

The propensity for CDCA utilization by *B. fragilis* NCTC 9343 to produce intermediate BA 7KetoLCA, an ability that is absent from *B. vulgatus* ATCC 8482 (**Figure 4.8 k**) prompted exploration of the microbial pathways that could lead to different intermediates through hydroxysteroid modification of the steroid rings of BAs moving from primary liver produced BAs CA and

227

CDCA (see **Figure 4.10** below for a summary of the currently proposed

modification).
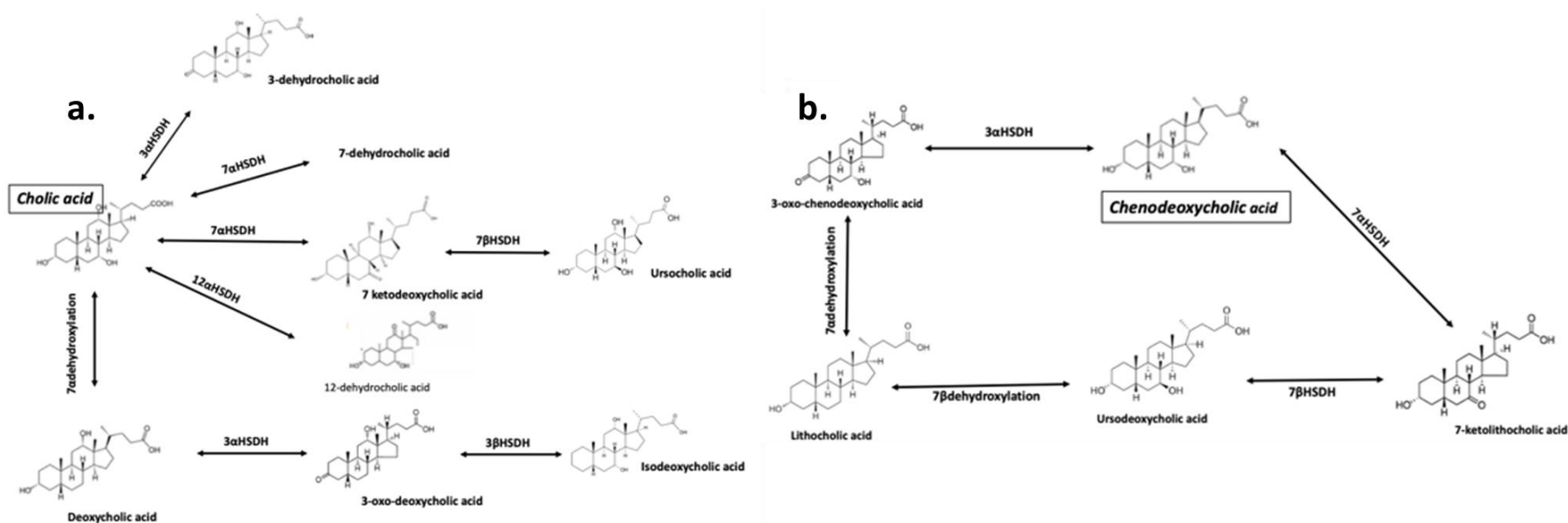
Figure 4.10 Overview of some potential alternative microbial Bile acid (BA) modification pathways: (a) Cholic acid (b) Chenodeoxycholic acid. HSDH represents hydroxysteroid dehydrogenase. The relevant carbon bonding and orientation of the bonds for action, are indicated by the number and by α, β respectively.

The reactions are noteworthy for two reasons, first, each of the modifications could be microbial in nature and second, they are reversible depending on bioenergetics and the availability of reducing or oxidizing power in the forms of NAD(P)H + Protons and NAD(P)+. Therefore, the energetic status of the microbes or the gut milieu would be critical in determining intermediate accumulation. The modifications include 7α-dehydroxylation of CA and CDCA to DCA and LCA respectively. 3α-dehydroxylation produces isoBAs, 7α-HSDH activity produces keto BAs while 7β-epimerization can produce UDCA downstream from other CDCA and LCA conversions (**Figure 4.10 a, b**).

Explorations of freed individual BAs CA and CDCA (1μM/ml final concentration in BHI) were next explored in the presence and absence of bacteria and individual co-incubation assays (n=3) with $1OD_{600}$ of each of B. *fragilis* NCTC 9343, *B. vulgatus* ATCC 8482 and with a third common gut isolate *B. thetaiotaomicron* strain VPI 5482. Incubations were allowed to proceed for 2 hours anaerobically at 37°C before BA extraction according to materials and methods **section 2.14**. Co-incubations assays with CA revealed potential spontaneous oxidation/reduction events to form deoxycholic acid ((DCA) normally a function of dehydroxylation via *bai* operon gene expression, and by 7α-dehydroxylation), 3-dehydrocholic acid (normally microbial 3α-HSDH activity) and Isodeoxycholic acid (IsoDCA) formation (a microbial 3β-HSDH activity) since all three of these BA moieties were elevated in control reactions (**Figure 4.11 b, c, g**). Interestingly, DCA and IsoDCA formation was reversed in the presence of *B. fragilis* and *B. thetaiotaomicron,* but not *B. vulgatus, to* potentially yield 3-oxoDCA.

However, concrete standards were not available at that time to allow discrimination and determination of this BA level. Similar BA modification abilities for *B. fragilis and B. thetaiotaomicron* were evident (**Figure 4.11 a-g**)*.* In these assays, these bacterial species appeared to significantly reduce CA levels by up to 50% relative to both bacteria negative control samples and to *B. vulgatus* co-incubations (**Figure 4.11 a**) with an accompanying accumulation of 7-dehydrocholic acid (a function of 7α-HSDH activity), 12-dehydrocholic acid (a function of 12α-HSDH activity) (**Figure 4.11 d, e**). Only urodeoxycholic acid (UCA) accumulated but not significantly, in the case of *B. vulgatus* co-incubations with CA.
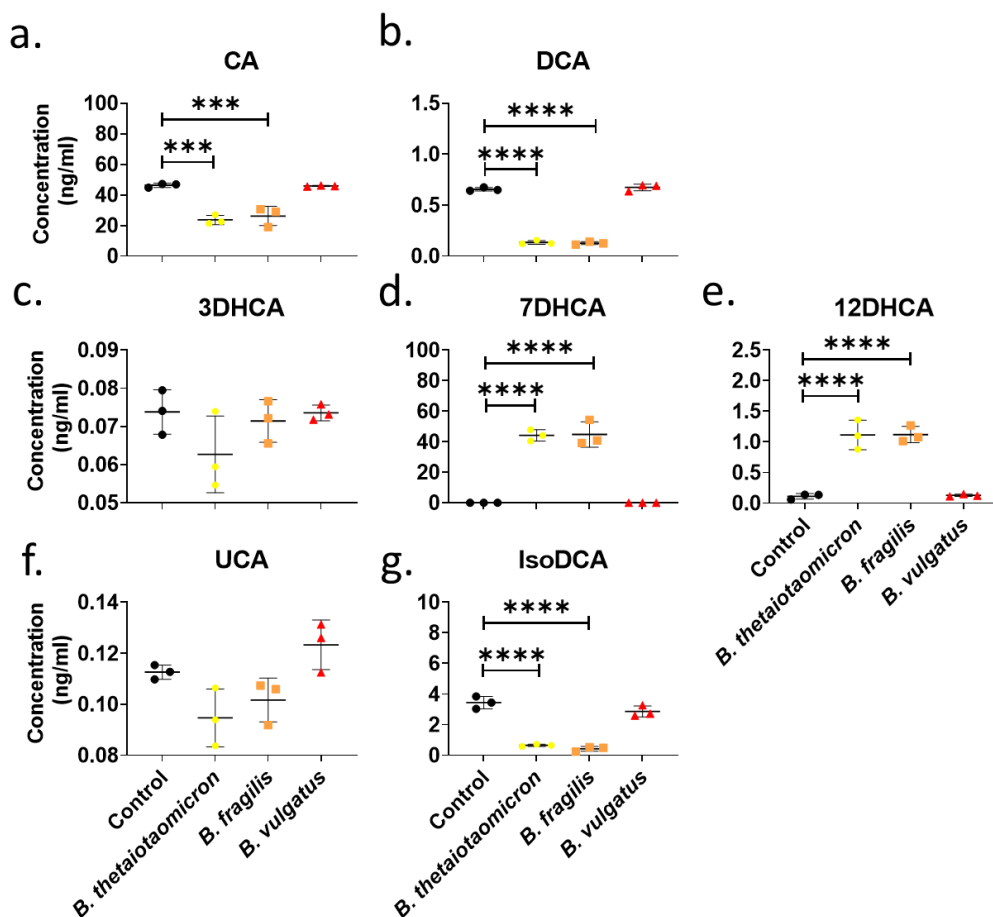
Figure 4.11 Potential metabolism of the primary bile acid cholic acid (CA) by Bacteroides species to generate intermediate bile acid products. Bile acid concentrations of individual BA intermediate moieties (a-g) determined post individual Bacteroides spp (B. fragilis NCTC 9343, B. vulgatus ATCC 8482, B. thetaiotaomicron VPI 5482) co-incubation with 1μM/ml of primary bile acids cholic acid (CA) relative to control, bacteria negative samples. Bile acids were normalised against internal standards and quantified using standard curves for each moiety using Waters® Targetlynx software. Data is presented as mean ± SD. n = 3 individual experiments from pooled triplicates. Statistical significance was calculated using one-way ANOVA with Dunnett's post-hoc test with the control column as control. * = p<0.05, ** = p<0.01, *** = p<0.001, and **** = p<0.0001. CA; cholic acid, DCA; deoxycholic acid, 3DCA; 3-dehydrocholic, 7DCA; 7-dehydrocholic acid, 12-dehydrocholic acid, UCA; urodeoxycholic acid, IsoDCA; Isodeoxycholic acid.

CDCA-based coincubations were associated with spontaneous LCA and UDCA formation (**Figure 12 b, d**), although again, *B. fragilis and B. thetaiotaomicron* maintained significantly lower levels of LCA in their respective assays. Indeed, both species again showed similar BA

modification abilities, this time from CDCA towards the production of 7-ketolithocholic acid (a function of 7βHSDH) and 3-oxo-chenodeoxycholic acid (a function of 3αHSDH) (see **Figure 4.12 c, e**). These data verify 7α-HSDH, 12α-HSDH, 7β-HSDH and 3α-HSDH as functions of *B. fragilis* and *B. thetaiotaomicron* but not of *B. vulgatus* when examined. The potential activities and the relative levels of activity, as well as significance, are indicated in Tables S4.2 and S4.3 and appendix IV.
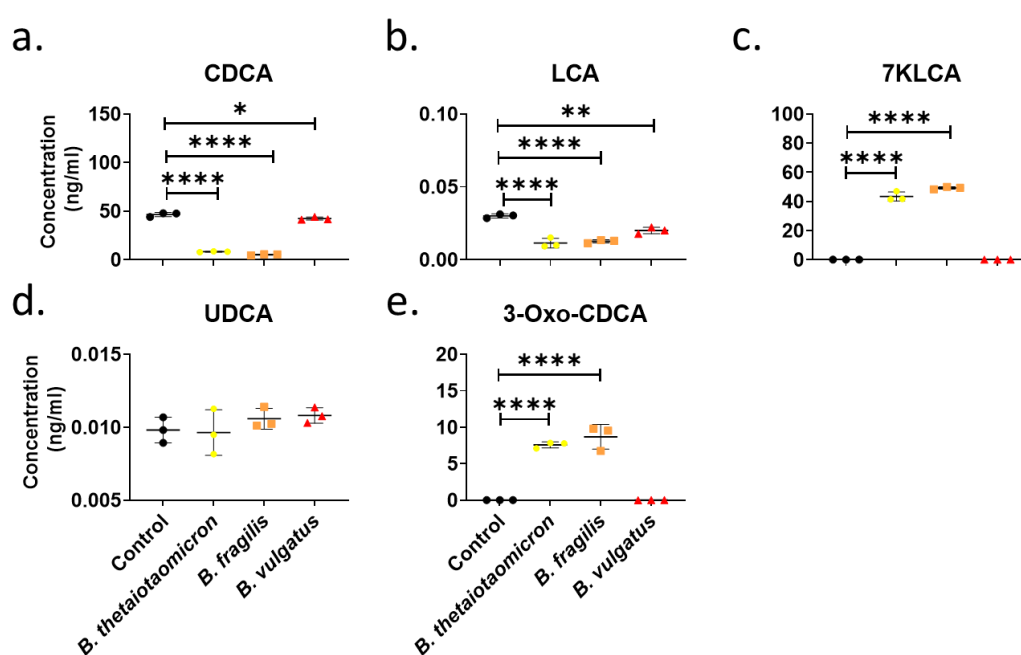
*Figure 4.12 Potential metabolism of the primary bile acid chenodeoxycholic acid (CDCA) by Bacteroides species to generate intermediate bile acid products. Bile acid concentrations of individual BA intermediate moieties (a-g) determined post individual Bacteroides spp (B. fragilis NCTC 9343, B. vulgatus ATCC 8482, B. thetaiotaomicron VPI 5482). co-incubation with 1μM/ml of primary bile acid chenodeoxycholic acid (CDCA) relative to control, bacteria negative samples. Bile acids were normalised against internal standards and quantified using standard curves for each moiety using Waters® Targetlynx software. Data is presented as mean ± SD. n = 3 individual experiments from pooled triplicates. Statistical significance was calculated using one-way ANOVA with Dunnett's post-hoc test with the control column as control. * = p<0.05, ** = p<0.01, *** = p<0.001, and **** = p<0.0001. CDCA; chenodeoxycholic acid, LCA; lithocholic acid, 7KLCA; 7-Keto lithocholic acid, UDCA; Ursodeoxycholic acid 3-Oxo -CDCA; 3-oxo-chenodeoxycholic acid.*

4.3.5 Bile acid alterations are dominated and negated, following antibiotic cocktail treatment, despite the introduction of individual *Bacteroides* species to these animals.

Given the species-specific BA modifications evident for *B. fragilis* NCTC 9343, *B. vulgatus* ATCC 8482 and *B. thetaiotaomicron* VPI 5482 *in vitro,* the question remained as to whether these conversions could translate and carry impact *in vivo.* Here, normal C57BL/6 mice were given no treatment (control n=5), and all the remaining groups (n=10) received an antibiotic cocktail (see materials and methods section 2.11 **Table 2.5**) for 13 days via oral gavage. 24 hours after treatment with an antibiotic cocktail one group was gavaged with PBS, and two other groups (n=10) were treated to 10^9 CFU of either *B. fragilis* NCTC 9343 or *B. vulgatus* ATCC 8482 on 2 consecutive days by gavage. Animals were sacrificed 9 days later. Relevant samples (gall bladder and bile, proximal colon tissue, faeces) were collected from each individual animal and frozen for further application to BA extraction for bile and faeces (materials and methods **section 2.14**) and RNA extraction and analysis (materials and methods **section 2.6**).

When gall bladder (GB) bile acids (BAs) were extracted and quantified against standard curves, post normalization a 2-log fold range of total BA was detected among animals from the different groups indicating a wide spectrum of BA content and filling in individual animals suggesting variation over the daytime culling (**Figure 4.13 a**). This range persisted across the groups, although antibiotic-treated animals tended to show higher levels of total BA, with a tighter range (2-fold). Still, this did not reach significance.

When the different microbial modifications -the general classes of BAs - were examined, there were no significant differences detected between the classes, relative to treatment. BSH activity normally reduces the levels of conjugated bile acids in favour of free and further microbially altered secondary BAs, however, no distinction was detected among these classes of modifications for GB BAs (**Figure 4.13 b-f**). The range of GB BAs in control animals remained consistently diverse throughout all further analyses. The control for bacterial treatment is the antibiotic control group. In comparison, no significant differences were detected between antibiotic-treated animals and those groups who received *Bacteroides* species for any class of microbial modification.

a.

Total Bile Acids

b.

Primary Bile Acids

c.

Secondary Bile Acids

d.

Free Bile Acids

e.

Tauro Conjugated Bile Acids

f.

Glyco Conjugated Bile Acids

Figure 4.13 Assessment of gallbladder bile acid concentrations following oral gavage of Bacteroides species in C57BL6 mice. Male mice were orally gavaged for 13 days with a full spectrum antibiotic cocktail consisting of 10 mg/mL metronidazole, 5 mg/mL vancomycin, 5 mg/mL neomycin, and 0.1 mg/mL amphotericin B and 1,000 mg/L ampicillin added to drinking water followed by oral gavage with 10^9 cfu B. fragilis NCTC 9343 and B. vulgatus ATCC 8482 for 2 consecutive days. On day 24, gallbladders were collected, and bile acids assessed. Concentration of bile acid are shown based on microbial modification (total, free, conjugated, and secondary BAs) (a-f). Bile acids were normalised against internal standards and quantified using standard curves for each moiety using Waters® Targetlynx software. Data is presented as mean ± SD. n=5-10/group. Statistical significance was calculated using one-way ANOVA with Dunnett's post-hoc test with the control column as Antibiotic. * = p<0.05, ** = p<0.01, *** = p<0.001, and **** = p<0.0001.

In examining GB BA individual moieties for microbial modifications, it is clear that the antibiotic cocktail significantly altered individual conjugated and freed moieties so that conjugates were significantly lower in the treated

236

groups (**Figure 4.14 a-h**).   Indeed, gavage of *Bacteroides* species had little effect on individual BAs, although a trend towards increased microbially formed DCA is evident in those animals treated with *B. fragilis* which did not reach significance (**Figure 4.14 a**). However, treatment with these bacteria did significantly elevate the levels of GUDCA (**Figure 4.14 b**). *B. vulgatus* had no effect in this antibiotic-treated background. Note, only a selection of the microbially modified BAs are shown here since no other significant alterations were detected among moieties (n=30) examined. Instead, classes, individual moieties, quantities, and statistical analysis are represented in Table S4.4 appendix IV.

*Figure 4.14 Assessment of gallbladder bile acid individual moieties, following oral gavage of Bacteroides species in C57BL6 mice. Male mice were orally gavaged for 13 days with a full spectrum antibiotic cocktail consisting of 10 mg/mL metronidazole, 5 mg/mL vancomycin, 5 mg/mL neomycin, and 0.1 mg/mL amphotericin B and 1,000 mg/L ampicillin added to drinking water followed by oral gavage with 10^9 cfu B. fragilis NCTC 9343 and B. vulgatus ATCC 8482 for 2 consecutive days. On day 24, gallbladders were collected, and bile acids assessed. Concentration of individual BA moieties are shown based on potential microbial modification with representation among free, conjugated, and secondary BAs (a-h). Bile acids were normalised against internal standards and quantified using standard curves for each moiety using Waters® Targetlynx software. Data is presented as mean ± SD. n=5-10/group. Statistical significance was calculated using one-way ANOVA with Dunnett's post-hoc test with the control column as Antibiotic. * = p<0.05, ** = p<0.01, *** = p<0.001, and **** = p<0.0001. DCA; Deoxycholic acid, UDCA; Ursodeoxycholic acid, HDCA; Hyodeoxycholic acid, HCA; Hyocholic acid, T and G indicated tauro and glyco conjugated moieties respectively.*

Next faecal BAs, relating to fermentation and high density microbial colonic colonization, were examined. Although the range in untreated animals varied only 3-fold for the different classes of microbial modification, total BAs tended to be higher in these animals and this was attributed to elevations in both free unconjugated and secondary BAs (both microbially produced), both were significantly elevated in control animals and levels were reduced

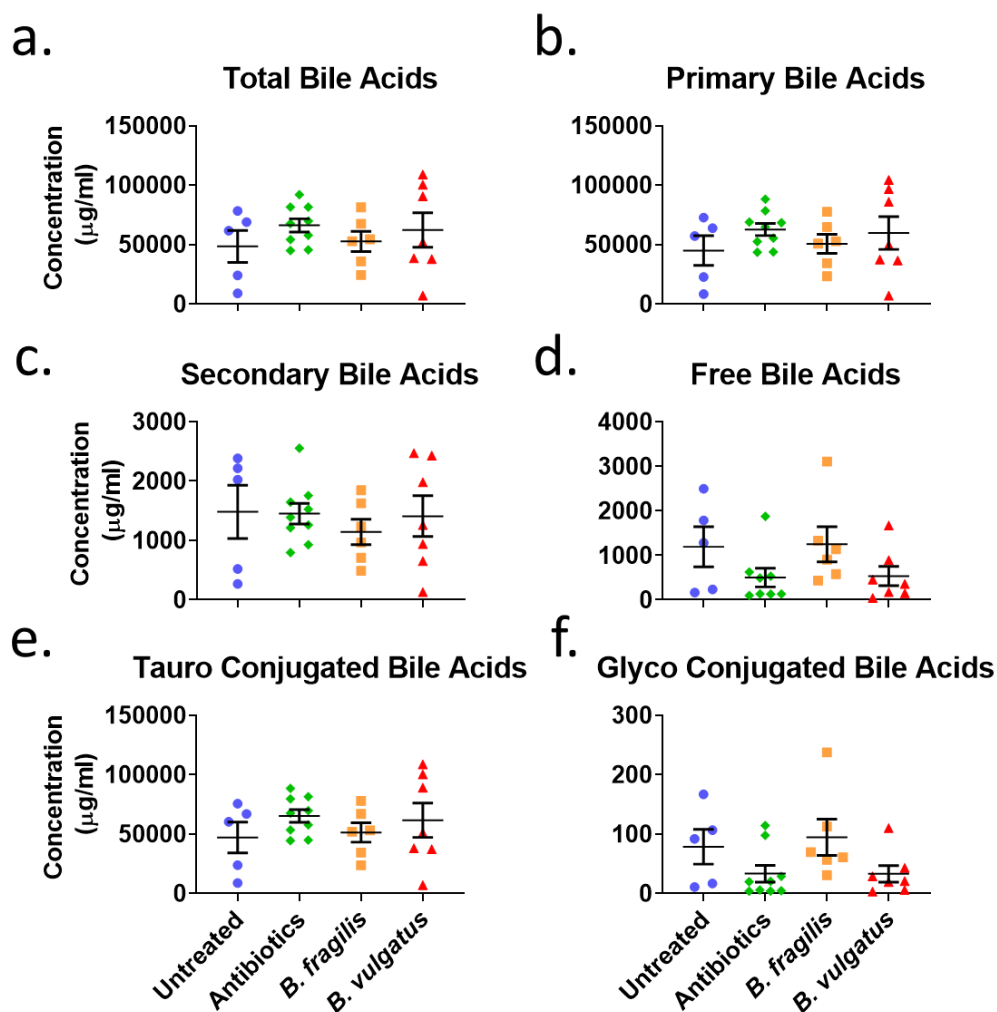up to 5-fold in any of the groups receiving antibiotic treatment (**Figure 4.15**

a, d, c).

*Figure 4.15 Assessment of faecal bile acid classes, following oral gavage of Bacteroides species in C57BL6 mice. Male mice were orally gavaged for 13 days with a full spectrum antibiotic cocktail consisting of 10 mg/mL metronidazole, 5 mg/mL vancomycin, 5 mg/mL neomycin, and 0.1 mg/mL amphotericin B and 1,000 mg/L ampicillin added to drinking water followed by oral gavage with 10^9 cfu B. fragilis NCTC 9343 and B. vulgatus ATCC 8482 for 2 consecutive days. On day 24, faecal samples were collected, and bile acids assessed. Concentration of individual BA moieties are shown based on potential microbial modification with representation among free, conjugated, and secondary BAs (a-h). Bile acids were normalised against internal standards and quantified using standard curves for each moiety using Waters® Targetlynx software. Data is presented as mean ± SD. n=5-10/group. Statistical significance was calculated using one-way ANOVA with Dunnett's post-hoc test with the control column as Antibiotics. * = p<0.05, ** = p<0.01, *** = p<0.001, and **** = p<0.0001.*

While no effect on faecal BAs was evident with *B. vulgatus, B. fragilis* significantly decreased TMCA, with a reciprocal increase in free BMCA detected, tauro conjugated CDCA was significantly reduced, however, this did not feed back to CDCA levels indicating possible further CDCA conversions, not analysed in this study, may have occurred here (**Figure 4.16 d, e, f**). The antibiotic depletion of individual moieties representing microbial modifications continued towards significant decreases for almost all moieties examined (**Figure 4.16 a-i, 4.17 a-i**).
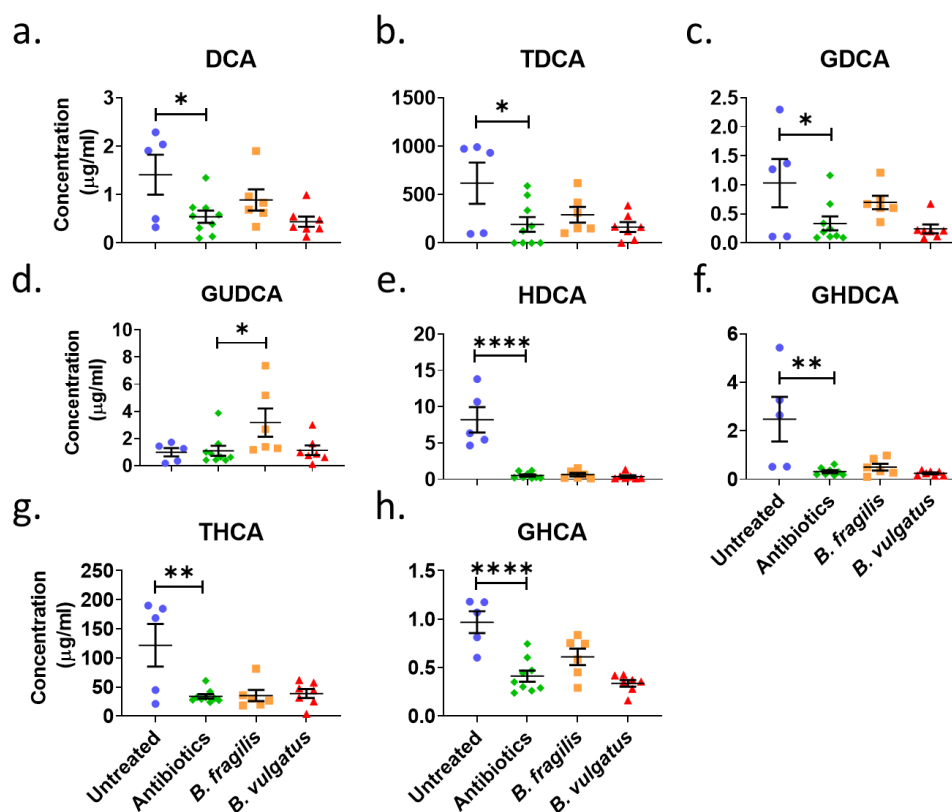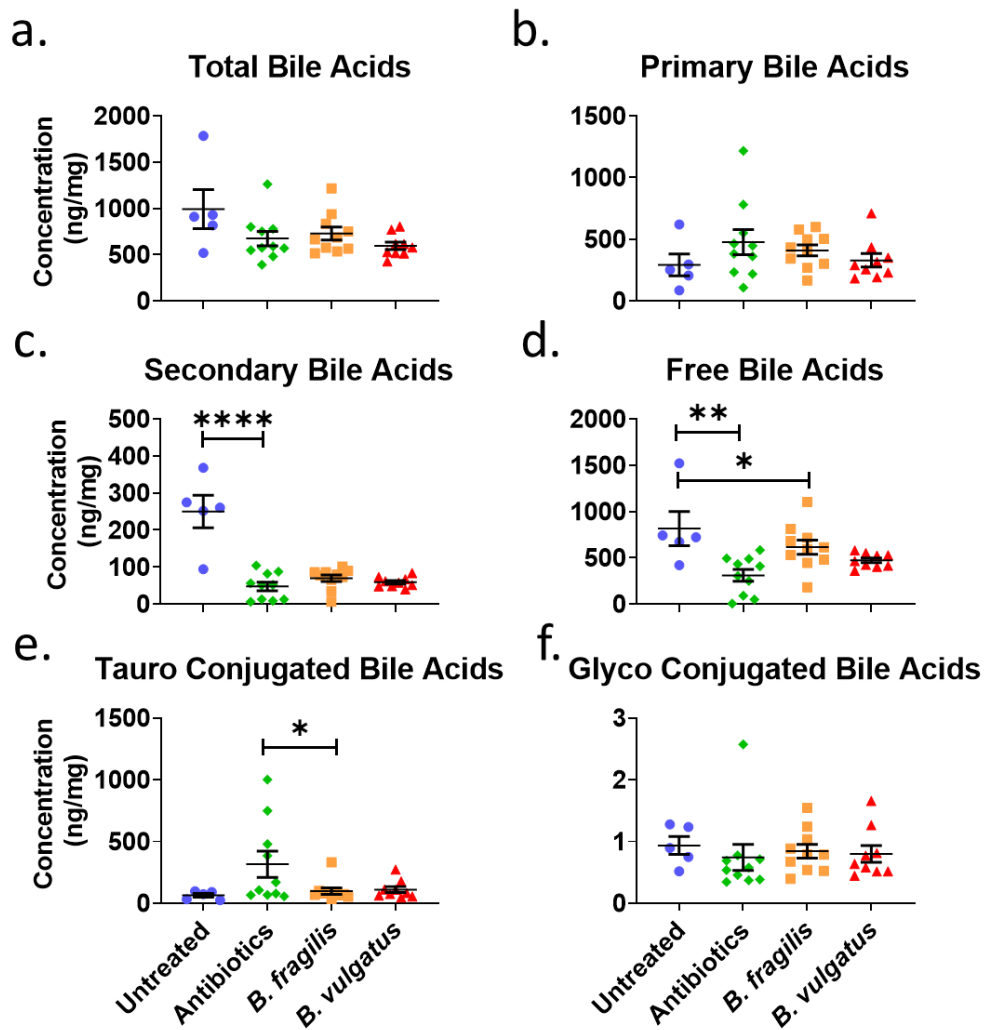
*Figure 4.16 Assessment of faecal bile acid individual moieties, following oral gavage of Bacteroides species in C57BL6 mice. Male mice were orally gavaged for 13 days with a full spectrum antibiotic cocktail consisting of 10 mg/mL metronidazole, 5 mg/mL vancomycin, 5 mg/mL neomycin, and 0.1 mg/mL amphotericin B and 1,000 mg/L ampicillin added to drinking water followed by oral gavage with 10^9 cfu B. fragilis NCTC 9343 and B. vulgatus ATCC 8482 for 2 consecutive days. On day 24, faecal samples were collected, and bile acids assessed. Concentration of individual BA moieties are shown based on potential microbial modification with representation among free, conjugated, and secondary BAs (a-h). Bile acids were normalised against internal standards and quantified using standard curves for each moiety using Waters® Targetlynx software. Data is presented as mean ± SD. n=5-10/group. Statistical significance was calculated using one-way ANOVA with Dunnett's post-hoc test with the control column as Antibiotics. * = p<0.05, ** = p<0.01, *** = p<0.001, and **** = p<0.0001. CA; Cholic acid, CDCA; Chenodeoxycholic acid, MCA; Muricholic acid, T and G indicated tauro and glyco conjugated moieties respectively.*

Comparing control antibiotic-treated animals to those antibiotic-treated animals, a significant increase in LCA (secondary bile acid) in the presence of *B. fragilis* was detected (**Figure 4.17 d**), interestingly a feature of *B. vulgatus* gavage was significantly increased GLCA (**Figure 4.17 f**), notably both species were associated with reduced TUDCA levels (**Figure 4.17 h**) an effect that did not transfer to elevate free UDCA (**Figure 4.17 g**). 7

ketoLCA levels were not detected as altered by either species. Note, only a selection of the microbially modified BAs are shown here since no other significant alterations were detected among moieties (n=30) examined. Instead, classes, individual moieties, quantities, and statistical analysis are represented in Table S4.5 appendix IV.
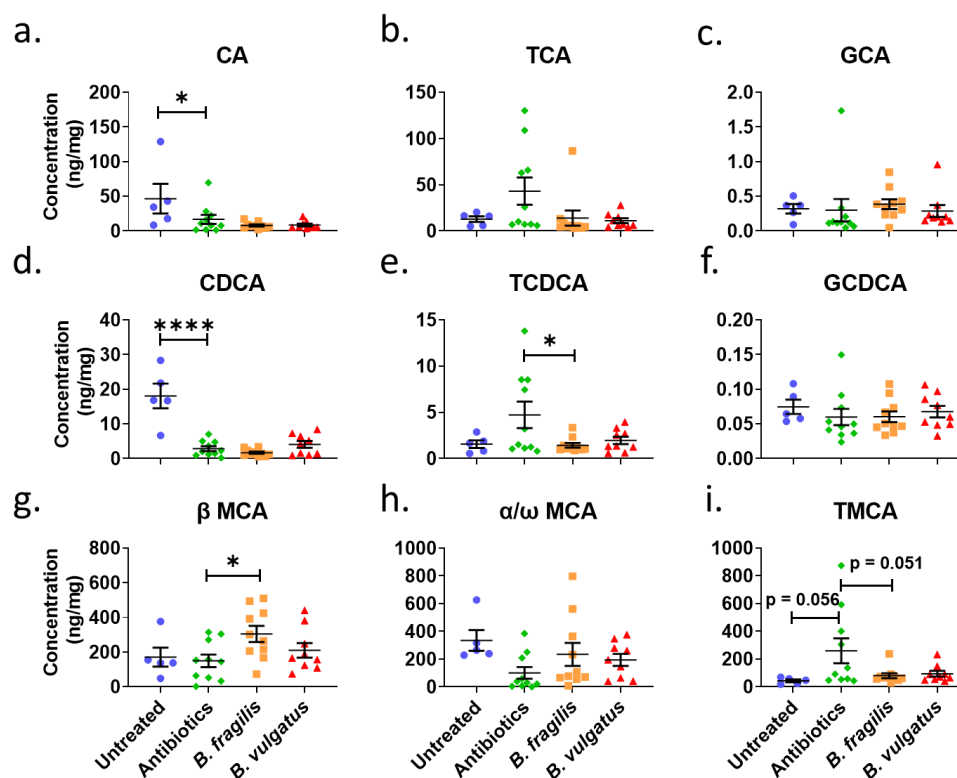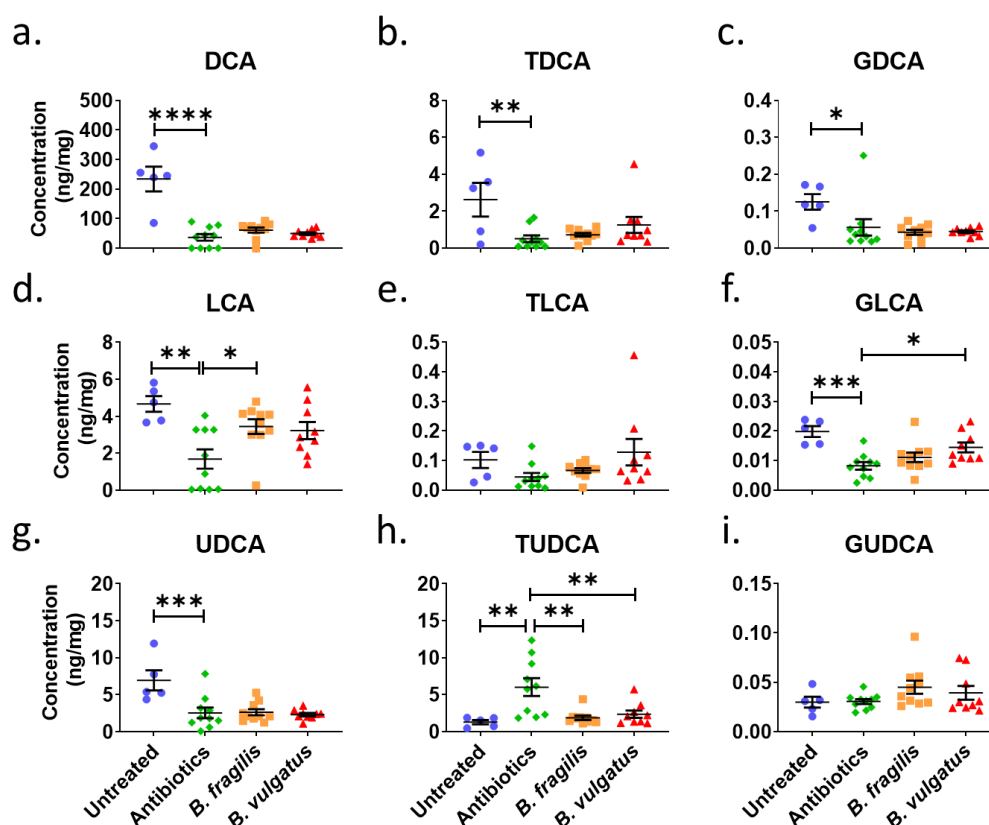
Figure 4.17 Assessment of faecal bile acid individual moieties, following oral gavage of *Bacteroides* species in C57BL6 mice. *Male mice were orally gavaged for 13 days with a full spectrum antibiotic cocktail consisting of 10 mg/mL metronidazole, 5 mg/mL vancomycin, 5 mg/mL neomycin, and 0.1 mg/mL amphotericin B and 1,000 mg/L ampicillin added to drinking water followed by oral gavage with 10^9 cfu B. fragilis NCTC 9343 and B. vulgatus ATCC 8482 for 2 consecutive days. On day 24, fecal samples were collected, and bile acids assessed. Concentration of individual BA moieties are shown based on potential microbial modification with representation among free, conjugated, and secondary BAs (a-h). Bile acids were normalised against internal standards and quantified using standard curves for each moiety using Waters® Targetlynx software. Data is presented as mean ± SD. n=5-10/group. Statistical significance was calculated using one-way ANOVA with Dunnett's post-hoc test with the control column as Antibiotics. * = p<0.05, ** = p<0.01, *** = p<0.001, and **** = p<0.0001.DCA; Deoxycholic acid, LCA; Lithocholic acid, UDCA; Ursodeoxycholic acid T and G indicated tauro and glyco conjugated moieties respectively.*

Although subtle alterations were determined at the level of each species, the dominant effect detected was through the antibiotic cocktail application. The microbiota was not assessed in these animal experiments, and the microbial colonization and viability of *Bacteroides* in the faeces were not assessed either. Therefore, conclusions on BA modifications in these

groups are abstract and could be the result of pathobiont or other outgrowth and are certainly representative of antibiotic microbial population culling rather than the input of *Bacteroides*.

Nevertheless, we examined potential relative receptor activation levels (**Figure 4.18**) to indicate that elevated receptor activation potential for the majority of receptors is associated with non-antibiotic treated animals except for FXR antagonism. Noteworthy is that GBAR1 (TGR5) receptor activation potential is significantly elevated (an LCA effect) in the presence of both *Bacteroides* species.
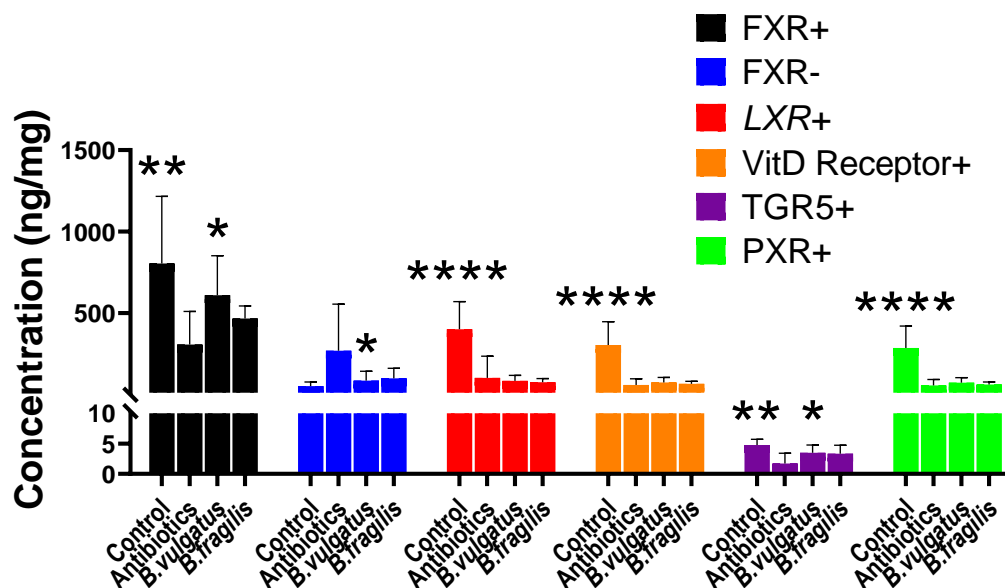
*Figure 4.18 The in vivo potential of antibiotic treatment and of Bacteroides gavage to modify BAs that activate nuclear, and G-protein coupled receptors is diminished and dominated by antibiotic treatment. Conversions were assessed for levels of those moieties that could collectively impact the Farnesoid X receptor (FXR), the liver X receptor (LX), Vitamin D Receptor (VitD), the Pregnane X receptor (PXR), G protein coupled receptor GBAR1 or alternatively named TGR5. Data is presented as mean ± SD. n=5-10/group. Significance was calculated using a student t-test between B. fragilis and B, vulgatus. * = p<0.05, ** = p<0.01, *** = p<0.001, and **** = p<0.0001.*

As a follow-up, a subset of the FXR-associated genes (FXR itself, LXR, Ost and MRP3 transporters and SHP (negative control)) were assessed for transcription by qPCR (**Figure 4.19**) where mRNA was extracted from the proximal colon region taken from each animal in the individual groups. A significant difference was detected for antibiotic-treated animals in Ostα gene expression an effect that was reversed in the presence of *Bacteroides* species. No other differences were detected at the RNA level.
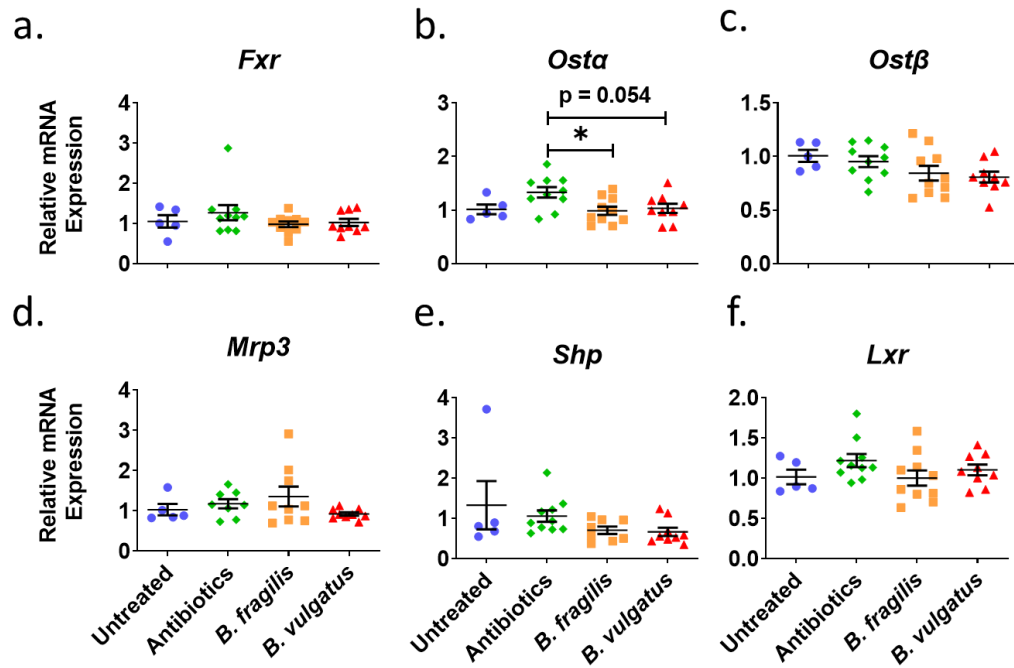
Figure 4.19 Assessment of gene expression of bile acid receptors and bile acid transporters in of C57Ll6 mice Male mice were orally gavaged for 13 days with a full spectrum antibiotic cocktail consisting of 10 mg/mL metronidazole, 5 mg/mL vancomycin, 5 mg/mL neomycin, and 0.1 mg/mL amphotericin B and 1,000 mg/L ampicillin added to drinking water followed by oral gavage with 10^9 cfu B. fragilis NCTC 9343 and B. vulgatus ATCC 8482 for 2 consecutive days. On day 24, colon samples were collected, and gene expression of (a) Fxr, (b) Ostα, (c) Ostβ, (d) Mrp3, (e) Shp and (f) Lxr was assayed by RT-qPCR. Data is presented as mean ± SD. n=5-10/group. Statistical significance was calculated using one-way ANOVA with Dunnett's post-hoc test with the control column as Antibiotics. * = p<0.05, ** = p<0.01, *** = p<0.001.

4.4 Discussion

Given a combined body of work to implicate reduced BA metabolism in IBDs (see introduction), we set out to determine whether *Bacteroides* species associated with IBD could impact BA signatures as mediators of metabolic and immune responses. This work was performed in 2016 when there was a sparsity of information on *Bacteroides* and their gut functional capacity. Investigations in this area have expanded since then.

Our analysis identified commonalities in key residue conservation indicating that the strains and the BSH enzymes selected, should be active. Differences in the loops and helices indicate a distance by *Bacteroides* from the crystal structure established for other microbes (*Bifidobacteria*, *Lactobacillus* and *Clostridia* spp BSHs) to point towards substrate variation and possible multiunit complexes as discussed above. Other regions of high conservation emerged that could serve as sites for future potential mutagenesis in determining range, interactions and indeed substrate preference for BSHs.

The established and conserved structures and residues for BSH have facilitated the search and design of inhibitor molecules to interfere with the enzyme catalytic site so that BSH manipulation towards weight gain or loss may be affected (Adhikari *et al.*, 2021). These authors modelled the *B. thetaiotaomicron* BSH and co-precipitated protein factors with purified BSH to identify potential inhibitors. They assayed deconjugation through ninhydrin amino acid liberation assays to detect patentable compounds of interest to support BSH inhibition. They further designed lithocholic acid

derivatives with modifications to its hydrocarbon side chains to impact and inhibit *Bacteroides* BSH relative to those of other genera (Adhikari *et al.*, 2021).   All these parameters showed inhibition in i*n vitro* assays with no toxicity effects on a subset of gut microbial represented groups.   They represent a next step manipulation of gut microbial function through BSH targeting.   However, the main focus or target is the highly conserved catalytic site, the effect *in vivo* would be general for BSH activity rather than bespoke.

Bacteroides BA modification was first identified in 1976 by Stellwag, to delimit functional BSH activity from purified protein from *B. fragilis* NCTC 9343*,* the same strain, applied to this study (Stellwag and Hylemon, 1976). A preference for TCA, TCDCA, TDCA but not LCA conjugates was identified for their BSH protein, but not for conjugates of LCA using thin layer chromatography.   In our hands with sensitive mass spectrometry and exact relative quantitation, GCA and TCA were not selected for deconjugation we also expanded the repertoire of BA metabolites to assign functionality and signature to *B. fragilis* NCTC 9343 (see Table 4.4 and Table 4.5).   The authors at that time suggested a non-selective role for BSHs, however, we subsequently know that this is not the case and that many different classes of BSH exist including 2 subclasses designated (T5 and T6) for *Bacteroides* by (Song *et al.*, 2019).   In their studies, they examined all *Bacteroides* representative sequences aligned to the gut environment, they then built a taxonomic picture of the isolates, from here site interrogation determined that those residues, later in the protein between 180 and 220 residues,

which we highlighted as conserved may serve as molecular docking sites including Gly218 for G/TCA, G/TCDCA, G/TCA, G/TCDA with interactions with Tyr189 important for TCA and TDCA conjugates and Ile 2219 important in terms of TUDCA interactions. Mutational analysis would confirm the interactive predictions and energetics of these reactions. They could also facilitate bespoke BSH construction to modulate and address specific conditions where specific BA levels are central to disease states.

The intrinsic properties of BSH liberated, and further microbially modified, BAs can alter signalling pathways. Indeed, modulating BA production through probiotic carrying BSHs (Jones, Martoni and Prakash, 2012; Joyce, MacSharry, *et al.*, 2014c; Hernández-Gómez *et al.*, 2021) has been applied to animals successfully but has delivered limited success in translation to humans in terms of metabolism and this may be related to the differences between rodents (98% tauro conjugated) and mammals (human bile are glycine: taurine conjugates at 3:1) in lipid metabolism and in the respective gut environments. However, the downstream products, bar the amino acids also liberated, are the same for the most part. Freed BAs represent potent receptor ligand BAs to modulate metabolism and immune responses mainly those to the FXR and GBAR1 (TGR5) (Chiang, 2013b). FXR can mediate a range of responses including BA uptake and synthesis, but it is promiscuous in nature for ligand binding and activation.

This study reveals the *in vitro* potential accumulation of FXR BA agonists (in potency order) CDCA>DCA>LCA>CA. Indeed, CA accumulation is

associated with *B. fragilis*, CDCA accumulation is associated to *B. vulgatus* suggesting different potential abilities to impact the FXR. among *Bacteroides* strains, FXR signalling feedback to the liver and alter BA synthesis, metabolic homeostasis particularly glucose and lipid metabolism (Joyce, MacSharry, *et al.*, 2014c). The effects of UDCA, also produced by *B. fragilis* on FXR are less clear with UDCA reported as an inhibitor of FXR agonists. LCA is a potent vitamin D receptor activation, neither strain showed the ability to generate LCA effectively in vitro. In terms of GBAR1, primarily activated by TLCA, a non-substrate for *Bacteroides* in our study. Activation is associated with systemic and local beneficial effects including increased gut motility (GLP hormone activation) (Pathak *et al.*, 2017). GBAR1 can activate macrophage inflammation response dampening (Pols *et al.*, 2011), it can induce browning of white adipose tissue (WAT to BAT) (Velazquez-Villegas *et al.*, 2018), it is documented to thyroxine-iodinase systems to influence of energy metabolism. Our animal work reveals that in the antibiotic-treated mice, *B. fragilis* promoted higher levels of GUDCA, an antagonist of the FXR. When gene expression analysis was interrogated by qPCR neither FXR nor GBAR1 levels were altered. However, post-translational modifications to their proteins, through either phosphorylation events or conformational changes can alter the activity of these proteins and their downstream effects. These aspects are not assayed by RNA assessments. Indeed, the FXR and GBAR1 are carried by both macrophages and by dendritic cells. Activation of the receptors causes polarization of macrophages to M2, they decrease dendritic cell maturation

and differentiation, and the combined effects here are to dampen inflammatory responses (Yang *et al.*, 2015; Ma *et al.*, 2018).

We observed the accumulation of 7ketoLCA, (or 7 oxo LCA) a functional output of identified 7-α HSDH enzymes and assigned to both *B. fragilis* and *B. thetaiotaomicron*. Indeed, our data suggests similarity in BA conversions for both strains implicating 7-α HSDH action similar to that of *B. fragilis* and that a single BSH is active in *B. thetaiotaomicron* VPI 5482. In contrast, *B. vulgatus* showed reduced substrate affinity, and an association to accumulate ursocholic acid from free CA. While intermediate BAs have remained largely ignored, it was not until a first role was assigned for intermediates in the differentiation of immune-associated cells that these BAs gained attention. (Campbell *et al.*, 2020b)) engineered strains (*Bacteroides)* to produce isoDCA and isoLCA that are central to T cell development. These BAs are the product of HSDH and epimerization actions, they can only be made once BSH has liberated and freed bile acids from amino acids as detailed in Figure 4.10 above. OxoBAs particularly 3-oxo-LCA are also associated with T Helper cell differentiation increasing the levels of Tregs (Hang *et al.*, 2019; Song *et al.*, 2019).

Animal experiments were conducted to examine whether those modifications detected *in vitro* in co-incubations assays with single bacteria could translate to *in vivo*, whole animal situations. Antibiotics were applied to niche clearance in advance of a 24 hour clear out time, before *Bacteroides* species introduction. Our data indicated the dominant effect of the antibiotic treatment -a severe combination of ampicillin, metronidazole,

vancomycin, neomycin and, amphotericin B- since modifications to BAs, a function of gut microbes was significantly altered. Antibiotic applications, by their very nature, are associated with negative shifting of microbial population density and diversity shifting, as well as in increasing pathobiont outgrowth opportunities, with resultant impacts on metabolism (reviewed by (Lange *et al.*, 2016)). Recovery of populations appears antibiotic-specific and can vary from months to years, in humans, depending on the antibiotic (nicely reviewed by (Yang *et al.*, 2021). It is also possible that the antibiotic cocktail may have residual effects to impact incoming *Bacteroides* species in the time frame. Indeed, vancomycin was shown to reduce *Bacteroides* representation, associated metabolites took 9 days in which to appear at levels of detection (Choo *et al.*, 2017), and ampicillin derivatives target *Bacteroides* populations among others (Oh *et al.*, 2016). Indeed, vancomycin and neomycin are broad-spectrum antibiotics, they not only alter microbial diversity including these Firmicutes, but they also adjust immune system responses (Harris *et al.*, 2018). Hence, in clearing a niche, consideration of short-term and longer-term colonization resistance should be considered going forward.

Chapter 5 Gender specific alterations in inflammatory response, microbiome, and downstream metabolite signalling in antibiotic microbiota depleted IL-10$^{-/-}$ mice and colonised with *B. vulgatus*.

5.1 Abstract

Crohn's disease (CD) is a chronic inflammatory condition of unknown aetiology, with the microbiota thought to be a major contributor to the disease. Previous *in vitro* studies indicate *Bacteroides vulgatus* provoked a higher inflammatory response, and impact epithelial cell homeostasis in a human colon cell line and murine organoids. In addition, *B. vulgatus* selectively affect bile acids (BA) *in vitro*. This study aims to translate these findings by using a genetically modified host, IL-10$^{-/-}$ mice, colonised with B. vulgatus. Thirty IL-10$^{-/-}$ mice were randomised into 3 groups, receiving PBS (control), an antibiotic cocktail and an antibiotic cocktail followed by *B. vulgatus* gavage. Faecal samples were collected over time for microbiota and BA analysis and colon samples were collected for gene expression analysis. Male IL10$^{-/-}$ mice colonised with *B. vulgatus* developed more intestinal inflammation based on an altered inflammatory and epithelial gene profile, microbiota and bile acid composition and histology. Notably, female IL10$^{-/-}$ mice with antibiotic-depleted-microbiota developed intestinal inflammation, not seen in male counterparts or female IL10$^{-/-}$ mice colonised with *B. vulgatus*. Collectively, our data indicate that *B. vulgatus* has a subtle but persistent effect on host and microbial responses, especially in males, in genetically susceptible individuals.

5.2 Introduction

In Chapter 3 we have demonstrated that *Bacteroides* species can elicit inflammatory responses *in vitro*, with *B. vulgatus* being the most pro-inflammatory. However, colonisation of a genetically intact host with *Bacteroides* spp did not recapitulate this inflammation *in vivo*. The genetic background represents a significant risk for the development of CD with monozygotic twins having a 58% concordance rate for CD development (Tysk *et al.*, 1988). Genome-wide association studies have further highlighted the link between genetics and CD where ~ 200 risk loci were associated with both CD and UC with mutations in NOD2, and ATG16L1 identified as major risk determinants for CD (Bianco, Girardelli and Tommasini, 2015). A single nucleotide polymorphism (SNP) in the promoter region of IL-10 has also been associated with increased CD risk with defective IL-10 production leading to more severe phenotypes of CD (Franke *et al.*, 2008; Correa *et al.*, 2009). Interleukin-10 is an immunoregulatory cytokine produced by immune cells such as macrophages, dendritic cells, and T cells and is crucial for the maintenance of intestinal homeostasis. It mediates its immunomodulatory functions through the suppression of Th1 and Th17 cells (Murray, 2006; Paul, Khare and Gasche, 2012). Mice that have IL-10 knocked out (IL-10$^{-/-}$ mice) develop spontaneous colitis with histological characteristics similar to CD (Kühn *et al.*, 1993b; Bleich *et al.*, 2004). They exhibit discontinuous transmural inflammation with inflammatory cell invasion to the lamina propria and submucosa, epithelial hyperplasia, mucin depletion, and crypt abscesses (Berg *et al.*, 1996b; Bleich *et al.*, 2004). Development of colitis

in IL-10$^{-/-}$ mice is dependent on the microbiota as germ-free IL-10$^{-/-}$ mice do not develop colitis (Sellon *et al.*, 1998b). This makes them an ideal model for investigating the impact of *B. vulgatus* on CD pathology as they constitute a genetically compromised host that will develop colitis in response to the gut microbiota.

In Chapter 4 we showed that *Bacteroides* spp, *in vitro*, possess the capacity to alter bile acids, generating intermediate moieties in the production of secondary bile acids by the gut microbiota. The CD-*Bacteroides* strains generated different impacts with *B. fragilis* having a high ability to modify bile acids, while *B. vulgatus*, was more selective e.g., conjugated bile acid substrates and in modifying single freed bile acids. A subtle effect was noticed in the *Bacteroides* colonised wild-type mice, which might be attributed to the dominant effect of the antibiotic cocktail.

In this chapter, we aimed to validate our *in vitro* findings from chapters 3 and 4 in an *in vivo* disease-relevant setting. For this purpose, we examined the causal role of *B. vulgatus* in intestinal inflammation by assaying its impact on the host immune and epithelial response, microbiota composition and bile acid metabolism and signalling in a genetically susceptible individual, IL10$^{-/-}$ mice.

5.3 Results

5.3.1 Characterisation of the inflammatory profile in an IL10$^{-/-}$ mouse model of colitis

Development of inflammation in IL-10$^{-/-}$ mice is dependent on genetic background and microbiota (Kühn *et al.*, 1993b; Mähler and Leiter, 2002). To assess the age and location that IL10$^{-/-}$ mice developed colitis a longitudinal study was designed (**Figure 5.1**). Each group consisted of males and females with n = 6-10 mice per group. Groups 1-5 contained IL10$^{-/-}$ mice aged 6, 9-10, 13, 16 and 19 weeks respectively with group 6 being wild-type (WT) mice aged 9-13 weeks. At each timepoint faeces and organs were collected and assessed for inflammation by physical measurements of the organs and analysis of inflammatory biomarkers and gene expression.
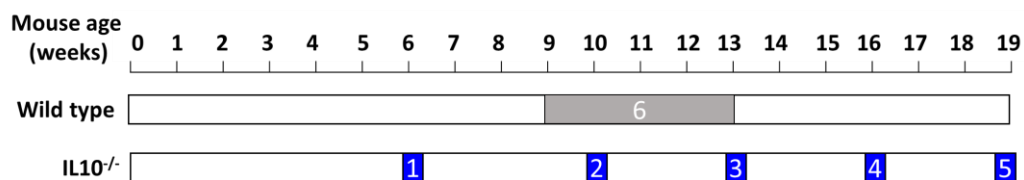
Group 1: IL10$^{-/-}$ 6 weeks (n=8, 4 males and 4 females)
Group 2: IL10$^{-/-}$ 9-10 weeks (n=8, 4 males and 4 females)
Group 3: IL10$^{-/-}$ 13 weeks (n=10, 5 males and 5 females)
Group 4: IL10$^{-/-}$ 16 weeks (n=8, 3 males and 5 females)
Group 5: IL10$^{-/-}$ 19 weeks (n=7, 2 males and 5 females)
Group 6: Wild type 9-13 weeks (n=6, 3 males and 3 females)

Figure 5.1 Schematic of longitudinal study design in IL10$^{-/-}$ mice, to characterise the progression of spontaneous colitis. Wild-type mice were euthanised at 9-13 weeks old and IL10$^{-/-}$ were euthanised at 6, 10, 13, 16, and 19 weeks old. Fluids, faecal, caecal, and intestinal samples were collected at the different timepoints.

5.3.1.1 IL10$^{-/-}$ mice develop colitis between 16 and 19 weeks old

Assessment of the colon in IL10$^{-/-}$ mice based on male and female distribution, showed no shortening of its length (**Figure 5.2 a and e**) relative to wild-type mice at any time point. However, the total colon weight was significantly increased in male IL10$^{-/-}$ mice at 19 weeks, when compared with WT controls, this increase in weight, was not seen in female IL10$^{-/-}$ mice (**Figure 5.2 b and f**). Though when the colon was examined in more detail it was seen that the proximal colon of male IL10$^{-/-}$ mice weighed significantly more than WT mice at 19 weeks old while the female IL10$^{-/-}$ mice proximal colon weighed significantly more than the WT mice at 16- and 19-weeks old (**Figure 5.2 c and g**). For the distal colon only a significant increase in weight, relative to WT mice, was seen in male IL10$^{-/-}$ mice aged 19 weeks (**Figure 5.2 d**). While there was no significant difference between the distal colon weights of female IL10$^{-/-}$ and WT mice it was evident that there was variability in the degree of inflammation in the female IL10$^{-/-}$ groups, which was also observed for total colon and proximal colon weights (**Figure 5.2 f-h**). Spleen and liver relative weights were insignificantly altered, for both genders, between IL10$^{-/-}$ and WT mice (**Figure 5.2 e**).
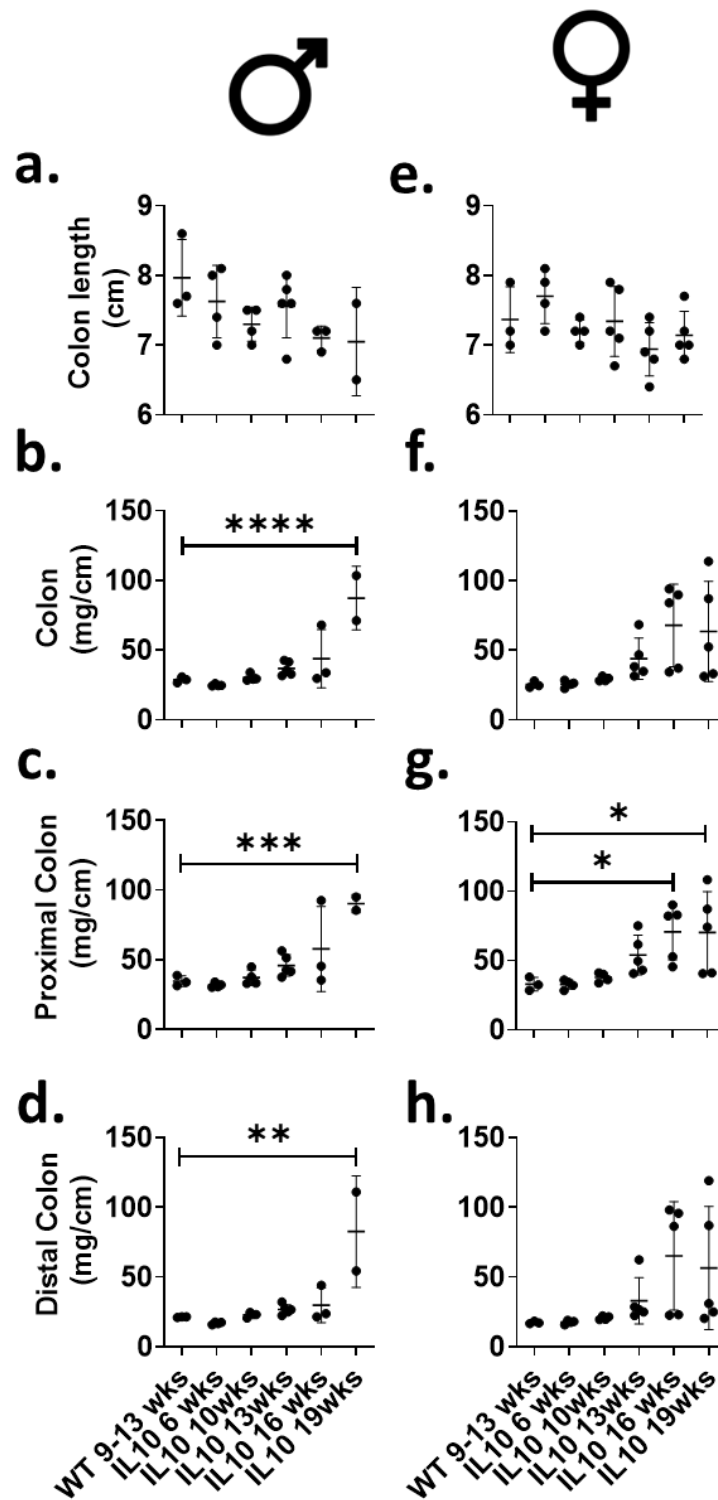
Figure 5.2 Colonic parameters of IL10$^{-/-}$ mice aged over time. Following euthanasia colon parameters - colon length and weights - were recorded from (a-d) male (e-h) and female mice. (a and e) Colon length; (b and f) colon weight; (c and g) proximal colon weight; (d and h) distal colon weight. Data is presented as mean ± SD. Statistical significance was calculated using one-way ANOVA with Dunnett's post-hoc test with the WT 9-13 wks column as control. * = p<0.05, ** = p<0.01, *** = p<0.001, and **** = p<0.0001. n=2-5/gender/group.

Similarly, to the colon weights seen in the female mice, there is the appearance of two populations for spleen weight, indicating systemic inflammation in some of the female IL10$^{-/-}$ mice (**Figure 5.3 e**). Faeces were collected and scored to assess the presence/degree of diarrhoea as a marker for colitis. Male IL10$^{-/-}$ mice faecal scores were not significantly different from WT mice however female IL10$^{-/-}$ mice at 6, 13, 16 and 19 weeks old had a significantly higher faecal score than WT mice (**Figure 5.3 a and d**).
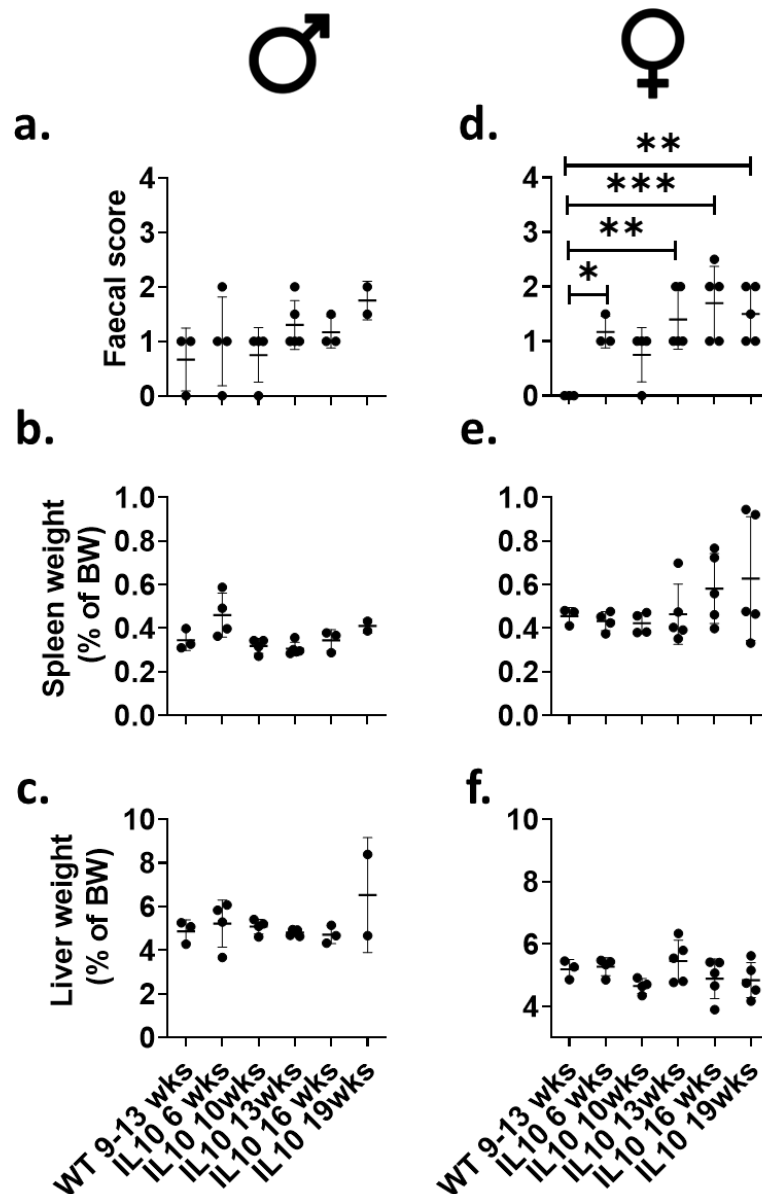
Figure 5.3 Physiological parameters of IL10⁻/⁻ mice aged over time. Following euthanasia weights of liver and spleen and faecal scoring was recorded from (a-d) male and (e-h) female mice. (a and d) Faecal score, (b and e) spleen weight and (c and f) liver weight is presented relative to body weight (% BW). Data is presented as mean ± SD. Statistical significance was calculated using one-way ANOVA with Dunnett's post-hoc test with the wild-type WT 9-13 wks column as control. * = p<0.05, ** = p<0.01, *** = p<0.001. n=2-5/gender/group.

Faecal calprotectin levels are often used as a reliable biomarker for neutrophil infiltration of the mucosa and so inflammation (Walsham and Sherwood, 2016). Here faecal calprotectin levels were measured via ELISA

and there was no significant difference between IL10$^{-/-}$ and wild WT mice (**Figure 5.4 a and b**). However, again it was apparent that there were two populations of IL10$^{-/-}$ mice. Faecal calprotectin levels in IL10$^{-/-}$ mice were elevated at 13 and 16 weeks for males and females, respectively, although this was obvious for a subset of mice in each group.
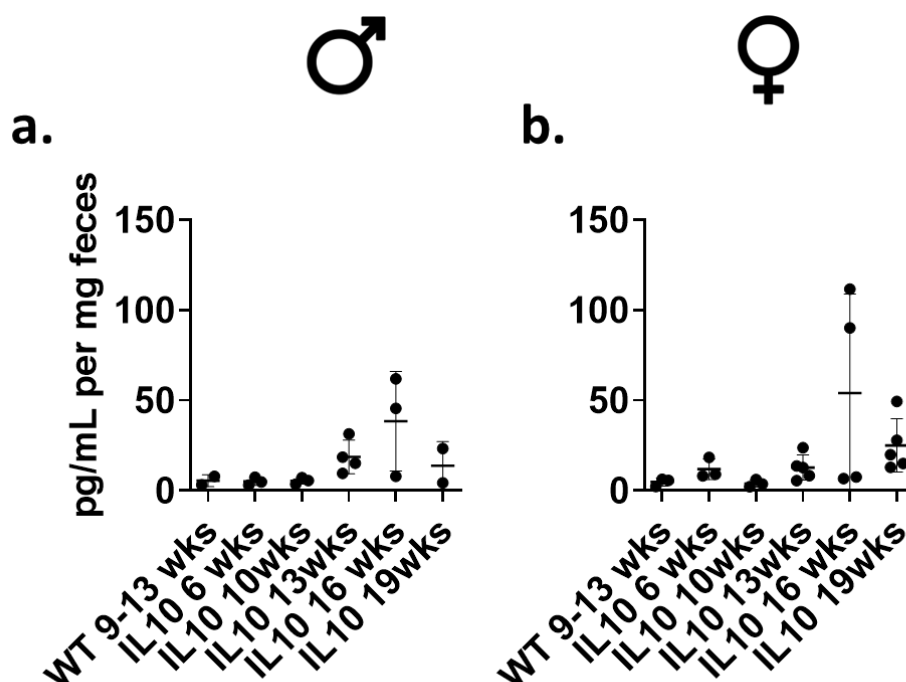
*Figure 5.4 Faecal calprotectin levels from IL10$^{-/-}$ mice aged over time. Faecal samples were collected at the time of euthanasia from (a) male and (b) female animals and calprotectin concentration assayed by ELISA. Data is presented as mean ± SD. Statistical significance was calculated using one-way ANOVA with Dunnett's post-hoc test with the wild-type (WT) 9-13 wks column as control. * = p<0.05, ** = p<0.01, *** = p<0.001. n=2-5/gender/group.*

These data suggest that in our facility IL10$^{-/-}$ mice develop spontaneous colitis between 16 and 19 weeks, as demonstrated by the increased weight of their colon. As previously reported in this genetic background of IL10$^{-/-}$ mice, the penetrance of colitis is not 100%, as demonstrated by the faecal calprotectin data and macroscopic markers of disease.

5.3.1.2 IL10$^{-/-}$ mice display increased inflammatory and decreased epithelial homeostatic gene expression

Following the assessment of organs and inflammatory biomarkers, RNA was isolated from the proximal colon for gene expression analysis. The proximal colon was chosen as it appeared to have the greatest level of inflammation due to its increased weight. Genes related to inflammation, immune receptors, cell junctions and epithelial homeostasis were assessed. Gene expression of inducible nitric oxide synthases (iNOS), a potent chemoattractant for neutrophils, was analysed and was significantly increased in male IL10$^{-/-}$ mice at 19 weeks compared to WT (**Figure 5.5 a**). There was no significant change observed in female IL10$^{-/-}$ mice (**Figure 5.4 e**) but there was a noticeable increase in iNOS expression at 16 and 19 weeks of age, with a consistent variability seen above. Similarly, to iNOS, the gene expression of the Th1 cytokine Interferon γ (IFNγ) was significantly increased in male IL10$^{-/-}$ mice at 19 weeks of age relative to WT with no significant, but variable, alteration in female IL10$^{-/-}$ mice (**Figure 5.4 b and d**). Contrary to IFNγ and iNOS, IL-1β expression was not significantly altered in either gender or age of IL10$^{-/-}$ mice relative to WT. TLR4 expression in male IL10$^{-/-}$ mice was not significantly different from WT mice but did appear to be decreased in mice aged 10-19 weeks. In female IL10$^{-/-}$ mice, TLR4 expression was decreased relative to WT at age 13-16 weeks but not at 19 weeks of age due to variability (**Figure 5.4 d and h**).
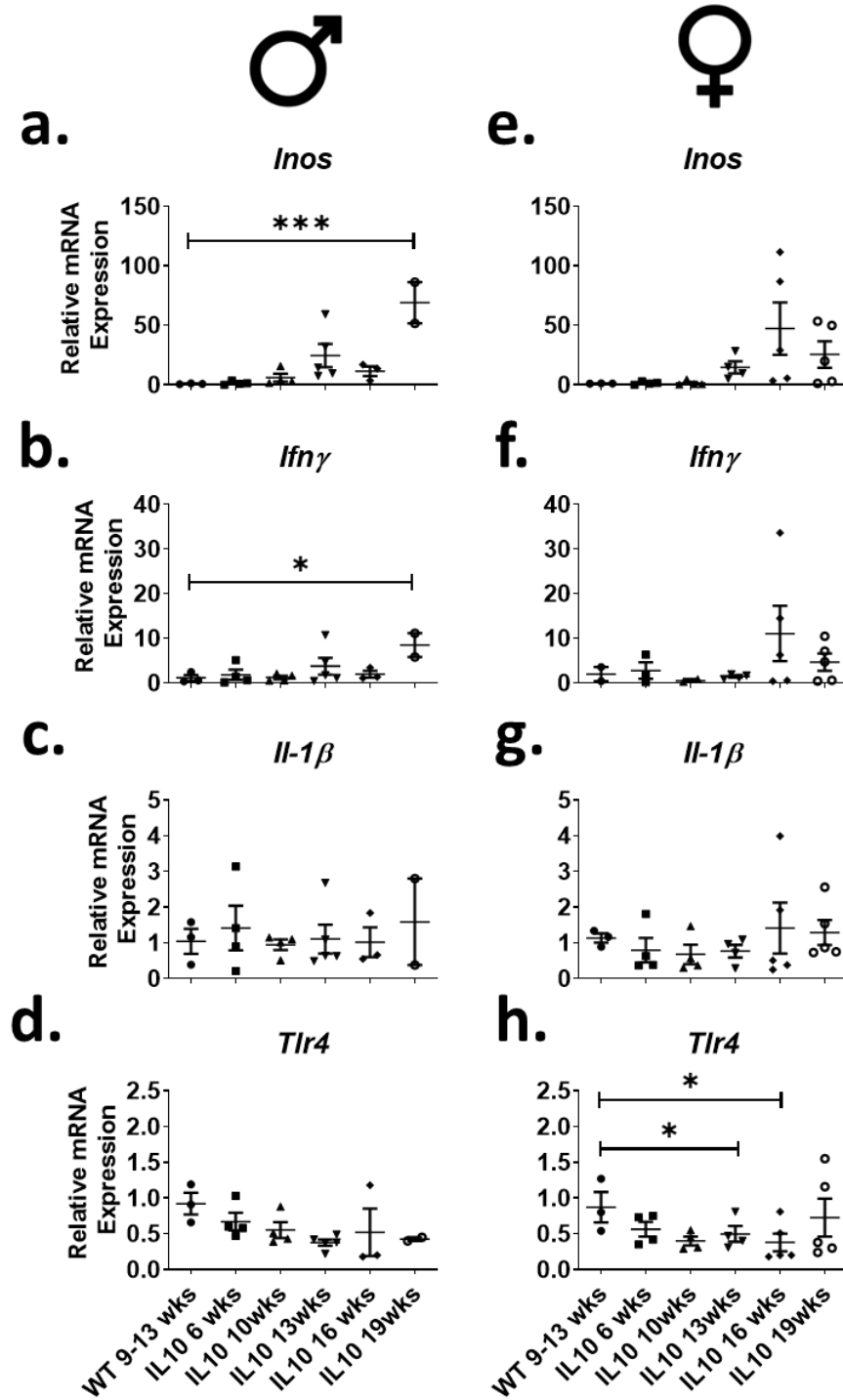
Figure 5.5 Gene expression analysis of colonic inflammatory markers of IL10$^{-/-}$ mice aged over time. Following euthanasia colons were collected from (a-d) male and (e-h) female IL10$^{-/-}$ mice and assayed for the expression of (a and e) Inos, (b and f) Ifnγ, (c and g) Il-1β, and (d and h) Tlr4 by RT-qPCR. Data is presented as mean ± SD. Statistical significance was calculated using one-way ANOVA with Dunnett's post-hoc test with the wild-type WT 9-13 wks column as control. * = p<0.05, ** = p<0.01, *** = p<0.001. n=2-5/gender/group.

The expression of CDH1, the gene for the adherens junction protein E-cadherin was analysed to evaluate if any disruption to the epithelial barrier was present in IL10$^{-/-}$ mice over time. There was no significant difference in CDH1 expression, for any gender or age, between IL10$^{-/-}$ mice and WT but there was a noticeable trend of decreased CDH1 expression in the IL10$^{-/-}$ mice (**Figure 5.6 a and d**). Claudin 2, coded for by the gene CLDN2, is a tight junction protein responsible for paracellular ion and water transport in the gut epithelium. In IL10$^{-/-}$ mice, of either gender, its expression is not altered relative to control.

Krüppel-like factor 4 (Klf4) is a gene vital for proliferation, differentiation, and homeostasis of the gut epithelium, with its depletion resulting in altered epithelial morphology and polarity (Yu et al 2012). Here we demonstrate that from as young as 6 weeks to 19 weeks the expression of Klf4 in IL10$^{-/-}$ mice, of both genders, is significantly decreased (**Figure 5.6 c and f**).
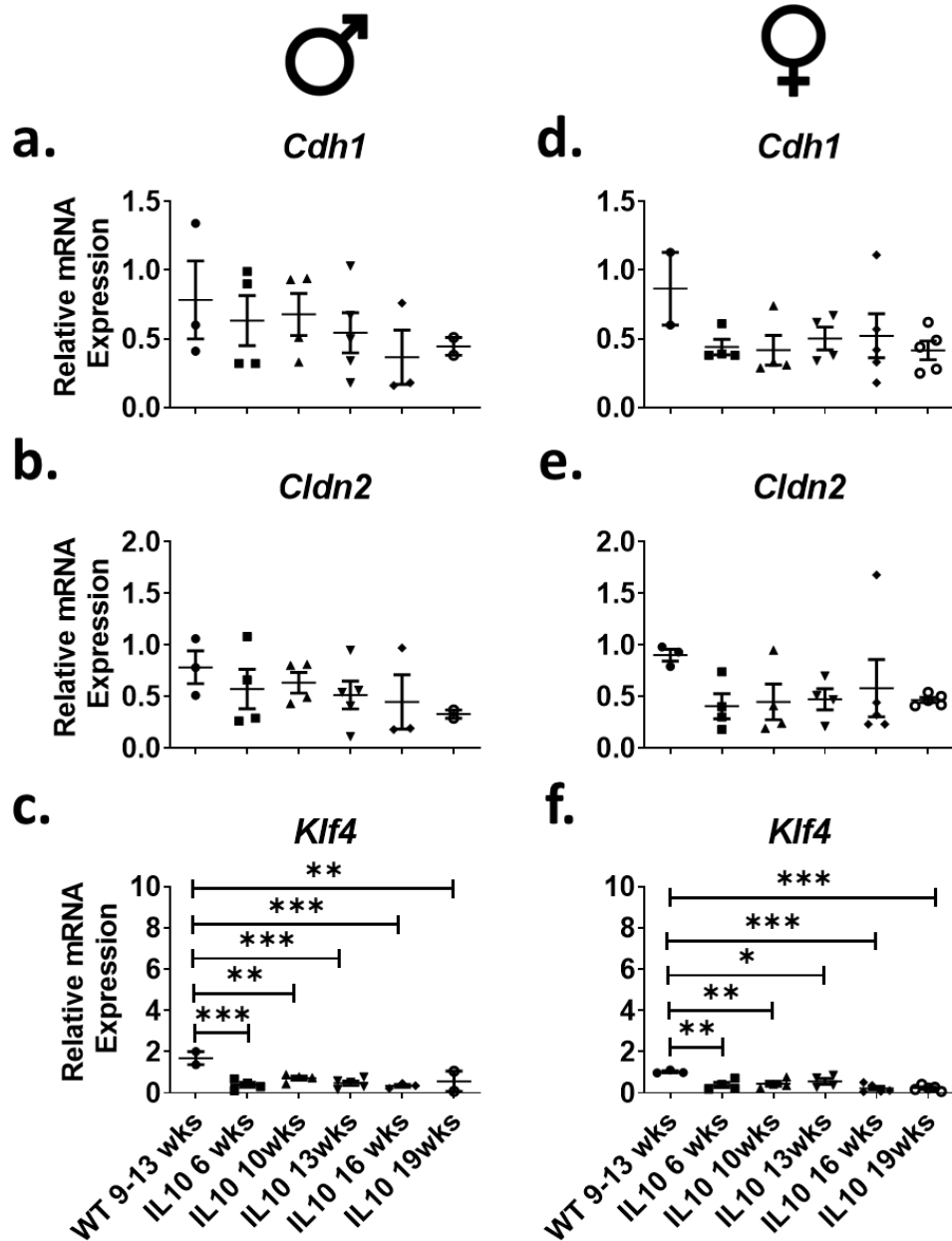
*Figure 5.6 Gene expression analysis of colonic epithelial markers of IL10$^{-/-}$ mice aged over time. Following euthanasia colons were collected from (a-c) male and (d-f) female IL10$^{-/-}$ mice and assayed for the expression of (a and d) Cdh1, (b and e) Cldn2, and (c and f) Klf4.by RT-qPCR. Data is presented as mean ± SD. Statistical significance was calculated using one-way ANOVA with Dunnett's post-hoc test with the wild-type WT 9-13 wks column as control. * = p<0.05, ** = p<0.01, *** = p<0.001. n=2-5/gender/group.*

These gene expression data corroborate the macroscopic data in **section 5.3.1** that colitis develops in IL10$^{-/-}$ mice between 16-19 weeks of age showing an increase in inflammatory gene expression at these time points.

These data agree with macroscopic markers of disease reported in the section above.

From these collected data, the age of 9-11 weeks of IL10$^{-/-}$ mice was selected as it represents an adult population and prior to the onset of inflammation which would be ideal to study the impact of *B. vulgatus* on the progression of colitis.

5.3.2 The impact of proinflammatory *B. vulgatus* colonisation on colitis progression in IL10$^{-/-}$ mice

In Chapter 3, *B. vulgatus* demonstrated the largest inflammatory potential and therefore this species was chosen for the *in-vivo* studies in the IL10$^{-/-}$ mice. An experiment was designed (**Figure 5.7**) where IL10$^{-/-}$ mice aged 9-11 weeks were randomised into3 treatment arms: Group 1: sham PBS oral gavage; Group 2: antibiotic cocktail (**Table 2.6**) and sham PBS oral gavage and Group 3: antibiotic cocktail and oral gavage of 200µl of 5X10^9 cfu/ml of *B. vulgatus*.

The IL10$^{-/-}$ mice were treated with an antibiotic cocktail for 13 days to deplete the gut microbiota and clear a niche to facilitate *B. vulgatus* colonisation (Reikvam *et al.*, 2011). IL10$^{-/-}$ mice were treated with antibiotics, or PBS, for 13 days following which they were rested for one day to allow both recovery and antibiotic washout of the mice. Then IL10$^{-/-}$ mice were inoculated with *B. vulgatus*, or PBS, for 3 days and this was repeated ~every 4 weeks. The study ran until the IL10$^{-/-}$ mice were 23-25 weeks old when, based on data from **Section 5.3.1**, some of the mice would be experiencing chronic inflammation. Body weight was monitored every 4 days during antibiotic treatment and then every ~3 days throughout the

experiment. Faeces were collected throughout the trial for faecal calprotectin monitoring, 16S analysis, and bile acid analysis.
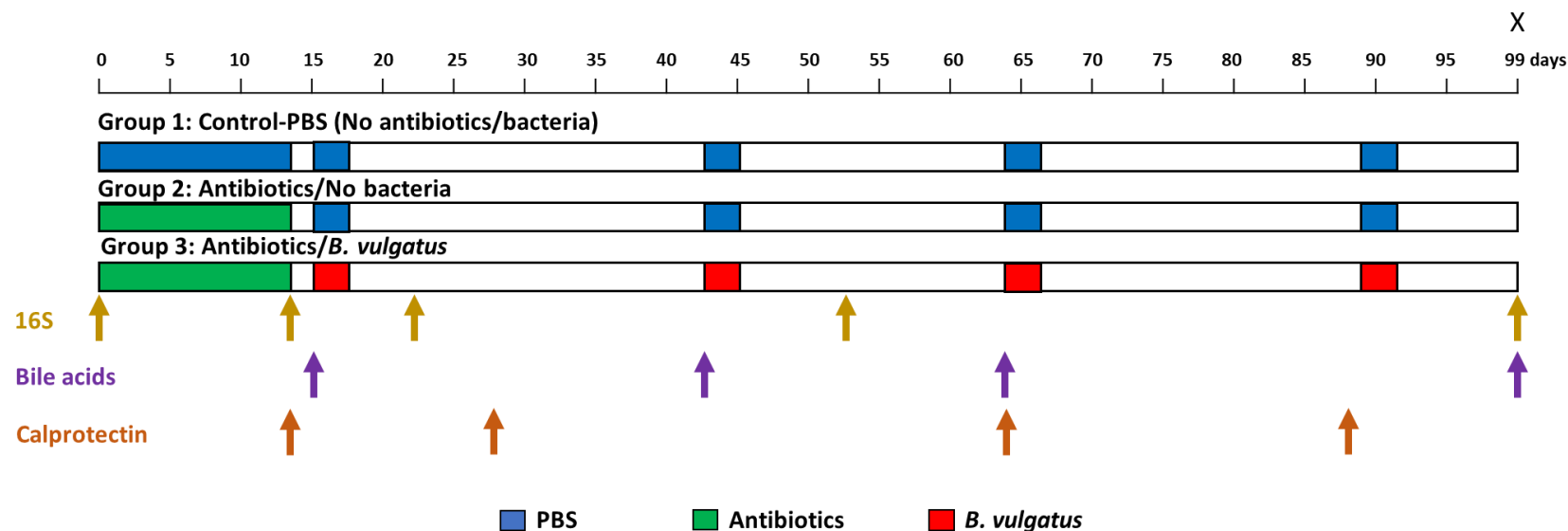
Figure 5.7 Schematic design of IL10-/- mice depleted of microbiota by full spectrum antibiotic treatment, followed by colonisation of the IBD associated Bacteroides vulgatus to determine its microbial, metabolome and inflammatory modulating potential. IL10$^{-/-}$ mice were treated with an antibiotic cocktail or vehicle (PBS), for 13 days via oral gavage followed by oral gavage of 1x10^9 cfu/200µl B. vulgatus, or vehicle (PBS), for 3 days. Oral gavage of B. vulgatus and PBS was repeated 3 times every 3-4 weeks (at days 15, 42, 64, 87). Group 1 received no antibiotics or bacteria but received sham PBS oral gavage. Group 2 received antibiotics for 13 days followed by sham PBS oral gavage in lieu of B. vulgatus. Group 3 received antibiotics for 13 days followed by oral gavage of B. vulgatus. During antibiotic treatment mouse weights were recorded every 4 days and every second day following that. Arrows indicate faeces collection for 16S analysis (gold arrows), bile acid analysis (purple arrow) and Calprotectin analysis (brown arrow). Animals were euthanised at day 99 post start and fluids, faecal, caecal and intestinal samples collec

269

5.3.2.1 *B. vulgatus* colonisation has a divergent effect, by gender, on macroscopic parameters of inflammation of IL10^{-/-} mice

Body weight was monitored throughout antibiotic treatment in IL10$^{-/-}$ mice in line with ethical approval and animal welfare. There was a significant drop in body weight, for both genders, at day 4 in the antibiotic-treated mice relative to the PBS-treated mice (**Figure 5.8 a and b**), followed by partial recovery to starting weight at the end of antibiotic-treatment. Weight monitoring was continued from day 30 of the experiment until day 99 with a significant difference in weight between antibiotic treated female mice and PBS-treated mice on day 90 (**Figure 5.8 d**). At the end of the experiment (day 99), a difference between groups and weight was evident, although not significant, between the genders with *B. vulgatus* treated mice weighing less in the male mice, while antibiotic-treated mice weighed less in the female mice (**Figure 5.8 c and d**).
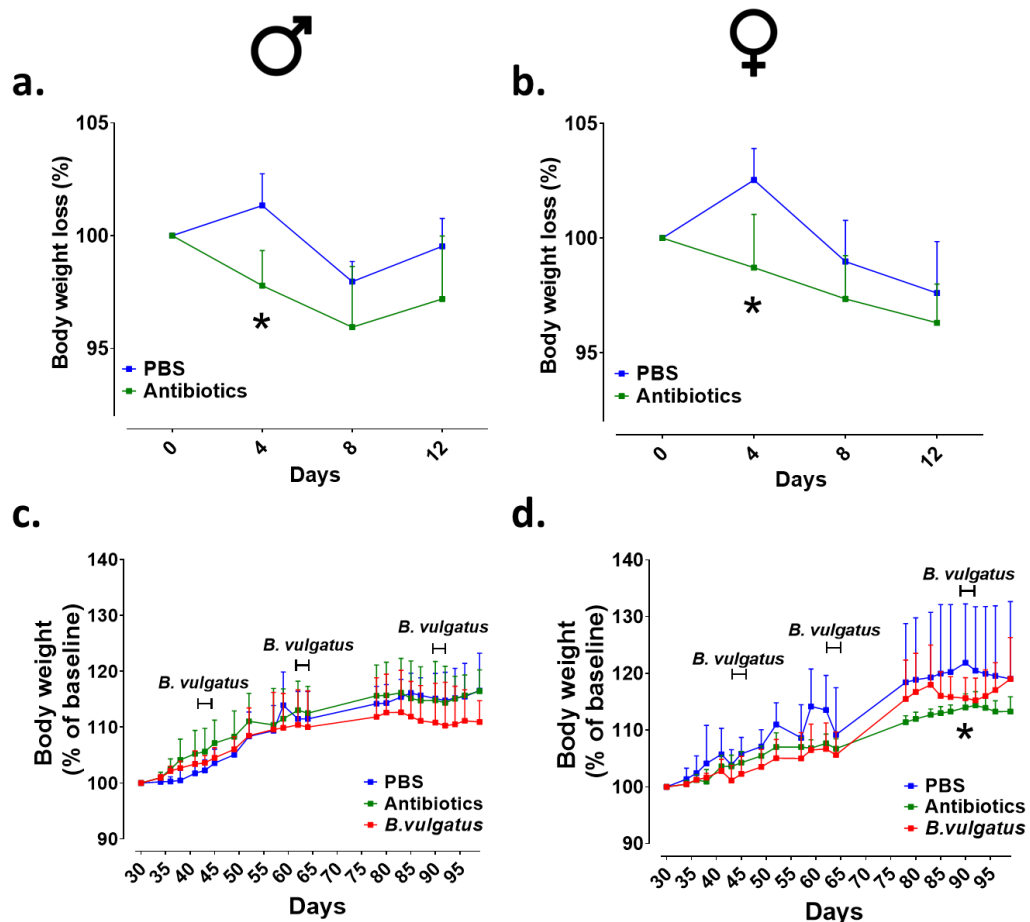
*Figure 5.8 Body weight monitoring in (a and c) male and (b and d) female IL10^{-/-} mice.(a) Male and (b) female IL10-/- mice were orally gavaged with a full spectrum antibiotic cocktail consisting of 10 mg/mL metronidazole, 5 mg/mL vancomycin, 5 mg/mL neomycin, 0.1 mg/mL amphotericin B, and 1,000 mg/L ampicillin added to the drinking water for 13 days. Body weight was recorded every 4th day. (c) Male and (d) female IL10-/- mice orally gavaged with PBS or 1x109 cfu/200μL of B. vulgatus for 3 consecutive days, repeated every 3-4 weeks, and body weight monitored every 3rd day. Data presented as mean ± SD. Statistical significance calculated using two-way ANOVA. * = p<0.05 n = 2-5 mice/gender/group.*

The weights of the dissected organs, colon, cecum, and spleen were determined, as indicators of mucosal and systemic inflammation. No significant difference in the length of the colon, for either gender, was seen between treatment arms (**Figure 5.9 a and e**). However, when weighed the colons showed a significant difference between groups characterised by gender. In male mice, total colon weight was significantly increased in the *B. vulgatus* treated mice relative to both PBS and antibiotic-treated male

mice (**Figure 5.9 b**). Whereas in female mice the colon weighed significantly more in the antibiotic-treated mice relative to PBS and *B. vulgatus* treated female mice (**Figure 5.9 f**). Proximal colon weights exhibited the same trend, with weight in male mice significantly increased in *B. vulgatus* treated mice relative to PBS treated mice (**Figure 5.9 c**). The weight in female mice was significantly increased relative to PBS and *B. vulgatus* treated mice (**Figure 5.9 g**). However, for the distal colon, in males, *B. vulgatus* treated mice weighed more relative to PBS treated mice with no significant difference between groups in weight seen in the female mice (**Figure 5.9 d and h**).

Figure 5.9 Colonic parameters of IL10$^{-/-}$ mice colonised with B. vulgatus. *(a-d) Male and (e-f) female mice were orally gavaged for 13 days with a full spectrum antibiotic cocktail consisting of 10 mg/mL metronidazole, 5 mg/mL vancomycin, 5 mg/mL neomycin, and 0.1 mg/mL amphotericin B and 1,000 mg/L ampicillin added to drinking water followed by oral gavage with B. vulgatus (10^9 cfu) for 3 consecutive days, repeated every 4 weeks. On day 99 colons were collected and colon parameters - length and weights - were recorded from (a-d) male and (e-h) female IL10$^{-/-}$ mice. (a and e) Colon length; (b and f) colon weight; (c and g) proximal colon weight; (d and h) distal colon weight). Data is presented as mean ± SD. Statistical significance was calculated using one-way ANOVA with Bonferroni post-hoc test. * = p<0.05, ** = p<0.01, *** = p<0.001. n=3-5 mice/gender/group.*

Cecal weight was significantly lower in male *B. vulgatus* treated mice relative to PBS treated but no difference was seen in the female groups (**Figure 5.10 b and d**). In contrast, the spleen weight was significantly increased in *B. vulgatus* treated males relative to PBS treated, with no significant difference seen in females (**Figure 5.10 a and c**).
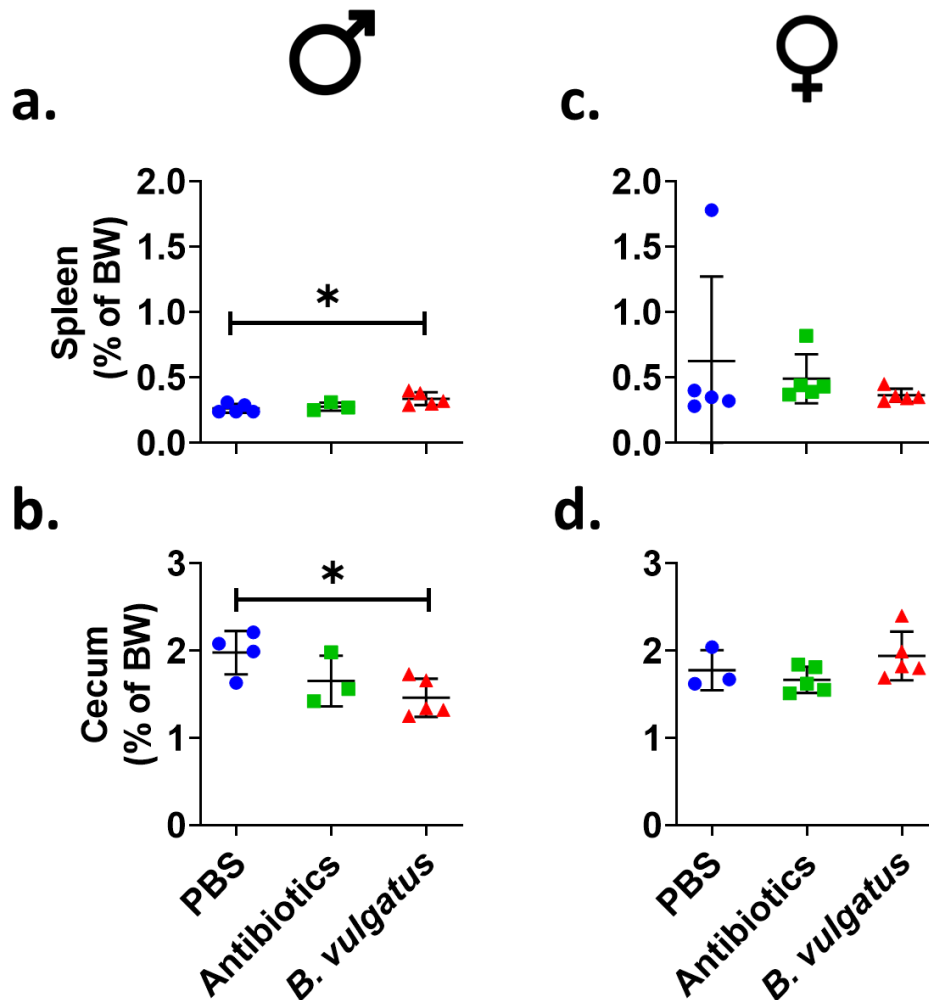
Figure 5.10 Spleen and cecum weights of IL10$^{-/-}$ mice colonised with B. vulgatus. (a-b) Male and (c-d) female mice were orally gavaged for 13 days with a full spectrum antibiotic cocktail consisting of 10 mg/mL metronidazole, 5 mg/mL vancomycin, 5 mg/mL neomycin, and 0.1 mg/mL amphotericin B and 1,000 mg/L ampicillin added to drinking water followed by oral gavage with B. vulgatus (10^9 cfu) for 3 consecutive days, repeated every 4 weeks. On day 99 organs were collected and weights of spleen and liver were recorded from male (a-b) and female (c-d) IL10$^{-/-}$ mice. (a and c) Spleen weight and (b and d) liver weight is presented relative to body weight (% BW). Data is presented as mean ± SD. Statistical significance was calculated using one-way ANOVA with Bonferroni post-hoc test. * = p<0.05. n=3-5 mice/gender/group.

Faecal calprotectin was assessed throughout the trial to monitor colitis (**Figure 5.11**); however, these data do not align with the macroscopic parameters outlined above. Data from faecal calprotectin ELISA shows that PBS-treated mice had significantly elevated faecal calprotectin levels relative to antibiotic-treated mice, regardless of gender. A similar profile was seen from day 27 until the end of the experiment (**Figure 5.11**). This directly contradicts the data on increased colon weight of male *B. vulgatus* treated mice and female antibiotics treated mice. Currently, we don't have an explanation for this discrepancy.
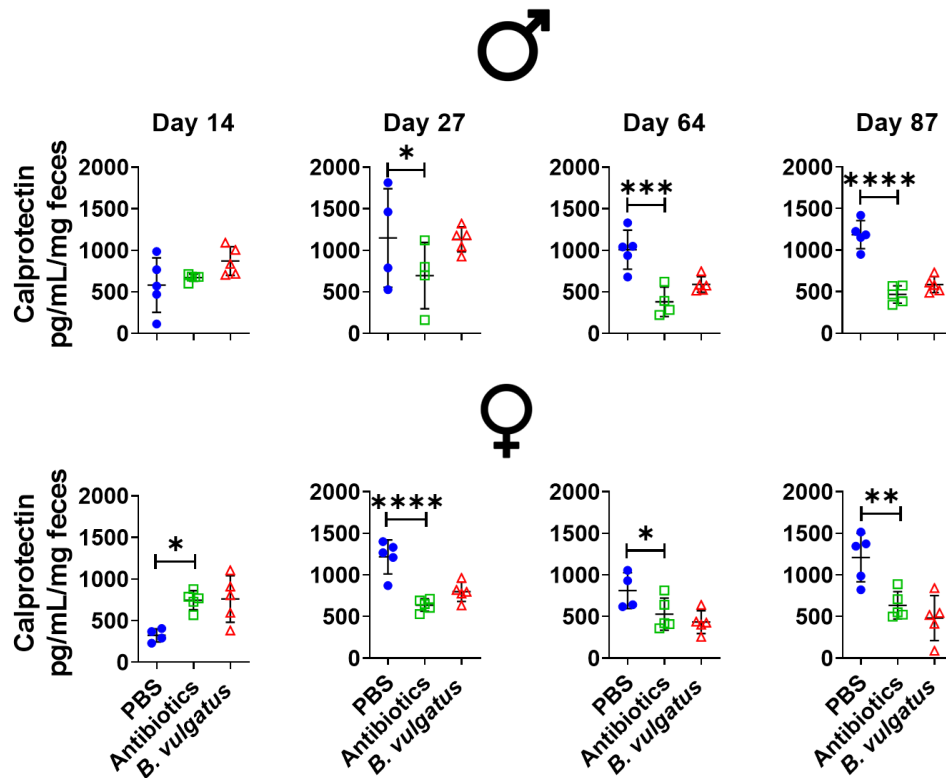
Figure 5.11 Faecal calprotectin levels from IL10$^{-/-}$ mice colonised with B. vulgatus. Faecal samples were collected at different time points along the study from male and female animals and calprotectin assayed by ELISA. Data is presented as mean ± SD. Statistical significance was calculated using one-way ANOVA with Dunnett's post-hoc test with the Antibiotics column as control. * = p<0.05, ** = p<0.01, *** = p<0.001, **** = p<0.0001. n=4-5 mice/gender/group.

Overall, these data indicate that male IL10$^{-/-}$ mice develop colitis upon colonisation with *B. vulgatus*, while female IL10$^{-/-}$ mice did not. Surprisingly, female IL10$^{-/-}$ mice develop colitis following an initial 13-day antibiotic treatment, while male IL10$^{-/-}$ mice did not, creating a divergent inflammatory effect, based on gender, in these mice and under these conditions.

5.3.2.2 *B. vulgatus* colonisation of IL10$^{-/-}$ mice impacted epithelial function and inflammation in a gender-dependent manner

In Chapter 3 supernatant from *B. vulgatus* demonstrated an ability to alter the expression of genes involved in the Wnt/β-Catenin and BMP pathways. These pathways are vital for the homeostatic functioning and lineage determination of the gut epithelium. To see if this effect of *B. vulgatus* conditioned media *in-vitro* was recapitulated *in-vivo*, gene expression analysis was performed by RT-qPCR on the proximal colon, the site of greatest visible inflammation in these mice. We assayed for lgr5, a marker of crypt stem cells, Axin2 a component in the Wnt/β-Catenin pathway, Smad5 a transcription factor in the BMP pathway, and hes1 a regulator that drives differentiation into the absorptive lineage. There was no significant difference in the gene expression of these markers between the three groups in male IL10$^{-/-}$ mice (**Figure 5.12 a-d**). However, in female IL10$^{-/-}$ mice *Lgr5* expression was decreased in antibiotic-treated mice relative to both PBS-treated and *B. vulgatus* colonised mice (**Figure 5.12 e**). Hes1 expression was also significantly increased in *B. vulgatus* colonised mice versus antibiotic-treated mice in female mice (**Figure 5.12 h**).

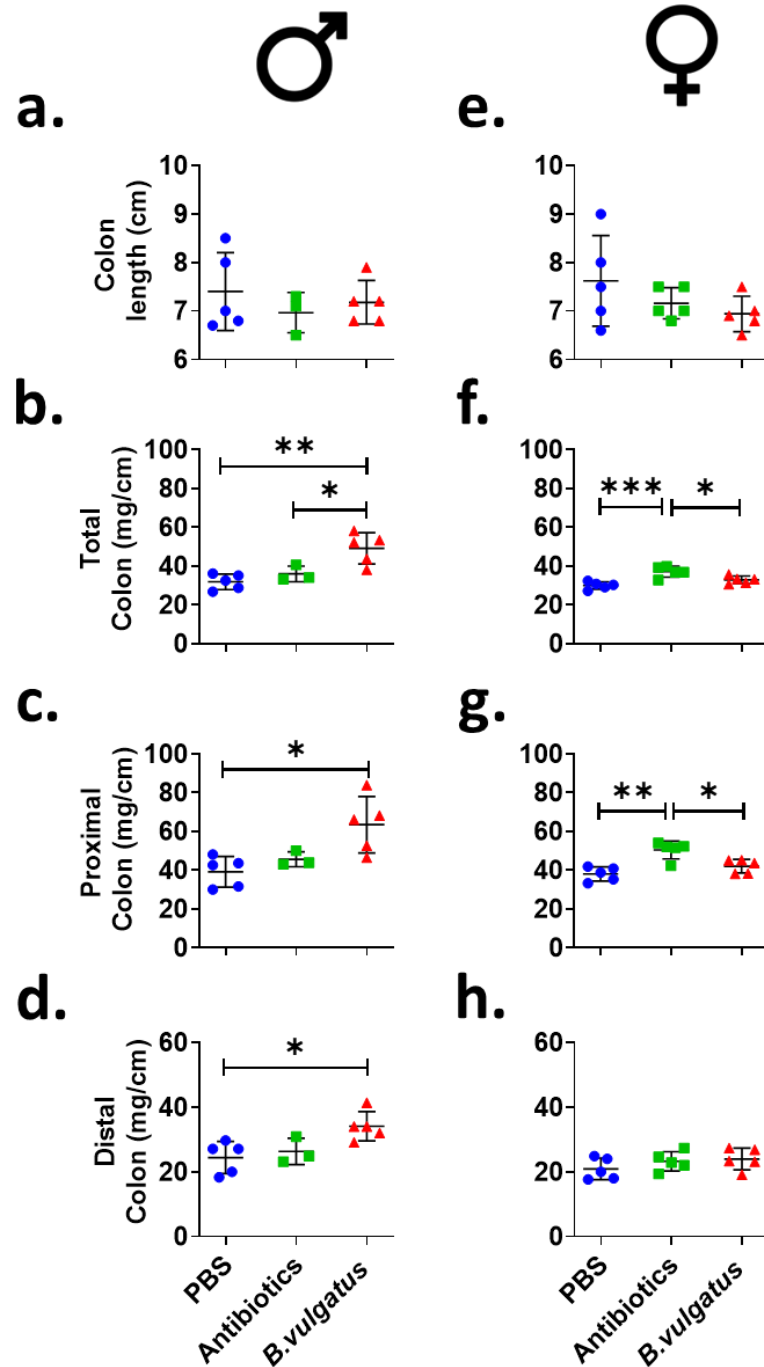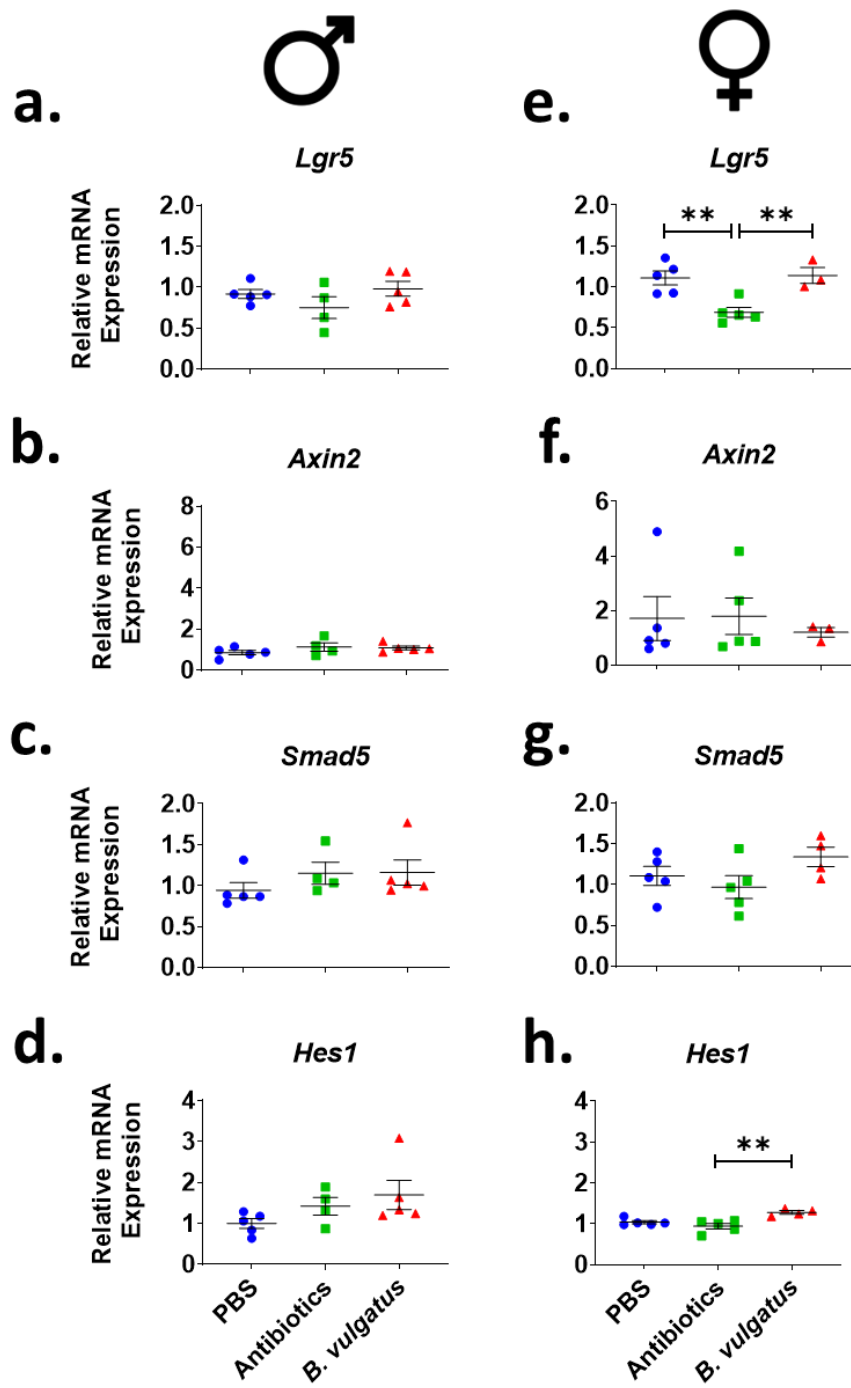**Figure 5.12 Gene expression of colonic epithelial stem cell niche signalling of IL10$^{-/-}$ mice colonised with B. vulgatus. (a-d) Male and (e-h) female mice were orally gavaged for 13 days with a full spectrum antibiotic cocktail consisting of 10 mg/mL metronidazole, 5 mg/mL vancomycin, 5 mg/mL neomycin, and 0.1 mg/mL amphotericin B and 1,000 mg/L ampicillin added to drinking water followed by oral gavage with B. vulgatus (10^9 cfu) for 3 consecutive days, repeated every 4 weeks. On day 99 colons were collected and assayed for the expression of (a and e) Lgr5, stem cell marker; (b and d) Axin2, Wnt-β-catenin pathway; (c and g) Smad5, BMP pathway; (d and h) Hes1, absorptive lineage by RT-qPCR. Data is presented as mean ± SD. Statistical significance was calculated using one-way ANOVA with Dunnett's post-hoc test with the Antibiotics column as control. ** = p<0.01. n=3-5 mice/gender/group.**

To further investigate this effect on epithelial stem cells and their signalling pathways we examined the expression of genes related to epithelial cell types as well as genes governing tight junctions and proliferation (**Figure 5.13 and Figure 5.14**). This demonstrated no significant changes in the male IL10$^{-/-}$ mice following either antibiotic treatment or *B. vulgatus* colonisation (**Figure 5.13 a-f**). However, in female IL10$^{-/-}$ mice, antibiotic treatment significantly decreased expression of the enteroendocrine cell marker CHGA which was significantly increased in mice colonised with *B. vulgatus* (**Figure 5.14 b**). The enterocyte marker Vil-1 was also significantly increased in *B. vulgatus* colonised female IL10$^{-/-}$ mice relative to antibiotic-treated ones (**Figure 5.14 d**). Expression of the ZO-1 and Klf4 genes were significantly increased in *B. vulgatus* colonised female IL10$^{-/-}$ mice relative to antibiotic treatment (**Figure 5.14 e and f**).

Figure 5.13 Gene expression of colonic epithelial cell lineage of male IL10^{-/-} mice colonised with B. vulgatus. *Male mice were orally gavaged for 13 days with a full spectrum antibiotic cocktail consisting of 10 mg/mL metronidazole, 5 mg/mL vancomycin, 5 mg/mL neomycin, and 0.1 mg/mL amphotericin B and 1,000 mg/L ampicillin added to drinking water followed by oral gavage with B. vulgatus (10^9 cfu) for 3 consecutive days, repeated every 4 weeks. On day 99 colons were collected and assayed for the expression of (a) lysozyme (Lyz Paneth cells); (b) chromogranin A (Chga, enteroendocrine cells); (c) Muc2 (goblet cells); (d) villin (Vil1, enterocytes); (e) Zo-1 (apical tight junction marker); (f) klf4 (proliferation/differentiation marker) by RT-qPCR. Data is presented as mean ± SD. Statistical significance was calculated using one-way ANOVA with Dunnett's post-hoc test with the Antibiotics column as control. * = p<0.05, ** = p<0.01. n=4-5 mice/gender/group.*

Figure 5.14 Gene expression of colonic epithelial cell lineage of female IL10^{-/-} mice

Figure 5.14 Gene expression of colonic epithelial cell lineage of female IL10$^{-/-}$ mice colonised with B. vulgatus. Female mice were orally gavaged for 13 days with a full spectrum antibiotic cocktail consisting of 10 mg/mL metronidazole, 5 mg/mL vancomycin, 5 mg/mL neomycin, and 0.1 mg/mL amphotericin B and 1,000 mg/L ampicillin added to drinking water followed by oral gavage with B. vulgatus (10^9 cfu) for 3 consecutive days, repeated every 4 weeks. On day 99 colons were collected and assayed for the expression of (a) lysozyme (Lyz Paneth cells); (b) chromogranin A (Chga, enteroendocrine cells); (c) Muc2 (goblet cells); (d) villin (Vil1, enterocytes); (e) Zo-1 (apical tight junction marker); (f) klf4 (proliferation/differentiation marker) by RT-qPCR. Data is presented as mean ± SD. Statistical significance was calculated using one-way ANOVA with Dunnett's post-hoc test with the Antibiotics column as control. * = p<0.05, ** = p<0.01. n=3-5 mice/gender/group.

These transcriptional data suggest that colonisation of IL10$^{-/-}$ mice with *B. vulgatus* affects epithelial homeostasis in a disparate manner dependant on gender. With male IL10$^{-/-}$ mice show no change in expression of markers related to stem cell functioning or epithelial homeostasis, whereas in female IL10$^{-/-}$ mice these genes were significantly decreased in antibiotic-treated relative to *B. vulgatus* colonised IL10-/- mice.

In **section 5.3.1.1** we observed that IL10$^{-/-}$ mice had increased colon weights indicating inflammation. To confirm this, we assayed for transcription of genes related to inflammatory mediators. This showed that male IL10$^{-/-}$ mice colonised with *B. vulgatus* had significantly increased transcription of iNOS and IFNγ (**Figure 5.15 a and c**). Also, while not significant, an increase was observed in IL-6, IL-17a, and CXCL2 (**Figure 5.15 b, d, and e**). Conversely, in antibiotic-treated female IL10$^{-/-}$ mice a significant increase in iNOS, IL-6, IL-17a, and CXCL2 was observed (**Figure 5.16 a, b, d, e**).
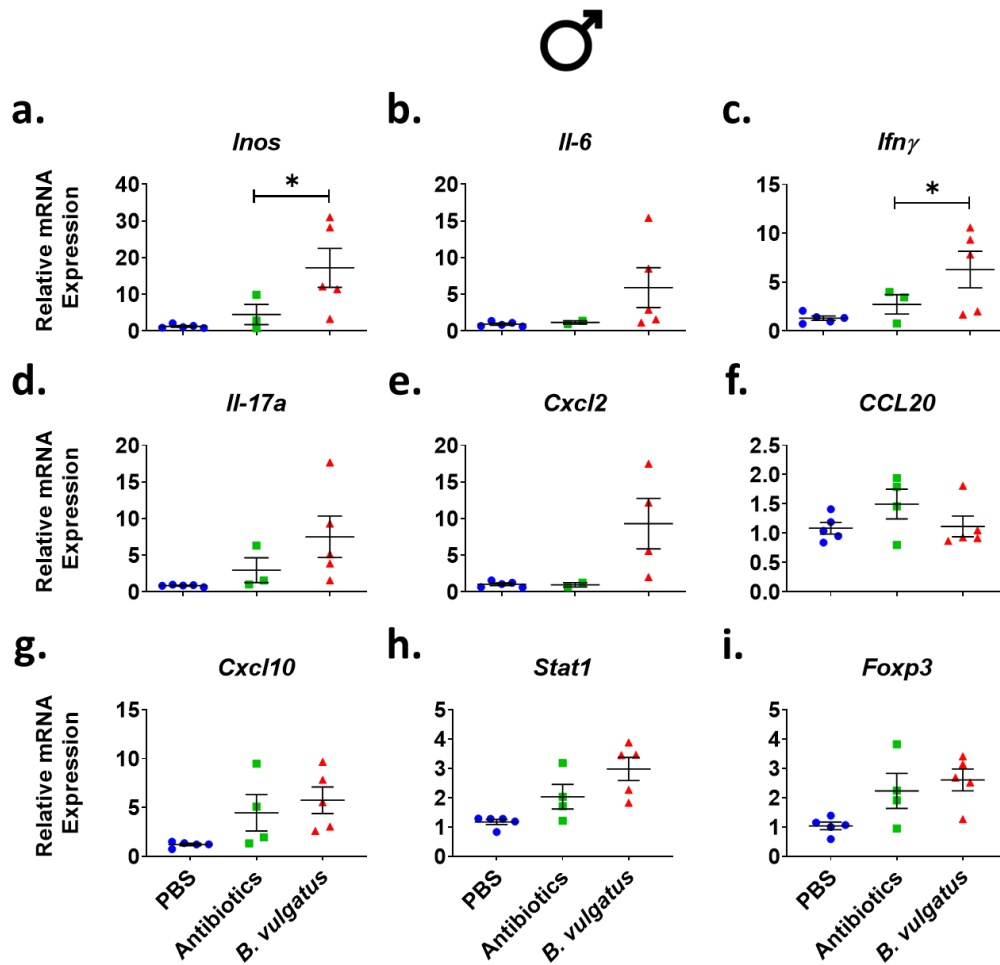
Figure 5.15 Gene expression of colonic inflammatory markers of male IL10$^{-/-}$ mice colonised with B. vulgatus. *Male mice were orally gavaged for 13 days with a full spectrum antibiotic cocktail consisting of 10 mg/mL metronidazole, 5 mg/mL vancomycin, 5 mg/mL neomycin, and 0.1 mg/mL amphotericin B and 1,000 mg/L ampicillin added to drinking water followed by oral gavage with B. vulgatus (10^9 cfu) for 3 consecutive days, repeated every 4 weeks. On day 99 colons were collected and assayed for the expression of (a) Inos, (b) Il6, (c) Ifnγ, (d) Il17a, (e) Cxcl2, (f) Ccl20, (g) Cxcl10, (h) Stat1, (i) Foxp3 by RT-qPCR. Data is presented as mean ± SD. Statistical significance was calculated using one-way ANOVA with Dunnett's post-hoc test with the Antibiotics column as control. * = p<0.05. n=3-5 mice/gender/group.*
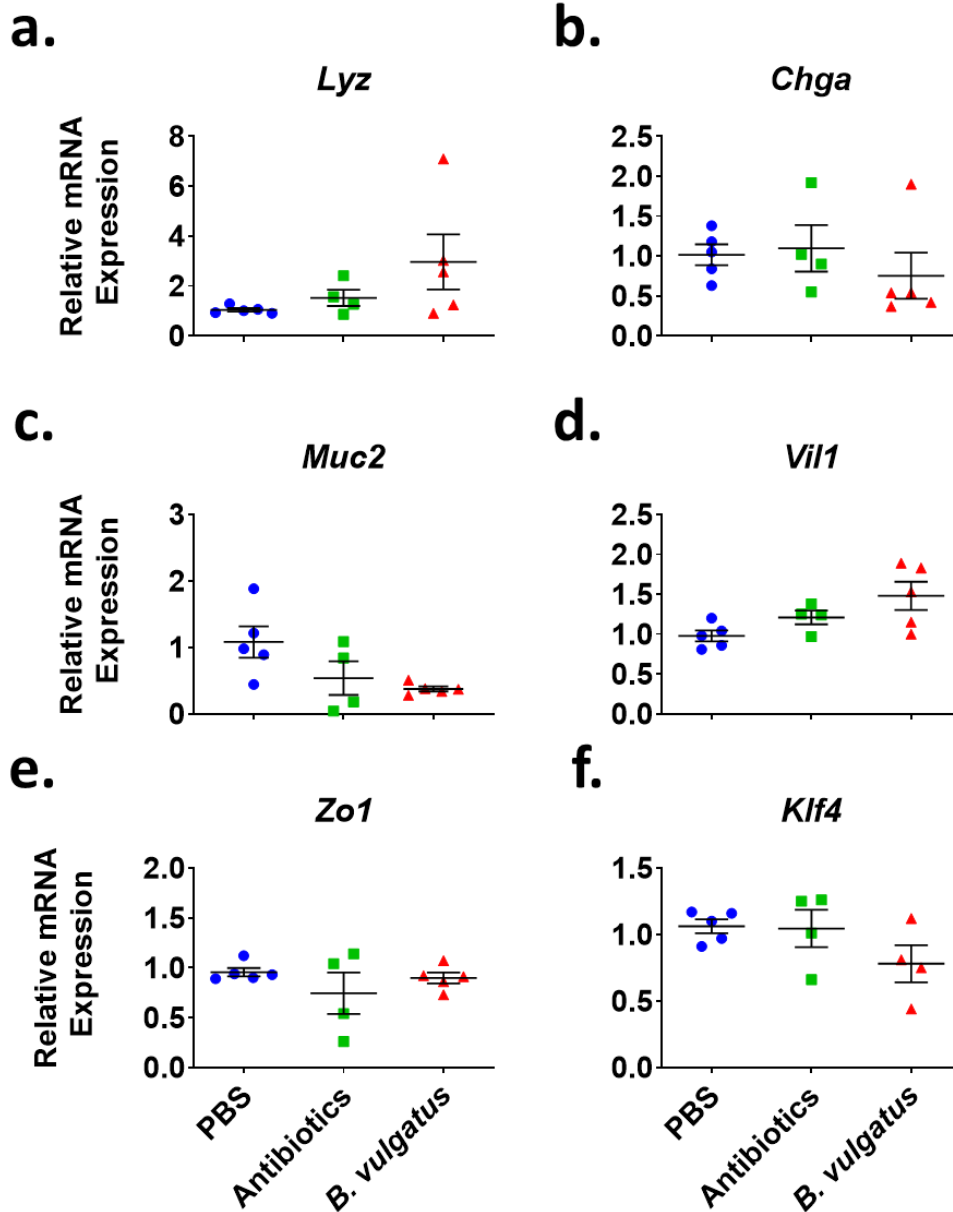
*Figure 5.16 Gene expression of colonic inflammatory markers of female IL10$^{-/-}$ mice colonised with B. vulgatus. Female mice were orally gavaged for 13 days with a full spectrum antibiotic cocktail consisting of 10 mg/mL metronidazole, 5 mg/mL vancomycin, 5 mg/mL neomycin, and 0.1 mg/mL amphotericin B and 1,000 mg/L ampicillin added to drinking water followed by oral gavage with B. vulgatus (10^9 cfu) for 3 consecutive days, repeated every 4 weeks. On day 99 colons were collected and assayed for the expression of (a) Inos, (b) Il6, (c) Ifnγ, (d) Il17a, (e) Cxcl2, (f) Ccl20, (g) Cxcl10, (h) Stat1, (i) Foxp3 by RT-qPCR. Data is presented as mean ± SD. Statistical significance was calculated using one-way ANOVA with Dunnett's post-hoc test with the Antibiotics column as control. * = p<0.05, ** = p<0.01, *** = p<0.001, **** = p<0.0001. n=3-5 mice/gender/group.*

To confirm this transcriptional data an immune assay was conducted targeting IL-1β, IL-6, and KC (murine IL-8 homologue). This demonstrated that *B. vulgatus* colonised male IL10$^{-/-}$ mice had significantly increased levels of IL-6 and, while not significant, elevated levels of KC (**Figure 5.17 b and c**). On the other hand, antibiotic-treated female IL-10$^{-/-}$ mice had significantly increased levels of KC and IL-1β (**Figure 5.17 f and d**).
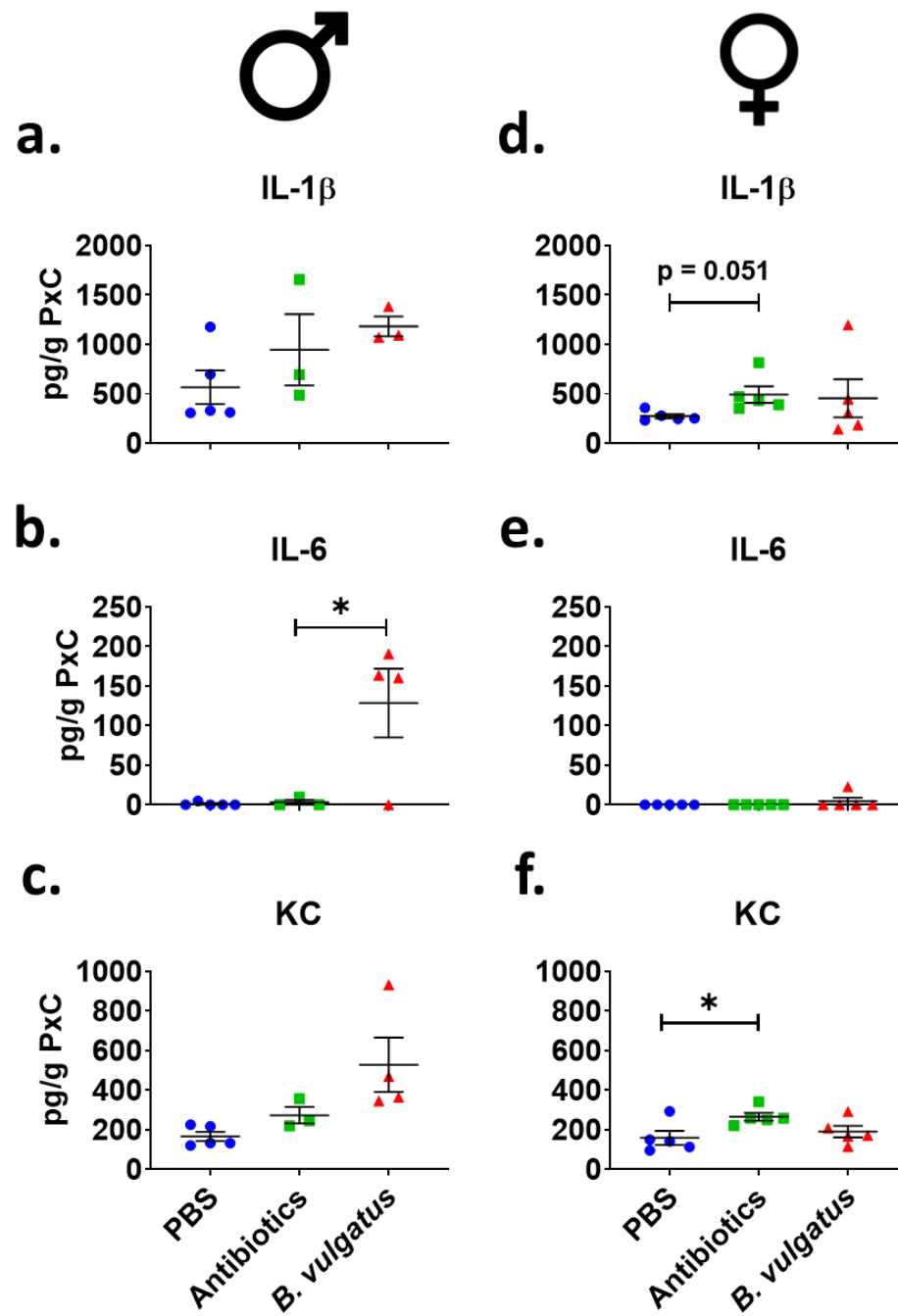
Figure 5.17 Assessment of cytokine/chemokine production in the colons of (a-c) male and (d-f) female IL10$^{-/-}$ mice colonised with B. vulgatus. Protein level was assayed by MSD on proximal colon homogenates for (a and d) IL1-β, (b and e) IL-6, and (f) KC. Data is presented as mean ± SD. Statistical significance was calculated using one-way ANOVA with Dunnett's post-hoc test with the Antibiotics column as control. * = p<0.05. n = 3-5 mice/gender/ group.
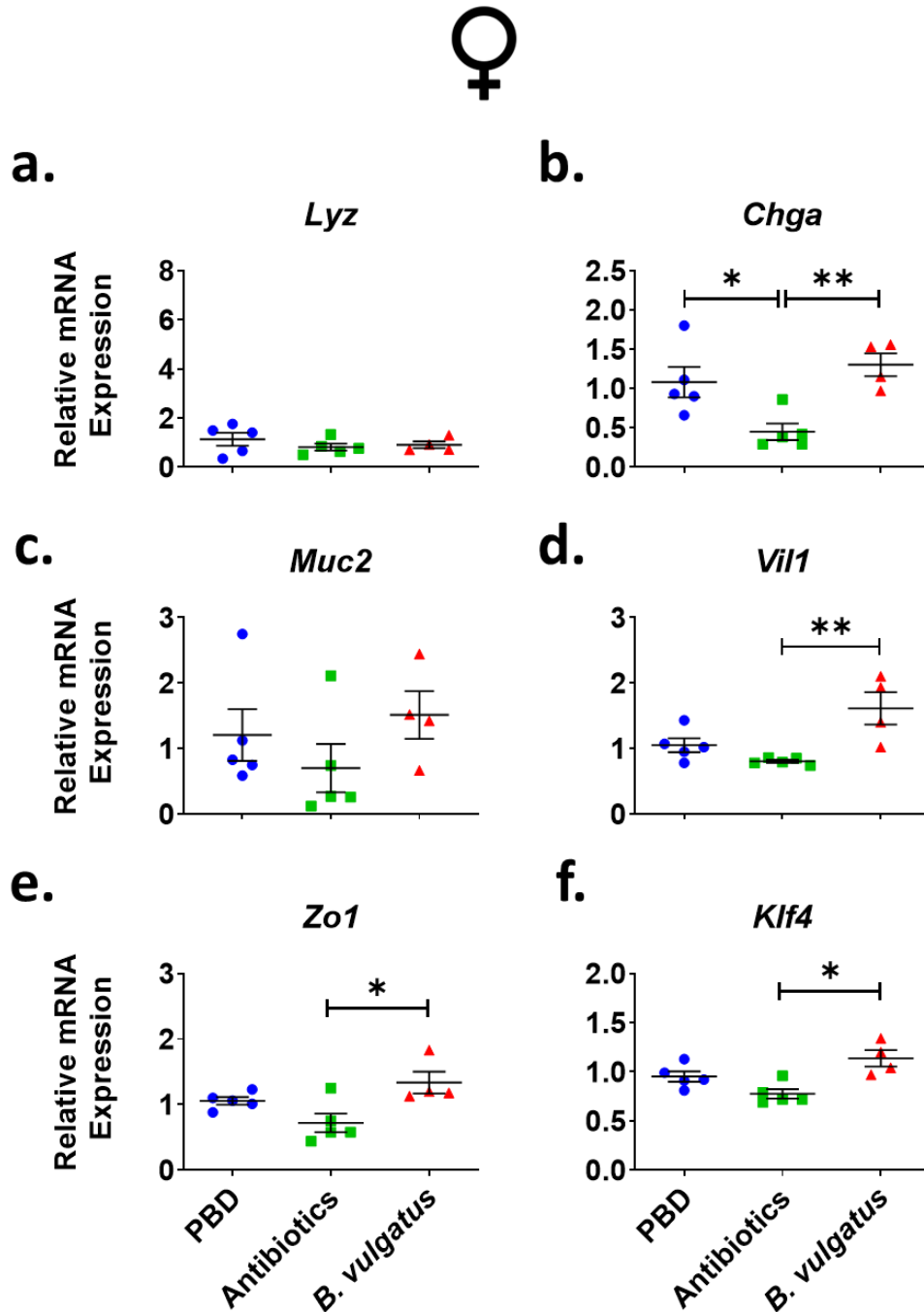
H&E staining was also performed on the proximal colon of IL10^{-/-} mice which confirmed inflammation in *B. vulgatus* colonised male mice which showed epithelial hyperplasia and immune cell infiltration (**Figure 5.18 c**).
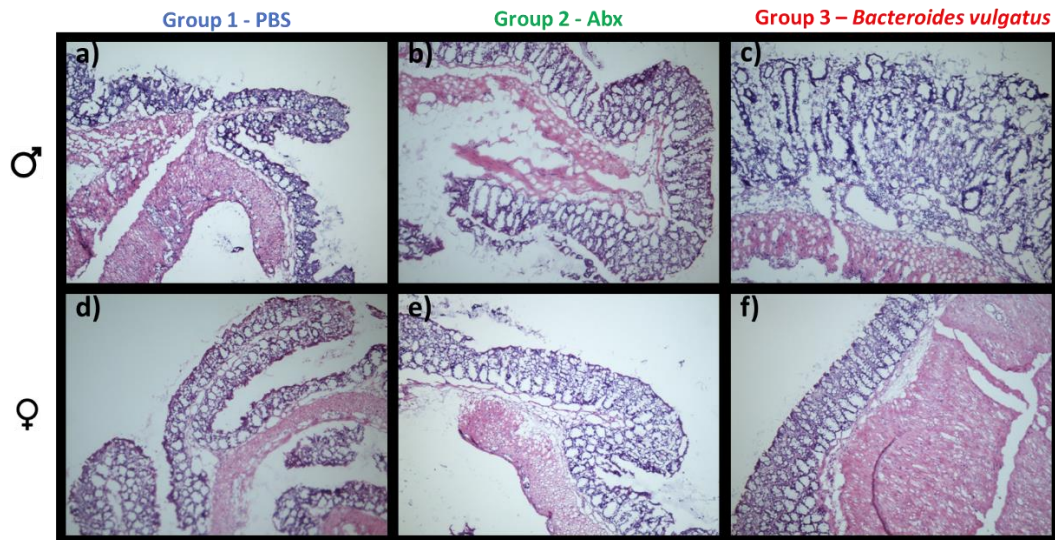
Figure 5.18 Haematoxylin and eosin-stained colon section from IL10^{-/-} mice colonised with B vulgatus. Proximal colon sections from (a-c) male and (d-f) female IL10^{-/-} mice. Representative pictures from each group and gender, 10x. n = 2-5 mice/gender/group.

5.3.3 Dynamic changes in the IL10^{-/-} mouse gut microbiota over time following *B. vulgatus* colonisation

In **sections 5.3.1 and 5.3.2** we identified a divergent inflammatory effect due to gender and antibiotic treatment in this model. We next wondered the following questions: is the antibiotic treatment impact on the host gender specific? Is the host response to *B. vulgatus* inherently different between genders due to IL-10 deficiency? Is the bacteria-host communication different between gender? Is the colonisation of *B. vulgatus* different between gender? How much does the composition of the microbiota at the gender level contribute to the subsequent response? To answer these questions 16S rRNA analyses were carried out on faecal samples collected from individual animals at selected time points for mapping microbiota

changes over time in IL10$^{-/-}$ mice. Briefly, bacterial DNA was isolated from faeces on; day 0 for a baseline read, day 14, post-antibiotic treatment, and day 22, post-B. *vulgatus*/PBS gavage, day 52, halfway through the experiment, after 2nd *B. vulgatus*/PBS gavage and day 99, the end of the experiment (**Figure 5.7**). Sequencing of the bacterial DNA was performed by Dr Fiona Crispie at Teagasc Food Research Centre, Ireland, as described in **Section 2.16**. Analysis of the sequence data was performed by Ms Julia Eckenberger as detailed in **Section 2.17**.

5.3.3.1 *B. vulgatus* colonisation altered IL10$^{-/-}$ mice microbiota in a gender-dependent manner

The gut microbiota composition of IL10$^{-/-}$ mice varied at the family level and this was dependent on the treatment arm and gender (**Figure 5.19**).

On day 0, before the experiment started, there were no significant differences in the relative abundances of the gut microbiota, at the family level, between the 3 treatment arms (**Table 5.1**). All 3 groups were dominated by the bacterial families *Muribaculaceae*, *Rikenellaceae*, *Lachnospiraceae*, and *Ruminococcaceae* (**Figure 5.19**).
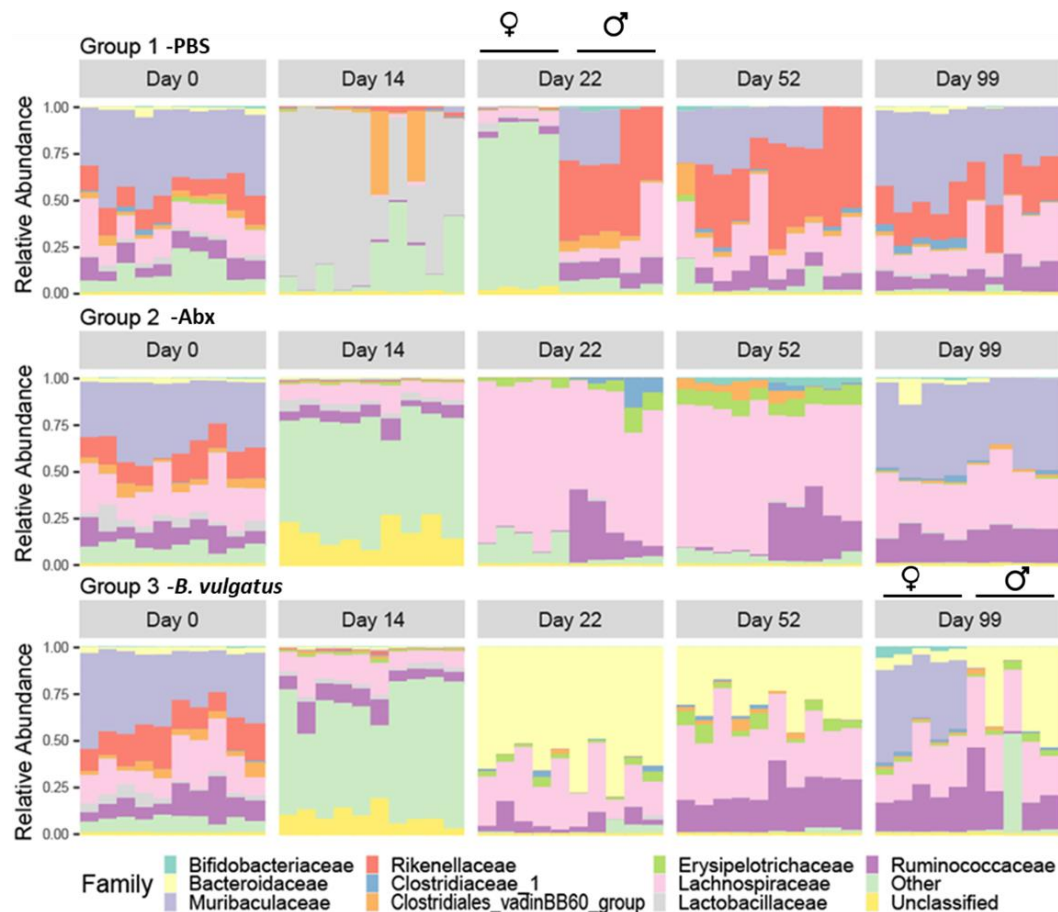
Figure 5.19 Longitudinal relative abundance of gut microbiota at the family level in IL10^{-/-} mice colonised with B. vulgatus. Mice were orally gavaged for 13 days with a full spectrum antibiotic cocktail consisting of 10 mg/mL metronidazole, 5 mg/mL vancomycin, 5 mg/mL neomycin, and 0.1 mg/mL amphotericin B and 1,000 mg/L ampicillin added to drinking water followed by oral gavage with B. vulgatus (10^9 cfu) for 3 consecutive days, repeated every 4 weeks. Faecal samples were collected at days 0, 14, 22, 52 and 99 along the study and relative abundance of gut microbiota at the family level was assessed and graphed. Faceted by group and time point. Group 1: Control (sham PBS gavage), Group 2: Antibiotics (antibiotic cocktail treatment with sham PBS oral gavage), Group 3: B. vulgatus (oral gavage of B. vulgatus). The first five columns in each subplot represent individual females belonging to that group and the other five columns are individual males. Exceptions: Group 1 Day 22, first 4 columns are female; Group 2 Day 99 3 last columns are male.

On day 14, post-antibiotic and PBS gavage, the gut microbiota composition was significantly changed from day 0 (**Table 5.1**). Unexpectedly the control PBS treated Group 1 was significantly altered and dominated by *Lactobacillaceae* and "other" (reads comprising <1% total abundance?) with two males showing an expansion of bacteria in *Clostridiales* vadinBB60 spp.

Antibiotic-treated Group 2 mice were not significantly different from antibiotic-treated Group 3 mice (**Table 5.1**) and their microbiota were dominated by unclassified and "other" bacteria with the families *Lachnospiraceae* and *Ruminococcaceae* comprising approximately 25% of the microbiota (**Figure 5.19**). Bacteria from the family *Rikenellaceae* were dramatically reduced in group 1 mice and absent from animals in Group 2 and Group 3.

Table 5.1 Multivariate test for differences in the overall composition between groups of samples via HMP

d0	xdc	p-value
Group 1 vs Group 2	8.870618	7.14E-01
Group 1 vs Group 3	10.27404	5.92E-01
Group 2 vs Group 3	4.110995	9.81E-01
d14	**xdc**	**p-value**
Group 1 vs Group 2	352.4692	0.00E+00
Group 1 vs Group 3	352.227	0.00E+00
Group 2 vs Group 3	18.68937	9.63E-02
d22	**xdc**	**p-value**
Group 1 vs Group 2	95.38765	4.44E-15
Group 1 vs Group 3	173.0823	0.00E+00
Group 2 vs Group 3	298.1296	0.00E+00
d52	**xdc**	**p-value**
Group 1 vs Group 2	197.6058	0.00E+00
Group 1 vs Group 3	298.1296	0.00E+00
Group 2 vs Group 3	237.5209	0.00E+00
d99	**xdc**	**p-value**
Group 1 vs Group 2	199.4036	0.00E+00
Group 1 vs Group 3	129.6813	0.00E+00
Group 2 vs Group 3	237.5209	0.00E+00

Group 1	xdc	p-value
Day 0 vs Day 14	336.81	0.00E+00
Day 14 vs Day 22	31.42	1.70E-03
Day 22 vs Day 52	52.68	4.70E-07
Day52 vs Day 99	70.65	2.42E-10
Day 99 vs Day 0	69.50	3.98E-10
Group 2	**xdc**	**p-value**
Day 0 vs Day 14	475.89	0.00E+00
Day 14 vs Day 22	423.40	0.00E+00
Day 22 vs Day 52	28.54	4.61E-03
Day52 vs Day 99	321.12	0.00E+00
Day 99 vs Day 0	193.67	0.00E+00
Group 3	**xdc**	**p-value**
Day 0 vs Day 14	450.87	0.00E+00
Day 14 vs Day 22	516.63	0.00E+00
Day 22 vs Day 52	151.92	0.00E+00
Day52 vs Day 99	112.84	0.00E+00
Day 99 vs Day 0	120.19	0.00E+00

Following oral gavage with either PBS (Group 1 and Group 2) or *B. vulgatus* from days 14-16 the microbiota composition of IL10$^{-/-}$ mice were assessed on day 22 and found that all 3 groups were significantly different from each other (**Table 5.1**), and each group was significantly different from previous

time points (**Table 5.1**). Mice in PBS-treated Group 1 showed a gut microbiota variation by gender with females exhibiting a similar abundance profile to day 14, while male mice in antibiotic-treated Group 2 have a similar abundance profile to day 0 and PBS-treated Group 1 mice showed a blooming of *Rikenellaceae* (**Figure 5.19**). Mice in antibiotic-treated Group 2 also appeared to have different abundances based on gender with females demonstrating an expansion of *Lachnospiraceae,* but lacking *Muribaculaceae,* whereas males presented an expansion in *Muribaculaceae* abundance (**Figure 5.19**). The relative abundance profile of *B. vulgatus*-treated Group 3 mice at day 22 was dominated (~50%) by *Bacteroidaceae*, indicating successful colonisation by *B. vulgatus* (**Figure 5.19**).

Halfway through the experiment on day 52 and one week after the 2nd *B. vulgatus* gavage, the relative abundance of all 3 groups was significantly different to each other (**Table 5.1**) and to the previous time points (**Table 5.1**). PBS-treated Group 1 displayed a similar abundance profile to day 0, for both genders, while antibiotic-treated group 2 maintained a similar profile to that seen on day 22 (**Figure 5.19**). The relative abundance profile for *B. vulgatus*-treated Group 3 was similar to day 22 but with a further decrease in the abundance of *Bacteroidaceae* and an increase in *Ruminococcaceae* abundance (**Figure 5.19**).

At the end of the study i.e., day 99 the relative abundances of all 3 groups were significantly different from each other (**Table 5.1**) and to their previous timepoints (**Table 5.1**) The microbial profile in mice in PBS-treated Group 1

resembles mostly to day 0. Mice in antibiotic-treated Group 2 mice also presented a similar profile but lacked members of the *Rikenellaceae* family (**Figure 5.19**). In contrast to the microbial profile and Groups 1 and 2, mice in *B. vulgatus*-treated Group 3 demonstrated a gender-specific relative abundance with female mice having decreased *Bacteroidaceae* abundance relative to males but an increase in *Muribaculaceae* bacteria which were absent in the males (**Figure 5.19**).

These data give a "bird's eye" view of the dynamic temporal changes in the microbiota of $IL10^{-/-}$ mice in response to PBS gavage, antibiotic gavage, or *B. vulgatus* colonisation. The observation that relative abundance appears to be different between genders, particularly in antibiotic and *B. vulgatus*-treated groups, where we saw disparate intestinal inflammation. Therefore, we decided to investigate the data with a greater resolution for diversity metrics and differential abundance with a focus between the three groups and genders.

5.3.3.2 Colonisation of $IL10^{-/-}$ mice with *B. vulgatus* altered alpha diversity in a gender-dependent manner

In the previous section, we demonstrated that all oral gavage treatments (PBS/antibiotic/*B. vulgatus*) altered the microbiota composition of $IL10^{-/-}$ mice, and the alterations appeared to have a gender component. Therefore, we analysed the alpha diversity using Chao1, Inverse Simpson, and Shannon diversity, of the faecal microbiota in a time point, treatment arm (**Figure 5.20**), and gender-wise (**Figures 5.21, 5.22, and 5.23**) manner. Analysing the alpha diversity measures within sample diversity, giving a

summary of the structure of the microbiota based on species richness and
their abundances.
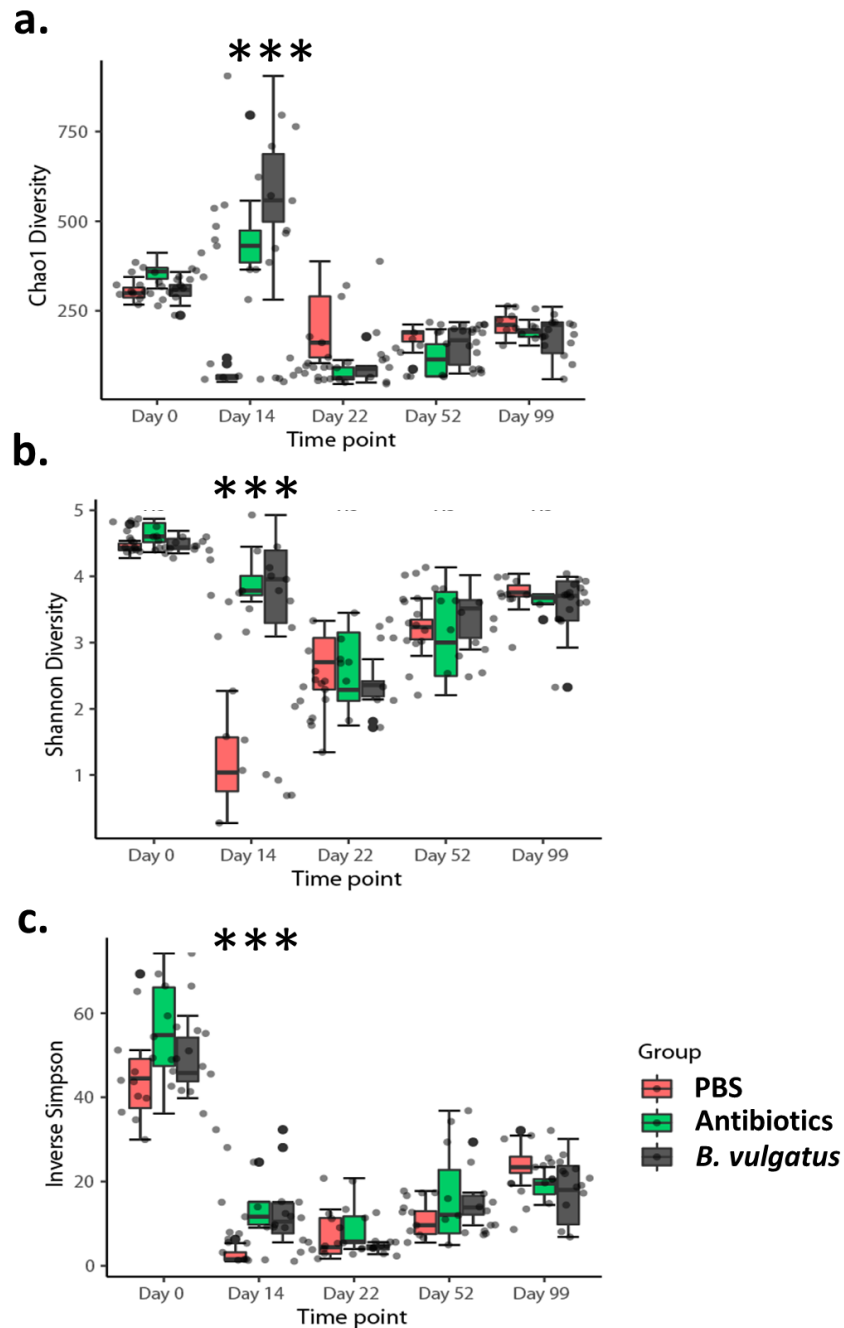
**Figure 5.20 Alpha diversity of gut microbiota in IL10⁻/⁻ mice colonised with B.
vulgatus. Faecal samples were collected on days 0, 14, 22, 52 and 99 throughout the
study where day 0 to 14 represent antibiotic treatment followed by B. vulgatus
colonisation from day 15 and forward. Alpha diversity of the gut microbiota was
assessed by (a) Chao1, Inverse (b) Shannon, and (c) Shannon diversity metrics.
Significance differences were tested using the Kruskal Wallis test. * = p<0.05, ** =
p<0.01, *** = p<0.001; ns – not significant**

When analysed by group, Chao1 diversity was significantly different between groups on days 0, 14 and 22 (**Figure 5.20, Table 5.2**). When compared in a pairwise manner on day 0, a significant difference in alpha diversity in PBS-Group 1 vs Antibiotic-Group 2 and Antibiotic-Group 2 vs *B. vulgatus*-Group 3 with there being no significant difference in PBS-Group 1 vs *B. vulgatus*-Group 3 (**Table 5.3**). Pairwise comparison of Chao1 diversity between groups at day 14 revealed there was no significant difference in alpha diversity between Antibiotic-Group 2 and *B. vulgatus*-Group 3 (pre-bacteria gavage), but that the alpha diversity in PBS-Group 1 was significantly different from both Antibiotic-Group 2 and *B. vulgatus*-Group 3, with this pattern sustained at day 22 (**Table 5.3**).

Table 5.2 Statistical analysis for differences in alpha diversity between groups at each time point in IL10$^{-/-}$ mice

	Chao1		Inverse Simpson		Shannon	
	p. value	p. adjust	p. value	p. adjust	p. value	p. adjust
Day 0	0.0013	0.0022	0.1304	0.163	0.0374	0.0935
Day 14	0	0.0002	0.0001	0.0005	0.0001	0.0004
Day 22	0.0004	0.001	0.0665	0.1109	0.484	0.573
Day 52	0.0464	0.058	0.2627	0.2627	0.5945	0.5945
Day 99	0.3964	0.3964	0.0309	0.0772	0.2585	0.4308

Significance was tested using Kruskal Wallis test, followed by Benjamini-Hochberg, where an adjusted p value of <0.05 was considered significant (green label). Gender is not a factor for analysis

Table 5.3 Statistical analysis for pairwise comparison of alpha diversity between groups and within timepoints in IL10$^{-/-}$ mice.

	Comparisons	Chao1 W	Chao1 p. value	Inverse Simpson W	Inverse Simpson p. value	Shannon W	Shannon p. value
Day 0	Gp1 vs Gp2	6	3.25x10-4	0	-	0	-
	Gp1 vs Gp3	44	6.84x10-1	0	-	0	-
	Gp2 vs Gp3	88	2.9x10-3	0	-	0	-
Day 14	Gp1 vs Gp2	0	2.17x10-5	0	2.17x10-5	0	2.17x10-5
	Gp1 vs Gp3	0	1.08x10-5	2	4.33x10-5	0	1.08x10-5
	Gp2 vs Gp3	22	0.065	53	0.55	45	1
Day 22	Gp1 vs Gp2	88	5.17x10-4	0	-	0	-
	Gp1 vs Gp3	85	4.11x10-4	0	-	0	-
	Gp2 vs Gp3	41.5	0.54	0	-	0	-
Day 52	Gp1 vs Gp2	0	-	0	-	0	-
	Gp1 vs Gp3	0	-	0	-	0	-
	Gp2 vs Gp3	0	-	0	-	0	-
Day 99	Gp1 vs Gp2	0	-	0	-	0	-
	Gp1 vs Gp3	0	-	0	-	0	-
	Gp2 vs Gp3	0	-	0	-	0	-

Significance was tested for pairwise group comparisons using the Mann Whitney U test where a p value <0.05 was considered significant (green label). Gp1 – PBS; Gp2 – antibiotics; Gp3 – B. vulgatus.

Next, using alpha diversity we investigated whether there were differences between the genders in each group at each time point. Statistics for each of the analyses are summarised in **Table 5.4**.

Table 5.4 Statistical analysis for comparison of gender within treatment groups and time points in IL10$^{-/-}$ mice.

Day	Group	Chao1		Inverse Simpson		Shannon	
		p. value	p. adjust	p. value	p. adjust	p. value	p. adjust
0	Gp1	0.841	0.9014	0.056	0.168	0.151	0.2517
	Gp2	0.841	0.9014	0.31	0.5167	0.31	0.465
	Gp3	0.016	0.048	1	1	0.056	0.12
14	Gp1	0.69	0.9014	0.056	0.168	0.056	0.12
	Gp2	0.41	0.6315	0.556	0.7582	0.73	0.9125
	Gp3	0.22	0.4125	0.151	0.3236	0.151	0.2517
22	Gp1	0.016	0.048	0.0159	0.0795	0.0159	0.0596
	Gp2	0.142	0.3043	0.0079	0.0593	0.0079	0.0395
	Gp3	0.421	0.6315	0.4206	0.6309	0.5476	0.7467
52	Gp1	0.8413	0.9014	0.8413	0.9707	0.8413	0.9707
	Gp2	0.0119	0.048	0.0079	0.0593	0.0079	0.0395
	Gp3	0.0079	0.048	0.2222	0.4166	0.0079	0.0395
99	Gp1	1	1	0.84	0.9707	1	1
	Gp2	0.0714	0.1785	1	1	1	1
	Gp3	0.0079	0.048	0.15	0.3236	0.056	0.12

Significance was tested using the Kruskal Wallis test where a p value <0.05 was considered significant (green label). Gp1 – PBS; Gp2 – antibiotics; Gp3 – B. vulgatus. Gender is a factor.

Chao1 diversity was significantly different between genders on days 0, 22, 52 and 99 (**Figure 5.21**). On day 0, in *B. vulgatus*-Group 3, female alpha diversity was significantly reduced relative to males (**Figure 5.21**). On day 22, PBS-Group 1, female alpha diversity was increased relative to the males (**Figure 5.21**). On day 52, Antibiotic-Group 2 females had decreased diversity vs males whereas *B. vulgatus*-Group 3 male alpha diversity was decreased relative to females with this trend continuing on day 99 for group 3 (**Figure 5.21**).
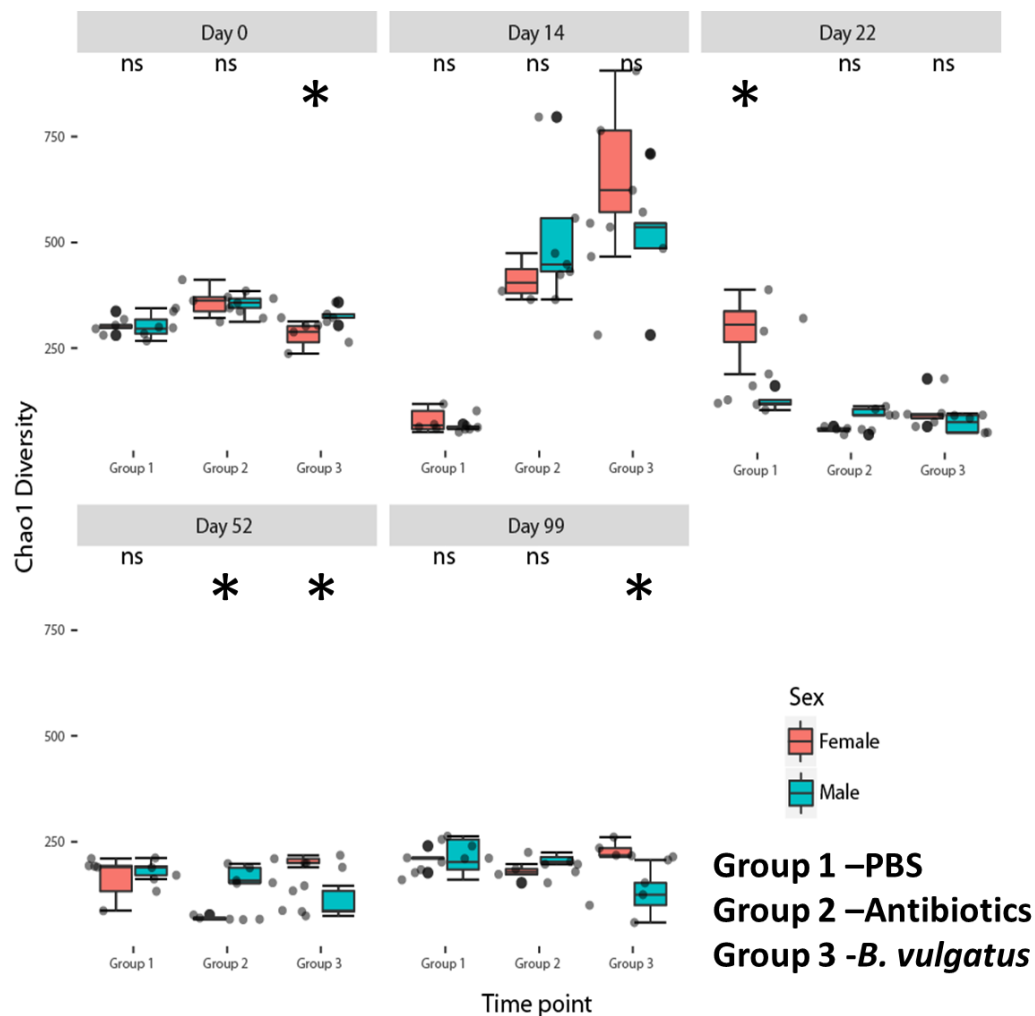
Figure 5.21 Comparison of the Chao1 diversity between gender and within groups and timepoints in B. vulgatus colonised IL10⁻/⁻ mice. Faecal samples were collected on days 0, 14, 22, 52 and 99 throughout the study, where day 0 to 14 represent antibiotic treatment followed by B. vulgatus colonisation from day 15 and forward. Significant differences were tested using the Kruskal Wallis test. * = p<0.05. ns- not significant.

In contrast to Chao1, analysis using Inverse Simpson revealed no significant differences between genders of any group at any time point (**Figure 5.22**). Analysis of Shannon diversity showed significant differences in alpha diversity between genders on days 22 and 52 (**Figure 5.23**). On day 22 in Antibiotic-Group 2 males, had significantly increased alpha diversity relative to females. Shannon diversity on day 52 showed a similar pattern to Chao1 diversity on day 52, i.e., a reduction in alpha diversity in Antibiotic-group 2 females and *B. vulgatus*-group 3 males (**Figure 5.23**).
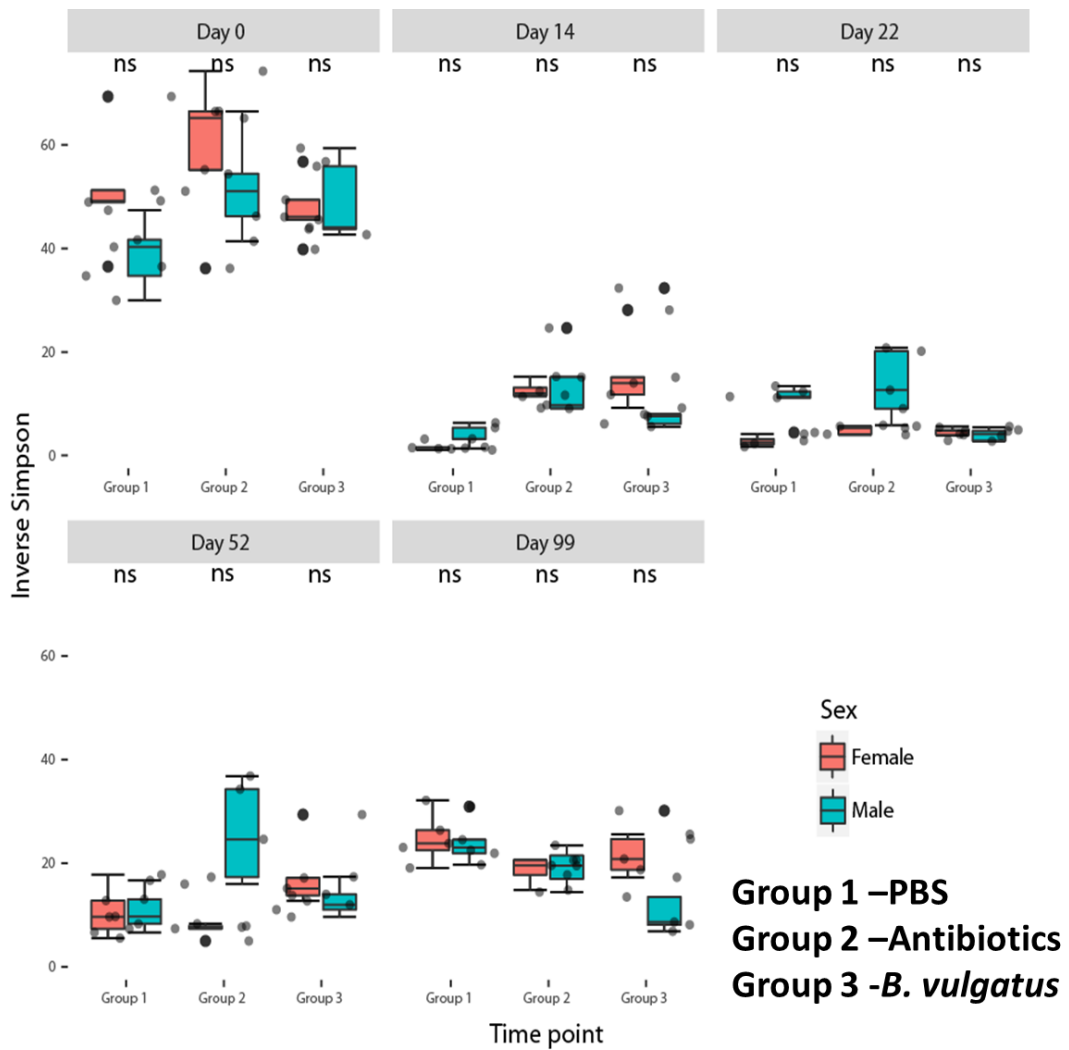
Figure 5.22 Comparison of the Inverse Simpson metric between gender and within groups and timepoints in B. vulgatus colonised IL10$^{-/-}$ mice. Faecal samples were collected on days 0, 14, 22, 52 and 99 throughout the study, where day 0 to 14 represent antibiotic treatment followed by B. vulgatus colonisation from day 15 and forward. Significant differences were tested using the Kruskal Wallis test. * = p<0.05. ns- not significant.
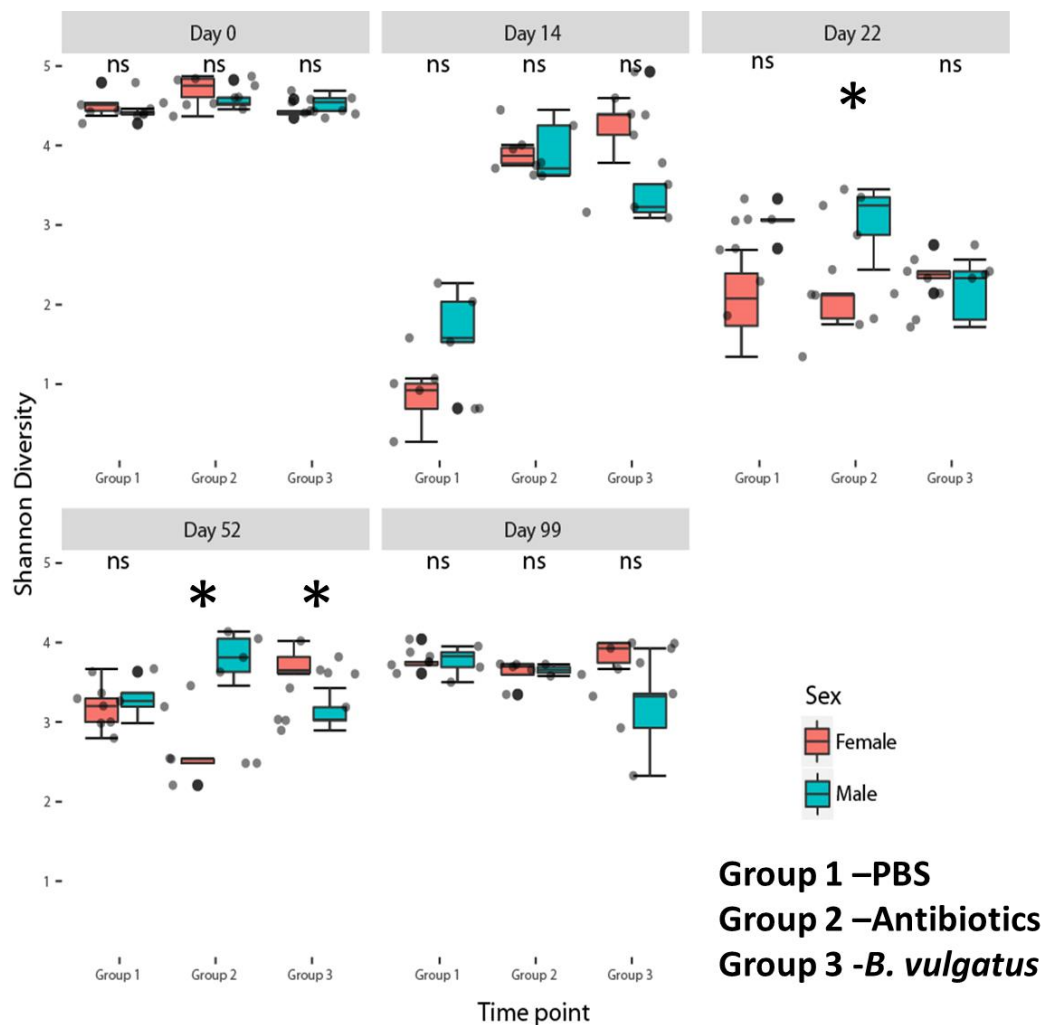
Figure 5.23 Comparison of the Shannon diversity between gender and within groups and timepoints in B. vulgatus colonised IL10$^{-/-}$ mice. Faecal samples were collected on days 0, 14, 22, 52 and 99 throughout the study, where day 0 to 14 represent antibiotic treatment followed by B. vulgatus colonisation from day 15 and forward. Significant differences were tested using the Kruskal Wallis test. * = p<0.05. ns- not significant.

These data demonstrate the long-term dramatic impact of antibiotics, and unexpectedly, PBS gavage on the diversity of the IL10$^{-/-}$ mouse microbiota. Showing a dramatic decrease in alpha diversity post-antibiotic/PBS gavage with slow recovery over time of diversity, however, this does not return to baseline levels even 85 days after treatment. The collected findings indicate significant alterations at day 52 in females of Antibiotic-Group 2 and in males in *B. vulgatus*-Group 3, which corresponds to the disparate

inflammation pattern seen in the tissue of these mice at the end of the study (**Section 5.3.3.2**).

5.3.3.3 *B. vulgatus* colonisation of IL10$^{-/-}$ mice delayed beta diversity recovery post-antibiotic treatment in male mice

Beta diversity measures dissimilarity between microbial populations allowing us to see how distinct differing microbiota populations are. Here we use beta diversity to investigate changes by treatment, time and, gender in the microbiota of IL10$^{-/-}$ mice after PBS/antibiotic/*B. vulgatus* gavage principal coordinate analysis (PCoA) was carried out using Bray-Curtis distances (**Figure 5.24**), and statistical significance was calculated with permutational multivariate analysis of variance (PERMANOVA) (**Table 5.5**).

Table 5.5 PERMANOVA comparison of gender within each group and time point.

Pairs	Df	SumsOfSqs	F.Model	R2	p.value	p.adjusted	sig
Gp1_d0_Female vs Gp1_d0_Male	1	0.2316	2.5796	0.2438	0.0152	0.0168	.
Gp2_d0_Female vs Gp2_d0_Male	1	0.2374	3.0355	0.2751	0.0089	0.0110	.
Gp3_d0_Female vs Gp3_d0_Male	1	0.2373	2.9613	0.2702	0.0092	0.0110	.
Gp1_d14_Female vs Gp1_d14_Male	1	0.4758	8.7026	0.5210	0.0175	0.0187	.
Gp2_d14_Female vs Gp2_d14_Male	1	0.0211	0.6079	0.0799	0.9020	0.9020	
Gp3_d14_Female vs Gp3_d14_Male	1	0.0744	1.2156	0.1319	0.3143	0.3150	
Gp1_d22_Female vs Gp1_d22_Male	1	1.8697	26.4250	0.7906	0.0084	0.0110	.
Gp2_d22_Female vs Gp2_d22_Male	1	1.6500	9.6754	0.5474	0.0070	0.0110	.
Gp3_d22_Female vs Gp3_d22_Male	1	0.1598	4.6538	0.3678	0.0102	0.0113	.
Gp1_d52_Female vs Gp1_d52_Male	1	0.5032	4.8480	0.3773	0.0067	0.0110	.
Gp2_d52_Female vs Gp2_d52_Male	1	1.8607	17.1210	0.6815	0.0067	0.0110	.
Gp3_d52_Female vs Gp3_d52_Male	1	0.8787	14.2493	0.6404	0.0080	0.0110	.
Gp1_d99_Female vs Gp1_d99_Male	1	0.3782	7.2182	0.4743	0.0090	0.0110	.
Gp2_d99_Female vs Gp2_d99_Male	1	0.2335	4.1484	0.4088	0.0190	0.0196	.
Gp3_d99_Female vs Gp3_d99_Male	1	1.1386	8.4109	0.5125	0.0097	0.0111	.
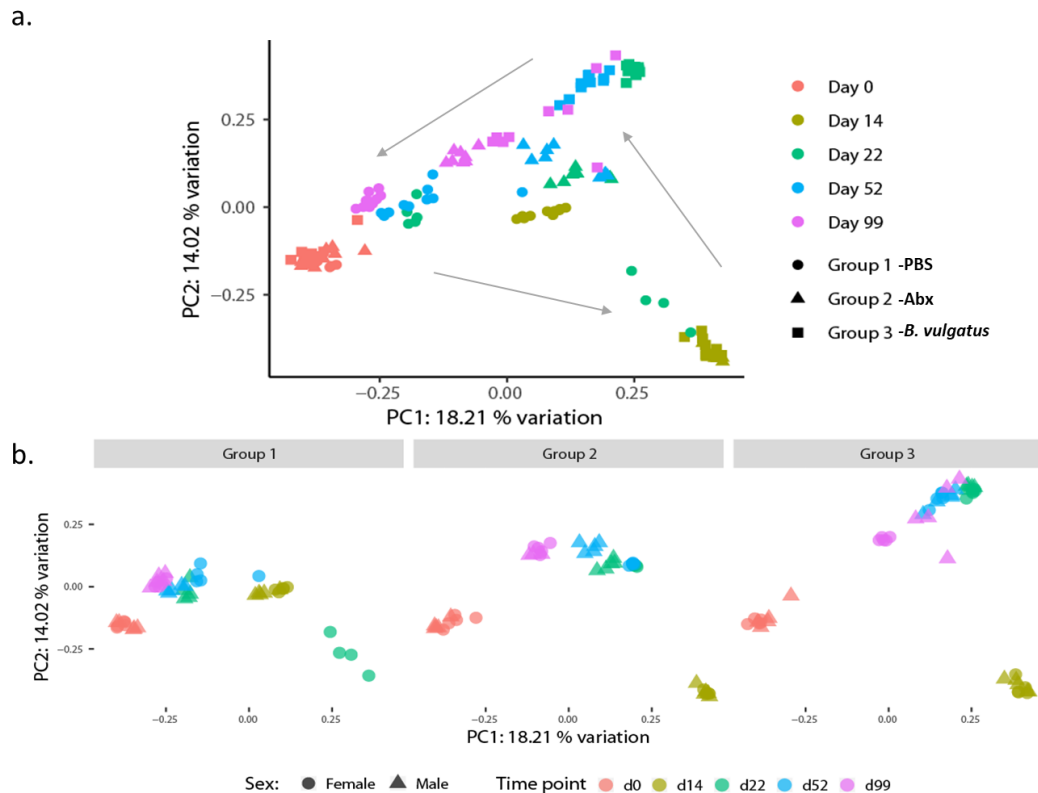
Figure 5.24 Beta diversity analysis of B. vulgatus colonised IL10⁻ᐟ⁻ mice. Faecal samples were collected on days 0, 14, 22, 52 and 99 along the study where day 0 to 14 represent antibiotic treatment followed by B. vulgatus colonisation from day 15 and forward. beta diversity of the gut microbiota was assessed. Principal Coordinate Analysis (PCoA) on Bray-Curtis distances grouped by time point and group with colours representing time points and shape indicating group. Arrows highlight direction of movement over time. Group 1: Control (sham PBS gavage), Group 2: Antibiotics (Abx - antibiotic cocktail treatment with sham PBS oral gavage), Group 3: B. vulgatus (oral gavage of B. vulgatus). (a). PCoA on Bray-Curtis distances grouped by time point and (b) faceted by group with circles indicating female and triangles indicating male mice.

Statistically significant differences in Bray-Curtis distances were seen for all groups and time points (excluding gender) except, on day 14 between Group 2 and Group 3 (before *B. vulgatus* gavage), between days 22 and 52 for Antibiotic-Group 2, and between days 52 and 99 for *B. vulgatus*-Group 3 (**Table 5.5**). Bray-Curtis PCoA demonstrates the dramatic effect that PBS and antibiotic gavage had on the microbiota of the IL10⁻ᐟ⁻ mice (**Figure 5.24 a**). In this figure, time points are represented as different colours with groups

denoted by the point shape and arrows indicating movement over time. It can be seen in **Figure 5.24 a** that antibiotic gavaged Group2 and Group 3 mice at day 14 (yellow) have moved dramatically away from day 0 (red) while PBS gavaged Group 1 mice have shifted, but not as severe as the antibiotic gavaged groups. The PCoA also demonstrates different "recovery" rates from antibiotic gavage for Group 2 and antibiotic-treated Group 3 with *B. vulgatus* colonisation, with Group 3 remaining the most dissimilar from the baseline. **Figure 5.24 b** shows the same PCoA but has been faceted by group with the point shape now representing gender. Statistical differences in Bray-Curtis distances were calculated using PERMANOVA and are summarised in **Table 5.5.** This showed that, except for Group 2 and Group 3, there was a significant difference in Bray-Curtis between all genders for all time points. Of particular interest is the separation, based on gender, seen in *B. vulgatus*-Group 3 at day 99, with the male mice being more dissimilar compared to baseline. Also, the differences observed between male and female mice in Antibiotic-Group 2 at day 99 with the females being the most dissimilar to the baseline diversity.

Analysis of the beta diversity further highlighted the fact that PBS/antibiotic gavage followed by *B. vulgatus* colonisation in IL10$^{-/-}$ mice led to alterations in the gut microbiota of these mice. This analysis also showed that these alterations to the IL10$^{-/-}$ gut microbiota occurred in a treatment and gender-dependent manner. Differential abundance analysis was applied to ascertain if these differences in diversities reflected a functionally different microbiota.

5.3.3.4 Colonisation with *B. vulgatus* in IL10$^{-/-}$ mice influenced microbiota recovery post-antibiotic treatment in a gender-dependent fashion

Significant differences were observed in the composition and alpha and beta diversities in IL10$^{-/-}$ mice. These were dependent on treatment, time point, and gender; therefore, a differential abundance analysis was performed using the ANOVA-like differential expression tool to identify potential taxa that can be correlated and contribute to the disparate inflammatory phenotype observed in Antibiotic-group 2 and *B. vulgatus*-group 3. Taxa were deemed significantly differentially abundant with an effect size greater than absolute one and an adjusted p-value of less than 0.05.

Differential abundance analysis identified a total of 147 taxa differentially abundant between the three groups across all time points **Table 5.6**.

Table 5.6 Differentially abundant genera by group in IL10$^{-/-}$ mice.

Group	Gp2 vs Gp3	Gp1 vs Gp3	Gp1 vs Gp2
Day 0	0	5	1
Day 14	1	29	33
Day 22	1	13	14
Day 52	9	14	10
Day 99	2	10	5

Data calculated using ANOVA-like differential expression tool (ALDEx2). Genera that demonstrated an effect size of bigger than absolute one and an adjusted p-value of less than 0.05 were deemed significantly differentially abundant. Group 1 –PBS, Group 2 –Abx, antibiotics, Group 3 –B. vulgatus.

Most of these taxa (134 taxa) were differentially abundant between PBS-Group 1 vs Antibiotic-Group 2 or PBS-Group 1 vs *B. vulgatus*-Group 3. Thirteen taxa that were differentially abundant between Antibiotic-Group 2 and *B. vulgatus*-Group 3 across all time points with the greatest difference seen at day 52, with 9 taxa. When differential abundance analysis was performed with gender as a factor it showed a total of 32 taxa as differentially abundant across all time points **Table 5.7**.

Table 5.7 Differentially abundant genera by gender in IL10$^{-/-}$ mice.

Gender	Group 1	Group 2	Group 3
Day 0	2	0	0
Day 14	0	0	0
Day 22	13	4	0
Day 52	2	6	0
Day 99	0	0	5

Data calculated using ANOVA-like differential expression tool (ALDEx2). Genera that demonstrated an effect size of bigger than absolute one and an adjusted p-value of less than 0.05 were deemed significantly differentially abundant. Group 1 –PBS, Group 2 –Abx, antibiotics, Group 3 –B. vulgatus.

An in-depth analysis of the different time points revealed the following alterations. On day 14 (**Figure 5.25**) the largest difference in differential abundance is seen between PBS-Group 1 and Antibiotic-Groups 2 and 3 (pre-*B. vulgatus* gavage) and demonstrates the effects of PBS vs antibiotic treatment. *Bifidobacterium* is the only taxon different with a higher abundance in Group 2 relative to Group 3 after 13 days of antibiotic treatment (**Figure 5.25**). There was no differential abundance observed on day 14 between genders in any of the groups.
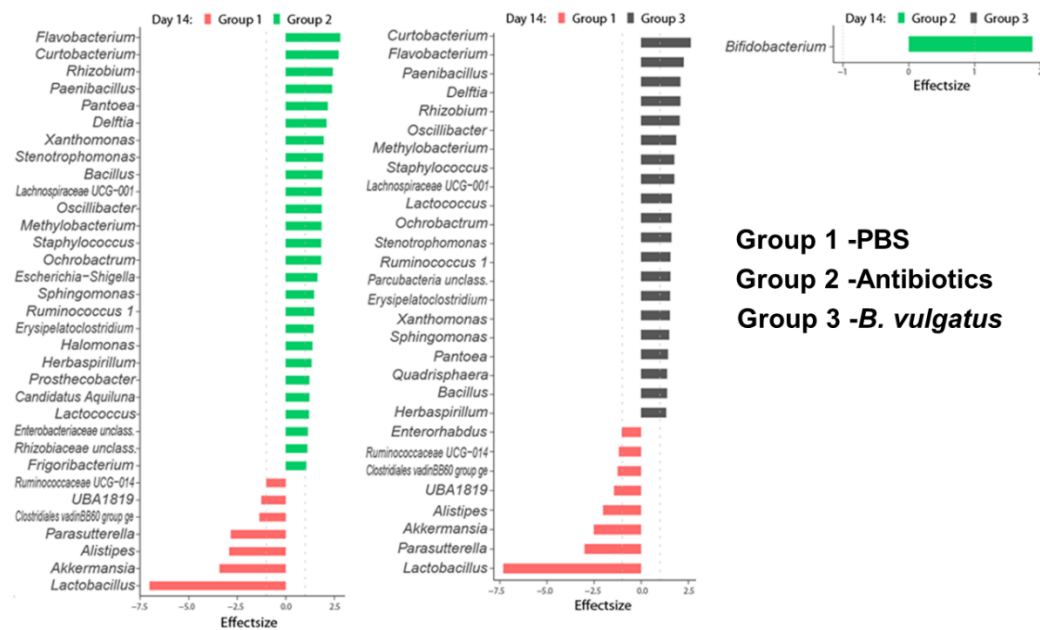
Figure 5.25 Differential abundance analysis on genera on day 14. Results are calculated using ANOVA-like differential expression tool (ALDEx2). Genera that demonstrated an effect size of bigger than absolute one and an adjusted p-value of less than 0.05 were deemed significantly differentially abundant. Group 1 –PBS, Group 2 –Abx, antibiotics, Group 3 –B. vulgatus.

On day 22, there was still a high number of taxa differentially abundant between Group 1 and Groups 2 and 3 post-antibiotic/PBS treatment, however, *Bacteroides* in Group 3 were differentially abundant relative to both PBS-Group 1 and Antibiotic-Group 2 confirming successful colonisation with *B. vulgatus* post oral gavage (**Figure 5.26**). Differential abundances were detected between the genders on day 22, predominantly in PBS-Group 1, mirroring the changes seen at the composition level in Figure 5.11. While in Antibiotic-Group 2, males showed increased *Ruminococcaceae* and *Clostridiaceae 1* while females had decreased *Paenibacillaceae* and *Enterococcaceae* relative to each other (**Figure 5.26**).
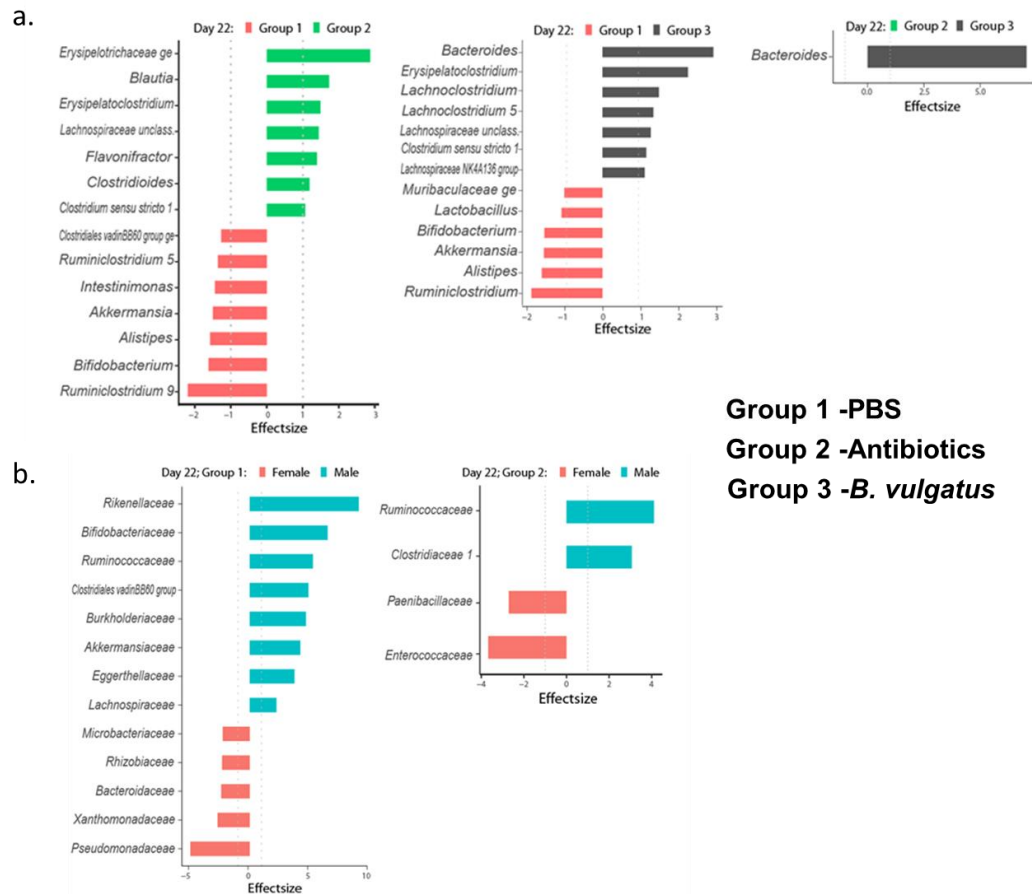
Figure 5.26 Differential abundance analysis on genera on day 22. Differentially abundant genera calculated between (a) groups and (b) gender. Results are calculated using ANOVA-like differential expression tool (ALDEx2). Genera that demonstrated an effect size of bigger than absolute one and an adjusted p-value of less than 0.05 were deemed significantly differentially abundant. Group 1 –PBS, Group 2 –Abx, Group 3 –B. vulgatus.

On day 52 many taxa are still differentially abundant between PBS-Group 1 and Antibiotic-Group 2 and *B. vulgatus*-Group 3 associated with a sustained impact of antibiotic treatment on microbiota abundance (**Figure 5.27**). *Bacteroides* are still increased in *B. vulgatus*-Group 3 relative to PBS-Group 1 and Antibiotic-Group 2 and *Lachnospiraceae* FCS020 group, *Anaerotruncus*, and *Ruminiclostridium* 9 are all enriched in *B. vulgatus*-Group 3, while *Bifidobacterium* and *Clostridioides* are depleted in Antibiotic-Group 2, relative to each other (**Figure 5.27**). There are no differentially

abundant taxa in *B. vulgatus*-Group 3 when analysed by gender, with Antibiotic-Group 2 demonstrating a similar abundance pattern as day 22 (**Figure 5.27**).
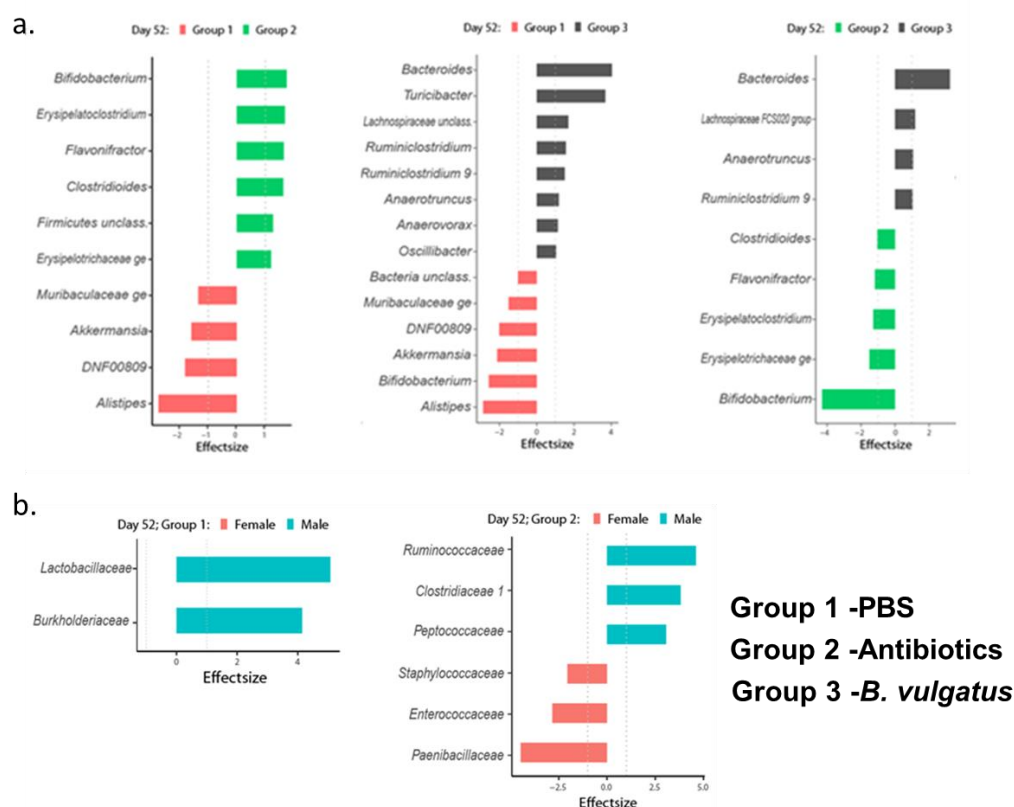
Figure 5.27 Differential abundance analysis day on genera on 52.. Differentially abundant genera calculated between (a) groups and (b) gender. Results are calculated using ANOVA-like differential expression tool (ALDEx2). Genera that demonstrated an effect size of bigger than absolute one and an adjusted p-value of less than 0.05 were deemed significantly differentially abundant. Group 1 –PBS, Group 2 –Abx, Group 3 –B. vulgatus.

On day 99 there were still many taxa differentially abundant between PBS-Group 1 and both Antibiotics-Group 2 and *B. vulgatus*-Group 3 however this was less than in previous time points (**Figure 5.28**). Between Antibiotics-Group 2 and *B. vulgatus*-Group 3 there were only two differentially abundant taxa, with Antibiotics-Group 2 having fewer unclassified bacteria and *Clostridium* ASF356 relative to *B. vulgatus*-Group 3 (**Figure 5.28**). There

were more differences in differentially abundant taxa by gender at day 99 in *B. vulgatus*-Group 3 than any other timepoint. Male mice had increased abundances of *Peptostreptococcaceae* and *Lachnospiraceae* relative to females while females had decreased abundances of *Bifidobacteriaceae*, *Muribaculaceae*, and unclassified bacteria relative to males (**Figure 5.28**).

a.

b.

Group 1 -PBS
Group 2 -Antibiotics
Group 3 -*B. vulgatus*
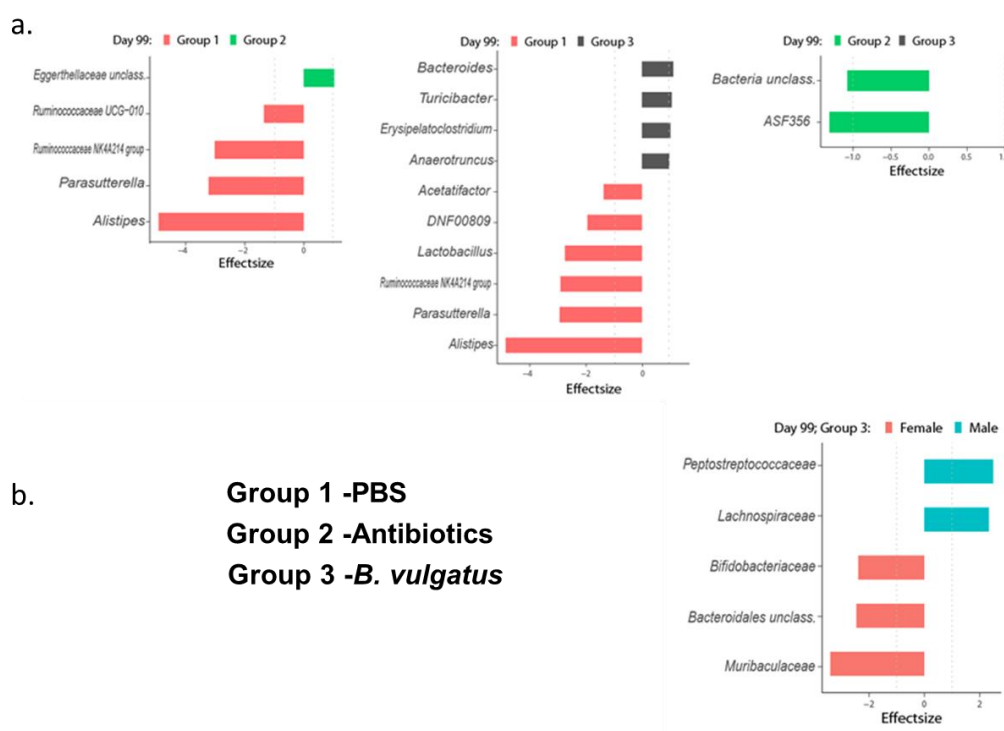
Figure 5.28 Differential abundance analysis on genera on day 99. Differentially abundant genera calculated between (a) groups and (b) gender. Results are calculated using ANOVA-like differential expression tool (ALDEx2). Genera that demonstrated an effect size of bigger than absolute one and an adjusted p-value of less than 0.05 were deemed significantly differentially abundant. Group 1 –PBS, Group 2 –Abx, Group 3 –B. vulgatus.

5.3.4 *B. vulgatus* colonisation of IL10^{-/-} mice altered the bile acid pool in a gender-dependent manner

Findings from Chapter 4 indicated that *Bacteroides* spp, possess the capacity to alter bile acids *in vitro*, we asked whether *B. vulgatus* colonisation *in vivo* could also alter bile acid profile. Faecal samples were

collected throughout the study, per **Figure 5.29 a**, for bile acid extraction and analysis as described in **section 2.14**. We conducted a targeted analysis of 39 bile acid moieties across four time points, on days 15, 43, 62 and 99 of the study. Preliminary examination of this data using principal component analysis (PCA), on all moieties investigated, and demonstrated separation due to both treatment and gender, over time (**Figure 5.29 b**). This was confirmed by generating a Spearman correlation heat plot using bile acid summaries (**Figure 5.29 c**).
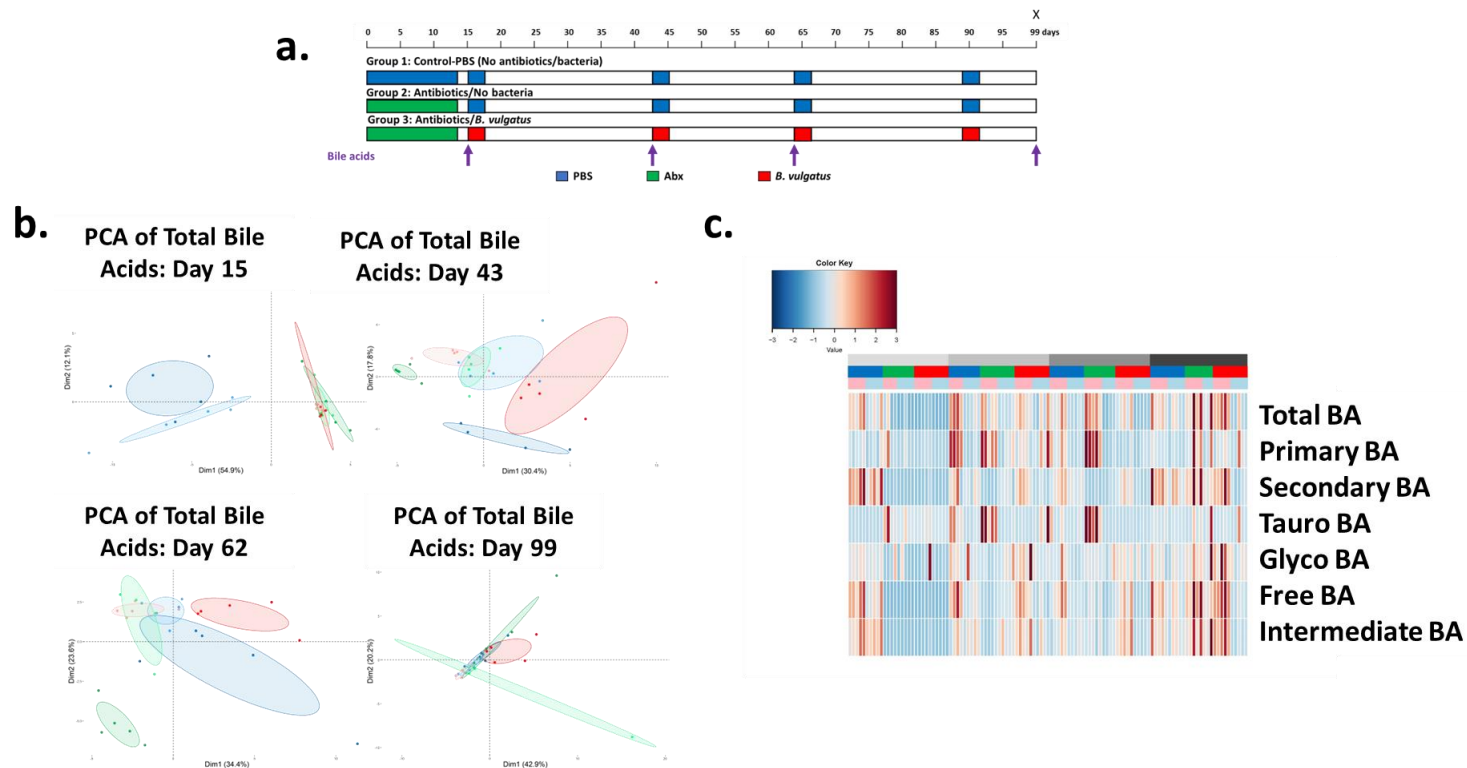
Figure 5.29 Overview of longitudinal changes in bile acid metabolism following antibiotic treatment and Bacteroides vulgatus colonisation in IL10$^{-/-}$ mice. (a) Study design highlighting faecal collection for bile acid analysis; (b) PCAs of the degree of separation incorporating all bile acid moieties (total bile acids) faceted by time points, where groups are designated by colour male mice lightly shaded and female mice darkly shaded. (c) Spearman correlation heatmap showing bile acid profile i.e., total, primary, secondary, Tauro and Glyco-conjugated, free and intermediates. Timepoints are illustrated with shades of grey, with treatment groups and gender by colour PBS (blue), antibiotics (Abx, green) and B. vulgatus (red) and male mice (light blue) and female mice (pink). The degree of correlation is indicated by colour, with dark red indicating a positive correlation and dark blue a negative one. n = 2-5/gender/group/timepoint

As the PCA on all bile acid moieties showed separation based on gender, group, and time point this analysis was repeated independently for each gender, this showed differences between male and female mice in their levels of total, primary, secondary, free, and *Bacteroides* associated intermediate bile acids (**Figure 5.30 a and Figure 31 a**). These analyses also highlighted the instability of the faecal bile acid pool post-antibiotic treatment, as such we focused all subsequent analyses on day 99, where stability appears to return.
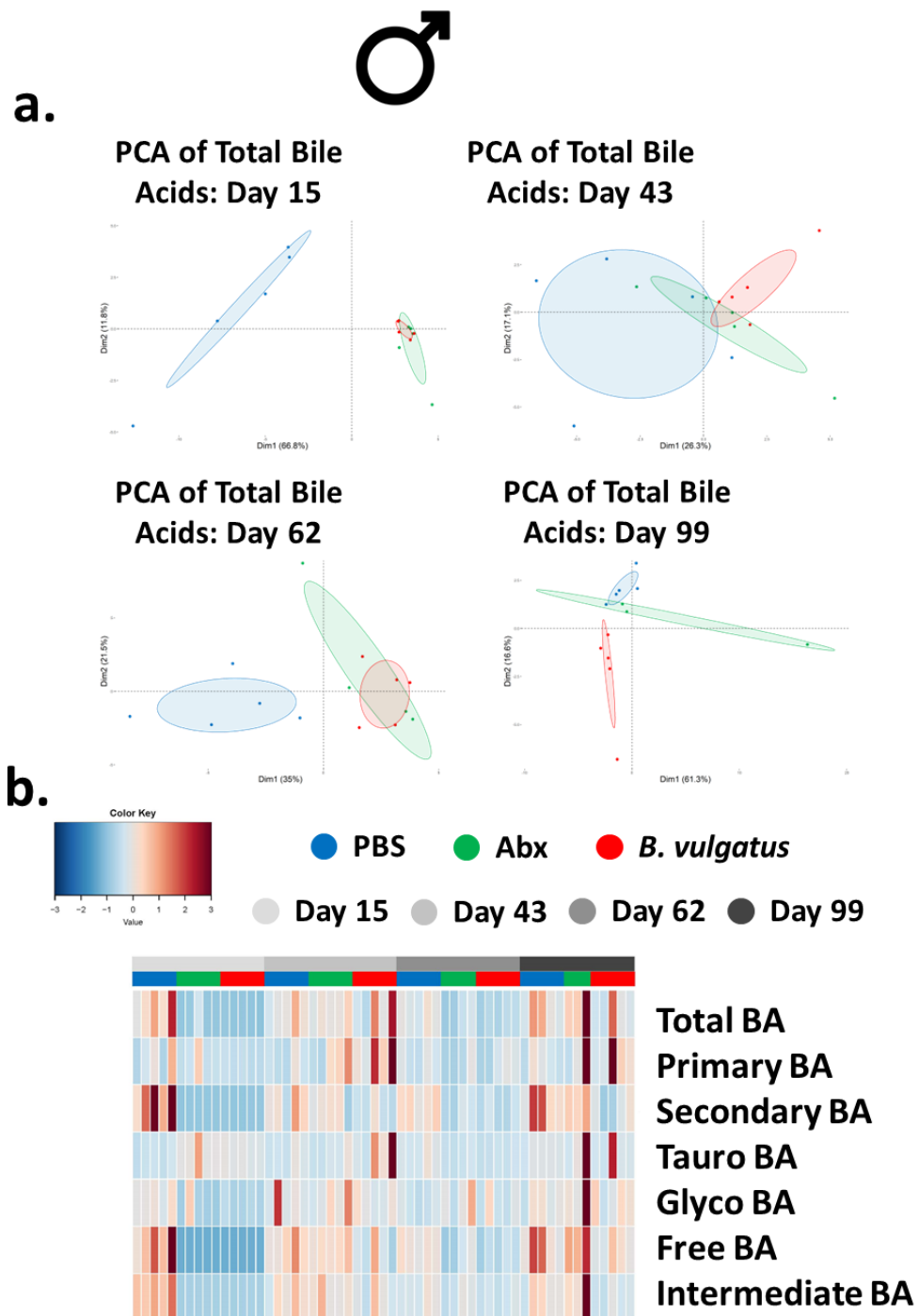
Figure 5.30 Overview of longitudinal changes in bile acid metabolism in male IL10$^{-/-}$ mice following antibiotic treatment and B. vulgatus colonisation over time. (a) PCAs of the degree of separation incorporating all bile acid moieties faceted by time points and gender with groups designated by colour. (b) Spearman correlation heatmap showing bile acid profile i.e., total, primary, secondary, Tauro and Glyco-conjugated, free and intermediates. Treatment groups PBS (blue), antibiotics (Abx, green) and B. vulgatus (red), male mice light blue and female mice pink. The degree of correlation is indicated by colour, with dark red indicating a positive correlation and dark blue a negative one. n = 2-5/gender/group/timepoint

Figure 5.31 Overview of longitudinal changes in bile acid metabolism in female IL10⁻
ᐟ⁻ mice following antibiotic treatment and B. vulgatus colonisation over time. (a)
PCAs of the degree of separation incorporating all bile acid moieties faceted by time
points and gender with groups designated by colour. (b) Spearman correlation
heatmap showing bile acid profile i.e., total, primary, secondary, Tauro and Glyco-
conjugated, free and intermediates. Treatment groups PBS (blue), antibiotics (Abx,
green) and B. vulgatus (red), male mice light blue and female mice pink. The degree
of correlation is indicated by colour, with dark red indicating a positive correlation
and dark blue a negative one. n = 2-5/gender/group/timepoint

When we examined for significance the levels of total, primary, conjugated, free, and secondary bile acids had no significant change in either male or female mice (**Figure 5.32 b-h and Figure 5.33 b-h**). There was a significant decrease in *Bacteroides*-associated bile acid intermediates in *B. vulgatus* colonised animals relative to antibiotic-treated mice for both males (p-value = 0.037, -0.58-fold change) and females (p-value 0.018, -0.62-fold change) (**Figure 5.32 i and Figure 5.33 i)**
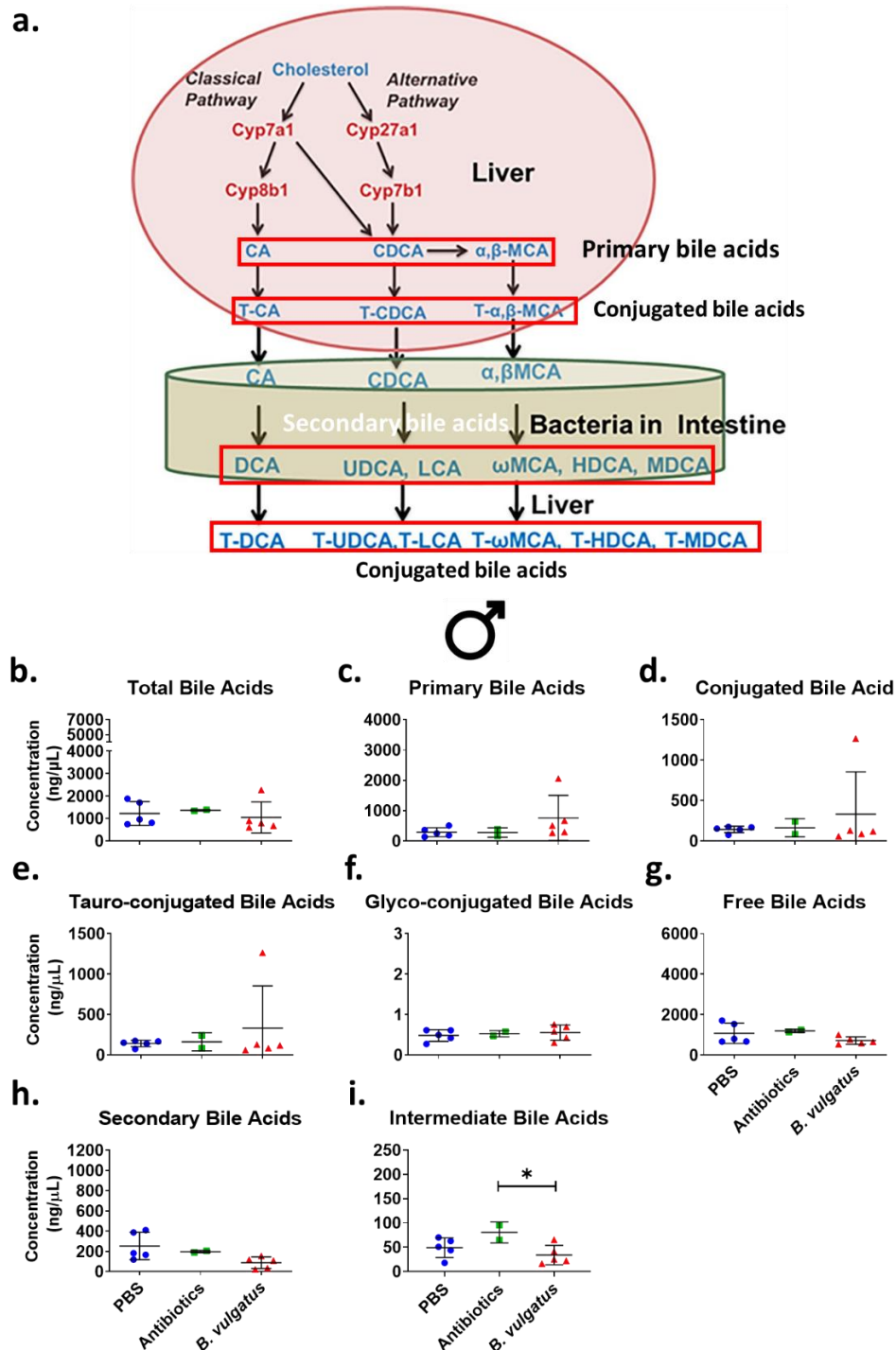
Figure 5.32 Assessment of faecal bile acid classes following oral gavage of B. vulgatus into male IL10$^{-/-}$ mice at day 99. (a) Schematic of Bile Acid synthesis and modification by gut bacteria. (b) Total bile acids, (c) Primary bile acids, (d) Conjugated bile acids, (e) Tauro-conjugated bile acids, (f) Glyco-conjugated bile acids, (g) Free bile acids, (h) Secondary bile acids, (I) Bacteroides associated intermediate bile acids. Bile acids were normalised against internal standards and quantified using standard curves for each moiety using Waters® Targetlynx software. Data is presented as mean ± SD. Statistical significance was calculated using one-way ANOVA with Dunnett's post-hoc test with the control column as Antibiotics. * = p<0.05. n= 2-5/gender/group.

Figure 5.33 : Assessment of faecal bile acid classes, following oral gavage of B. vulgatus into female IL10^(-/-) mice at day 99. (a) Schematic of Bile Acid synthesis and modification by gut bacteria. (b) Total bile acids, (c) Primary bile acids, (d) Conjugated bile acids, (e) Tauro-conjugated bile acids, (f) Glyco-conjugated bile acids, (g) Free bile acids, (h) Secondary bile acids, (I) Bacteroides associated intermediate bile acids. Bile acids were normalised against internal standards and quantified using standard curves for each moiety using Waters® Targetlynx software. Data is presented as mean ± SD. Statistical significance was calculated using one-way ANOVA with Dunnett's post-hoc test with the control column as Antibiotics. * = p<0.05. n= 2-5/gender/group.

Individual analysis of these *Bacteroides*-associated moieties revealed that male *B. vulgatus* colonised mice had decreased levels, relative to male Antibiotic-treated mice, of 12-DHCA (p-value 0.001, -0.62-fold change), 12-KLCA (p-value 0.013, -0.77-fold change), 7,12-DKLCA (p-value <0.0001, -0.81-fold change), and 24-Nor-UDCA (p-value 0.0002, -0.67-fold change) Interestingly 3-oxo CDCA and IsoDCA are also decreased but significantly so in the presence of *B. vulgatus* relative to antibiotic-treated animals (**Figure 5.34 c, e, f, and i**). There were no significant differences in these moieties in female mice with either treatment (**Figure 5.35**)
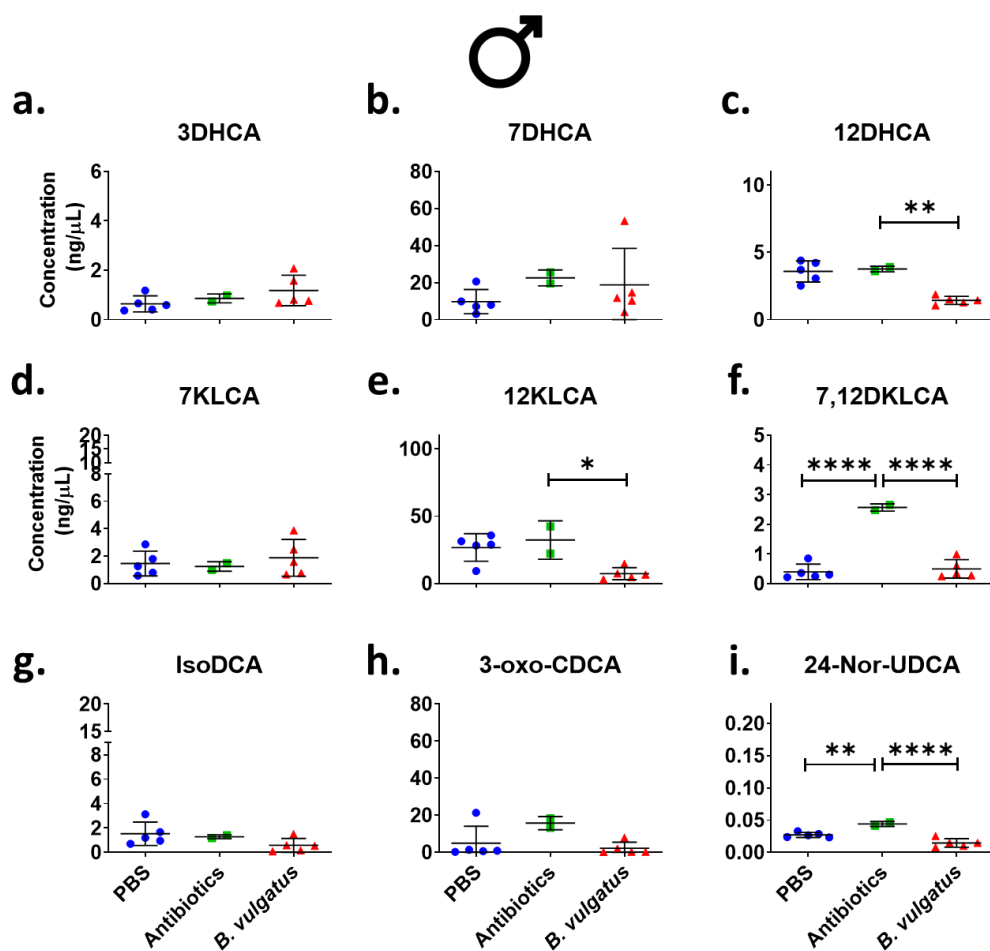
Figure 5.34 Assessment of B. vulgatus colonisation on Bacteroides associated bile acid intermediates in male IL10$^{-/-}$ mice. (a) 3-DHCA, (b) 7-DHCA, (c) 12-DHCA, (d) 7-KLCA, (e) 12-KLCA, (f) 7,12-DKLCA, (g) IsoDCA, (h) 3-oxo-CDCA, (i) 24-Nor-UDCA. Bile acids were normalised against internal standards and quantified using standard curves for each moiety using Waters® Targetlynx software. Data presented as mean ± SD. Statistical significance was calculated using one-way ANOVA with Dunnett's post-hoc test with the antibiotic column as control. * = p<0.05, ** = p<0.01, *** = p<0.001. n= 2-5/gender/group. DHCA = dihydroxycholic acid, KLCA = ketolithocholic acid, DCA = deoxycholic acid, CDCA = chenodeoxycholic acid, UDCA = ursodeoxycholic acid.
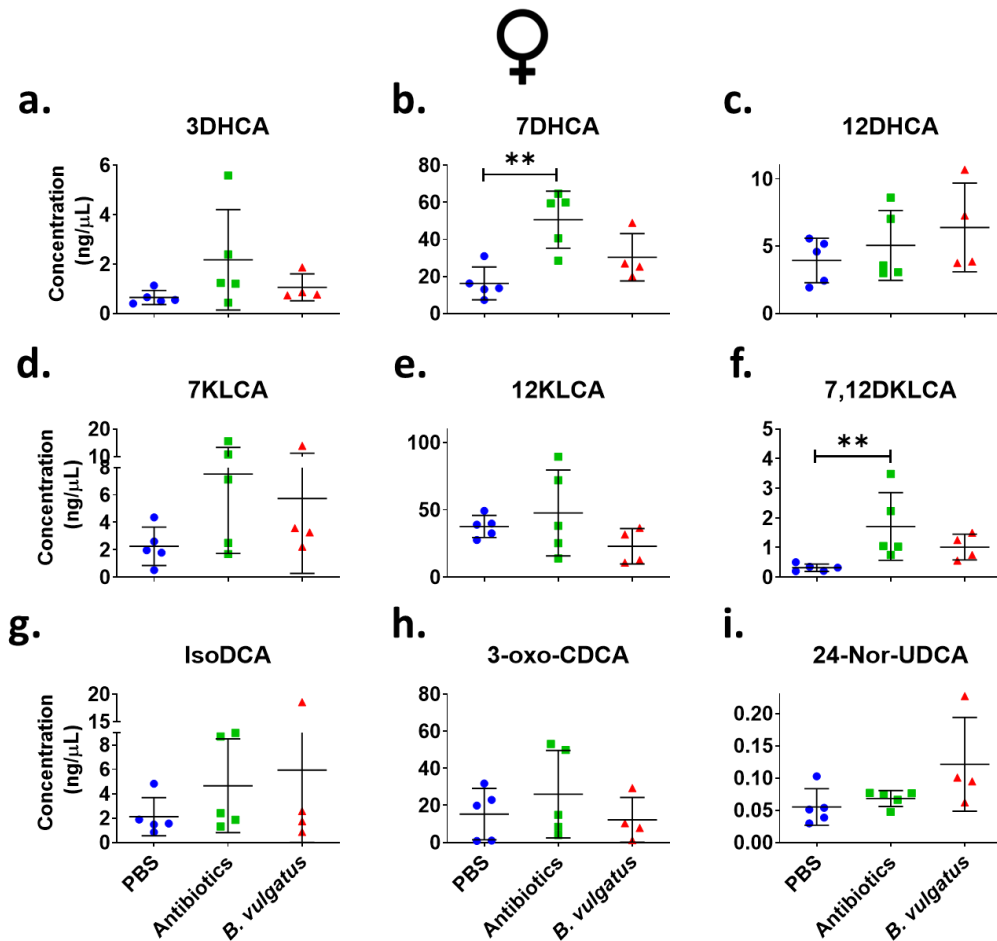
*Figure 5.35 : Assessment of B. vulgatus colonisation on bacteroides associated bile acid intermediates in female IL10$^{-/-}$ mice. (a) 3-DHCA, (b) 7-DHCA, (c) 12-DHCA, (d) 7-KLCA, (e) 12-KLCA, (f) 7,12-DKLCA, (g) IsoDCA, (h) 3-oxo-CDCA, (i) 24-Nor-UDCA. Bile acids were normalised against internal standards and quantified using standard curves for each moiety using Waters® Targetlynx software. Data is presented as mean ± SD. Statistical significance was calculated using one-way ANOVA with Dunnett's post-hoc test with the antibiotic column as control. * = p<0.05, ** = p<0.01, *** = p<0.001. n= 2-5/gender/group. DHCA = dihydroxycholic acid, KLCA = ketolithocholic acid, DCA = deoxycholic acid, CDCA = chenodeoxycholic acid, UDCA = ursodeoxycholic acid.*

We next examined if there was a differential between the predicted lower gut activation of nuclear and G protein coupled receptors based on BA levels for each treatment and in males relative to females (**Figure 5.36**). Here the antibiotic treatment altered BAs towards an FXR and a GBAR1

(TGR5) activating phenotype potential in male mice only. No other receptor appeared altered for activation based on these BA signatures.

a.

Receptors	Activating bile acids
FXR Agonist	CA, CDCA, DCA, a-MCA, B-MCA
FXR Antagonist	UDCA, TUDCA, GUDCA, T-MCA
LXR Agonist	CA, LCA, DCA, CDCA, HDCA
VDR Agonist	LCA, CDCA, DCA, CA
TGR5 Agonist	TLCA, LCA
PXR Agonist	LCA, DCA, CA

b.

c.
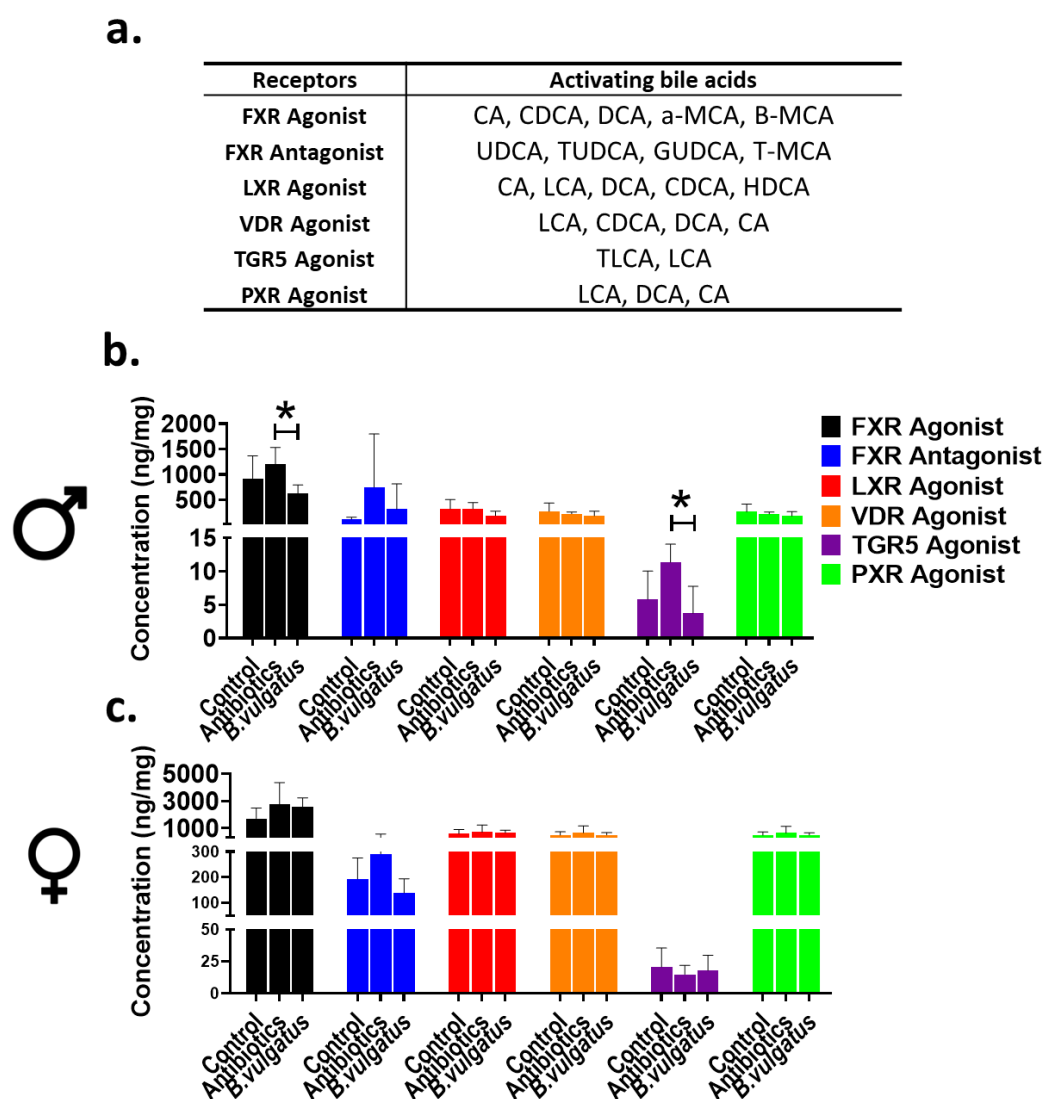
*Figure 5.36 Investigating the potential of colonisation with B. vulgatus in IL10$^{-/-}$ mice to alter bile acids which activate nuclear, and G-protein coupled receptors FXR, LXR, VDR, TGR5 and PXR. (a) Table of bile acid moieties which activate the different receptors. (b) Levels of receptor activating bile acid moieties in male IL10$^{-/-}$ mice. (c) Levels of receptor activating bile acid moieties in female IL10-/- mice. Bile acids were normalised against internal standards and quantified using standard curves for each moiety using Waters® Targetlynx software. Data is presented as mean ± SD. n = 2-5 mice/gender/group. Significance was calculated using one-way ANOVA with Dunnett's post-hoc test with the control column as Abx. * = p<0.05.*

To assess whether actual activation by BA was occurring though further up in the SI, we performed qPCR to examine the levels of bile acid associated

receptors and their select downstream targets (**Figure 5.30**). Interestingly, for antibiotic-treated animals, increased NR mRNA was not detected in the antibiotic-treated group, however, the mRNA tended towards elevation but was not significant for all male mice. This same trend applied to the levels of mRNA detected for all 3 FXR targets examined. Female mice showed significant mRNA level alterations for the FXR when treated with antibiotics and tended to increase in the *B. vulgatus* treated mice, this effect was translated to downstream FXR target genes where significant levels of FXR target genes were elevated in female mice. It is possible that a change in FXR activity is not simply a function of mRNA, the activation of FXR may be post-transcriptional. Interestingly, both FXR and the cognate heterodimer for it and FXR were significantly increased in the tissues of these female animals (**Figure 5.30**).
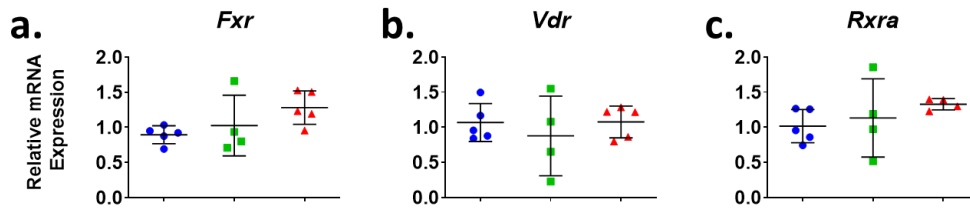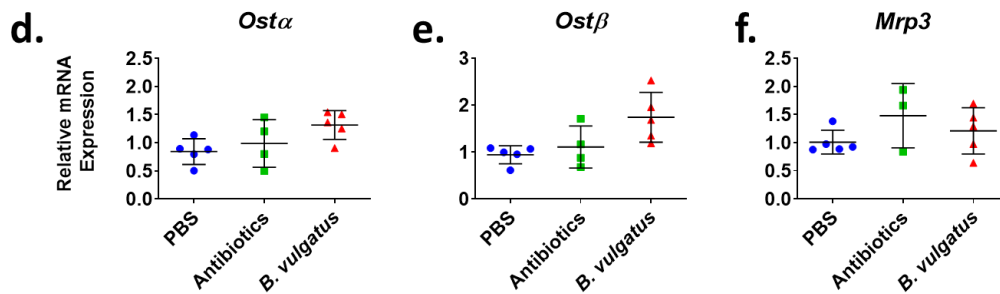
Figure 5.37 Colonic gene expression analysis of bile acid activated receptors and transporters in B. vulgatus colonised male IL10$^{-/-}$ mice. Transcription changes in colonic samples collected on day 99 for bile acid activated receptors (a-c) and bile acid reabsorption transporters (d-e) in male IL10$^{-/-}$ mice following B. vulgatus colonisation. Data is presented as mean ± SD. n = 2-5 mice/gender/group. Significance was calculated using one-way ANOVA with Dunnett's post-hoc test with the control column as Antibiotics. * = p<0.05, ** = p<0.01, *** = p<0.001.
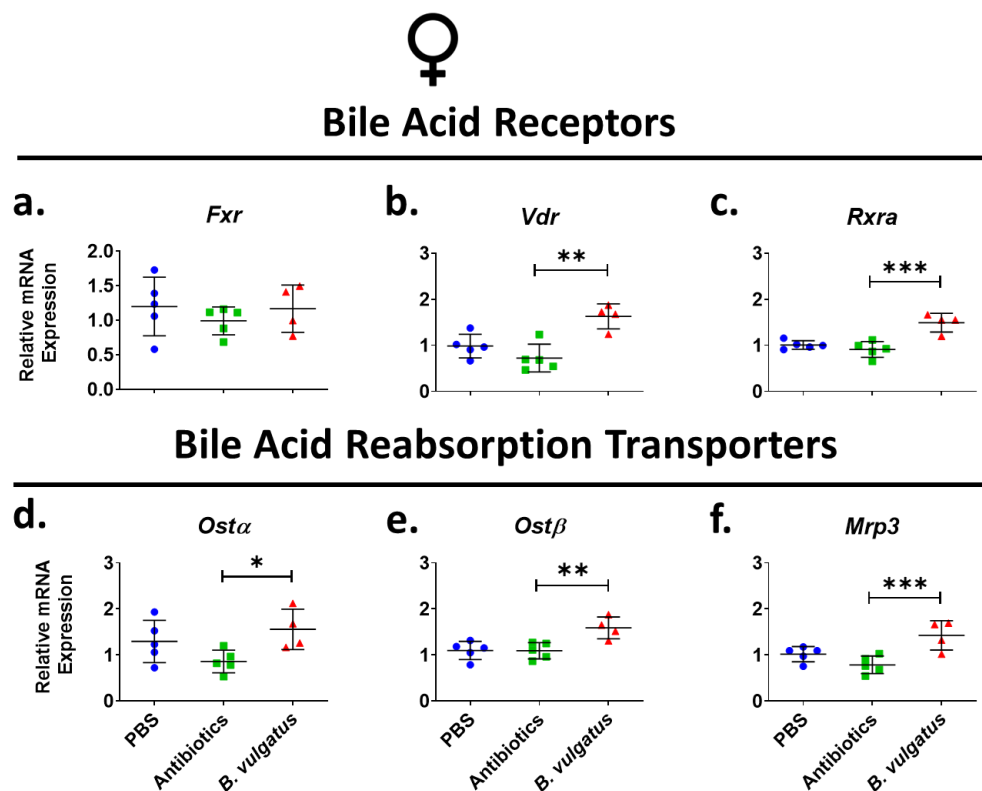
Figure 5.38 Colonic gene expression analysis of bile acid activated receptors and transporters in B. vulgatus colonised female IL10^{-/-} mice. Transcription changes in colon samples collected on day 99 for bile acid activated receptors (a-c) and bile acid reabsorption transporters (d-e) in female IL10^{-/-} mice following B. vulgatus colonisation. Data is presented as mean ± SD. n = 2-5 mice/gender/group. Significance was calculated using one-way ANOVA with Dunnett's post-hoc test with the control column as Antibiotics. * = p<0.05, ** = p<0.01, *** = p<0.001.

5.4 Discussion

In this chapter, we investigated the causal role of *B. vulgatus* in intestinal inflammation by assaying its impact on the host immune and epithelial response, microbiota composition and bile acid signalling in a genetically susceptible individual, IL10^{-/-} mice. A broad-spectrum antibiotic cocktail was used to establish colonisation of *B. vulgatus* in IL10^{-/-} mice. This resulted in impaired colitis and changes in microbiota composition towards a more pro-inflammatory profile in male IL10^{-/-} mice but not in female mice. Surprisingly, female IL10^{-/-} mice also developed colitis which was associated with an altered pro-inflammatory bacterial profile, three months after cessation of a broad-spectrum antibiotic cocktail treatment used to reduce microbiota to allow *B. vulgatus* colonisation. This data indicates a gender-specific response to *B. vulgatus* based on microbiota and host response, in genetic susceptible animals.

Based on previous results in Chapter 3, *B. vulgatus* was seen as the most inflammatory Bacteroides spp which negatively affected the epithelial response in cell lines and organoids but did not provoke major changes in gene expression profile in wild-type animals after two weeks' colonisation. Previous studies in TcRalpha^{-/-}, NOD2^{-/-} and Itch^{-/-} mice reported an expansion of *B. vulgatus* associated with colonic inflammation (Kishi *et al.*, 2000; Ramanan *et al.*, 2014b; Kathania *et al.*, 2020), indicating the increased capacity of *B. vulgatus* to colonise and behaving as a pathobiont in a susceptible individual and contributing to in colitis development.

In this study, we chose the IL10^{-/-} mice, due to reported increased CD risk and severe CD phenotype with defective IL-10 production (Franke *et al.*,

2008; Correa *et al.*, 2009). In line with previous reports, the disease penetrance in our IL10^{-/-} colony was as expected low, potentially due to the genetic background (the resistant C57BL/6 strain) and the lack of certain bacterial strains such as *Helicobacter hepaticus*, *Bilophila wadsworthia* in our animal facility (Kullberg *et al.*, 1998; Bristol *et al.*, 2000; Mähler and Leiter, 2002; Yang *et al.*, 2013), indicating the relevance of genetic susceptibility and microbial profile for colitis progression in these mice. Based on the initial clinical and gene expression profiling of our IL10^{-/-} colony, animals at an age of 9-11weeks were chosen for this study due to the lack of spontaneous inflammation, but deficiencies in the epithelial barrier, as shown to be necessary for *B. vulgatus* to provoke inflammation in IL10^{-/-} mice (Sydora *et al.*, 2007).

Studies investigating the role of *B. vulgatus* in CD pathogenesis using experimental models have to date been conflicting. Co-association of germ IL10^{-/-} mice with *B. vulgatus* and *Clostridium sordellii* did not induce intestinal inflammation over 22 weeks period (Sydora *et al.*, 2005). *B. vulgatus* was also reported to reduce inflammation provoked by *E. coli*-colonisation of gnotobiotic IL-2^{-/-} mice, by preventing maturation of dendritic cells and upregulating peroxisome proliferator-activated receptor-□ regulated genes (Waidmann *et al.*, 2003; Bohn *et al.*, 2006; Müller *et al.*, 2008). In contrast, *B. vulgatus* monocolonisation of germ-free HLA-B27 transgenic rats or TCRalpha^{-/-} mice induced inflammation, indicating a host-specific response to the invading microbe (Rath *et al.*, 1996; Kishi *et al.*, 2000). One explanation for the lack of *B. vulgatus* induced inflammation in germ-free IL10^{-/-} mice was the presence of an intact barrier in these animals

(Sydora *et al.*, 2007). Therefore, administration of a barrier breacher, indomethacin, to germ-free IL10^{-/-} mice resulted in increased inflammation upon *B. vulgatus* colonisation (Sydora *et al.*, 2007). Interestingly, a reduction in the barrier-related markers Claudin-2 and E-cadherin are detected at baseline in IL10^{-/-} raised in our colony, potentially contributing to the inflammation induced by *B. vulgatus* in this study.

The colitis progression provoked by *B. vulgatus* in male IL10^{-/-} mice corroborates previous findings in *Helicobacter hepaticus*-infected IL-10^{-/-} male mice. In this study, a more severe disease was associated with a higher degree of *H. hepaticus* survival and virulence as well as higher bone loss (Irwin *et al.*, 2013). Preliminary data in our group also indicate a higher degree of colonisation and colitis in IL10^{-/-} mice colonised with another CD-pathobiont Adherent and invasive *E. coli* (unpublished observation). In contrast, the colitis progression observed in female IL10^{-/-} mice three months after broad-spectrum antibiotic exposure was an unexpected finding. Previous studies have shown antibiotic treatment before disease onset prevents colitis in IL10^{-/-} mice, while antibiotics are less efficacious in mice with established disease (Madsen *et al.*, 2000b; Hoentjen *et al.*, 2003). One difference between our study and previous studies is the broad-spectrum antibiotic cocktail used in the current study compared to the two antibiotic treatment combinations (vancomycin-imipenem or neomycin-metronidazole) or the individual antibiotic treatment (ciprofloxacin or metronidazole) and the genetic background, the less susceptible C57BL/6 compared to the more susceptible C57BL/6-129/Ola mixed background and 129 Sv/Ev background (Madsen *et al.*, 2000b; Mähler and Leiter, 2002;

Hoentjen *et al.*, 2003). In contrast to these preventive studies in IL10$^{-/-}$ mice, Knoop et al, 2016 reported the promotion of inflammation as early as day 4 after treatment with a broad-spectrum antibiotic cocktail, similar to our cocktail, in WT, CX3CR1-transgene and Myd88-/- mice, followed by the translocation of commensal bacteria, such as *Enterococcus faecalis* and *Escherichia coli,* to mesenteric lymph nodes, inducing inflammatory responses, and predisposing the mice to increased colitis upon chemical stimuli (Knoop *et al.*, 2016). Although this study did not address whether the antibiotic-induced inflammation was gender-dependent or whether the inflammatory phenotype was sustained over a longer period post-antibiotic ease but based on our findings similar outcome could be expected in the longer term. Contrary to our results, Shen et al, recently reported that broad-spectrum antibiotic treatment of adult male IL10$^{-/-}$ mice developed more severe colitis than the littermates exposed to water (Shen *et al.*, 2019). IL10$^{-/-}$ mice used in this study belonged to the C3H/HejBir background, which is more susceptible to intestinal inflammation due to the activation of pathogenic T cells by enteric bacterial antigens and a mutation in the LPS receptor TLR4 (Elson, Cong and Sundberg, 2000; Mähler and Leiter, 2002; Shen *et al.*, 2019) compared to the more resistant C57BL/6 strain used in our study. Other differences include the dominance of the phylum Proteobacteria and *Pseudomonas* genera after antibiotic treatment (Shen *et al.*, 2019), a profile not seen in our study. Interestingly, antibiotic-treated male IL10$^{-/-}$ mice presented a faster recovery on days 22 and 52 associated with the higher abundance of *Ruminococcaceae* and *Clostridiaceae,* taxa known for their beneficial role in inflammation and infection (Atarashi *et al.*,

2013; Kim *et al.*, 2017), potentially contributing to the lack of intestinal inflammation in antibiotic-treated male IL10$^{-/-}$ mice at the end of the study. Previous studies have identified gender differences in microbiota composition in wild-type animals, as shown by hormone replacement or gonadectomy and vice versa i.e., the microbiota also regulated the level of hormones (Markle *et al.*, 2013; Yurkovetskiy *et al.*, 2013; Org *et al.*, 2016). A similar observation has been reported in mice developing autoimmune diseases, where the transfer of male microbiota to female mice modified diabetes development (Markle *et al.*, 2013). Although these reports indicate differences in microbiota composition by gender, a recent study reported no major differences in species richness and diversity between genders in IL10$^{-/-}$ animals, although their diversity was somewhat reduced compared to WT mice (Son *et al.*, 2019). In line with the latter paper, no major differences in abundances at the family level were observed between genders at the start of our experiment (on day 0). Thirteen days of antibiotic treatment resulted in reduced alpha diversity in the two groups, regardless of gender and a reduced abundance of what is regarded as beneficial bacteria including Lactobacillus and Akkermansia and increases in pathogenic bacteria such as Escherichia/Shigella, (In contrast to day 0, bacteria differences based on gender were observed at day 22 and 52 post-antibiotic treatment with the presence of the genera *Ruminococcaceae* and *Clostridiaceae,* known for their beneficial role in inflammation and infection (Atarashi *et al.*, 2013; Kim *et al.*, 2017), preferentially found in male IL10$^{-/-}$ mice, potentially contributing to their fast recovery post-antibiotic-treatment. Interestingly, these taxa are largely underrepresented in IBD and contribute to the reduced presence of

beneficial short-chain fatty acids, known to promote barrier function and anti-inflammatory potential (Frank *et al.*, 2007; Schirmer *et al.*, 2019; Ryan *et al.*, 2020). The expansion of the potentially harmful bacteria *Enterococcaceae* observed on days 22 and 52 in antibiotic-treated female mice potentially contributed to the increased inflammation seen on day 99 in these mice. In line with these findings, gender-specific responses associated with an increase in *Enterococcaceae* abundance were observed in the adoptive T cell transfer Rag2$^{-/-}$ model exposed to antibiotic treatment (Harrison *et al.*, 2019). In addition, this study also reported that the epithelial Na+ /H+ exchanger NHE3 was significantly elevated in the colon of antibiotic-treated female mice, but not in males, indicating NHE3 might be responsible for gender-specific response (Harrison *et al.*, 2019). However, we were not able to corroborate this result in our study, since *B. vulgatus* protected female IL10$^{-/-}$ mice presented a significantly higher NHE3 expression than antibiotic-treated females (data not shown). These data indicate that alterations in certain microbial taxa as a response to antibiotic cocktail and *B. vulgatus* colonisation appear to dictate the intestinal disease outcome in a gender-dependent manner.

Interestingly, oral gavage of the vehicle PBS for 13 days to IL10$^{-/-}$ mice resulted in dominance in the abundance of Lactobacillaceae and "other" bacteria, which was similar in gender on day 14 but diverge between genders from days 22 to 52, returning to similar microbial profile as day 0 at the end of the study on day 99. To our knowledge, this is the first time an effect of PBS on microbiota composition over 3 months have been identified

and this can be of relevance for the interpretation of studies where continuous gavaging with PBS is used as vehicle control.

Data generated *in vitro* in Chapter 4, indicated *Bacteroides* spp could play an important role in bile acid metabolism thereby contributing to the inflammation process seen in IBD. However, *B, vulgatus* elicited the least effect on BA moiety generation among the strains examined. From that chapter male mice fed *B. vulgatus* retained the conjugates of LCA (GBAR1 /TGR5 agonists), it also retained FXR antagonist GUDCA. These changes did not translate to activation of these receptors in the IL-10$^{-/-}$ males since only antibiotic treatment elicited any effects on receptors and only in female mice. Similar to the gender-specific changes in the microbiota, gender-specific alterations were also observed in the bile acid profile along disease progression. Few bile acid alterations were correlated to the inflammatory phenotype observed at day 99, except for a reduction in certain intermediate moieties such as 24Nor UDCA in *B. vulgatus*-colonised males and an increase in 7,12 DKLCA in antibiotic-treated females. 24-Nor UDCA is a conjugation-resistant UDCA derivative, which has shown anti-inflammatory effects in models of Sclerosing Cholangitis and hepatic inflammation by reshaping the immunometabolism of CD8 T cells (Fickert *et al.*, 2006; Zhu *et al.*, 2021). A recent preprint reported that 24-Nor UDCA reduced intestinal inflammation in an adoptive T cell transfer model by targeting the immunometabolism of Th17 and Tregs. When summarising the profile of bile acid moieties according to their bile acid receptors, a reduction in FXR and TGR5 agonist bile acids was found which was not accompanied by altered expression of bile acid receptors in the tissue of *B. vulgatus-*

colonised male IL10$^{-/-}$ mice. In contrast, a reduced expression in VDR and FXR-associated genes was detected in antibiotic-treated IL10$^{-/-}$ female mice, while no major changes in bile acid composition were observed in this group. Overall, the collected data set indicate that *B. vulgatus* do not appear to regulate bile acid metabolism and contribute to the increased inflammation in IL10$^{-/-}$ mice under the conditions studied in this chapter.

When we then investigated the host response to *B. vulgatus* colonisation, we confirmed an induction in inflammation, supported by changes in colonic markers, an array of epithelial and immune cell associated cytokines and chemokines and increased infiltration of immune cells in the colon of male IL10$^{-/-}$ mice colonised with *B. vulgatus*, supporting the *in vitro* findings from Chapter 3 and previous reports in mice and rat (Rath *et al.*, 1996; Bloom *et al.*, 2011b; Kathania *et al.*, 2020). A reduction in MUC2 gene expression and goblet cells was observed in *B. vulgatus* colonised IL10$^{-/-}$ male mice. This is in agreement with our findings from *B. vulgatus* conditioned media acute treated organoids (Chapter 3) and previous observations in the small intestine of NOD2$^{-/-}$ mice (Ramanan et al, 2014) and Itch$^{-/-}$ mice (Kathania *et al.*, 2020). Goblet cells are important as a first line of defence to the intestine as the production of mucin generates the mucus layer that inhibits bacterial penetrance and protects the colonic crypts (Johansson and Hansson, 2016b). Studies in antibiotic-treated mice indicated the formation of goblet cell associated antigen passages (GAPs), where antigens or bacteria can be transported and recognised by dendritic cells in the lamina propria (Knoop *et al.*, 2016), suggesting a mechanism whereby the depletion of microbiota by antibiotics not only creates a beneficial niche for

B. vulgatus to colonise the intestine but also to penetrate the intestinal tissue and sustain the immune response observed in our mice.

An increase in the expression of villin-1, both in colon homogenates and organoids was observed in Chapter 3, potentially indicating an impact of *B. vulgatus* on the normal functioning of enterocytes e.g., in the regulation of apoptosis (Wang et al., 2008). Some discrepancies were observed between the small intestinal organoids and colon homogenates in regards to *B. vulgatus* regulation of epithelial genes e.g., the expression of lysozyme was reduced in organoids but increased expression in colon homogenates. Similarly, alterations of members of the BMP and Wnt/β-catenin pathway detected in the organoids were not corroborated in the colon of IL10$^{-/-}$ mice. The reason for this discrepancy might be due to acute vs long-term exposure to bacteria/metabolites, small intestinal organoids vs proximal colon, WT vs IL10$^{-/-}$ mice. Further studies are needed to address the relevance of these results.

The findings from this study provide support for *B. vulgatus* as a regulator of intestinal inflammation by altering microbial profile and host response in a gender-specific manner. We also provide evidence of a gender-specific response to broad-spectrum antibiotics in promoting intestinal inflammation long after antibiotics pressure is released, indicating the long-term impact of antibiotics in females. This data further supports antibiotics as a risk factor for autoimmune disorders and functional gastrointestinal disorders such as irritable bowel syndrome in female individuals.

Chapter 6 General discussion

Crohn's disease is a chronic gastrointestinal disorder affecting the quality of life of its sufferers and it's becoming a global disease with an increased incidence worldwide. Crohn's disease aetiology is unknown but the collective evidence to date indicates its dependent on environmental, microbial, genetic factors, and dysregulated immune responses.

Research in the last decade and improvement in NGS technology has deepened our knowledge of altered microbiota composition and reduced microbial diversity to Crohn's disease. However, much of the research to date has revealed correlations of bacteria genera to different disease states while less is known on mechanisms causing the disease by specific bacteria or bacteria consortia. Among bacteria often reported in Crohn's disease is *Bacteroides* spp, especially *B. fragilis* and *B. vulgatus*. Studies to date have been conflicted with some studies showing increased abundance, while others show reduced abundance. These discrepancies could be attributed to several factors including the sample studied i.e., faeces vs tissue, techniques i.e., 16S rRNA vs metagenomics, or differences in software used. A recent study from our group on paired colonic biopsies from inflamed and non-inflamed patients with IBD showed significant enrichment of *Bacteroides fragilis* in inflamed mucosal biopsies from patients with Crohn's disease and an increased abundance of *Bacteroides vulgatus* in a cluster associated with decreased diversity but no disease state (Ryan et al., 2020). The literature demonstrates no consensus on the abundance of *Bacteroides* species in Crohn's disease, with some reporting increased and others decreased abundance, as recently published as a systematic review (Aldars-García et al., 2021).

Microorganisms can generate bacterial metabolites such as bile acids. Recent studies indicate bile acids can have immunomodulatory potential by promoting Tregs or reducing the presence of inflammatory Th17 cells, besides regulating metabolism.

This thesis aimed to investigate if *Bacteroides* spp play a role in the pathology of Crohn's disease. For this, we targeted our analyses to the colonic epithelium as this represents the first barrier to the microbiota and acts as a central coordinator of immune responses in the gut.

In chapter 3, we examined the pro-inflammatory potential of *B. fragilis* and *B. vulgatus* strains and their metabolites on disease-relevant inflammatory mechanisms and assessed their impact on epithelial homeostasis in a human colon cell line and murine organoids and mice. Whole *Bacteroides* species, and their metabolites, were able to induce an inflammatory response associated with NF-κB and JAK/STAT and altered the expression of members of the Wnt/β-catenin and BMP-pathways and Paneth cell maturation, suggesting a regulatory role of *Bacteroides* on epithelial cell proliferation and maturation. These effects were, however, not replicated in wild-type mice colonized with *B. fragilis* or *B. vulgatu*s for 2 weeks.

While the literature is conflicted on the potential role of *Bacteroides* species in CD pathology, our findings from the in vitro studies indicate the potential of both *Bacteroides* not only to affect epithelial cell immune response but also the proliferation and maturation of the cells. Previous studies on *B, fragilis* have been on its enterotoxin-producing strain, which is expressed in less than 11% of patients with active CD (Becker *et al.*, 2021). Therefore, the results obtained in this chapter would be representative of the *B. fragilis*

strain present in the majority of patients with CD. Animal studies have indicated that deletion of the CD susceptibility gene NOD2 results in the expansion of *B. vulgatus* resulting in inflammation and abnormalities in the intestinal epithelium, especially Paneth cells (Ramanan *et al.*, 2014a). This data is in support of our findings in the murine organoids cultured with *B. vulgatus* metabolites, where we observed an alteration in genes associated with Paneth cells' maturation potentially relating to the Paneth cell dysfunction linked to CD (Perminow et al., 2010).

To our knowledge, this is the first time that an effect on Wnt/β-catenin and BMP pathway has been reported by *B. vulgatus*. This could indicate a shift towards proliferation with less differentiation which can result in an impairment in the renewal and composition of the epithelium. Increased proliferation in the epithelium is generally associated with increased cancer risk. Interestingly a positive association of *B. vulga*tus with inflammatory markers and higher tumour burden was recently reported in a murine model of colitis-associated cancer (Song et al 2021). The metabolites produced by *B. vulgatus* induced the secretion of CCL20 in the cell line, a chemokine which is relevant for dendritic cell and Th17 migration, both associated with CD (Li *et al.*, 2013). In contrast, CCL20 was reduced in the organoids exposed to these metabolites. The reason for this discrepancy and the relevance for CD pathogenesis need to be investigated in more detail. Although we did not characterise the content of the conditioned media produced by the *Bacteroides* species, there is a possibility that it can contain OMVs. Although very little research has been reported on *B. vulgatus* OMVs, these appear to have immunomodulatory potential by either

silencing DCs (Maerz *et al.*, 2018) or activating NF-κB and IL-8 production (Di Lorenzo *et al.*, 2020). Future studies aiming to identify and characterise OMVs, or metabolites produced by Bacteroides species would shed a light on the role of these metabolites in the pathogenesis of IBD.

Our findings in the wild-type mice corroborate previous findings where *B. vulgatus* did not induce colitis in a genetically intact host but did in genetically deficient hosts (Bloom *et al.,* 2011) or in a host with disrupted barrier function (Sydora *et al.,* 2007). Overall, our data suggest that in a genetically intact host with a functional epithelial barrier, CD-associated *Bacteroides* species behave as commensals, while in a compromised host these same *Bacteroides* species may induce or sustain inflammation.

To provide a deeper insight into *Bacteroides'* potential to regulate inflammation and epithelial cell pathways such as BMP and Wnt/β-catenin, protein analysis and small molecule inhibitor or siRNA treatment studies are required. In addition, the use of human 3D organoids or inverted organoids generated would also provide a deeper understanding of the impact of *Bacteroides* species on epithelial cells and disease.

In chapter 4 we examined the BA metabolizing ability of *Bacteroides* species (*B. fragilis* NCTC 9343, *B. vulgatus* ATCC 8482, *B. thetaiotaomicron* VPI 5482) to determine if they carried differential activity. The rationale for this work was a documented deficiency in the representation of *Bacteroides* in IBDs, in essence, representation was reported as lower (Zhou *et al.,* (2016)). Indeed, Delday *et al.,* (2019) attributed the anti-inflammatory effect to whole and engineered *Bacteroides thetaiotaomicron* in the DSS murine model of colitis. At the same time a range of studies identified BA

metabolism, both a readout of microbial fitness to function and of potential to activate different nuclear and G protein coupled receptors as altered in the IBD contexts (reviewed by Biagioli *et al.,* 2021). The range of receptors attributed to BA activation is staggering including FXR, VDR, CAR SIPR, LXR, PXR, PPAR and indeed GBAR1 among others. Importantly they can be activated by different BAs, mainly by those that are microbially modified whilst a range of antagonists are also BAs but of the conjugated type.

Our data confirmed that the gateway to modification enzymes - BSHs - carried in *B. vulgatus* and *B. fragilis* carried conserved key residues and predicted overlay structure with established structures to suggest activity by the enzymes (Lambert (2008). We confirmed these activities experimentally. Furthermore, the differing loop regions and interspaces suggested divergence in interactions with BAs and there were also detected, a lower range of substrates and activity attributed to *B. vulgatus.* Our work highlighted other potential sites of conservation that may be useful in the context of mutation and application so that future bespoke BSHs could be designed for targeted deconjugation and to effectively alter conditions, where IBD and other diseases are related to the convergence of BA signatures.

We next examined the ability to deliver a range of secondary BAs and their intermediates. These secondary acids are central as potent signalling molecules for macrophage differentiation to M2 and the intermediates are effectors of T helper cell differentiation and Treg population determination (Ma *et al.,* 2018; Song *et al.,* 2020; Campbell et al., 2020). Indeed, we showed that for the intermediates examined, inflammation dampening *B.*

thetaiotaomicron could alter BA profiles similarly to *B. fragilis.* When we applied *B. fragilis* and *B. vulgatus* to normal male mice to determine any BA effects, following microbial knock down treatment through antibiotics, BAs alterations were dominated by the treatment, this is not unusual (Harris *et al.,* 2018). Effectively, *B. fragilis* was associated with faecal and gall bladder BA alteration, less so in the gall bladder bile as expected, since repair and replenishing occur here. In the lower intestine, the faecal BA signatures were altered significantly by this strain and less so by *B. vulgatus.* Our data represented a snapshot and a lower intestinal view of BA metabolism in these animals. It may not be representative of *Bacteroides'* complete functionality and a GF model may prove of better use in this context. Nevertheless, this work points to specific BA modifications that merit further investigations in the context of HSDH-modified BAs. It informs future experimentation to examine the suite of intermediate metabolites for specific strain linkage. This work also points to the inclusion of flow cytometry analysis to determine cell differentiation functions going forward with both male and female mice.

In Chapter 5, we aimed to examine whether the potential of *B. vulgatus* in inducing an inflammatory response, altering proliferation and maturation of epithelium and modifications on bile acid moieties could influence the development of intestinal inflammation in a genetically susceptible individual, IL10$^{-/-}$ mice. Our data indicated a gender-specific response whereby male IL10$^{-/-}$ developed more intestinal inflammation by inducing inflammatory markers and altering gut microbiota towards a pro-inflammatory environment before the development of intestinal

inflammation. Our data is in line with previous studies showing the necessity of a genetic predisposition for B. vulgatus to colonise and expand and behave as a pathobiont (Kishi *et al.*, 2000; Ramanan *et al.*, 2014b; Kathania *et al.*, 2020).

The *in vitro* findings from Chapter 4, indicated that *Bacteroides* spp could modify bile acid metabolism thereby contributing to the inflammation process seen in IBD. However, *B, vulgatus* elicited a low effect on bile acid moiety generation compared to *B. fragilis* and male wild-type mice colonised with *B. vulgatus* retained the conjugates of LCA (GBAR1 /TGR5 agonists) and the FXR antagonist - GUDCA. These changes were not observed in the male IL10$^{-/-}$ mice and only antibiotic treatment elicited any effects on the receptors but only in the female IL10$^{-/-}$ mice. This data suggests a low-level effect of *B. vulgatus* in modifying bile acids regardless of genetic background.

Although male and female individuals are at equal risk to develop CD, sex is a relevant factor in autoimmunity and microbiota composition, often associated with hormone regulation (Markle *et al.*, 2013; Yurkovetskiy *et al.*, 2013; Org *et al.*, 2016; (Markle *et al.*, 2013)). Our higher colonisation with *B. vulgatus* in male IL10$^{-/-}$ mice could be correlated to beneficial factors produced by the host and regulated by IL10 since no difference in the microbiota composition was observed at the start of the study between genders in these mice. This finding is in agreement with a recent publication in IL10$^{-/-}$ mice (Son *et al.*, 2019). Gender-associated differences in bacteria composition were identified ~ 3 months after antibiotic treatment ceased, with male IL10$^{-/-}$ treated with antibiotics presenting a higher abundance of

Ruminococcaceae and *Clostridiaceae,* known for their beneficial role in inflammation and infection (Atarashi *et al.*, 2013; Kim *et al.*, 2017), while antibiotic-treated female IL10$^{-/-}$ mice presented a higher abundance of the potentially harmful bacteria *Enterococcaceae*. This difference may explain the gender-different inflammatory phenotype observed in the animals at the end of the study. Similarly, a gender-specific higher abundance in *Enterococcaceae* was observed in the adoptive T cell transfer Rag2$^{-/-}$ model exposed to antibiotic treatment (Harrison *et al.*, 2019). We also observed a gender-specific microbiota profile in the IL10$^{-/-}$ male mice colonised with *B. vulgatus*. Interestingly, the more pro-inflammatory environment found in the *B. vulgatus* colonised male IL10$^{-/-}$ also appeared to provide a suitable environment for Bacteroides to expand, which was not seen in the female mice. This data thus indicates the necessity to create a host-microbial niche that will help expand a pathobiont thereby affecting the host immune and epithelial response in promoting or sustaining inflammation. Longitudinal studies on microbiota and microbial metabolites in newly diagnosed patients with CD would provide a platform for identifying how changes in microbiota over time affect the expansion or reduction of pathobionts or commensal regulatory bacteria, respectively.

Throughout the course of this thesis, we have made a variety of novel observations demonstrating that CD-associated *Bacteroides* species can influence epithelial development, along with the metabolic landscape and inflammatory tone of the gastrointestinal tract. However, the scope of this project was of such breadth that further investigation of some of these observations was not feasible due to time and material constraints.

Identification of the contents of *Bacteroides* conditioned media through proteomics could potentially help to determine immunoactive proteins responsible for the immune responses we observed through application of *Bacteroides* conditioned media to epithelial cell lines and organoids. Further to this, *Bacteroides* produce OMVs which may also be the mediator of immune signals from *Bacteroides* conditioned media to the epithelium. As such, isolating and exposing these OMVs to the epithelial systems used in this thesis may shed further light on the mechanism(s) by which *Bacteroides* metabolites relay signals to the epithelium. Much of our investigations into the inflammatory potential of *Bacteroides* (both whole bacterial cell and conditioned media) focused on the expression and production of downstream chemokines, future experiments could seek to identify which immune receptors and signalling pathways are activated by *Bacteroides* species, potentially by utilizing reporter cell lines or knocking down the expression of the receptors by siRNA or CRISP/Cas9 editing. We have observed that *Bacteroides* conditioned media altered the expression of genes responsible for epithelial lineage determination in organoid models. This work could be expanded, and this effect fully investigated using flow cytometry and cell sorting to characterise the changes in epithelial cell populations following exposure of organoids to *Bacteroides* conditioned media. This work also demonstrated that *Bacteroides* species contain BSH enzymes with varying substrate specificity and as such specific deconjugation ability. Amino acid residues critical for function can be mutated to allow a greater understanding of the functioning of the BSH enzyme which can potentially lead to the creation of synthetic "bespoke"

BSHs with defined deconjugation abilities. The presence of HSDH enzymes in *Bacteroides* species should also be further investigated and characterised as these may catalyse reactions generating exotic intermediate bile acids, for which there is currently very little research conducted on. Our observation that oral gavage of PBS had a large impact on the microbiota of IL10$^{-/-}$ mice was unexpected and may constitute a confounding variable on previous, and future, microbiota studies where it is used as a vehicle control. A potential reason for this perturbation to the microbiota is LPS contamination of the PBS. Analysing the PBS used in these experiments for the presence of LPS may provide an answer for the perturbations to the microbiota and indicate testing for LPS as good practice for future experiments.

Chapter 7 References

Abdelkarim, M. *et al.* (2010) 'The farnesoid X receptor regulates adipocyte differentiation and function by promoting peroxisome proliferator-activated receptor-gamma and interfering with the Wnt/beta-catenin pathways', *The Journal of biological chemistry*, 285(47), pp. 36759–36767. Available at: https://doi.org/10.1074/JBC.M110.166231.

Abrahamsson, T.R. *et al.* (2014) 'Low gut microbiota diversity in early infancy precedes asthma at school age', *Clinical and experimental allergy : journal of the British Society for Allergy and Clinical Immunology*, 44(6), pp. 842–850. Available at: https://doi.org/10.1111/CEA.12253.

Abreu, M.T. (2010) 'Toll-like receptor signalling in the intestinal epithelium: how bacterial recognition shapes intestinal function', *Nature reviews. Immunology*, 10(2), pp. 131–143. Available at: https://doi.org/10.1038/NRI2707.

Adhikari, A.A. *et al.* (2021) 'A Gut-Restricted Lithocholic Acid Analog as an Inhibitor of Gut Bacterial Bile Salt Hydrolases', *ACS chemical biology*, 16(8), pp. 1401–1412. Available at: https://doi.org/10.1021/ACSCHEMBIO.1C00192.

Adlerberth, I. and Wold, A.E. (2009) 'Establishment of the gut microbiota in Western infants', *Acta paediatrica (Oslo, Norway : 1992)*, 98(2), pp. 229–238. Available at: https://doi.org/10.1111/J.1651-2227.2008.01060.X.

De Aguiar Vallim, T.Q., Tarling, E.J. and Edwards, P.A. (2013) 'Pleiotropic roles of bile acids in metabolism', *Cell metabolism*, 17(5), pp. 657–669. Available at: https://doi.org/10.1016/J.CMET.2013.03.013.

Akare, S. *et al.* (2006) 'Ursodeoxycholic acid modulates histone acetylation and induces differentiation and senescence', *International journal of cancer*, 119(12), pp. 2958–2969. Available at: https://doi.org/10.1002/IJC.22231.

Akira, S., Uematsu, S. and Takeuchi, O. (2006) 'Pathogen recognition and innate immunity', *Cell*, 124(4), pp. 783–801. Available at: https://doi.org/10.1016/J.CELL.2006.02.015.

Alatshan, A. and Benkő, S. (2021) 'Nuclear Receptors as Multiple Regulators of NLRP3 Inflammasome Function', *Frontiers in Immunology*, 12, p. 503. Available at: https://doi.org/10.3389/FIMMU.2021.630569/BIBTEX.

Aldars-García, L., Chaparro, M. and Gisbert, J.P. (2021) *Systematic review: The gut microbiome and its potential clinical application in inflammatory bowel disease*, *Microorganisms*. Available at: https://doi.org/10.3390/microorganisms9050977.

Al-Lahham, S.H. *et al.* (2010) 'Regulation of adipokine production in human adipose tissue by propionic acid', *European journal of clinical investigation*, 40(5), pp. 401–407. Available at: https://doi.org/10.1111/J.1365-2362.2010.02278.X.

Ananthakrishnan, A.N. *et al.* (2012) 'Aspirin, nonsteroidal anti-inflammatory drug use, and risk for crohn disease and ulcerative colitis', *Annals of Internal Medicine*, 156(5), pp. 350–359. Available at: https://doi.org/10.7326/0003-4819-156-5-201203060-00007.

Ananthakrishnan, A.N. *et al.* (2013) 'A prospective study of long-term intake of dietary fiber and risk of Crohn's disease and ulcerative colitis', *Gastroenterology*, 145(5), pp. 970–977. Available at: https://doi.org/10.1053/j.gastro.2013.07.050.

Ananthakrishnan, A.N. *et al.* (2018) 'Environmental triggers in IBD: A review of progress and evidence', *Nature Reviews Gastroenterology and Hepatology*. Nature Publishing Group, pp. 39–49. Available at: https://doi.org/10.1038/nrgastro.2017.136.

Anderson, J.M. and Van Itallie, C.M. (2009) 'Physiology and function of the tight junction', *Cold Spring Harbor perspectives in biology*, 1(2). Available at: https://doi.org/10.1101/CSHPERSPECT.A002584.

Annunziato, F. *et al.* (2007) 'Phenotypic and functional features of human Th17 cells', *The Journal of experimental medicine*, 204(8), pp. 1849–1861. Available at: https://doi.org/10.1084/JEM.20070663.

Ansari, N. *et al.* (2006) 'Comparison of RANTES expression in Crohn's disease and ulcerative colitis: An aid in the differential diagnosis?', *Journal of Clinical Pathology*, 59(10), pp. 1066–1072. Available at: https://doi.org/10.1136/jcp.2005.034983.

Arboleya, S. *et al.* (2012) 'Establishment and development of intestinal microbiota in preterm neonates', *FEMS microbiology ecology*, 79(3), pp. 763–772. Available at: https://doi.org/10.1111/J.1574-6941.2011.01261.X.

Arumugam, M. *et al.* (2011) 'Enterotypes of the human gut microbiome', *Nature*, 473(7346), pp. 174–180. Available at: https://doi.org/10.1038/NATURE09944.

Asakuma, S. *et al.* (2011) 'Physiology of consumption of human milk oligosaccharides by infant gut-associated bifidobacteria', *The Journal of biological chemistry*, 286(40), pp. 34583–34592. Available at: https://doi.org/10.1074/JBC.M111.248138.

Atarashi, K. *et al.* (2013) 'Treg induction by a rationally selected mixture of Clostridia strains from the human microbiota', *Nature 2013 500:7461*, 500(7461), pp. 232–236. Available at: https://doi.org/10.1038/nature12331.

Attinkara, R. *et al.* (2012) 'Association of genetic variation in the NR1H4 gene, encoding the nuclear bile acid receptor FXR, with inflammatory bowel disease', *BMC Research Notes*, 5, p. 461. Available at: https://doi.org/10.1186/1756-0500-5-461.

Bäckhed, F. *et al.* (2005) 'Host-bacterial mutualism in the human intestine', *Science (New York, N.Y.)*, 307(5717), pp. 1915–1920. Available at: https://doi.org/10.1126/SCIENCE.1104816.

Bäckhed, F. *et al.* (2015) 'Dynamics and Stabilization of the Human Gut Microbiome during the First Year of Life', *Cell host & microbe*, 17(5), pp. 690–703. Available at: https://doi.org/10.1016/J.CHOM.2015.04.004.

Badi, S.A. *et al.* (2019) 'Induction Effects of Bacteroides fragilis Derived Outer Membrane Vesicles on Toll Like Receptor 2, Toll Like Receptor 4 Genes Expression and Cytokines Concentration in Human Intestinal Epithelial Cells', *Cell journal*, 21(1), pp. 57–61. Available at: https://doi.org/10.22074/CELLJ.2019.5750.

Barker, N. *et al.* (2007) 'Identification of stem cells in small intestine and colon by marker gene Lgr5', *Nature 2007 449:7165*, 449(7165), pp. 1003–1007. Available at: https://doi.org/10.1038/nature06196.

Barker, N. *et al.* (2009) 'Crypt stem cells as the cells-of-origin of intestinal cancer', *Nature*, 457(7229), pp. 608–611. Available at: https://doi.org/10.1038/nature07602.

Barrett, J.C. *et al.* (2008) 'Genome-wide association defines more than 30 distinct susceptibility loci for Crohn's disease', *Nature Genetics*, 40(8), pp. 955–962. Available at: https://doi.org/10.1038/ng.175.

Basak, O. *et al.* (2017) 'Induced Quiescence of Lgr5+ Stem Cells in Intestinal Organoids Enables Differentiation of Hormone-Producing Enteroendocrine Cells', *Cell Stem Cell*, 20(2), pp. 177-190.e4. Available at: https://doi.org/10.1016/j.stem.2016.11.001.

Basson, A. (2012) 'Nutrition management in the adult patient with crohn's disease', *South African Journal of Clinical Nutrition*, 25(4), pp. 164–172. Available at: https://doi.org/10.1080/16070658.2012.11734423.

BAUER, H. *et al.* (1963) 'The Response of the Lymphatic Tissue to the Microbial Flora. Studies on Germfree Mice', *The American Journal of Pathology*, 42(4), p. 471.

Baümler, A.J. and Sperandio, V. (2016) 'Interactions between the microbiota and pathogenic bacteria in the gut', *Nature 2016 535:7610*, 535(7610), pp. 85–93. Available at: https://doi.org/10.1038/nature18849.

Becker, H.E.F. *et al.* (2021) 'Higher Prevalence of Bacteroides fragilis in Crohn's Disease Exacerbations and Strain-Dependent Increase of Epithelial Resistance', *Frontiers in Microbiology*, 12, p. 1305. Available at: https://doi.org/10.3389/FMICB.2021.598232/BIBTEX.

Begley, M. *et al.* (2005a) 'Contribution of three bile-associated loci, bsh, pva, and btlB, to gastrointestinal persistence and bile tolerance of Listeria monocytogenes', *Infection and immunity*, 73(2), pp. 894–904. Available at: https://doi.org/10.1128/IAI.73.2.894-904.2005.

Begley, M. *et al.* (2005b) 'Contribution of three bile-associated loci, bsh, pva, and btlB, to gastrointestinal persistence and bile tolerance of Listeria monocytogenes', *Infection and immunity*, 73(2), pp. 894–904. Available at: https://doi.org/10.1128/IAI.73.2.894-904.2005.

Begley, M., Hill, C. and Gahan, C.G.M. (2006) 'Bile salt hydrolase activity in probiotics', *Applied and environmental microbiology*, 72(3), pp. 1729–1738. Available at: https://doi.org/10.1128/AEM.72.3.1729-1738.2006.

Bell, J.K. *et al.* (2003) 'Leucine-rich repeats and pathogen recognition in Toll-like receptors', *Trends in immunology*, 24(10), pp. 528–533. Available at: https://doi.org/10.1016/S1471-4906(03)00242-4.

Bennett, M.J., McKnight, S.L. and Coleman, J.P. (2003) 'Cloning and characterization of the NAD-dependent 7alpha-Hydroxysteroid dehydrogenase from Bacteroides fragilis', *Current microbiology*, 47(6), pp. 475–484. Available at: https://doi.org/10.1007/S00284-003-4079-4.

Berg, D.J. *et al.* (1996a) 'Enterocolitis and colon cancer in interleukin-10-deficient mice are associated with aberrant cytokine production and CD4(+) TH1-like responses.', *Journal of Clinical Investigation*, 98(4), p. 1010. Available at: https://doi.org/10.1172/JCI118861.

Berg, D.J. *et al.* (1996b) 'Enterocolitis and colon cancer in interleukin-10-deficient mice are associated with aberrant cytokine production and CD4(+) TH1-like responses.', *Journal of Clinical Investigation*, 98(4), p. 1010. Available at: https://doi.org/10.1172/JCI118861.

Den Besten, G. *et al.* (2013) 'The role of short-chain fatty acids in the interplay between diet, gut microbiota, and host energy metabolism', *Journal of Lipid Research*, 54(9), pp. 2325–2340. Available at: https://doi.org/10.1194/JLR.R036012.

Bettelli, E. *et al.* (2006) 'Reciprocal developmental pathways for the generation of pathogenic effector TH17 and regulatory T cells', *Nature*, 441(7090), pp. 235–238. Available at: https://doi.org/10.1038/NATURE04753.

Beumer, J. and Clevers, H. (2020) 'Cell fate specification and differentiation in the adult mammalian intestine', *Nature Reviews Molecular Cell Biology 2020 22:1*, 22(1), pp. 39–53. Available at: https://doi.org/10.1038/s41580-020-0278-0.

Beutler, B. (2004) 'Innate immunity: an overview', *Molecular immunology*, 40(12), pp. 845–859. Available at: https://doi.org/10.1016/J.MOLIMM.2003.10.005.

Biagioli, M. *et al.* (2017) 'The Bile Acid Receptor GPBAR1 Regulates the M1/M2 Phenotype of Intestinal Macrophages and Activation of GPBAR1 Rescues Mice from Murine Colitis', *Journal of immunology (Baltimore, Md. :*

1950), 199(2), pp. 718–733. Available at: https://doi.org/10.4049/JIMMUNOL.1700183.

Biagioli, M. *et al.* (2021) 'Bile Acids Activated Receptors in Inflammatory Bowel Disease', *Cells*, 10(6). Available at: https://doi.org/10.3390/CELLS10061281.

Bianco, A.M., Girardelli, M. and Tommasini, A. (2015) 'Genetics of inflammatory bowel disease from multifactorial to monogenic forms', *World Journal of Gastroenterology*. WJG Press, pp. 12296–12310. Available at: https://doi.org/10.3748/wjg.v21.i43.12296.

Birrenbach, T. and Böcker, U. (2004) 'Inflammatory bowel disease and smoking. A review of epidemiology, pathophysiology, and therapeutic implications', *Inflammatory Bowel Diseases*. Inflamm Bowel Dis, pp. 848–859. Available at: https://doi.org/10.1097/00054725-200411000-00019.

Bleich, A. *et al.* (2004) 'Refined histopathologic scoring system improves power to detect colitis QTL in mice', *Mammalian genome : official journal of the International Mammalian Genome Society*, 15(11), pp. 865–871. Available at: https://doi.org/10.1007/S00335-004-2392-2.

Bloom, S.M. *et al.* (2011a) 'Commensal Bacteroides species induce colitis in host-genotype-specific fashion in a mouse model of inflammatory bowel disease', *Cell host & microbe*, 9(5), p. 390. Available at: https://doi.org/10.1016/J.CHOM.2011.04.009.

Bloom, S.M. *et al.* (2011b) 'Commensal Bacteroides species induce colitis in host-genotype-specific fashion in a mouse model of inflammatory bowel disease', *Cell host & microbe*, 9(5), pp. 390–403. Available at: https://doi.org/10.1016/J.CHOM.2011.04.009.

Blottière, H.M. *et al.* (2011) 'Identification of NF-κB Modulation Capabilities within Human Intestinal Commensal Bacteria', *Journal of Biomedicine and Biotechnology*, 2011. Available at: https://doi.org/10.1155/2011/282356.

Bohn, E. *et al.* (2006) 'Host gene expression in the colon of gnotobiotic interleukin-2-deficient mice colonized with commensal colitogenic or noncolitogenic bacterial strains: common patterns and bacteria strain specific signatures', *Inflammatory bowel diseases*, 12(9), pp. 853–862. Available at: https://doi.org/10.1097/01.MIB.0000231574.73559.75.

Botos, I., Segal, D.M. and Davies, D.R. (2011) 'The structural biology of Toll-like receptors', *Structure (London, England : 1993)*, 19(4), pp. 447–459. Available at: https://doi.org/10.1016/J.STR.2011.02.004.

Boyapati, R.K. *et al.* (2016) 'Gut mucosal DAMPs in IBD: from mechanisms to therapeutic implications', *Mucosal immunology*, 9(3), pp. 567–582. Available at: https://doi.org/10.1038/MI.2016.14.

Boyer, J.L. (2013) 'Bile formation and secretion', *Comprehensive Physiology*, 3(3), pp. 1035–1078. Available at: https://doi.org/10.1002/CPHY.C120027.

Breese, E. *et al.* (1993) 'Interleukin-2- and interferon-gamma-secreting T cells in normal and diseased human intestinal mucosa.', *Immunology*, 78(1), p. 127.

Bristol, I.J. *et al.* (2000) 'Heritable Susceptibility for Colitis in Mice Induced by IL-10 Deficiency', *Inflammatory Bowel Diseases*, 6(4), pp. 290–302. Available at: https://doi.org/10.1097/00054725-200011000-00006.

Britton, R.A. and Young, V.B. (2014) 'Role of the Intestinal Microbiota in Resistance to Colonization by Clostridium difficile', *Gastroenterology*, 146(6), pp. 1547–1553. Available at: https://doi.org/10.1053/J.GASTRO.2014.01.059.

Buisine, M.P. *et al.* (1999) 'Abnormalities in mucin gene expression in Crohn's disease', *Inflammatory bowel diseases*, 5(1), pp. 24–32. Available at: https://doi.org/10.1097/00054725-199902000-00004.

Bunker, J.J. *et al.* (2017) 'Natural polyreactive IgA antibodies coat the intestinal microbiota', *Science (New York, N.Y.)*, 358(6361). Available at: https://doi.org/10.1126/SCIENCE.AAN6619.

Burnat, G., Majka, J. and Konturek, P.C. (2010) 'Bile acids are multifunctional modulators of the Barrett's carcinogenesis', *Journal of physiology and pharmacology : an official journal of the Polish Physiological Society*, 61(2), pp. 185–192.

Campbell, C. *et al.* (2020a) 'Bacterial metabolism of bile acids promotes generation of peripheral regulatory T cells', *Nature*, 581(7809), pp. 475–479. Available at: https://doi.org/10.1038/S41586-020-2193-0.

Campbell, C. *et al.* (2020b) 'Bacterial metabolism of bile acids promotes generation of peripheral regulatory T cells', *Nature*, 581(7809), pp. 475–479. Available at: https://doi.org/10.1038/S41586-020-2193-0.

Cani, P.D. (2018) 'Human gut microbiome: hopes, threats and promises', *Gut*, 67(9), pp. 1716–1725. Available at: https://doi.org/10.1136/GUTJNL-2018-316723.

Capaldo, C.T. and Macara, I.G. (2007) 'Depletion of E-cadherin disrupts establishment but not maintenance of cell junctions in Madin-Darby canine kidney epithelial cells', *Molecular biology of the cell*, 18(1), pp. 189–200. Available at: https://doi.org/10.1091/MBC.E06-05-0471.

Carlson, A.L. *et al.* (2018) 'Infant Gut Microbiome Associated With Cognitive Development', *Biological psychiatry*, 83(2), pp. 148–159. Available at: https://doi.org/10.1016/J.BIOPSYCH.2017.06.021.

Carroll, I.M. *et al.* (2012) 'Alterations in composition and diversity of the intestinal microbiota in patients with diarrhea-predominant irritable bowel syndrome', *Neurogastroenterology and motility : the official journal of the European Gastrointestinal Motility Society*, 24(6). Available at: https://doi.org/10.1111/J.1365-2982.2012.01891.X.

Caruso, R. *et al.* (2014) 'NOD1 and NOD2: Signaling, host defense, and inflammatory disease', *Immunity*. Cell Press, pp. 898–908. Available at: https://doi.org/10.1016/j.immuni.2014.12.010.

Caruso, R. *et al.* (2019) 'A specific gene-microbe interaction drives the development of Crohn's disease-like colitis in mice', *Science immunology*, 4(34). Available at: https://doi.org/10.1126/SCIIMMUNOL.AAW4341.

Cerutti, A. (2008) 'The regulation of IgA class switching', *Nature reviews. Immunology*, 8(6), pp. 421–434. Available at: https://doi.org/10.1038/NRI2322.

Cerutti, A. and Rescigno, M. (2008) 'The biology of intestinal immunoglobulin A responses', *Immunity*, 28(6), pp. 740–750. Available at: https://doi.org/10.1016/J.IMMUNI.2008.05.001.

Chan, S.S.M. *et al.* (2011) 'Aspirin in the aetiology of Crohn's disease and ulcerative colitis: A European prospective cohort study', *Alimentary Pharmacology and Therapeutics*, 34(6), pp. 649–655. Available at: https://doi.org/10.1111/j.1365-2036.2011.04784.x.

Chang, S.Y., Ko, H.J. and Kweon, M.N. (2014) 'Mucosal dendritic cells shape mucosal immunity', *Experimental & Molecular Medicine 2014 46:3*, 46(3), pp. e84–e84. Available at: https://doi.org/10.1038/emm.2014.16.

Cheifetz, A.S. (2013) 'Management of active Crohn disease', *JAMA - Journal of the American Medical Association*. American Medical Association, pp. 2150–2158. Available at: https://doi.org/10.1001/jama.2013.4466.

Cheng, H. and Leblond, C.P. (1974) 'Origin, differentiation and renewal of the four main epithelial cell types in the mouse small intestine. V. Unitarian Theory of the origin of the four epithelial cell types', *The American journal of anatomy*, 141(4), pp. 537–561. Available at: https://doi.org/10.1002/AJA.1001410407.

Chiang, J.Y.L. (2013a) 'Bile acid metabolism and signaling', *Comprehensive Physiology*, 3(3), pp. 1191–1212. Available at: https://doi.org/10.1002/CPHY.C120023.

Chiang, J.Y.L. (2013b) 'Bile acid metabolism and signaling', *Comprehensive Physiology*, 3(3), pp. 1191–1212. Available at: https://doi.org/10.1002/CPHY.C120023.

Chikai, T., Nakao, H. and Uchida, K. (1987) 'Deconjugation of bile acids by human intestinal bacteria implanted in germ-free rats', *Lipids 1987 22:9*, 22(9), pp. 669–671. Available at: https://doi.org/10.1007/BF02533948.

Choo, J.M. *et al.* (2017) 'Divergent Relationships between Fecal Microbiota and Metabolome following Distinct Antibiotic-Induced Disruptions', *mSphere*, 2(1). Available at: https://doi.org/10.1128/MSPHERE.00005-17.

Christ, A., Lauterbach, M. and Latz, E. (2019) 'Western Diet and the Immune System: An Inflammatory Connection', *Immunity*, 51(5), pp. 794–811. Available at: https://doi.org/10.1016/J.IMMUNI.2019.09.020.

Chu, H. *et al.* (2016a) 'Gene-microbiota interactions contribute to the pathogenesis of inflammatory bowel disease', *Science*, 352(6289), pp. 1116–1120. Available at: https://doi.org/10.1126/science.aad9948.

Chu, H. *et al.* (2016b) 'Gene-Microbiota Interactions Contribute to the Pathogenesis of Inflammatory Bowel Disease', *Science (New York, N.Y.)*, 352(6289), p. 1116. Available at: https://doi.org/10.1126/SCIENCE.AAD9948.

Chung, Y. *et al.* (2009) 'Critical regulation of early Th17 cell differentiation by interleukin-1 signaling', *Immunity*, 30(4), pp. 576–587. Available at: https://doi.org/10.1016/J.IMMUNI.2009.02.007.

Claesson, M.J. *et al.* (2010) 'Comparison of two next-generation sequencing technologies for resolving highly complex microbiota composition using tandem variable 16S rRNA gene regions', *Nucleic acids research*, 38(22). Available at: https://doi.org/10.1093/NAR/GKQ873.

Claesson, M.J. *et al.* (2011) 'Composition, variability, and temporal stability of the intestinal microbiota of the elderly', *Proceedings of the National Academy of Sciences of the United States of America*, 108(SUPPL. 1), pp. 4586–4591. Available at: https://doi.org/10.1073/PNAS.1000097107/-/DCSUPPLEMENTAL.

Claesson, M.J. *et al.* (2012) 'Gut microbiota composition correlates with diet and health in the elderly', *Nature*, 488(7410), pp. 178–184. Available at: https://doi.org/10.1038/NATURE11319.

Coccia, M. *et al.* (2012) 'IL-1β mediates chronic intestinal inflammation by promoting the accumulation of IL-17A secreting innate lymphoid cells and CD4 + Th17 cells', *Journal of Experimental Medicine*, 209(9), pp. 1595–1609. Available at: https://doi.org/10.1084/jem.20111453.

Cong, Y. *et al.* (1998) 'CD4+ T cells reactive to enteric bacterial antigens in spontaneously colitic C3H/HeJBir mice: increased T helper cell type 1 response and ability to transfer disease', *The Journal of experimental medicine*, 187(6), pp. 855–864. Available at: https://doi.org/10.1084/JEM.187.6.855.

Conlon, M.A. and Bird, A.R. (2014) 'The impact of diet and lifestyle on gut microbiota and human health', *Nutrients*, 7(1), pp. 17–44. Available at: https://doi.org/10.3390/NU7010017.

Correa, I. *et al.* (2009) 'Defective IL-10 production in severe phenotypes of Crohn's disease', *Journal of Leukocyte Biology*, 85(5), pp. 896–903. Available at: https://doi.org/10.1189/JLB.1108698.

Corthésy, B. (2013) 'Role of secretory IgA in infection and maintenance of homeostasis', *Autoimmunity reviews*, 12(6), pp. 661–665. Available at: https://doi.org/10.1016/J.AUTREV.2012.10.012.

Coskun, M. (2014) 'Intestinal epithelium in inflammatory bowel disease', *Frontiers in Medicine*, 1(AUG), pp. 1–5. Available at: https://doi.org/10.3389/fmed.2014.00024.

Cosnes, J. *et al.* (2004) 'Gender differences in the response of colitis to smoking', *Clinical Gastroenterology and Hepatology*, 2(1), pp. 41–48. Available at: https://doi.org/10.1016/S1542-3565(03)00290-8.

Cotton, J.A. *et al.* (2016) 'Interleukin-8 in gastrointestinal inflammation and malignancy: Induction and clinical consequences', *International Journal of Interferon, Cytokine and Mediator Research*, 8, pp. 13–34. Available at: https://doi.org/10.2147/IJICMR.S63682.

Coyne, M.J. *et al.* (2008) 'Role of glycan synthesis in colonization of the mammalian gut by the bacterial symbiont Bacteroides fragilis', *Proceedings of the National Academy of Sciences of the United States of America*, 105(35), pp. 13099–13104. Available at: https://doi.org/10.1073/PNAS.0804220105.

Daig, R. *et al.* (1996) 'Increased interleukin 8 expression in the colon mucosa of patients with inflammatory bowel disease', *Gut*, 38(2), pp. 216–222. Available at: https://doi.org/10.1136/gut.38.2.216.

Dalal, S.R. and Chang, E.B. (2014) 'The microbial basis of inflammatory bowel diseases', *The Journal of clinical investigation*, 124(10), pp. 4190–4196. Available at: https://doi.org/10.1172/JCI72330.

Dan, Z. *et al.* (2020) 'Altered gut microbial profile is associated with abnormal metabolism activity of Autism Spectrum Disorder', *Gut microbes*, 11(5), pp. 1246–1267. Available at: https://doi.org/10.1080/19490976.2020.1747329.

Darwich, A.S. *et al.* (2014) 'Meta-analysis of the turnover of intestinal epithelia in preclinical animal species and humans', *Drug metabolism and disposition: the biological fate of chemicals*, 42(12), pp. 2016–2022. Available at: https://doi.org/10.1124/DMD.114.058404.

David, L.A. *et al.* (2013) 'Diet rapidly and reproducibly alters the human gut microbiome', *Nature 2013 505:7484*, 505(7484), pp. 559–563. Available at: https://doi.org/10.1038/nature12820.

David, L.A. *et al.* (2014) 'Diet rapidly and reproducibly alters the human gut microbiome', *Nature*, 505(7484), pp. 559–563. Available at: https://doi.org/10.1038/nature12820.

Decker, E., Hornef, M. and Stockinger, S. (2011) 'Cesarean delivery is associated with celiac disease but not inflammatory bowel disease in children', *Gut microbes*, 2(2). Available at: https://doi.org/10.4161/GMIC.2.2.15414.

Delday, M. *et al.* (2019a) 'Bacteroides thetaiotaomicron Ameliorates Colon Inflammation in Preclinical Models of Crohn's Disease', *Inflammatory bowel diseases*, 25(1), pp. 85–96. Available at: https://doi.org/10.1093/IBD/IZY281.

Delday, M. *et al.* (2019b) 'Bacteroides thetaiotaomicron Ameliorates Colon Inflammation in Preclinical Models of Crohn's Disease', *Inflammatory bowel diseases*, 25(1), pp. 85–96. Available at: https://doi.org/10.1093/IBD/IZY281.

Devlin, A.S. and Fischbach, M.A. (2015) 'A biosynthetic pathway for a prominent class of microbiota-derived bile acids', *Nature chemical biology*, 11(9), pp. 685–690. Available at: https://doi.org/10.1038/NCHEMBIO.1864.

D'Haens, G.R. *et al.* (1998) 'Early lesions of recurrent Crohn's disease caused by infusion of intestinal contents in excluded ileum', *Gastroenterology*, 114(2), pp. 262–267. Available at: https://doi.org/10.1016/S0016-5085(98)70476-7.

Dianda, L. *et al.* (1997) 'T cell receptor-alpha beta-deficient mice fail to develop colitis in the absence of a microbial environment.', *The American Journal of Pathology*, 150(1), p. 91.

DiGiulio, D.B. *et al.* (2008) 'Microbial prevalence, diversity and abundance in amniotic fluid during preterm labor: a molecular and culture-based investigation', *PloS one*, 3(8). Available at: https://doi.org/10.1371/JOURNAL.PONE.0003056.

Ding, L. *et al.* (2015) 'Bile acid nuclear receptor FXR and digestive system diseases', *Acta pharmaceutica Sinica. B*, 5(2), pp. 135–144. Available at: https://doi.org/10.1016/J.APSB.2015.01.004.

Ding, N.S. *et al.* (2020) 'Metabonomics and the Gut Microbiome Associated With Primary Response to Anti-TNF Therapy in Crohn's Disease', *Journal of Crohn's & colitis*, 14(8), pp. 1090–1102. Available at: https://doi.org/10.1093/ECCO-JCC/JJAA039.

Dogaru, C.M. *et al.* (2014) 'Breastfeeding and childhood asthma: systematic review and meta-analysis', *American journal of epidemiology*, 179(10), pp. 1153–1167. Available at: https://doi.org/10.1093/AJE/KWU072.

Dominguez-Bello, M.G. *et al.* (2010) 'Delivery mode shapes the acquisition and structure of the initial microbiota across multiple body habitats in

newborns', *Proceedings of the National Academy of Sciences of the United States of America*, 107(26), pp. 11971–11975. Available at: https://doi.org/10.1073/PNAS.1002601107/-/DCSUPPLEMENTAL.

Duboc, H. *et al.* (2013a) 'Connecting dysbiosis, bile-acid dysmetabolism and gut inflammation in inflammatory bowel diseases', *Gut*, 62(4), pp. 531–539. Available at: https://doi.org/10.1136/GUTJNL-2012-302578.

Duboc, H. *et al.* (2013b) 'Connecting dysbiosis, bile-acid dysmetabolism and gut inflammation in inflammatory bowel diseases', *Gut*, 62(4), pp. 531–539. Available at: https://doi.org/10.1136/GUTJNL-2012-302578.

Duboc, H., Taché, Y. and Hofmann, A.F. (2014) 'The bile acid TGR5 membrane receptor: from basic research to clinical application', *Digestive and liver disease : official journal of the Italian Society of Gastroenterology and the Italian Association for the Study of the Liver*, 46(4), pp. 302–312. Available at: https://doi.org/10.1016/J.DLD.2013.10.021.

Duerr, R.H. *et al.* (2006) 'A genome-wide association study identifies IL23R as an inflammatory bowel disease gene', *Science*, 314(5804), pp. 1461–1463. Available at: https://doi.org/10.1126/science.1135245.

Duparc, T. *et al.* (2017) 'Original article: Hepatocyte MyD88 affects bile acids, gut microbiota and metabolome contributing to regulate glucose and lipid metabolism', *Gut*, 66(4), p. 620. Available at: https://doi.org/10.1136/GUTJNL-2015-310904.

Dwinell, M.B. *et al.* (2001) 'Regulated production of interferon-inducible T-cell chemoattractants by human intestinal epithelial cells', *Gastroenterology*, 120(1), pp. 49–59. Available at: https://doi.org/10.1053/gast.2001.20914.

Elson, C.O. *et al.* (1995) 'Experimental models of inflammatory bowel disease', *Gastroenterology*, 109(4), pp. 1344–1367. Available at: https://doi.org/10.1016/0016-5085(95)90599-5.

Elson, C.O. *et al.* (2007) 'Monoclonal anti-interleukin 23 reverses active colitis in a T cell-mediated model in mice', *Gastroenterology*, 132(7), pp. 2359–2370. Available at: https://doi.org/10.1053/J.GASTRO.2007.03.104.

Elson, C.O., Cong, Y. and Sundberg, J. (2000) 'The C3H/HeJBir mouse model: a high susceptibility phenotype for colitis', *International reviews of immunology*, 19(1), pp. 63–75. Available at: https://doi.org/10.3109/08830180009048390.

Enright, E.F. *et al.* (2016) 'Focus: Microbiome: The Impact of the Gut Microbiota on Drug Metabolism and Clinical Outcome', *The Yale Journal of Biology and Medicine*, 89(3), p. 375.

Van Es, J.H. *et al.* (2005) 'Notch/γ-secretase inhibition turns proliferative cells in intestinal crypts and adenomas into goblet cells', *Nature*, 435(7044), pp. 959–963. Available at: https://doi.org/10.1038/nature03659.

van Es, J.H. *et al.* (2012) 'A Critical Role for the Wnt Effector Tcf4 in Adult Intestinal Homeostatic Self-Renewal', *Molecular and Cellular Biology*, 32(10), pp. 1918–1927. Available at: https://doi.org/10.1128/mcb.06288-11.

Van Es, J.H. *et al.* (2019) 'Enteroendocrine and tuft cells support Lgr5 stem cells on Paneth cell depletion', *Proceedings of the National Academy of Sciences of the United States of America*, 116(52), pp. 26599–26605. Available at: https://doi.org/10.1073/PNAS.1801888117.

Eun, C.S. *et al.* (2016) 'Does the intestinal microbial community of Korean Crohn's disease patients differ from that of western patients?', *BMC Gastroenterology*, 16(1), pp. 1–11. Available at: https://doi.org/10.1186/S12876-016-0437-0/FIGURES/7.

Faith, J.J. *et al.* (2013) 'The long-term stability of the human gut microbiota', *Science (New York, N.Y.)*, 341(6141). Available at: https://doi.org/10.1126/SCIENCE.1237439.

Fanning, S. *et al.* (2017) 'A review on the applications of next generation sequencing technologies as applied to food-related microbiome studies', *Frontiers in Microbiology*, 8(SEP), p. 1829. Available at: https://doi.org/10.3389/FMICB.2017.01829/BIBTEX.

Fantini, M.C. *et al.* (2009) 'Smad7 controls resistance of colitogenic T cells to regulatory T cell-mediated suppression', *Gastroenterology*, 136(4). Available at: https://doi.org/10.1053/J.GASTRO.2008.12.053.

Faubion, W.A. *et al.* (2001) 'The natural history of corticosteroid therapy for inflammatory bowel disease: A population-based study', *Gastroenterology*, 121(2), pp. 255–260. Available at: https://doi.org/10.1053/gast.2001.26279.

Feagan, B.G. *et al.* (2016) 'Ustekinumab as Induction and Maintenance Therapy for Crohn's Disease', *The New England journal of medicine*, 375(20), pp. 1946–1960. Available at: https://doi.org/10.1056/NEJMOA1602773.

Fickert, P. *et al.* (2006) '24-norUrsodeoxycholic acid is superior to ursodeoxycholic acid in the treatment of sclerosing cholangitis in Mdr2 (Abcb4) knockout mice', *Gastroenterology*, 130(2), pp. 465–481. Available at: https://doi.org/10.1053/J.GASTRO.2005.10.018.

De Filippis, F. *et al.* (2016) 'High-level adherence to a Mediterranean diet beneficially impacts the gut microbiota and associated metabolome', *Gut*, 65(11). Available at: https://doi.org/10.1136/GUTJNL-2015-309957.

Fiorucci, S. *et al.* (2018) 'Bile Acids Activated Receptors Regulate Innate Immunity', *Frontiers in immunology*, 9(AUG). Available at: https://doi.org/10.3389/FIMMU.2018.01853.

Fowler, E. V. *et al.* (2008) 'ATG16L1 T300A shows strong associations with disease subgroups in a large Australian IBD population: Further support for significant disease heterogeneity', *American Journal of Gastroenterology*,

103(10), pp. 2519–2526. Available at: https://doi.org/10.1111/j.1572-0241.2008.02023.x.

Frank, D.N. *et al.* (2007) 'Molecular-phylogenetic characterization of microbial community imbalances in human inflammatory bowel diseases', *Proceedings of the National Academy of Sciences of the United States of America*, 104(34), p. 13780. Available at: https://doi.org/10.1073/PNAS.0706625104.

Franke, A. *et al.* (2008) 'Sequence variants in IL10, ARPC2 and multiple other loci contribute to ulcerative colitis susceptibility', *Nature Genetics 2008 40:11*, 40(11), pp. 1319–1323. Available at: https://doi.org/10.1038/ng.221.

Franzosa, E.A. *et al.* (2019) 'Gut microbiome structure and metabolic activity in inflammatory bowel disease', *Nature microbiology*, 4(2), pp. 293–305. Available at: https://doi.org/10.1038/S41564-018-0306-4.

Fu, L. *et al.* (2016) 'Investigation of JAKs/STAT-3 in lipopolysaccharide-induced intestinal epithelial cells', *Clinical and Experimental Immunology*, 186(1), p. 75. Available at: https://doi.org/10.1111/CEI.12835.

Fu, T. *et al.* (2016) 'FXR Primes the Liver for Intestinal FGF15 Signaling by Transient Induction of β-Klotho', *Molecular endocrinology (Baltimore, Md.)*, 30(1), pp. 92–103. Available at: https://doi.org/10.1210/ME.2015-1226.

Fujiie, S. *et al.* (2001) 'Proinflammatory cytokines induce liver and activation-regulated chemokine/macrophage inflammatory protein-3α/CCL20 in mucosal epithelial cells through NF-κB', *International Immunology*, 13(10), pp. 1255–1263. Available at: https://doi.org/10.1093/INTIMM/13.10.1255.

Fujino, S. *et al.* (2003) 'Increased expression of interleukin 17 in inflammatory bowel disease', *Gut*, 52(1), pp. 65–70. Available at: https://doi.org/10.1136/GUT.52.1.65.

Fukiya, S. *et al.* (2009) 'Conversion of cholic acid and chenodeoxycholic acid into their 7-oxo derivatives by Bacteroides intestinalis AM-1 isolated from human feces', *FEMS microbiology letters*, 293(2), pp. 263–270. Available at: https://doi.org/10.1111/J.1574-6968.2009.01531.X.

Furrie, E. *et al.* (2005) 'Toll-like receptors-2, -3 and -4 expression patterns on human colon and their regulation by mucosal-associated bacteria', *Immunology*, 115(4), pp. 565–574. Available at: https://doi.org/10.1111/J.1365-2567.2005.02200.X.

Furuse, M. *et al.* (1993) 'Occludin: a novel integral membrane protein localizing at tight junctions', *The Journal of cell biology*, 123(6 Pt 2), pp. 1777–1788. Available at: https://doi.org/10.1083/JCB.123.6.1777.

Furuse, M. *et al.* (1998) 'Claudin-1 and -2: novel integral membrane proteins localizing at tight junctions with no sequence similarity to occludin', *The*

Journal of cell biology, 141(7), pp. 1539–1550. Available at: https://doi.org/10.1083/JCB.141.7.1539.

Gadaleta, R.M. *et al.* (2020) 'Fibroblast Growth Factor 19 modulates intestinal microbiota and inflammation in presence of Farnesoid X Receptor', *EBioMedicine*, 54. Available at: https://doi.org/10.1016/J.EBIOM.2020.102719.

Gaffen, S. (2015) 'IL-17 receptor composition', *Nature Reviews Immunology 2015 16:1*, 16(1), pp. 4–4. Available at: https://doi.org/10.1038/nri.2015.2.

Garcia-Mantrana, I. *et al.* (2018) 'Shifts on Gut Microbiota Associated to Mediterranean Diet Adherence and Specific Dietary Intakes on General Adult Population', *Frontiers in microbiology*, 9(MAY). Available at: https://doi.org/10.3389/FMICB.2018.00890.

Gareau, M.G. *et al.* (2011) 'Bacterial infection causes stress-induced memory dysfunction in mice', *Gut*, 60(3), pp. 307–317. Available at: https://doi.org/10.1136/GUT.2009.202515.

Garrido, D. *et al.* (2015) 'Comparative transcriptomics reveals key differences in the response to milk oligosaccharides of infant gut-associated bifidobacteria', *Scientific Reports 2015 5:1*, 5(1), pp. 1–18. Available at: https://doi.org/10.1038/srep13517.

Gasche, C. *et al.* (2000) 'A simple classification of Crohn's disease: Report of the working party for the world congresses of gastroenterology, Vienna 1998', *Inflammatory Bowel Diseases*, 6(1), pp. 8–15. Available at: https://doi.org/10.1097/00054725-200002000-00002.

Gaudier, E. *et al.* (2004) 'Butyrate specifically modulates MUC gene expression in intestinal epithelial goblet cells deprived of glucose', *American journal of physiology. Gastrointestinal and liver physiology*, 287(6). Available at: https://doi.org/10.1152/AJPGI.00219.2004.

Gay, N.J. *et al.* (2014) 'Assembly and localization of Toll-like receptor signalling complexes', *Nature reviews. Immunology*, 14(8), pp. 546–558. Available at: https://doi.org/10.1038/NRI3713.

Gensollen, T. *et al.* (2016a) 'How colonization by microbiota in early life shapes the immune system', *Science*, 352(6285), pp. 539–544. Available at: https://doi.org/10.1126/SCIENCE.AAD9378/ASSET/2F91909F-0DF5-4161-88BB-078F2A92D227/ASSETS/GRAPHIC/352_539_F3.JPEG.

Gensollen, T. *et al.* (2016b) 'How colonization by microbiota in early life shapes the immune system', *Science (New York, N.Y.)*, 352(6285), pp. 539–544. Available at: https://doi.org/10.1126/SCIENCE.AAD9378.

Geremia, A. and Arancibia-Cárcamo, C. V. (2017) 'Innate Lymphoid Cells in Intestinal Inflammation', *Frontiers in immunology*, 8(OCT). Available at: https://doi.org/10.3389/FIMMU.2017.01296.

Gevers, D. *et al.* (2014) 'The treatment-naive microbiome in new-onset Crohn's disease', *Cell host & microbe*, 15(3), pp. 382–392. Available at: https://doi.org/10.1016/J.CHOM.2014.02.005.

Gewirtz, A.T. *et al.* (2001) 'Cutting edge: bacterial flagellin activates basolaterally expressed TLR5 to induce epithelial proinflammatory gene expression', *Journal of immunology (Baltimore, Md. : 1950)*, 167(4), pp. 1882–1885. Available at: https://doi.org/10.4049/JIMMUNOL.167.4.1882.

Ghaleb, A.M. *et al.* (2008) 'Notch inhibits expression of the Krüppel-like factor 4 tumor suppressor in the intestinal epithelium', *Molecular Cancer Research*, 6(12), pp. 1920–1927. Available at: https://doi.org/10.1158/1541-7786.MCR-08-0224.

Ghaleb, A.M. *et al.* (2011) 'Altered intestinal epithelial homeostasis in mice with intestine-specific deletion of the Krüppel-like factor 4 gene', *Developmental Biology*, 349(2), pp. 310–320. Available at: https://doi.org/10.1016/j.ydbio.2010.11.001.

Gill, S.R. *et al.* (2006) 'Metagenomic Analysis of the Human Distal Gut Microbiome', *Science (New York, N.Y.)*, 312(5778), p. 1355. Available at: https://doi.org/10.1126/SCIENCE.1124234.

Girardin, S.E. *et al.* (2003) 'Nod1 detects a unique muropeptide from gram-negative bacterial peptidoglycan', *Science (New York, N.Y.)*, 300(5625), pp. 1584–1587. Available at: https://doi.org/10.1126/SCIENCE.1084677.

Glocker, E.-O. *et al.* (2009a) 'Inflammatory Bowel Disease and Mutations Affecting the Interleukin-10 Receptor', *New England Journal of Medicine*, 361(21), pp. 2033–2045. Available at: https://doi.org/10.1056/nejmoa0907206.

Glocker, E.-O. *et al.* (2009b) 'Inflammatory Bowel Disease and Mutations Affecting the Interleukin-10 Receptor', *New England Journal of Medicine*, 361(21), pp. 2033–2045. Available at: https://doi.org/10.1056/NEJMOA0907206/SUPPL_FILE/NEJM_GLOCKER _2033SA1.PDF.

Gonçalves, P., Araújo, J.R. and Di Santo, J.P. (2018) 'A Cross-Talk Between Microbiota-Derived Short-Chain Fatty Acids and the Host Mucosal Immune System Regulates Intestinal Homeostasis and Inflammatory Bowel Disease', *Inflammatory bowel diseases*, 24(3), pp. 558–572. Available at: https://doi.org/10.1093/IBD/IZX029.

Gonsky, R. *et al.* (2014) 'IFNG rs1861494 polymorphism is associated with IBD disease severity and functional changes in both IFNG methylation and protein secretion', *Inflammatory Bowel Diseases*, 20(10), pp. 1794–1801. Available at: https://doi.org/10.1097/MIB.0000000000000172.

Goodwin, B. *et al.* (2000) 'A Regulatory Cascade of the Nuclear Receptors FXR, SHP-1, and LRH-1 Represses Bile Acid Biosynthesis', *Molecular Cell*,

6(3), pp. 517–526. Available at: https://doi.org/10.1016/S1097-2765(00)00051-4.

Grier, A. *et al.* (2017) 'Impact of prematurity and nutrition on the developing gut microbiome and preterm infant growth', *Microbiome*, 5(1), p. 158. Available at: https://doi.org/10.1186/S40168-017-0377-0.

Groman, R.P. (2009) 'Gram-Negative Infections', *Small Animal Critical Care Medicine*, pp. 469–473. Available at: https://doi.org/10.1016/B978-1-4160-2591-7.10109-2.

Guaraldi, F. and Salvatori, G. (2012) 'Effect of Breast and Formula Feeding on Gut Microbiota Shaping in Newborns', *Frontiers in Cellular and Infection Microbiology*, 2, p. 94. Available at: https://doi.org/10.3389/FCIMB.2012.00094.

Gupta, V.K., Paul, S. and Dutta, C. (2017) 'Geography, ethnicity or subsistence-specific variations in human microbiome composition and diversity', *Frontiers in Microbiology*. Frontiers Media S.A., p. 1162. Available at: https://doi.org/10.3389/fmicb.2017.01162.

Haller, D. *et al.* (2004) 'Differential effect of immune cells on non-pathogenic Gram-negative bacteria-induced nuclear factor-kappaB activation and pro-inflammatory gene expression in intestinal epithelial cells', *Immunology*, 112(2), pp. 310–320. Available at: https://doi.org/10.1111/J.1365-2567.2004.01874.X.

Halliday, J.S. *et al.* (2012) 'A unique clinical phenotype of primary sclerosing cholangitis associated with Crohn's disease', *Journal of Crohn's and Colitis*, 6(2), pp. 174–181. Available at: https://doi.org/10.1016/j.crohns.2011.07.015.

Hamilton, J.P. *et al.* (2007) 'Human cecal bile acids: concentration and spectrum', *American journal of physiology. Gastrointestinal and liver physiology*, 293(1). Available at: https://doi.org/10.1152/AJPGI.00027.2007.

Han, Y.M. *et al.* (2017) 'NF-kappa B activation correlates with disease phenotype in Crohn's disease', *PLoS ONE*, 12(7). Available at: https://doi.org/10.1371/JOURNAL.PONE.0182071.

Hanauer, S.B. *et al.* (2002) 'Maintenance infliximab for Crohn's disease: The ACCENT I randomised trial', *Lancet*, 359(9317), pp. 1541–1549. Available at: https://doi.org/10.1016/S0140-6736(02)08512-4.

Hang, S. *et al.* (2019) 'Bile acid metabolites control T H 17 and T reg cell differentiation', *Nature*, 576(7785), pp. 143–148. Available at: https://doi.org/10.1038/S41586-019-1785-Z.

Hansson, G.C. and Johansson, M.E.V. (2010) 'The inner of the two Muc2 mucin-dependent mucus layers in colon is devoid of bacteria',

https://doi.org/10.4161/gmic.1.1.10470, 1(1), pp. 51–54. Available at: https://doi.org/10.4161/GMIC.1.1.10470.

Hapfelmeier, S. *et al.* (2010) 'Reversible microbial colonization of germ-free mice reveals the dynamics of IgA immune responses', *Science (New York, N.Y.)*, 328(5986), pp. 1705–1709. Available at: https://doi.org/10.1126/SCIENCE.1188454.

Harbord, M. *et al.* (2016) 'The first european evidence-based consensus on extra-intestinal manifestations in inflammatory bowel disease', *Journal of Crohn's and Colitis*, 10(3), pp. 239–254. Available at: https://doi.org/10.1093/ecco-jcc/jjv213.

Hardenberg, G., Steiner, T.S. and Levings, M.K. (2011) 'Environmental influences on T regulatory cells in inflammatory bowel disease', *Seminars in immunology*, 23(2), pp. 130–138. Available at: https://doi.org/10.1016/J.SMIM.2011.01.012.

Harris, V.C. *et al.* (2018) 'Effect of Antibiotic-Mediated Microbiome Modulation on Rotavirus Vaccine Immunogenicity: A Human, Randomized-Control Proof-of-Concept Trial.', *Cell Host & Microbe*, 24(2), pp. 197-207.e4. Available at: https://doi.org/10.1016/J.CHOM.2018.07.005.

Harrison, C.A. *et al.* (2019) 'Sexual Dimorphism in the Response to Broad-spectrum Antibiotics During T Cell-mediated Colitis', *Journal of Crohn's and Colitis*, 13(1), pp. 115–126. Available at: https://doi.org/10.1093/ECCO-JCC/JJY144.

Hausmann, M. *et al.* (2002) 'Toll-like receptors 2 and 4 are up-regulated during intestinal inflammation', *Gastroenterology*, 122(7), pp. 1987–2000. Available at: https://doi.org/10.1053/GAST.2002.33662.

He, X.C. *et al.* (2004) 'BMP signaling inhibits intestinal stem cell self-renewal through suppression of Wnt-β-catenin signaling', *Nature Genetics*, 36(10), pp. 1117–1121. Available at: https://doi.org/10.1038/ng1430.

Heel, K.A. *et al.* (1997) 'Review: Peyer's patches', *Journal of gastroenterology and hepatology*, 12(2), pp. 122–136. Available at: https://doi.org/10.1111/J.1440-1746.1997.TB00395.X.

Heinken, A. *et al.* (2019) 'Systematic assessment of secondary bile acid metabolism in gut microbes reveals distinct metabolic capabilities in inflammatory bowel disease', *Microbiome*, 7(1), pp. 1–18. Available at: https://doi.org/10.1186/S40168-019-0689-3/FIGURES/4.

Helander, H.F. and Fändriks, L. (2014) 'Surface area of the digestive tract - revisited', *Scandinavian journal of gastroenterology*, 49(6), pp. 681–689. Available at: https://doi.org/10.3109/00365521.2014.898326.

Hernández-Gómez, J.G. *et al.* (2021) 'In Vitro Bile Salt Hydrolase (BSH) Activity Screening of Different Probiotic Microorganisms', *Foods 2021, Vol.*

10, Page 674, 10(3), p. 674. Available at: https://doi.org/10.3390/FOODS10030674.

Higuchi, L.M. *et al.* (2012) 'A prospective study of cigarette smoking and the risk of inflammatory bowel disease in women', *American Journal of Gastroenterology*, 107(9), pp. 1399–1406. Available at: https://doi.org/10.1038/ajg.2012.196.

Ho, N.T. *et al.* (2018) 'Meta-analysis of effects of exclusive breastfeeding on infant gut microbiota across populations', *Nature communications*, 9(1). Available at: https://doi.org/10.1038/S41467-018-06473-X.

Hodkinson, B.P. and Grice, E.A. (2015) 'Next-Generation Sequencing: A Review of Technologies and Tools for Wound Microbiome Research', *https://home.liebertpub.com/wound*, 4(1), pp. 50–58. Available at: https://doi.org/10.1089/WOUND.2014.0542.

Hoentjen, F. *et al.* (2003) 'Antibiotics with a selective aerobic or anaerobic spectrum have different therapeutic activities in various regions of the colon in interleukin 10 gene deficient mice', *Gut*, 52(12), pp. 1721–1727. Available at: https://doi.org/10.1136/GUT.52.12.1721.

Hornung, V. *et al.* (2002) 'Quantitative Expression of Toll-Like Receptor 1–10 mRNA in Cellular Subsets of Human Peripheral Blood Mononuclear Cells and Sensitivity to CpG Oligodeoxynucleotides', *The Journal of Immunology*, 168(9), pp. 4531–4537. Available at: https://doi.org/10.4049/JIMMUNOL.168.9.4531.

Horta, B.L., Loret De Mola, C. and Victora, C.G. (2015) 'Long-term consequences of breastfeeding on cholesterol, obesity, systolic blood pressure and type 2 diabetes: a systematic review and meta-analysis', *Acta paediatrica (Oslo, Norway : 1992)*, 104(467), pp. 30–37. Available at: https://doi.org/10.1111/APA.13133.

Hugon, P. *et al.* (2015) 'A comprehensive repertoire of prokaryotic species identified in human beings', *The Lancet. Infectious diseases*, 15(10), pp. 1211–1219. Available at: https://doi.org/10.1016/S1473-3099(15)00293-5.

Hugot, J.P. *et al.* (2001) 'Association of NOD2 leucine-rich repeat variants with susceptibility to Crohn's disease', *Nature*, 411(6837), pp. 599–603. Available at: https://doi.org/10.1038/35079107.

Huttenhower, C. *et al.* (2012) 'Structure, function and diversity of the healthy human microbiome', *Nature 2012 486:7402*, 486(7402), pp. 207–214. Available at: https://doi.org/10.1038/nature11234.

Iimura, M. *et al.* (2005) 'Cathelicidin Mediates Innate Intestinal Defense against Colonization with Epithelial Adherent Bacterial Pathogens', *The Journal of Immunology*, 174(8), pp. 4901–4907. Available at: https://doi.org/10.4049/JIMMUNOL.174.8.4901.

Ikenouchi, J. *et al.* (2007) 'Requirement of ZO-1 for the formation of belt-like adherens junctions during epithelial cell polarization', *The Journal of Cell Biology*, 176(6), p. 779. Available at: https://doi.org/10.1083/JCB.200612080.

Imbeaud, S. *et al.* (2005) 'Towards standardization of RNA quality assessment using user-independent classifiers of microcapillary electrophoresis traces', *Nucleic Acids Research*, 33(6), p. e56. Available at: https://doi.org/10.1093/NAR/GNI054.

Inohara, N. *et al.* (2003) 'Host recognition of bacterial muramyl dipeptide mediated through NOD2. Implications for Crohn's disease', *The Journal of biological chemistry*, 278(8), pp. 5509–5512. Available at: https://doi.org/10.1074/JBC.C200673200.

Irwin, R. *et al.* (2013) 'Colitis induced bone loss is gender dependent and associated with increased inflammation', *Inflammatory bowel diseases*, 19(8), p. 1586. Available at: https://doi.org/10.1097/MIB.0B013E318289E17B.

Islam, K.B.M.S. *et al.* (2011) 'Bile acid is a host factor that regulates the composition of the cecal microbiota in rats', *Gastroenterology*, 141(5), pp. 1773–1781. Available at: https://doi.org/10.1053/J.GASTRO.2011.07.046.

Ivanov, A.I. (2012) 'Structure and regulation of intestinal epithelial tight junctions: current concepts and unanswered questions', *Advances in experimental medicine and biology*, 763, pp. 132–148. Available at: https://doi.org/10.1007/978-1-4614-4711-5_6.

Ivanov, I.I. *et al.* (2006) 'The orphan nuclear receptor RORgammat directs the differentiation program of proinflammatory IL-17+ T helper cells', *Cell*, 126(6), pp. 1121–1133. Available at: https://doi.org/10.1016/J.CELL.2006.07.035.

Ivanov, I.I. *et al.* (2009) 'Induction of intestinal Th17 cells by segmented filamentous bacteria', *Cell*, 139(3), p. 485. Available at: https://doi.org/10.1016/J.CELL.2009.09.033.

Iwasaki, A. and Medzhitov, R. (2004) 'Toll-like receptor control of the adaptive immune responses', *Nature Immunology 2004 5:10*, 5(10), pp. 987–995. Available at: https://doi.org/10.1038/ni1112.

Jakobsson, H.E. *et al.* (2014) 'Decreased gut microbiota diversity, delayed Bacteroidetes colonisation and reduced Th1 responses in infants delivered by caesarean section', *Gut*, 63(4), pp. 559–566. Available at: https://doi.org/10.1136/GUTJNL-2012-303249.

Jeffery, I.B. *et al.* (2012) 'Categorization of the gut microbiota: enterotypes or gradients?', *Nature Reviews Microbiology 2012 10:9*, 10(9), pp. 591–592. Available at: https://doi.org/10.1038/nrmicro2859.

Jenny, M. *et al.* (2002) 'Neurogenin3 is differentially required for endocrine cell fate specification in the intestinal and gastric epithelium', *EMBO Journal*, 21(23), pp. 6338–6347. Available at: https://doi.org/10.1093/emboj/cdf649.

Jho, E. *et al.* (2002) 'Wnt/β-Catenin/Tcf Signaling Induces the Transcription of Axin2, a Negative Regulator of the Signaling Pathway', *Molecular and Cellular Biology*, 22(4), pp. 1172–1183. Available at: https://doi.org/10.1128/mcb.22.4.1172-1183.2002.

Jiménez, E. *et al.* (2005) 'Isolation of commensal bacteria from umbilical cord blood of healthy neonates born by cesarean section', *Current microbiology*, 51(4), pp. 270–274. Available at: https://doi.org/10.1007/S00284-005-0020-3.

Jiménez, E. *et al.* (2008) 'Is meconium from healthy newborns actually sterile?', *Research in microbiology*, 159(3), pp. 187–193. Available at: https://doi.org/10.1016/J.RESMIC.2007.12.007.

Johansson, M.E.V. and Hansson, G.C. (2016a) 'Immunological aspects of intestinal mucus and mucins', *Nature reviews. Immunology*, 16(10), pp. 639–649. Available at: https://doi.org/10.1038/NRI.2016.88.

Johansson, M.E.V. and Hansson, G.C. (2016b) 'Immunological aspects of intestinal mucus and mucins', *Nature Reviews Immunology 2016 16:10*, 16(10), pp. 639–649. Available at: https://doi.org/10.1038/nri.2016.88.

Johnston, R.D. and Logan, R.F.A. (2008) 'What is the peak age for onset of IBD?', *Inflammatory Bowel Diseases*, 14(suppl_2), pp. S4–S5. Available at: https://doi.org/10.1002/ibd.20545.

Jones, B. V. *et al.* (2008a) 'Functional and comparative metagenomic analysis of bile salt hydrolase activity in the human gut microbiome', *Proceedings of the National Academy of Sciences of the United States of America*, 105(36), pp. 13580–13585. Available at: https://doi.org/10.1073/PNAS.0804437105.

Jones, B. V. *et al.* (2008b) 'Functional and comparative metagenomic analysis of bile salt hydrolase activity in the human gut microbiome', *Proceedings of the National Academy of Sciences of the United States of America*, 105(36), pp. 13580–13585. Available at: https://doi.org/10.1073/PNAS.0804437105/SUPPL_FILE/0804437105SI.PDF.

Jones, E.J. *et al.* (2020) 'The Uptake, Trafficking, and Biodistribution of Bacteroides thetaiotaomicron Generated Outer Membrane Vesicles', *Frontiers in Microbiology*, 11, p. 57. Available at: https://doi.org/10.3389/FMICB.2020.00057/BIBTEX.

Jones, M.L., Martoni, C.J. and Prakash, S. (2012) 'Cholesterol lowering and inhibition of sterol absorption by Lactobacillus reuteri NCIMB 30242: a

randomized controlled trial', *European journal of clinical nutrition*, 66(11), pp. 1234–1241. Available at: https://doi.org/10.1038/EJCN.2012.126.

Jostins, L. *et al.* (2012a) 'Host-microbe interactions have shaped the genetic architecture of inflammatory bowel disease', *Nature*, 491(7422), pp. 119–124. Available at: https://doi.org/10.1038/nature11582.

Jostins, L. *et al.* (2012b) 'Host-microbe interactions have shaped the genetic architecture of inflammatory bowel disease', *Nature*, 491(7422), pp. 119–124. Available at: https://doi.org/10.1038/nature11582.

Joyce, S.A., Shanahan, F., *et al.* (2014) 'Bacterial bile salt hydrolase in host metabolism: Potential for influencing gastrointestinal microbe-host crosstalk', *Gut microbes*, 5(5), pp. 669–674. Available at: https://doi.org/10.4161/19490976.2014.969986.

Joyce, S.A., MacSharry, J., *et al.* (2014a) 'Regulation of host weight gain and lipid metabolism by bacterial bile acid modification in the gut', *Proceedings of the National Academy of Sciences of the United States of America*, 111(20), pp. 7421–7426. Available at: https://doi.org/10.1073/PNAS.1323599111/-/DCSUPPLEMENTAL.

Joyce, S.A., MacSharry, J., *et al.* (2014b) 'Regulation of host weight gain and lipid metabolism by bacterial bile acid modification in the gut', *Proceedings of the National Academy of Sciences of the United States of America*, 111(20), pp. 7421–7426. Available at: https://doi.org/10.1073/PNAS.1323599111.

Joyce, S.A., MacSharry, J., *et al.* (2014c) 'Regulation of host weight gain and lipid metabolism by bacterial bile acid modification in the gut', *Proceedings of the National Academy of Sciences of the United States of America*, 111(20), pp. 7421–7426. Available at: https://doi.org/10.1073/PNAS.1323599111/SUPPL_FILE/PNAS.201323599SI.PDF.

Joyce, S.A. and Gahan, C.G.M. (2014) 'The gut microbiota and the metabolic health of the host', *Current opinion in gastroenterology*, 30(2), pp. 120–127. Available at: https://doi.org/10.1097/MOG.0000000000000039.

Joyce, S.A. and Gahan, C.G.M. (2016) 'Bile Acid Modifications at the Microbe-Host Interface: Potential for Nutraceutical and Pharmaceutical Interventions in Host Health', *Annual review of food science and technology*, 7, pp. 313–333. Available at: https://doi.org/10.1146/ANNUREV-FOOD-041715-033159.

Jurjus, A.R., Khoury, N.N. and Reimund, J.M. (2004) 'Animal models of inflammatory bowel disease', *Journal of pharmacological and toxicological methods*, 50(2), pp. 81–92. Available at: https://doi.org/10.1016/J.VASCN.2003.12.002.

Kabiri, Z. *et al.* (2014) 'Stroma provides an intestinal stem cell niche in the absence of epithelial Wnts', *Development*, 141(11), pp. 2206–2215. Available at: https://doi.org/10.1242/DEV.104976.

Kaetzel, C.S. (2005) 'The polymeric immunoglobulin receptor: bridging innate and adaptive immune responses at mucosal surfaces', *Immunological reviews*, 206, pp. 83–99. Available at: https://doi.org/10.1111/J.0105-2896.2005.00278.X.

Kamada, N. *et al.* (2008) 'Unique CD14 intestinal macrophages contribute to the pathogenesis of Crohn disease via IL-23/IFN-gamma axis', *The Journal of clinical investigation*, 118(6), pp. 2269–2280. Available at: https://doi.org/10.1172/JCI34610.

Kang, D.J. *et al.* (2008) 'Clostridium scindens baiCD and baiH genes encode stereo-specific 7alpha/7beta-hydroxy-3-oxo-delta4-cholenoic acid oxidoreductases', *Biochimica et biophysica acta*, 1781(1–2), pp. 16–25. Available at: https://doi.org/10.1016/J.BBALIP.2007.10.008.

Kang, D.W. *et al.* (2013) 'Reduced Incidence of Prevotella and Other Fermenters in Intestinal Microflora of Autistic Children', *PLOS ONE*, 8(7), p. e68322. Available at: https://doi.org/10.1371/JOURNAL.PONE.0068322.

Kang, J.Y. *et al.* (2009) 'Recognition of lipopeptide patterns by Toll-like receptor 2-Toll-like receptor 6 heterodimer', *Immunity*, 31(6), pp. 873–884. Available at: https://doi.org/10.1016/J.IMMUNI.2009.09.018.

Kaplan, G.G. (2015) 'The global burden of IBD: From 2015 to 2025', *Nature Reviews Gastroenterology and Hepatology*. Nature Publishing Group, pp. 720–727. Available at: https://doi.org/10.1038/nrgastro.2015.150.

Kaplan, G.G. and Ng, S.C. (2017) 'Understanding and Preventing the Global Increase of Inflammatory Bowel Disease', *Gastroenterology*, 152(2), pp. 313-321.e2. Available at: https://doi.org/10.1053/j.gastro.2016.10.020.

Kaser, A. *et al.* (2004) 'Increased expression of CCL20 in human inflammatory bowel disease', *Journal of Clinical Immunology*, 24(1), pp. 74–85. Available at: https://doi.org/10.1023/B:JOCI.0000018066.46279.6b.

Kathania, M. *et al.* (2020) 'Gut Microbiota Contributes to Spontaneous Colitis in E3 Ligase Itch-Deficient Mice', *Journal of immunology (Baltimore, Md. : 1950)*, 204(8), pp. 2277–2284. Available at: https://doi.org/10.4049/JIMMUNOL.1701478.

Katz, J.P. *et al.* (2002) 'The zinc-finger transcription factor Klf4 is required for terminal differentiation of goblet cells in the colon', *Development (Cambridge, England)*, 129(11), p. 2619. Available at: https://doi.org/10.1242/dev.129.11.2619.

Kawada, M., Arihiro, A. and Mizoguchi, E. (2007) 'Insights from advances in research of chemically induced experimental models of human

inflammatory bowel disease', *World Journal of Gastroenterology : WJG*, 13(42), p. 5581. Available at: https://doi.org/10.3748/WJG.V13.I42.5581.

Kawai, T. and Akira, S. (2011) 'Toll-like receptors and their crosstalk with other innate receptors in infection and immunity', *Immunity*, 34(5), pp. 637–650. Available at: https://doi.org/10.1016/J.IMMUNI.2011.05.006.

Kawamoto, K., Horibe, I. and Uchida, K. (1989) 'Purification and characterization of a new hydrolase for conjugated bile acids, chenodeoxycholyltaurine hydrolase, from Bacteroides vulgatus', *Journal of biochemistry*, 106(6), pp. 1049–1053. Available at: https://doi.org/10.1093/OXFORDJOURNALS.JBCHEM.A122962.

Keubler, L.M. *et al.* (2015) 'A Multihit Model: Colitis Lessons from the Interleukin-10–deficient Mouse', *Inflammatory Bowel Diseases*, 21(8), p. 1967. Available at: https://doi.org/10.1097/MIB.0000000000000468.

Kim, Y.G. *et al.* (2017) 'Neonatal acquisition of Clostridia species protects against colonization by bacterial pathogens', *Science (New York, N.Y.)*, 356(6335), pp. 315–319. Available at: https://doi.org/10.1126/SCIENCE.AAG2029.

Kirsner, J.B. (1958) 'Ulcerative Colitis—A Challenge', *A.M.A. Archives of Internal Medicine*, 101(1), pp. 3–8. Available at: https://doi.org/10.1001/ARCHINTE.1958.00260130017002.

Kishi, D. *et al.* (2000) 'Alteration of V beta usage and cytokine production of CD4+ TCR beta beta homodimer T cells by elimination of Bacteroides vulgatus prevents colitis in TCR alpha-chain-deficient mice', *Journal of immunology (Baltimore, Md. : 1950)*, 165(10), pp. 5891–5899. Available at: https://doi.org/10.4049/JIMMUNOL.165.10.5891.

Knights, D. *et al.* (2014) 'Rethinking "enterotypes"', *Cell host & microbe*, 16(4), pp. 433–437. Available at: https://doi.org/10.1016/J.CHOM.2014.09.013.

Knoop, K.A. *et al.* (2016) 'Antibiotics promote inflammation through the translocation of native commensal colonic bacteria', *Gut*, 65(7), pp. 1100–1109. Available at: https://doi.org/10.1136/GUTJNL-2014-309059.

Kobayashi, K.S. *et al.* (2005) 'Nod2-dependent regulation of innate and adaptive immunity in the intestinal tract', *Science*, 307(5710), pp. 731–734. Available at: https://doi.org/10.1126/SCIENCE.1104911/SUPPL_FILE/KOBAYASHI.SOM.PDF.

Kobayashi, T. *et al.* (2008) 'IL23 differentially regulates the Th1/Th17 balance in ulcerative colitis and Crohn's disease', *Gut*, 57(12), pp. 1682–1689. Available at: https://doi.org/10.1136/GUT.2007.135053.

Koblansky, A.A. *et al.* (2013) 'Recognition of profilin by Toll-like receptor 12 is critical for host resistance to Toxoplasma gondii', *Immunity*, 38(1), pp. 119–130. Available at: https://doi.org/10.1016/J.IMMUNI.2012.09.016.

Koenig, J.E. *et al.* (2011) 'Succession of microbial consortia in the developing infant gut microbiome', *Proceedings of the National Academy of Sciences of the United States of America*, 108(SUPPL. 1), pp. 4578–4585. Available at: https://doi.org/10.1073/PNAS.1000081107/-/DCSUPPLEMENTAL.

Koh, A. *et al.* (2016) 'From Dietary Fiber to Host Physiology: Short-Chain Fatty Acids as Key Bacterial Metabolites', *Cell*, 165(6), pp. 1332–1345. Available at: https://doi.org/10.1016/J.CELL.2016.05.041.

Kosinski, C. *et al.* (2007) 'Gene expression patterns of human colon tops and basal crypts and BMP antagonists as intestinal stem cell niche factors', *Proceedings of the National Academy of Sciences*, 104(39), pp. 15418–15423. Available at: https://doi.org/10.1073/PNAS.0707210104.

Kotb, M.A. (2012) 'Molecular mechanisms of ursodeoxycholic acid toxicity & side effects: ursodeoxycholic acid freezes regeneration & induces hibernation mode', *International journal of molecular sciences*, 13(7), pp. 8882–8914. Available at: https://doi.org/10.3390/IJMS13078882.

Kotlarz, D. *et al.* (2012) 'Loss of interleukin-10 signaling and infantile inflammatory bowel disease: Implications for diagnosis and therapy', *Gastroenterology*, 143(2), pp. 347–355. Available at: https://doi.org/10.1053/j.gastro.2012.04.045.

Krajina, T. *et al.* (2003) 'Colonic lamina propria dendritic cells in mice with CD4+ T cell-induced colitis', *European journal of immunology*, 33(4), pp. 1073–1083. Available at: https://doi.org/10.1002/EJI.200323518.

Kronman, M.P. *et al.* (2012) 'Antibiotic exposure and IBD development among children: A population-based cohort study', *Pediatrics*, 130(4). Available at: https://doi.org/10.1542/peds.2011-3886.

Kugathasan, S. *et al.* (2007) 'Mucosal T-cell immunoregulation varies in early and late inflammatory bowel disease', *Gut*, 56(12), p. 1696. Available at: https://doi.org/10.1136/GUT.2006.116467.

Kühn, R. *et al.* (1993a) 'Interleukin-10-deficient mice develop chronic enterocolitis', *Cell*, 75(2), pp. 263–274. Available at: https://doi.org/10.1016/0092-8674(93)80068-P.

Kühn, R. *et al.* (1993b) 'Interleukin-10-deficient mice develop chronic enterocolitis', *Cell*, 75(2), pp. 263–274. Available at: https://doi.org/10.1016/0092-8674(93)80068-P.

Kuiper, G.G.J.M., Klootwijk, W. and Visser, T.J. (2002) 'Substitution of cysteine for a conserved alanine residue in the catalytic center of type II

iodothyronine deiodinase alters interaction with reducing cofactor', *Endocrinology*, 143(4), pp. 1190–1198. Available at: https://doi.org/10.1210/ENDO.143.4.8738.

Kullberg, M.C. *et al.* (1998) 'Helicobacter hepaticus triggers colitis in specific-pathogen-free interleukin-10 (IL-10)-deficient mice through an IL-12- and gamma interferon-dependent mechanism', *Infection and immunity*, 66(11), pp. 5157–5166. Available at: https://doi.org/10.1128/IAI.66.11.5157-5166.1998.

Kulp, A. and Kuehn, M.J. (2010) 'Biological functions and biogenesis of secreted bacterial outer membrane vesicles', *Annual review of microbiology*, 64, pp. 163–184. Available at: https://doi.org/10.1146/ANNUREV.MICRO.091208.073413.

Kumar, R.S. *et al.* (2006) 'Structural and functional analysis of a conjugated bile salt hydrolase from Bifidobacterium longum reveals an evolutionary relationship with penicillin V acylase', *The Journal of biological chemistry*, 281(43), pp. 32516–32525. Available at: https://doi.org/10.1074/JBC.M604172200.

Labbé, A. *et al.* (2014) 'Bacterial Bile Metabolising Gene Abundance in Crohn's, Ulcerative Colitis and Type 2 Diabetes Metagenomes', *PLOS ONE*, 9(12), p. e115175. Available at: https://doi.org/10.1371/JOURNAL.PONE.0115175.

Lakatos, P.L., Szamosi, T. and Lakatos, L. (2007) 'Smoking in inflammatory bowel diseases: Good, bad or ugly?', *World Journal of Gastroenterology*, 13(46), p. 6134. Available at: https://doi.org/10.3748/wjg.v13.i46.6134.

Lambert, J.M. *et al.* (2008) 'Functional analysis of four bile salt hydrolase and penicillin acylase family members in Lactobacillus plantarum WCFS1', *Applied and environmental microbiology*, 74(15), pp. 4719–4726. Available at: https://doi.org/10.1128/AEM.00137-08.

Lange, K. *et al.* (2016) 'Effects of Antibiotics on Gut Microbiota', *Digestive diseases (Basel, Switzerland)*, 34(3), pp. 260–268. Available at: https://doi.org/10.1159/000443360.

Langrish, C.L. *et al.* (2005) 'IL-23 drives a pathogenic T cell population that induces autoimmune inflammation', *The Journal of experimental medicine*, 201(2), pp. 233–240. Available at: https://doi.org/10.1084/JEM.20041257.

Lapaquette, P. *et al.* (2010) 'Crohn's disease-associated adherent-invasive E. coli are selectively favoured by impaired autophagy to replicate intracellularly', *Cellular Microbiology*, 12(1), pp. 99–113. Available at: https://doi.org/10.1111/j.1462-5822.2009.01381.x.

Larabi, A., Barnich, N. and Nguyen, H.T.T. (2020) 'New insights into the interplay between autophagy, gut microbiota and inflammatory responses

in IBD', *Autophagy*, 16(1), pp. 38–51. Available at: https://doi.org/10.1080/15548627.2019.1635384.

de Lau, W. *et al.* (2014) 'The R-spondin/Lgr5/Rnf43 module: Regulator of Wnt signal strength', *Genes and Development*, 28(4), pp. 305–316. Available at: https://doi.org/10.1101/gad.235473.113.

Lavelle, A. and Sokol, H. (2020) 'Gut microbiota-derived metabolites as key actors in inflammatory bowel disease', *Nature reviews. Gastroenterology & hepatology*, 17(4), pp. 223–237. Available at: https://doi.org/10.1038/S41575-019-0258-Z.

Lee, B.C. *et al.* (2005) 'Induction of interleukin-8 production via nuclear factor-κB activation in human intestinal epithelial cells infected with Vibrio vulnificus', *Immunology*, 115(4), p. 506. Available at: https://doi.org/10.1111/J.1365-2567.2005.02185.X.

Lee, J. *et al.* (2006) 'Maintenance of colonic homeostasis by distinctive apical TLR9 signalling in intestinal epithelial cells', *Nature cell biology*, 8(12), pp. 1327–1336. Available at: https://doi.org/10.1038/NCB1500.

Lee, J.S. and Polin, R.A. (2003) 'Treatment and prevention of necrotizing enterocolitis', *Seminars in neonatology : SN*, 8(6), pp. 449–459. Available at: https://doi.org/10.1016/S1084-2756(03)00123-4.

Lee, J.W. *et al.* (2008) 'Differential Regulation of Chemokines by IL-17 in Colonic Epithelial Cells', *The Journal of Immunology*, 181(9), pp. 6536–6545. Available at: https://doi.org/10.4049/JIMMUNOL.181.9.6536.

Lee, S.M. *et al.* (2013) 'Bacterial colonization factors control specificity and stability of the gut microbiota', *Nature*, 501(7467), pp. 426–429. Available at: https://doi.org/10.1038/nature12447.

Lepercq, P. *et al.* (2004) 'Epimerization of chenodeoxycholic acid to ursodeoxycholic acid by Clostridium baratii isolated from human feces', *FEMS microbiology letters*, 235(1), pp. 65–72. Available at: https://doi.org/10.1016/J.FEMSLE.2004.04.011.

Lewis, J.D. and Abreu, M.T. (2017) 'Diet as a Trigger or Therapy for Inflammatory Bowel Diseases', *Gastroenterology*, 152(2), pp. 398-414.e6. Available at: https://doi.org/10.1053/j.gastro.2016.10.019.

Li, J. *et al.* (2014) 'An integrated catalog of reference genes in the human gut microbiome', *Nature Biotechnology 2014 32:8*, 32(8), pp. 834–841. Available at: https://doi.org/10.1038/nbt.2942.

Li, J. *et al.* (2016) 'Profiles of Lamina Propria T Helper Cell Subsets Discriminate Between Ulcerative Colitis and Crohn's Disease', *Inflammatory bowel diseases*, 22(8), pp. 1779–1792. Available at: https://doi.org/10.1097/MIB.0000000000000811.

Li, Q. *et al.* (2008) 'Interferon-γ and tumor necrosis factor-α disrupt epithelial barrier function by altering lipid composition in membrane microdomains of tight junction', *Clinical Immunology*, 126(1), pp. 67–80. Available at: https://doi.org/10.1016/j.clim.2007.08.017.

Li, Q. *et al.* (2013) 'Recruitment of CCR6-expressing Th17 cells by CCL20 secreted from plasmin-stimulated macrophages', *Acta biochimica et biophysica Sinica*, 45(7), pp. 593–600. Available at: https://doi.org/10.1093/ABBS/GMT049.

Li, T. and Chiang, J.Y.L. (2014) 'Bile acid signaling in metabolic disease and drug therapy', *Pharmacological reviews*, 66(4), pp. 948–983. Available at: https://doi.org/10.1124/PR.113.008201.

Lichtenstein, G.R. *et al.* (2006) 'Serious Infections and Mortality in Association With Therapies for Crohn's Disease: TREAT Registry', *Clinical Gastroenterology and Hepatology*, 4(5), pp. 621–630. Available at: https://doi.org/10.1016/j.cgh.2006.03.002.

Ligumsky, M. (1990) 'Role of interleukin 1 in inflammatory bowel disease-enhanced production during active disease', *Gut*, 31(6), pp. 686–689. Available at: https://doi.org/10.1136/gut.31.6.686.

Lin, B.C. *et al.* (2007) 'Liver-specific activities of FGF19 require Klotho beta', *The Journal of biological chemistry*, 282(37), pp. 27277–27284. Available at: https://doi.org/10.1074/JBC.M704244200.

Lin, Z. *et al.* (2017) 'Genetic association and epistatic interaction of the interleukin-10 signaling pathway in pediatric inflammatory bowel disease', *World Journal of Gastroenterology*, 23(27), pp. 4897–4909. Available at: https://doi.org/10.3748/wjg.v23.i27.4897.

Liu, B. and Newburg, D.S. (2013) 'Human Milk Glycoproteins Protect Infants Against Human Pathogens', *Breastfeeding Medicine*, 8(4), p. 354. Available at: https://doi.org/10.1089/BFM.2013.0016.

Liu, J.Z. *et al.* (2015) 'Association analyses identify 38 susceptibility loci for inflammatory bowel disease and highlight shared genetic risk across populations', *Nature Genetics*, 47(9), pp. 979–986. Available at: https://doi.org/10.1038/ng.3359.

Liu, T. *et al.* (2017) 'NF-κB signaling in inflammation', *Signal Transduction and Targeted Therapy 2017 2:1*, 2(1), pp. 1–9. Available at: https://doi.org/10.1038/sigtrans.2017.23.

Liu, Z. *et al.* (2011) 'The increased expression of IL-23 in inflammatory bowel disease promotes intraepithelial and lamina propria lymphocyte inflammatory responses and cytotoxicity', *Journal of Leukocyte Biology*, 89(4), pp. 597–606. Available at: https://doi.org/10.1189/jlb.0810456.

Livak, K.J. and Schmittgen, T.D. (2001) 'Analysis of relative gene expression data using real-time quantitative PCR and the 2(-Delta Delta

C(T)) Method', *Methods (San Diego, Calif.)*, 25(4), pp. 402–408. Available at: https://doi.org/10.1006/METH.2001.1262.

Lloyd-Price, J. *et al.* (2019) 'Multi-omics of the gut microbial ecosystem in inflammatory bowel diseases', *Nature 2019 569:7758*, 569(7758), pp. 655–662. Available at: https://doi.org/10.1038/s41586-019-1237-9.

Long, S.L., Gahan, C.G.M. and Joyce, S.A. (2017) 'Interactions between gut bacteria and bile in health and disease', *Molecular aspects of medicine*, 56, pp. 54–65. Available at: https://doi.org/10.1016/J.MAM.2017.06.002.

López-Díaz, L. *et al.* (2007) 'Intestinal Neurogenin 3 directs differentiation of a bipotential secretory progenitor to endocrine cell rather than goblet cell fate', *Developmental Biology*, 309(2), pp. 298–305. Available at: https://doi.org/10.1016/j.ydbio.2007.07.015.

Di Lorenzo, F. *et al.* (2020) 'Pairing bacteroides vulgatus LPS structure with its immunomodulatory effects on human cellular models', *ACS Central Science*, 6(9), pp. 1602–1616. Available at: https://doi.org/10.1021/ACSCENTSCI.0C00791/SUPPL_FILE/OC0C0079 1_SI_001.PDF.

Louca, S., Doebeli, M. and Parfrey, L.W. (2018) 'Correcting for 16S rRNA gene copy numbers in microbiome surveys remains an unsolved problem', *Microbiome*, 6(1), pp. 1–12. Available at: https://doi.org/10.1186/S40168-018-0420-9/FIGURES/4.

Lukonin, I. *et al.* (2020) 'Phenotypic landscape of intestinal organoid regeneration', *Nature*, 586(7828), pp. 275–280. Available at: https://doi.org/10.1038/s41586-020-2776-9.

Lytle, C. *et al.* (2005) 'the Peroxisome Proliferator-Activated Receptor γ Ligand Rosiglitazone Delays the Onset of Inflammatory Bowel Disease in Mice With Interleukin 10 Deficiency', *Inflammatory Bowel Diseases*, 11(3), pp. 231–243. Available at: https://doi.org/10.1097/01.MIB.0000160805.46235.EB.

Ma, C. *et al.* (2018) 'Gut microbiome-mediated bile acid metabolism regulates liver cancer via NKT cells', *Science (New York, N.Y.)*, 360(6391). Available at: https://doi.org/10.1126/SCIENCE.AAN5931.

Ma, H., Tao, W. and Zhu, S. (2019) 'T lymphocytes in the intestinal mucosa: defense and tolerance', *Cellular & Molecular Immunology 2019 16:3*, 16(3), pp. 216–224. Available at: https://doi.org/10.1038/s41423-019-0208-2.

Ma, T.Y. (1997) 'Intestinal epithelial barrier dysfunction in Crohn's disease', *Proceedings of the Society for Experimental Biology and Medicine*, 214(4), pp. 318–327. Available at: https://doi.org/10.3181/00379727-214-44099.

Macpherson, A.J. and Uhr, T. (2004) 'Induction of protective IgA by intestinal dendritic cells carrying commensal bacteria', *Science (New York,*

N.Y.), 303(5664), pp. 1662–1665. Available at: https://doi.org/10.1126/SCIENCE.1091334.

Madara, J.L. (1987) 'Intestinal absorptive cell tight junctions are linked to cytoskeleton', *https://doi.org/10.1152/ajpcell.1987.253.1.C171*, 253(1 (22/1)). Available at: https://doi.org/10.1152/AJPCELL.1987.253.1.C171.

Madsen, K.L. *et al.* (2000a) 'Antibiotic therapy attenuates colitis in interleukin 10 gene-deficient mice', *Gastroenterology*, 118(6), pp. 1094–1105. Available at: https://doi.org/10.1016/S0016-5085(00)70362-3.

Madsen, K.L. *et al.* (2000b) 'Antibiotic therapy attenuates colitis in interleukin 10 gene-deficient mice', *Gastroenterology*, 118(6), pp. 1094–1105. Available at: https://doi.org/10.1016/S0016-5085(00)70362-3.

Maerz, J.K. *et al.* (2018) 'Outer membrane vesicles blebbing contributes to B. vulgatus mpk-mediated immune response silencing', *Gut microbes*, 9(1), pp. 1–12. Available at: https://doi.org/10.1080/19490976.2017.1344810.

Mahid, S.S. *et al.* (2006) 'Smoking and inflammatory bowel disease: A meta-analysis', *Mayo Clinic Proceedings*, 81(11), pp. 1462–1471. Available at: https://doi.org/10.4065/81.11.1462.

Mähler, M. and Leiter, E.H. (2002) 'Genetic and Environmental Context Determines the Course of Colitis Developing in IL–10-Deficient Mice', *Inflammatory Bowel Diseases*, 8(5), pp. 347–355. Available at: https://doi.org/10.1097/00054725-200209000-00006.

Makishima, M. *et al.* (1999) 'Identification of a nuclear receptor for bile acids', *Science (New York, N.Y.)*, 284(5418), pp. 1362–1365. Available at: https://doi.org/10.1126/SCIENCE.284.5418.1362.

Malmström, V. *et al.* (2001) 'CD134L expression on dendritic cells in the mesenteric lymph nodes drives colitis in T cell-restored SCID mice', *Journal of immunology (Baltimore, Md. : 1950)*, 166(11), pp. 6972–6981. Available at: https://doi.org/10.4049/JIMMUNOL.166.11.6972.

Manetti, R. *et al.* (1993) 'Natural killer cell stimulatory factor (interleukin 12 [IL-12]) induces T helper type 1 (Th1)-specific immune responses and inhibits the development of IL-4-producing Th cells', *The Journal of experimental medicine*, 177(4), pp. 1199–1204. Available at: https://doi.org/10.1084/JEM.177.4.1199.

Marcobal, A. *et al.* (2013) 'A refined palate: bacterial consumption of host glycans in the gut', *Glycobiology*, 23(9), pp. 1038–1046. Available at: https://doi.org/10.1093/GLYCOB/CWT040.

Markle, J.G.M. *et al.* (2013) 'Sex differences in the gut microbiome drive hormone-dependent regulation of autoimmunity', *Science (New York, N.Y.)*, 339(6123), pp. 1084–1088. Available at: https://doi.org/10.1126/SCIENCE.1233521.

Martínez-Maqueda, D., Miralles, B. and Recio, I. (2015) 'HT29 Cell Line', *The Impact of Food Bioactives on Health: In Vitro and Ex Vivo Models*, pp. 113–124. Available at: https://doi.org/10.1007/978-3-319-16104-4_11.

Martinon, F., Mayor, A. and Tschopp, J. (2009) 'The inflammasomes: guardians of the body', *Annual review of immunology*, 27, pp. 229–265. Available at: https://doi.org/10.1146/ANNUREV.IMMUNOL.021908.132715.

Martinot, E. *et al.* (2017) 'Bile acids and their receptors', *Molecular aspects of medicine*, 56, pp. 2–9. Available at: https://doi.org/10.1016/J.MAM.2017.01.006.

Martìn-Padura, I. *et al.* (1998) 'Junctional adhesion molecule, a novel member of the immunoglobulin superfamily that distributes at intercellular junctions and modulates monocyte transmigration', *The Journal of cell biology*, 142(1), pp. 117–127. Available at: https://doi.org/10.1083/JCB.142.1.117.

Maynard, C.L. *et al.* (2012) 'Reciprocal interactions of the intestinal microbiota and immune system', *Nature 2012 489:7415*, 489(7415), pp. 231–241. Available at: https://doi.org/10.1038/nature11551.

Mazmanian, S.K. *et al.* (2005) 'An immunomodulatory molecule of symbiotic bacteria directs maturation of the host immune system', *Cell*, 122(1), pp. 107–118. Available at: https://doi.org/10.1016/J.CELL.2005.05.007.

Mazzucchelli, L. *et al.* (1996) 'Differential in situ expression of the genes encoding the chemokines MCP-1 and RANTES in human inflammatory bowel disease', *Journal of Pathology*, 178(2), pp. 201–206. Available at: https://doi.org/10.1002/(SICI)1096-9896(199602)178:2<201::AID-PATH440>3.0.CO;2-4.

McCarroll, S.A. *et al.* (2008) 'Deletion polymorphism upstream of IRGM associated with altered IRGM expression and Crohn's disease', *Nature Genetics*, 40(9), pp. 1107–1112. Available at: https://doi.org/10.1038/ng.215.

McGeachy, M.J. and Cua, D.J. (2008) 'Th17 cell differentiation: the long and winding road', *Immunity*, 28(4), pp. 445–453. Available at: https://doi.org/10.1016/J.IMMUNI.2008.03.001.

McGovern, D. and Powrie, F. (2007) 'The IL23 axis plays a key role in the pathogenesis of IBD', *Gut.* Gut, pp. 1333–1336. Available at: https://doi.org/10.1136/gut.2006.115402.

Meier, P.J. and Stieger, B. (2002) 'Bile salt transporters', *Annual review of physiology*, 64, pp. 635–661. Available at: https://doi.org/10.1146/ANNUREV.PHYSIOL.64.082201.100300.

Melgar, S., Karlsson, A. and Michaëlsson, E. (2005) 'Acute colitis induced by dextran sulfate sodium progresses to chronicity in C57BL/6 but not in

BALB/c mice: correlation between symptoms and inflammation', *American journal of physiology. Gastrointestinal and liver physiology*, 288(6). Available at: https://doi.org/10.1152/AJPGI.00467.2004.

Methé, B.A. *et al.* (2012) 'A framework for human microbiome research', *Nature 2012 486:7402*, 486(7402), pp. 215–221. Available at: https://doi.org/10.1038/nature11209.

Mitsou, E.K. *et al.* (2017) 'Adherence to the Mediterranean diet is associated with the gut microbiota pattern and gastrointestinal characteristics in an adult population', *The British journal of nutrition*, 117(12), pp. 1645–1655. Available at: https://doi.org/10.1017/S0007114517001593.

Mizoguchi, A. (2012) 'Animal models of inflammatory bowel disease', *Progress in molecular biology and translational science*, 105, pp. 263–320. Available at: https://doi.org/10.1016/B978-0-12-394596-9.00009-3.

Moller, F.T. *et al.* (2015) 'Familial risk of inflammatory bowel disease: A population-based cohort study 1977-2011', *American Journal of Gastroenterology*, 110(4), pp. 564–571. Available at: https://doi.org/10.1038/ajg.2015.50.

Molodecky, N.A. *et al.* (2012) 'Increasing incidence and prevalence of the inflammatory bowel diseases with time, based on systematic review', *Gastroenterology*, 142(1). Available at: https://doi.org/10.1053/j.gastro.2011.10.001.

Monte, M.J. *et al.* (2009) 'Bile acids: Chemistry, physiology, and pathophysiology', *World Journal of Gastroenterology : WJG*, 15(7), p. 804. Available at: https://doi.org/10.3748/WJG.15.804.

Monteleone, G. *et al.* (2015) ' Mongersen, an Oral SMAD7 Antisense Oligonucleotide, and Crohn's Disease ', *New England Journal of Medicine*, 372(12), pp. 1104–1113. Available at: https://doi.org/10.1056/NEJMOA1407250/SUPPL_FILE/NEJMOA1407250_DISCLOSURES.PDF.

Moossavi, S. *et al.* (2019) 'Composition and Variation of the Human Milk Microbiota Are Influenced by Maternal and Early-Life Factors', *Cell host & microbe*, 25(2), pp. 324-335.e4. Available at: https://doi.org/10.1016/J.CHOM.2019.01.011.

Moran, C.J. *et al.* (2015) 'Very early-onset inflammatory bowel disease: Gaining insight through focused discovery', *Inflammatory Bowel Diseases*, 21(5), pp. 1166–1175. Available at: https://doi.org/10.1097/MIB.0000000000000329.

Mörbe, U.M. *et al.* (2021) 'Human gut-associated lymphoid tissues (GALT); diversity, structure, and function', *Mucosal Immunology*, 14(4), pp. 793–802. Available at: https://doi.org/10.1038/S41385-021-00389-4.

Mori-Akiyama, Y. *et al.* (2007) 'SOX9 Is Required for the Differentiation of Paneth Cells in the Intestinal Epithelium', *Gastroenterology*, 133(2), pp. 539–546. Available at: https://doi.org/10.1053/j.gastro.2007.05.020.

Morishima, N. *et al.* (2009) 'TGF-beta is necessary for induction of IL-23R and Th17 differentiation by IL-6 and IL-23', *Biochemical and biophysical research communications*, 386(1), pp. 105–110. Available at: https://doi.org/10.1016/J.BBRC.2009.05.140.

Mowat, A.M. and Agace, W.W. (2014) 'Regional specialization within the intestinal immune system', *Nature reviews. Immunology*, 14(10), pp. 667–685. Available at: https://doi.org/10.1038/NRI3738.

Moya, A. and Ferrer, M. (2016) 'Functional Redundancy-Induced Stability of Gut Microbiota Subjected to Disturbance', *Trends in microbiology*, 24(5), pp. 402–413. Available at: https://doi.org/10.1016/J.TIM.2016.02.002.

Muise, A.M. *et al.* (2009a) 'Polymorphisms in E-cadherin (CDH1) result in a mislocalised cytoplasmic protein that is associated with Crohn's disease', *Gut*, 58(8), pp. 1121–1127. Available at: https://doi.org/10.1136/gut.2008.175117.

Muise, A.M. *et al.* (2009b) 'Polymorphisms in E-cadherin (CDH1) result in a mislocalised cytoplasmic protein that is associated with Crohn's disease', *Gut*, 58(8), pp. 1121–1127. Available at: https://doi.org/10.1136/gut.2008.175117.

Müller, M. *et al.* (2008) 'Intestinal Colonization of IL-2 Deficient Mice with Non-Colitogenic B. vulgatus Prevents DC Maturation and T-Cell Polarization', *PLOS ONE*, 3(6), p. e2376. Available at: https://doi.org/10.1371/JOURNAL.PONE.0002376.

Murray, P.J. (2006) 'Understanding and exploiting the endogenous interleukin-10/STAT3-mediated anti-inflammatory response', *Current opinion in pharmacology*, 6(4), pp. 379–386. Available at: https://doi.org/10.1016/J.COPH.2006.01.010.

Nagpal, R. *et al.* (2018) 'Gut Microbiome Composition in Non-human Primates Consuming a Western or Mediterranean Diet', *Frontiers in Nutrition*, 5, p. 28. Available at: https://doi.org/10.3389/FNUT.2018.00028/BIBTEX.

Natividad, J.M.M. and Verdu, E.F. (2013) 'Modulation of intestinal barrier by intestinal microbiota: pathological and therapeutic implications', *Pharmacological research*, 69(1), pp. 42–51. Available at: https://doi.org/10.1016/J.PHRS.2012.10.007.

Negroni, A. *et al.* (2018) 'NOD2 and inflammation: Current insights', *Journal of Inflammation Research*. Dove Medical Press Ltd, pp. 49–60. Available at: https://doi.org/10.2147/JIR.S137606.

Neish, A.S. (2009) 'Microbes in Gastrointestinal Health and Disease', *Gastroenterology*, 136(1), pp. 65–80. Available at: https://doi.org/10.1053/J.GASTRO.2008.10.080.

Neurath, M.F. *et al.* (2002) 'The Transcription Factor T-bet Regulates Mucosal T Cell Activation in Experimental Colitis and Crohn's Disease', *The Journal of Experimental Medicine*, 195(9), p. 1129. Available at: https://doi.org/10.1084/JEM.20011956.

Neurath, M.F. (2014) 'Cytokines in inflammatory bowel disease', *Nature Reviews Immunology*, 14(5), pp. 329–342. Available at: https://doi.org/10.1038/nri3661.

Ng, S.C. *et al.* (2017) 'Worldwide incidence and prevalence of inflammatory bowel disease in the 21st century: a systematic review of population-based studies', *The Lancet*, 390(10114), pp. 2769–2778. Available at: https://doi.org/10.1016/S0140-6736(17)32448-0.

Nishi, K. *et al.* (2009) 'Cyclin D1 Downregulation is Important for Permanent Cell Cycle Exit and Initiation of Differentiation Induced by Anchorage-Deprivation in Human Keratinocytes', *Journal of cellular biochemistry*, 106(1), p. 63. Available at: https://doi.org/10.1002/JCB.21978.

Nusse, R. and Clevers, H. (2017) 'Wnt/β-Catenin Signaling, Disease, and Emerging Therapeutic Modalities', *Cell*, 169(6), pp. 985–999. Available at: https://doi.org/10.1016/j.cell.2017.05.016.

Ó Cuív, P. *et al.* (2017) 'The gut bacterium and pathobiont Bacteroides vulgatus activates NF-κB in a human gut epithelial cell line in a strain and growth phase dependent manner', *Anaerobe*, 47, pp. 209–217. Available at: https://doi.org/10.1016/J.ANAEROBE.2017.06.002.

Oeckinghaus, A. and and Ghosh, S. (2009) 'The nuclear factor- k B (NF-k B) family of transcription factors', *Cold Spring Harbor Perspectives in Biology*, 1(4), pp. 1–15.

Oh, B. *et al.* (2016) 'The Effect of Probiotics on Gut Microbiota during the Helicobacter pylori Eradication: Randomized Controlled Trial', *Helicobacter*, 21(3), pp. 165–174. Available at: https://doi.org/10.1111/HEL.12270.

Okayasu, I. *et al.* (1990) 'A novel method in the induction of reliable experimental acute and chronic ulcerative colitis in mice', *Gastroenterology*, 98(3), pp. 694–702. Available at: https://doi.org/10.1016/0016-5085(90)90290-H.

Oki, M. *et al.* (2005) 'Accumulation of CCR5+ T cells around RANTES+ granulomas in Crohn's disease: A pivotal site of Th1-shifted immune response?', *Laboratory Investigation*, 85(1), pp. 137–145. Available at: https://doi.org/10.1038/labinvest.3700189.

Oldenburg, M. *et al.* (2012) 'TLR13 recognizes bacterial 23S rRNA devoid of erythromycin resistance-forming modification', *Science (New York, N.Y.)*,

337(6098), pp. 1111–1115. Available at: https://doi.org/10.1126/SCIENCE.1220363.

Ooi, L.G. *et al.* (2010) 'Lactobacillus gasseri [corrected] CHO-220 and inulin reduced plasma total cholesterol and low-density lipoprotein cholesterol via alteration of lipid transporters', *Journal of dairy science*, 93(11), pp. 5048–5058. Available at: https://doi.org/10.3168/JDS.2010-3311.

Org, E. *et al.* (2016) 'Sex differences and hormonal effects on gut microbiota composition in mice', *Gut Microbes*, 7(4), p. 313. Available at: https://doi.org/10.1080/19490976.2016.1203502.

Ostaff, M.J., Stange, E.F. and Wehkamp, J. (2013) 'Antimicrobial peptides and gut microbiota in homeostasis and pathology', *EMBO Molecular Medicine*, 5(10), pp. 1465–1483. Available at: https://doi.org/10.1002/EMMM.201201773.

Ostanin, D. V. *et al.* (2009) 'T cell transfer model of chronic colitis: concepts, considerations, and tricks of the trade', *American journal of physiology. Gastrointestinal and liver physiology*, 296(2). Available at: https://doi.org/10.1152/AJPGI.90462.2008.

Østvik, A.E. *et al.* (2013) 'Enhanced expression of CXCL10 in inflammatory bowel disease: Potential role of mucosal toll-like receptor 3 stimulation', *Inflammatory Bowel Diseases*, 19(2), pp. 265–274. Available at: https://doi.org/10.1002/ibd.23034.

Pagliai, G. *et al.* (2020) 'Influence of a 3-month low-calorie Mediterranean diet compared to the vegetarian diet on human gut microbiota and SCFA: the CARDIVEG Study', *European journal of nutrition*, 59(5), pp. 2011–2024. Available at: https://doi.org/10.1007/S00394-019-02050-0.

Paik, D. *et al.* (2021) 'Human gut bacteria produce TH17-modulating bile acid metabolites', *bioRxiv*, p. 2021.01.08.425913. Available at: https://doi.org/10.1101/2021.01.08.425913.

Parkes, M. *et al.* (2007) 'Sequence variants in the autophagy gene IRGM and multiple other replicating loci contribute to Crohn's disease susceptibility', *Nature Genetics*, 39(7), pp. 830–832. Available at: https://doi.org/10.1038/ng2061.

Pascal, V. *et al.* (2017) 'A microbial signature for Crohn's disease', *Gut*, 66(5), pp. 813–822. Available at: https://doi.org/10.1136/GUTJNL-2016-313235.

Pathak, P. *et al.* (2017) 'Farnesoid X receptor induces Takeda G-protein receptor 5 cross-talk to regulate bile acid synthesis and hepatic metabolism', *The Journal of biological chemistry*, 292(26), pp. 11055–11069. Available at: https://doi.org/10.1074/JBC.M117.784322.

Pathmanathan, S.G. *et al.* (2020) 'Gut bacteria characteristic of the infant microbiota down-regulate inflammatory transcriptional responses in HT-29

cells', *Anaerobe*, 61. Available at: https://doi.org/10.1016/J.ANAEROBE.2019.102112.

Paul, G., Khare, V. and Gasche, C. (2012) 'Inflamed gut mucosa: downstream of interleukin-10', *European journal of clinical investigation*, 42(1), pp. 95–109. Available at: https://doi.org/10.1111/J.1365-2362.2011.02552.X.

Perminow, G. *et al.* (2010) 'Defective paneth cell-mediated host defense in pediatric ileal Crohn's disease', *The American journal of gastroenterology*, 105(2), pp. 452–459. Available at: https://doi.org/10.1038/AJG.2009.643.

Perše, M. and Cerar, A. (2012) 'Dextran sodium sulphate colitis mouse model: traps and tricks', *Journal of biomedicine & biotechnology*, 2012. Available at: https://doi.org/10.1155/2012/718617.

Peterson, M.D. and Mooseker, M.S. (1992) 'Characterization of the enterocyte-like brush border cytoskeleton of the C2BBe clones of the human intestinal cell line, Caco-2', *Journal of cell science*, 102 (Pt 3)(3), pp. 581–600. Available at: https://doi.org/10.1242/JCS.102.3.581.

Pols, T.W.H. *et al.* (2011) 'The bile acid membrane receptor TGR5 as an emerging target in metabolism and inflammation', *Journal of hepatology*, 54(6), pp. 1263–1272. Available at: https://doi.org/10.1016/J.JHEP.2010.12.004.

Pols, T.W.H. *et al.* (2017) 'Lithocholic acid controls adaptive immune responses by inhibition of Th1 activation through the Vitamin D receptor', *PloS one*, 12(5). Available at: https://doi.org/10.1371/JOURNAL.PONE.0176715.

Prawitt, J. *et al.* (2011) 'Farnesoid X receptor deficiency improves glucose homeostasis in mouse models of obesity', *Diabetes*, 60(7), pp. 1861–1871. Available at: https://doi.org/10.2337/DB11-0030/-/DC1.

Prescott, N.J. *et al.* (2010) 'Independent and population-specific association of risk variants at the IRGM locus with Crohn's disease', *Human Molecular Genetics*, 19(9), pp. 1828–1839. Available at: https://doi.org/10.1093/hmg/ddq041.

Prete, R. *et al.* (2020) 'Beneficial bile acid metabolism from Lactobacillus plantarum of food origin', *Scientific Reports 2020 10:1*, 10(1), pp. 1–11. Available at: https://doi.org/10.1038/s41598-020-58069-5.

Qin, J. *et al.* (2010) 'A human gut microbial gene catalogue established by metagenomic sequencing', *Nature 2010 464:7285*, 464(7285), pp. 59–65. Available at: https://doi.org/10.1038/nature08821.

Quadrilatero, J. and Hoffman-Goetz, L. (2003) 'Physical activity and colon cancer. A systematic review of potential mechanisms.', *undefined* [Preprint].

Quince, C. *et al.* (2017) 'Shotgun metagenomics, from sampling to analysis', *Nature Biotechnology 2017 35:9*, 35(9), pp. 833–844. Available at: https://doi.org/10.1038/nbt.3935.

Rajilić-Stojanović, M. and de Vos, W.M. (2014) 'The first 1000 cultured species of the human gastrointestinal microbiota', *FEMS Microbiology Reviews*, 38(5), pp. 996–1047. Available at: https://doi.org/10.1111/1574-6976.12075.

Ramanan, D. *et al.* (2014a) 'Bacterial sensor Nod2 prevents inflammation of the small intestine by restricting the expansion of the commensal Bacteroides vulgatus', *Immunity*, 41(2), pp. 311–324. Available at: https://doi.org/10.1016/J.IMMUNI.2014.06.015.

Ramanan, D. *et al.* (2014b) 'Bacterial sensor Nod2 prevents inflammation of the small intestine by restricting the expansion of the commensal Bacteroides vulgatus', *Immunity*, 41(2), pp. 311–324. Available at: https://doi.org/10.1016/J.IMMUNI.2014.06.015.

Rao, A. *et al.* (2008) 'The organic solute transporter alpha-beta, Ostalpha-Ostbeta, is essential for intestinal bile acid transport and homeostasis', *Proceedings of the National Academy of Sciences of the United States of America*, 105(10), pp. 3891–3896. Available at: https://doi.org/10.1073/PNAS.0712328105.

Rath, H.C. *et al.* (1996) 'Normal luminal bacteria, especially Bacteroides species, mediate chronic colitis, gastritis, and arthritis in HLA-B27/human beta2 microglobulin transgenic rats', *The Journal of clinical investigation*, 98(4), pp. 945–953. Available at: https://doi.org/10.1172/JCI118878.

Regan, T. *et al.* (2013) 'Identification of TLR10 as a Key Mediator of the Inflammatory Response to Listeria monocytogenes in Intestinal Epithelial Cells and Macrophages', *The Journal of Immunology*, 191(12), pp. 6084–6092. Available at: https://doi.org/10.4049/JIMMUNOL.1203245.

Rehman, A. *et al.* (2016) 'Geographical patterns of the standing and active human gut microbiome in health and IBD', *Gut*, 65(2), pp. 238–248. Available at: https://doi.org/10.1136/GUTJNL-2014-308341.

Reikvam, D.H. *et al.* (2011) 'Depletion of Murine Intestinal Microbiota: Effects on Gut Mucosa and Epithelial Gene Expression', *PLOS ONE*, 6(3), p. e17996. Available at: https://doi.org/10.1371/JOURNAL.PONE.0017996.

Reinisch, W. *et al.* (2010) 'Fontolizumab in moderate to severe Crohn's disease: a phase 2, randomized, double-blind, placebo-controlled, multiple-dose study', *Inflammatory bowel diseases*, 16(2), pp. 233–242. Available at: https://doi.org/10.1002/IBD.21038.

Renz-Polster, H. *et al.* (2005) 'Caesarean section delivery and the risk of allergic disorders in childhood', *Clinical and experimental allergy : journal of*

the British Society for Allergy and Clinical Immunology, 35(11), pp. 1466–1472. Available at: https://doi.org/10.1111/J.1365-2222.2005.02356.X.

Resta-Lenert, S., Smitham, J. and Barrett, K.E. (2005) 'Epithelial dysfunction associated with the development of colitis in conventionally housed mdr1a-/- mice', *American Journal of Physiology - Gastrointestinal and Liver Physiology*, 289(1 52-1), pp. 153–162. Available at: https://doi.org/10.1152/ajpgi.00395.2004.

Ridlon, J.M., Kang, D.J. and Hylemon, P.B. (2006) 'Bile salt biotransformations by human intestinal bacteria', *Journal of Lipid Research*, 47(2), pp. 241–259. Available at: https://doi.org/10.1194/JLR.R500013-JLR200.

Rinninella, E. *et al.* (2019) 'Food Components and Dietary Habits: Keys for a Healthy Gut Microbiota Composition', *Nutrients*, 11(10). Available at: https://doi.org/10.3390/NU11102393.

Rintala, A. *et al.* (2017) 'Gut Microbiota Analysis Results Are Highly Dependent on the 16S rRNA Gene Target Region, Whereas the Impact of DNA Extraction Is Minor', *Journal of biomolecular techniques : JBT*, 28(1), pp. 19–30. Available at: https://doi.org/10.7171/JBT.17-2801-003.

Rodríguez, J.M. *et al.* (2015) 'The composition of the gut microbiota throughout life, with an emphasis on early life', *Microbial ecology in health and disease*, 26(0). Available at: https://doi.org/10.3402/MEHD.V26.26050.

Rodriguez-Antequera, M. *et al.* (2019) 'P041 Differences in NOTCH signalling between stricturing and penetrating behaviour in Crohn's disease', *Journal of Crohn's and Colitis*, 13(Supplement_1), pp. S107–S107. Available at: https://doi.org/10.1093/ECCO-JCC/JJY222.165.

Rodríguez-Colman, M.J. *et al.* (2017) 'Interplay between metabolic identities in the intestinal crypt supports stem cell function', *Nature*, 543(7645), pp. 424–427. Available at: https://doi.org/10.1038/NATURE21673.

Rolhion, N. and Darfeuille-Michaud, A. (2007) 'Adherent-invasive Escherichia coli in inflammatory bowel disease', *Inflammatory Bowel Diseases*, 13(10), pp. 1277–1283. Available at: https://doi.org/10.1002/IBD.20176.

Rossocha, M. *et al.* (2005) 'Conjugated bile acid hydrolase is a tetrameric N-terminal thiol hydrolase with specific recognition of its cholyl but not of its tauryl product', *Biochemistry*, 44(15), pp. 5739–5748. Available at: https://doi.org/10.1021/BI0473206.

Rougé, C. *et al.* (2010) 'Investigation of the intestinal microbiota in preterm infants using different methods', *Anaerobe*, 16(4), pp. 362–370. Available at: https://doi.org/10.1016/J.ANAEROBE.2010.06.002.

Rubtsov, Y.P. *et al.* (2008) 'Regulatory T cell-derived interleukin-10 limits inflammation at environmental interfaces', *Immunity*, 28(4), pp. 546–558. Available at: https://doi.org/10.1016/J.IMMUNI.2008.02.017.

Rutgeerts, P. *et al.* (1991) 'Effect of faecal stream diversion on recurrence of Crohn's disease in the neoterminal ileum', *Lancet (London, England)*, 338(8770), pp. 771–774. Available at: https://doi.org/10.1016/0140-6736(91)90663-A.

Ryan, F.J. *et al.* (2020) 'Colonic microbiota is associated with inflammation and host epigenomic alterations in inflammatory bowel disease', *Nature Communications*, 11(1), pp. 1–12. Available at: https://doi.org/10.1038/s41467-020-15342-5.

Sadabad, M.S. *et al.* (2015) 'The ATG16L1-T300A allele impairs clearance of pathosymbionts in the inflamed ileal mucosa of Crohn's disease patients', *Gut*, 64(10), pp. 1546–1552. Available at: https://doi.org/10.1136/gutjnl-2014-307289.

Sahoo, M. *et al.* (2011) 'Role of the Inflammasome, IL-1β, and IL-18 in Bacterial Infections', *The Scientific World Journal*, 11, p. 2037. Available at: https://doi.org/10.1100/2011/212680.

Saiz-Gonzalo, G. *et al.* (2021) 'Regulation of CEACAM Family Members by IBD-Associated Triggers in Intestinal Epithelial Cells, Their Correlation to Inflammation and Relevance to IBD Pathogenesis', *Frontiers in Immunology*, 12, p. 2986. Available at: https://doi.org/10.3389/FIMMU.2021.655960/BIBTEX.

Salas, A. *et al.* (2020) 'JAK–STAT pathway targeting for the treatment of inflammatory bowel disease', *Nature Reviews Gastroenterology & Hepatology 2020 17:6*, 17(6), pp. 323–337. Available at: https://doi.org/10.1038/s41575-020-0273-0.

Sancho, R., Cremona, C.A. and Behrens, A. (2015) 'Stem cell and progenitor fate in the mammalian intestine: Notch and lateral inhibition in homeostasis and disease', *EMBO reports*, 16(5), pp. 571–581. Available at: https://doi.org/10.15252/embr.201540188.

Sandborn, W.J. *et al.* (2013) 'Vedolizumab as induction and maintenance therapy for Crohn's disease', *The New England journal of medicine*, 369(8), pp. 711–721. Available at: https://doi.org/10.1056/NEJMOA1215739.

Sands, B.E. *et al.* (2020) 'Mongersen (GED-0301) for Active Crohn's Disease: Results of a Phase 3 Study', *The American journal of gastroenterology*, 115(5), pp. 738–745. Available at: https://doi.org/10.14309/AJG.0000000000000493.

Saraiva, M. and O'Garra, A. (2010) 'The regulation of IL-10 production by immune cells', *Nature Reviews Immunology*. Nature Publishing Group, pp. 170–181. Available at: https://doi.org/10.1038/nri2711.

Sartor, R.B. (2008) 'Microbial Influences in Inflammatory Bowel Diseases', *Gastroenterology*, 134(2), pp. 577–594. Available at: https://doi.org/10.1053/j.gastro.2007.11.059.

Saruta, M. *et al.* (2007) 'Characterization of FOXP3+CD4+ regulatory T cells in Crohn's disease', *Clinical immunology (Orlando, Fla.)*, 125(3), pp. 281–290. Available at: https://doi.org/10.1016/J.CLIM.2007.08.003.

Sato, T. *et al.* (2010) 'Paneth cells constitute the niche for Lgr5 stem cells in intestinal crypts', *Nature 2010 469:7330*, 469(7330), pp. 415–418. Available at: https://doi.org/10.1038/nature09637.

Sato, T. and Clevers, H. (2013a) 'Growing self-organizing mini-guts from a single intestinal stem cell: Mechanism and applications', *Science*, 340(6137), pp. 1190–1194. Available at: https://doi.org/10.1126/SCIENCE.1234852/SUPPL_FILE/SATO.SM.COVER.PAGE.PDF.

Sato, T. and Clevers, H. (2013b) 'Growing self-organizing mini-guts from a single intestinal stem cell: Mechanism and applications', *Science*, 340(6137), pp. 1190–1194. Available at: https://doi.org/10.1126/science.1234852.

Satokari, R. *et al.* (2009) 'Bifidobacterium and Lactobacillus DNA in the human placenta', *Letters in applied microbiology*, 48(1), pp. 8–12. Available at: https://doi.org/10.1111/J.1472-765X.2008.02475.X.

Satsangi, J. *et al.* (2006) 'The Montreal classification of inflammatory bowel disease: Controversies, consensus, and implications', *Gut*. Gut, pp. 749–753. Available at: https://doi.org/10.1136/gut.2005.082909.

Sayin, S.I. *et al.* (2013) 'Gut microbiota regulates bile acid metabolism by reducing the levels of tauro-beta-muricholic acid, a naturally occurring FXR antagonist', *Cell metabolism*, 17(2), pp. 225–235. Available at: https://doi.org/10.1016/J.CMET.2013.01.003.

Schaubeck, M. *et al.* (2016) 'Dysbiotic gut microbiota causes transmissible Crohn's disease-like ileitis independent of failure in antimicrobial defence', *Gut*, 65(2), pp. 225–237. Available at: https://doi.org/10.1136/GUTJNL-2015-309333.

Scher, J.U. *et al.* (2015) 'Decreased bacterial diversity characterizes the altered gut microbiota in patients with psoriatic arthritis, resembling dysbiosis in inflammatory bowel disease', *Arthritis & rheumatology (Hoboken, N.J.)*, 67(1), pp. 128–139. Available at: https://doi.org/10.1002/ART.38892.

Schippa, S. *et al.* (2010) 'A distinctive "microbial signature" in celiac pediatric patients', *BMC Microbiology*, 10(1), pp. 1–10. Available at: https://doi.org/10.1186/1471-2180-10-175/TABLES/2.

Schirmer, M. *et al.* (2019) 'Microbial genes and pathways in inflammatory bowel disease', *Nature Reviews Microbiology 2019 17:8*, 17(8), pp. 497–511. Available at: https://doi.org/10.1038/s41579-019-0213-6.

Schmidt, A., Oberle, N. and Krammer, P.H. (2012) 'Molecular mechanisms oftreg-mediatedt cell suppression', *Frontiers in Immunology*, 3(MAR), p. 51. Available at: https://doi.org/10.3389/FIMMU.2012.00051/BIBTEX.

Schnoor, M. (2015) 'E-cadherin Is Important for the Maintenance of Intestinal Epithelial Homeostasis Under Basal and Inflammatory Conditions', *Digestive Diseases and Sciences*, 60(4), pp. 816–818. Available at: https://doi.org/10.1007/s10620-015-3622-z.

Schreiner, P. *et al.* (2020) 'Nutrition in Inflammatory Bowel Disease', *Digestion*, 101(Suppl. 1), pp. 120–135. Available at: https://doi.org/10.1159/000505368.

Schroder, K. and Tschopp, J. (2010) 'The inflammasomes', *Cell*, 140(6), pp. 821–832. Available at: https://doi.org/10.1016/J.CELL.2010.01.040.

Schugar, R.C. *et al.* (2017) 'The TMAO-Producing Enzyme Flavin-Containing Monooxygenase 3 (FMO3) Regulates Obesity and the Beiging of White Adipose Tissue', *Cell reports*, 19(12), p. 2451. Available at: https://doi.org/10.1016/J.CELREP.2017.05.077.

Sellon, R.K. *et al.* (1998a) 'Resident enteric bacteria are necessary for development of spontaneous colitis and immune system activation in interleukin-10-deficient mice', *Infection and immunity*, 66(11), pp. 5224–5231. Available at: https://doi.org/10.1128/IAI.66.11.5224-5231.1998.

Sellon, R.K. *et al.* (1998b) 'Resident enteric bacteria are necessary for development of spontaneous colitis and immune system activation in interleukin-10-deficient mice', *Infection and immunity*, 66(11), pp. 5224–5231. Available at: https://doi.org/10.1128/IAI.66.11.5224-5231.1998.

Sender, R., Fuchs, S. and Milo, R. (2016) 'Revised Estimates for the Number of Human and Bacteria Cells in the Body', *PLOS Biology*, 14(8), p. e1002533. Available at: https://doi.org/10.1371/JOURNAL.PBIO.1002533.

Shanmugam, M. *et al.* (2005) 'Bacterial-induced inflammation in germ-free rabbit appendix', *Inflammatory bowel diseases*, 11(11), pp. 992–996. Available at: https://doi.org/10.1097/01.MIB.0000182869.74648.0F.

Shao, Y. *et al.* (2019) 'Stunted microbiota and opportunistic pathogen colonization in caesarean-section birth', *Nature 2019 574:7776*, 574(7776), pp. 117–121. Available at: https://doi.org/10.1038/s41586-019-1560-1.

Shaw, S.Y., Blanchard, J.F. and Bernstein, C.N. (2010) 'Association between the use of antibiotics in the first year of life and pediatric inflammatory bowel disease', *American Journal of Gastroenterology*, 105(12), pp. 2687–2692. Available at: https://doi.org/10.1038/ajg.2010.398.

Shen, B. *et al.* (2019) 'Antibiotics exacerbated colitis by affecting the microbiota, Treg cells and SCFAs in IL10-deficient mice', *Biomedicine & pharmacotherapy = Biomedecine & pharmacotherapie*, 114. Available at: https://doi.org/10.1016/J.BIOPHA.2019.108849.

Sherman, M.P. *et al.* (2005) 'Paneth cells and antibacterial host defense in neonatal small intestine', *Infection and immunity*, 73(9), pp. 6143–6146. Available at: https://doi.org/10.1128/IAI.73.9.6143-6146.2005.

Sherrod, J.A. and Hylemon, P.B. (1977) 'Partial purification and characterization of NAD-dependent 7alpha-hydroxysteroid dehydrogenase from Bacteroides thetaiotaomicron', *Biochimica et biophysica acta*, 486(2), pp. 351–358. Available at: https://doi.org/10.1016/0005-2760(77)90031-5.

Sidiq, T. *et al.* (2016) 'Nod2: A critical regulator of ileal microbiota and Crohn's disease', *Frontiers in Immunology*. Frontiers Media S.A., p. 1. Available at: https://doi.org/10.3389/fimmu.2016.00367.

Sierro, F. *et al.* (2001) 'Flagellin stimulation of intestinal epithelial cells triggers CCL20-mediated migration of dendritic cells', *Proceedings of the National Academy of Sciences*, 98(24), pp. 13722–13727. Available at: https://doi.org/10.1073/PNAS.241308598.

Singh, P., Ananthakrishnan, A. and Ahuja, V. (2017) 'Pivot to Asia: inflammatory bowel disease burden', *Intestinal Research*, 15(1), p. 138. Available at: https://doi.org/10.5217/IR.2017.15.1.138.

Singh, R.K. *et al.* (2017) 'Influence of diet on the gut microbiome and implications for human health', *Journal of translational medicine*, 15(1). Available at: https://doi.org/10.1186/S12967-017-1175-Y.

Singh, U.P. *et al.* (2016) 'Chemokine and cytokine levels in inflammatory bowel disease patients', *Cytokine*, 77, pp. 44–49. Available at: https://doi.org/10.1016/j.cyto.2015.10.008.

Sinha, S.R. *et al.* (2020) 'Dysbiosis-Induced Secondary Bile Acid Deficiency Promotes Intestinal Inflammation', *Cell host & microbe*, 27(4), pp. 659-670.e5. Available at: https://doi.org/10.1016/J.CHOM.2020.01.021.

Sjögren, Y.M. *et al.* (2009) 'Influence of early gut microbiota on the maturation of childhood mucosal and systemic immune responses', *Clinical and experimental allergy : journal of the British Society for Allergy and Clinical Immunology*, 39(12), pp. 1842–1851. Available at: https://doi.org/10.1111/J.1365-2222.2009.03326.X.

Skovdahl, H.K. *et al.* (2015) 'Expression of CCL20 and its corresponding receptor CCR6 is enhanced in active inflammatory bowel disease, and TLR3 mediates CCL20 expression in colonic epithelial cells', *PLoS ONE*, 10(11), pp. 1–17. Available at: https://doi.org/10.1371/journal.pone.0141710.

Van der Sluis, M. *et al.* (2006) 'Muc2-Deficient Mice Spontaneously Develop Colitis, Indicating That MUC2 Is Critical for Colonic Protection', *Gastroenterology*, 131(1), pp. 117–129. Available at: https://doi.org/10.1053/J.GASTRO.2006.04.020.

Snippert, H.J. *et al.* (2014) 'Biased competition between Lgr5 intestinal stem cells driven by oncogenic mutation induces clonal expansion', *EMBO Reports*, 15(1), pp. 62–69. Available at: https://doi.org/10.1002/embr.201337799.

Sokol, H. *et al.* (2009) 'Low counts of Faecalibacterium prausnitzii in colitis microbiota', *Inflammatory bowel diseases*, 15(8), pp. 1183–1189. Available at: https://doi.org/10.1002/IBD.20903.

Sokol, H. and Seksik, P. (2010) 'The intestinal microbiota in inflammatory bowel diseases: Time to connect with the host', *Current Opinion in Gastroenterology*, 26(4), pp. 327–331. Available at: https://doi.org/10.1097/MOG.0b013e328339536b.

Solá, S. *et al.* (2007) 'Game and Players: Mitochondrial Apoptosis and the Therapeutic Potential of Ursodeoxycholic Acid', *Current Issues in Molecular Biology 2007, Vol. 9, Pages 123-139*, 9(2), pp. 123–139. Available at: https://doi.org/10.21775/CIMB.009.123.

Son, H.J. *et al.* (2019) 'Sex-related Alterations of Gut Microbiota in the C57BL/6 Mouse Model of Inflammatory Bowel Disease', *Journal of cancer prevention*, 24(3), pp. 173–182. Available at: https://doi.org/10.15430/JCP.2019.24.3.173.

Song, E.J., Lee, E.S. and Nam, Y. Do (2018) 'Progress of analytical tools and techniques for human gut microbiome research', *Journal of microbiology (Seoul, Korea)*, 56(10), pp. 693–705. Available at: https://doi.org/10.1007/S12275-018-8238-5.

Song, X. *et al.* (2020) 'Microbial bile acid metabolites modulate gut RORγ + regulatory T cell homeostasis', *Nature*, 577(7790), pp. 410–415. Available at: https://doi.org/10.1038/S41586-019-1865-0.

Song, Z. *et al.* (2019) 'Taxonomic profiling and populational patterns of bacterial bile salt hydrolase (BSH) genes based on worldwide human gut microbiome', *Microbiome*, 7(1), pp. 1–16. Available at: https://doi.org/10.1186/S40168-019-0628-3/FIGURES/6.

Sorrentino, G. *et al.* (2020) 'Bile Acids Signal via TGR5 to Activate Intestinal Stem Cells and Epithelial Regeneration', *Gastroenterology*, 159(3), pp. 956-968.e8. Available at: https://doi.org/10.1053/J.GASTRO.2020.05.067.

De Souza, H.S.P. and Fiocchi, C. (2015) 'Immunopathogenesis of IBD: current state of the art', *Nature Reviews Gastroenterology & Hepatology 2015 13:1*, 13(1), pp. 13–27. Available at: https://doi.org/10.1038/nrgastro.2015.186.

Spencer, D.M. *et al.* (2002) 'Distinct inflammatory mechanisms mediate early versus late colitis in mice', *Gastroenterology*, 122(1), pp. 94–105. Available at: https://doi.org/10.1053/GAST.2002.30308.

Spits, H. and Cupedo, T. (2012) 'Innate lymphoid cells: emerging insights in development, lineage relationships, and function', *Annual review of immunology*, 30, pp. 647–675. Available at: https://doi.org/10.1146/ANNUREV-IMMUNOL-020711-075053.

Stagg, A.J. (2018) 'Intestinal Dendritic Cells in Health and Gut Inflammation', *Frontiers in Immunology*, 9, p. 2883. Available at: https://doi.org/10.3389/FIMMU.2018.02883/BIBTEX.

Staley, C. *et al.* (2017) 'Interaction of gut microbiota with bile acid metabolism and its influence on disease states', *Applied microbiology and biotechnology*, 101(1), pp. 47–64. Available at: https://doi.org/10.1007/S00253-016-8006-6.

Stellwag, E.J. and Hylemon, P.B. (1976) 'Purification and characterization of bile salt hydrolase from Bacteroides fragilis subsp. fragilis', *Biochimica et biophysica acta*, 452(1), pp. 165–176. Available at: https://doi.org/10.1016/0005-2744(76)90068-1.

Su, C.W. *et al.* (2011) 'Duodenal helminth infection alters barrier function of the colonic epithelium via adaptive immune activation', *Infection and immunity*, 79(6), pp. 2285–2294. Available at: https://doi.org/10.1128/IAI.01123-10.

Suau, A. *et al.* (1999) 'Direct analysis of genes encoding 16S rRNA from complex communities reveals many novel molecular species within the human gut', *Applied and environmental microbiology*, 65(11), pp. 4799–4807. Available at: https://doi.org/10.1128/AEM.65.11.4799-4807.1999.

Sundberg, J.P. *et al.* (1994) 'Spontaneous, heritable colitis in a new substrain of C3H/HeJ mice', *Gastroenterology*, 107(6), pp. 1726–1735. Available at: https://doi.org/10.1016/0016-5085(94)90813-3.

Sydora, B.C. *et al.* (2005) 'Association with selected bacteria does not cause enterocolitis in IL-10 gene-deficient mice despite a systemic immune response', *Digestive diseases and sciences*, 50(5), pp. 905–913. Available at: https://doi.org/10.1007/S10620-005-2663-0.

Sydora, B.C. *et al.* (2007) 'Epithelial barrier disruption allows nondisease-causing bacteria to initiate and sustain IBD in the IL-10 gene-deficient mouse', *Inflammatory bowel diseases*, 13(8), pp. 947–954. Available at: https://doi.org/10.1002/IBD.20155.

Takeichi, M. (2014) 'Dynamic contacts: rearranging adherens junctions to drive epithelial remodelling', *Nature reviews. Molecular cell biology*, 15(6), pp. 397–410. Available at: https://doi.org/10.1038/NRM3802.

Tamana, S.K. *et al.* (2021) 'Bacteroides-dominant gut microbiome of late infancy is associated with enhanced neurodevelopment', *Gut Microbes*, 13(1), pp. 1–17. Available at: https://doi.org/10.1080/19490976.2021.1930875/SUPPL_FILE/KGMI_A_1930875_SM9588.DOCX.

Tamburini, S. *et al.* (2016) 'The microbiome in early life: implications for health outcomes', *Nature Medicine 2016 22:7*, 22(7), pp. 713–722. Available at: https://doi.org/10.1038/nm.4142.

Tan, T.G. *et al.* (2016) 'Identifying species of symbiont bacteria from the human gut that, alone, can induce intestinal Th17 cells in mice', *Proceedings of the National Academy of Sciences of the United States of America*, 113(50), pp. E8141–E8150. Available at: https://doi.org/10.1073/PNAS.1617460113.

Tashiro, Y. *et al.* (2010) 'Variation of Physiochemical Properties and Cell Association Activity of Membrane Vesicles with Growth Phase in Pseudomonas aeruginosa', *APPLIED AND ENVIRONMENTAL MICROBIOLOGY*, 76(11), pp. 3732–3739. Available at: https://doi.org/10.1128/AEM.02794-09.

Teo, J.L. and Kahn, M. (2010) 'The Wnt signaling pathway in cellular proliferation and differentiation: A tale of two coactivators', *Advanced Drug Delivery Reviews*, 62(12), pp. 1149–1155. Available at: https://doi.org/10.1016/J.ADDR.2010.09.012.

Testro, A.G. and Visvanathan, K. (2009) 'Toll-like receptors and their role in gastrointestinal disease', *Journal of gastroenterology and hepatology*, 24(6), pp. 943–954. Available at: https://doi.org/10.1111/J.1440-1746.2009.05854.X.

Thieu, V.T. *et al.* (2008) 'Signal transducer and activator of transcription 4 is required for the transcription factor T-bet to promote T helper 1 cell-fate determination', *Immunity*, 29(5), pp. 679–690. Available at: https://doi.org/10.1016/J.IMMUNI.2008.08.017.

Trauner, M. and Boyer, J.L. (2003) 'Bile salt transporters: molecular characterization, function, and regulation', *Physiological reviews*, 83(2), pp. 633–671. Available at: https://doi.org/10.1152/PHYSREV.00027.2002.

Troncone, E. *et al.* (2021) 'Involvement of smad7 in inflammatory diseases of the gut and colon cancer', *International Journal of Molecular Sciences*, 22(8). Available at: https://doi.org/10.3390/ijms22083922.

Turnbaugh, P.J. *et al.* (2008) 'A core gut microbiome in obese and lean twins', *Nature 2008 457:7228*, 457(7228), pp. 480–484. Available at: https://doi.org/10.1038/nature07540.

Tysk, C. *et al.* (1988) 'Ulcerative colitis and Crohn's disease in an unselected population of monozygotic and dizygotic twins. A study of

heritability and the influence of smoking', *Gut*, 29(7), pp. 990–996. Available at: https://doi.org/10.1136/gut.29.7.990.

Uhlig, H.H. *et al.* (2014) 'The diagnostic approach to monogenic very early onset inflammatory bowel disease', *Gastroenterology*. W.B. Saunders, pp. 990-1007.e3. Available at: https://doi.org/10.1053/j.gastro.2014.07.023.

Ungaro, R. *et al.* (2014) 'Antibiotics Associated With Increased Risk of New-Onset Crohn's Disease But Not Ulcerative Colitis: A Meta-Analysis', *American Journal of Gastroenterology*, 109(11), pp. 1728–1738. Available at: https://doi.org/10.1038/ajg.2014.246.

Vandenplas, Y. *et al.* (2020) 'Factors affecting early-life intestinal microbiota development', *Nutrition (Burbank, Los Angeles County, Calif.)*, 78. Available at: https://doi.org/10.1016/J.NUT.2020.110812.

VanDussen, K.L. and Samuelson, L.C. (2010) 'Mouse Atonal Homolog 1 Directs Intestinal Progenitors to Secretory Cell Rather than Absorptive Cell Fate', *Developmental biology*, 346(2), p. 215. Available at: https://doi.org/10.1016/J.YDBIO.2010.07.026.

Vantrappen, G. *et al.* (1977) 'Bile acid studies in uncomplicated Crohn's disease.', *Gut*, 18(9), p. 730. Available at: https://doi.org/10.1136/GUT.18.9.730.

Vavricka, S.R. *et al.* (2011) 'Frequency and risk factors for extraintestinal manifestations in the swiss inflammatory bowel disease cohort', *American Journal of Gastroenterology*, 106(1), pp. 110–119. Available at: https://doi.org/10.1038/ajg.2010.343.

Velazquez-Villegas, L.A. *et al.* (2018) 'TGR5 signalling promotes mitochondrial fission and beige remodelling of white adipose tissue', *Nature communications*, 9(1). Available at: https://doi.org/10.1038/S41467-017-02068-0.

te Velde, A.A. *et al.* (2003) 'Increased expression of DC-SIGN+IL-12+IL-18+ and CD83+IL-12-IL-18- dendritic cell populations in the colonic mucosa of patients with Crohn's disease', *European journal of immunology*, 33(1), pp. 143–151. Available at: https://doi.org/10.1002/IMMU.200390017.

Verhoeckx, K. *et al.* (2015) 'The Impact of Food Bioactives on Health: in vitro and ex vivo models [Internet]', *The Impact of Food Bioactives on Health: In Vitro and Ex Vivo Models*, pp. 1–327. Available at: https://doi.org/10.1007/978-3-319-16104-4.

Wadwa, M. *et al.* (2016) 'IL-10 downregulates CXCR3 expression on Th1 cells and interferes with their migration to intestinal inflammatory sites', *Mucosal Immunology*, 9(5), pp. 1263–1277. Available at: https://doi.org/10.1038/mi.2015.132.

Waidmann, M. *et al.* (2003) 'Bacteroides vulgatus protects against Escherichia coli-induced colitis in gnotobiotic interleukin-2-deficient mice',

Gastroenterology, 125(1), pp. 162–177. Available at: https://doi.org/10.1016/S0016-5085(03)00672-3.

Walker, J.A. and McKenzie, A.N.J. (2018) 'T H 2 cell development and function', *Nature reviews. Immunology*, 18(2), pp. 121–133. Available at: https://doi.org/10.1038/NRI.2017.118.

Walsham, N.E. and Sherwood, R.A. (2016) 'Fecal calprotectin in inflammatory bowel disease', *Clinical and Experimental Gastroenterology*, 9, p. 21. Available at: https://doi.org/10.2147/CEG.S51902.

Wang, L. *et al.* (2017) 'Breastfeeding Reduces Childhood Obesity Risks', *Childhood obesity (Print)*, 13(3), pp. 197–204. Available at: https://doi.org/10.1089/CHI.2016.0210.

Wang, Y. *et al.* (2008) 'A novel role for villin in intestinal epithelial cell survival and homeostasis', *Journal of Biological Chemistry*, 283(14), pp. 9454–9464. Available at: https://doi.org/10.1074/jbc.M707962200.

Wang, Y. *et al.* (2021) 'Microbial and metabolic features associated with outcome of infliximab therapy in pediatric Crohn's disease', *Gut Microbes*, 13(1), pp. 1–18. Available at: https://doi.org/10.1080/19490976.2020.1865708.

Watanabe, T. *et al.* (2004) 'NOD2 is a negative regulator of Toll-like receptor 2-mediated T helper type 1 responses', *Nature immunology*, 5(8), pp. 800–808. Available at: https://doi.org/10.1038/NI1092.

Weaver, C.T. *et al.* (2013) 'The Th17 pathway and inflammatory diseases of the intestines, lungs, and skin', *Annual review of pathology*, 8, pp. 477–512. Available at: https://doi.org/10.1146/ANNUREV-PATHOL-011110-130318.

Wehkamp, J. *et al.* (2005) 'Reduced Paneth cell alpha-defensins in ileal Crohn's disease', *Proceedings of the National Academy of Sciences of the United States of America*, 102(50), pp. 18129–18134. Available at: https://doi.org/10.1073/PNAS.0505256102.

Westbrook, A.M., Szakmary, A. and Schiestl, R.H. (2016) 'Mouse models of intestinal inflammation and cancer', *Archives of toxicology*, 90(9), pp. 2109–2130. Available at: https://doi.org/10.1007/S00204-016-1747-2.

Van de Wetering, M. *et al.* (2002) 'The beta-catenin/TCF-4 complex imposes a crypt progenitor phenotype on colorectal cancer cells', *Cell*, 111(2), pp. 241–250. Available at: https://doi.org/10.1016/S0092-8674(02)01014-0.

Wick, E.C. *et al.* (2014) 'Stat3 activation in murine colitis induced by enterotoxigenic Bacteroides fragilis', *Inflammatory bowel diseases*, 20(5), pp. 821–834. Available at: https://doi.org/10.1097/MIB.0000000000000019.

Willemsen, L.E.M. *et al.* (2003) 'Short chain fatty acids stimulate epithelial mucin 2 expression through differential effects on prostaglandin E(1) and E(2) production by intestinal myofibroblasts', *Gut*, 52(10), pp. 1442–1447. Available at: https://doi.org/10.1136/GUT.52.10.1442.

Wilson, A.J. *et al.* (2010) 'Apoptotic sensitivity of colon cancer cells to histone deacetylase inhibitors is mediated by an Sp1/Sp3-activated transcriptional program involving immediate-early gene induction', *Cancer research*, 70(2), pp. 609–620. Available at: https://doi.org/10.1158/0008-5472.CAN-09-2327.

Windsor, J.W. and Kaplan, G.G. (2019) 'Evolving Epidemiology of IBD', *Current Gastroenterology Reports*. Current Medicine Group LLC 1. Available at: https://doi.org/10.1007/s11894-019-0705-6.

Wirtz, S. *et al.* (2017) 'Chemically induced mouse models of acute and chronic intestinal inflammation', *Nature protocols*, 12(7), pp. 1295–1309. Available at: https://doi.org/10.1038/NPROT.2017.044.

Woznicki, J.A. *et al.* (2021) 'TNF-α synergises with IFN-γ to induce caspase-8-JAK1/2-STAT1-dependent death of intestinal epithelial cells', *Cell Death & Disease 2021 12:10*, 12(10), pp. 1–15. Available at: https://doi.org/10.1038/s41419-021-04151-3.

Wrzosek, L. *et al.* (2013) 'Bacteroides thetaiotaomicron and Faecalibacterium prausnitzii influence the production of mucus glycans and the development of goblet cells in the colonic epithelium of a gnotobiotic model rodent', *BMC biology*, 11. Available at: https://doi.org/10.1186/1741-7007-11-61.

Xu, F. *et al.* (2016) 'Crystal structure of bile salt hydrolase from Lactobacillus salivarius', *Acta crystallographica. Section F, Structural biology communications*, 72(Pt 5), pp. 376–381. Available at: https://doi.org/10.1107/S2053230X16005707.

Xu, L. *et al.* (2017) 'Systematic review with meta-analysis: breastfeeding and the risk of Crohn's disease and ulcerative colitis', *Alimentary pharmacology & therapeutics*, 46(9), pp. 780–789. Available at: https://doi.org/10.1111/APT.14291.

Yamada, A. *et al.* (2016) 'Role of regulatory T cell in the pathogenesis of inflammatory bowel disease', *World Journal of Gastroenterology*, 22(7), p. 2195. Available at: https://doi.org/10.3748/WJG.V22.I7.2195.

Yan, K.S. *et al.* (2012) 'The intestinal stem cell markers Bmi1 and Lgr5 identify two functionally distinct populations', *Proceedings of the National Academy of Sciences of the United States of America*, 109(2), pp. 466–471. Available at: https://doi.org/10.1073/pnas.1118857109.

Yang, C.S. *et al.* (2015) 'Small heterodimer partner interacts with NLRP3 and negatively regulates activation of the NLRP3 inflammasome', *Nature communications*, 6. Available at: https://doi.org/10.1038/NCOMMS7115.

Yang, I. *et al.* (2013) 'Intestinal Microbiota Composition of Interleukin-10 Deficient C57BL/6J Mice and Susceptibility to Helicobacter hepaticus-Induced Colitis', *PLOS ONE*, 8(8), p. e70783. Available at: https://doi.org/10.1371/JOURNAL.PONE.0070783.

Yang, L. *et al.* (2021) 'The varying effects of antibiotics on gut microbiota', *AMB Express*, 11(1). Available at: https://doi.org/10.1186/S13568-021-01274-W.

Yang, Q. *et al.* (2001) 'Requirement of Math1 for secretory cell lineage commitment in the mouse intestine', *Science*, 294(5549), pp. 2155–2158. Available at: https://doi.org/10.1126/science.1065718.

Yatsunenko, T. *et al.* (2012) 'Human gut microbiome viewed across age and geography', *Nature*, 486(7402), pp. 222–227. Available at: https://doi.org/10.1038/NATURE11053.

Yen, D. *et al.* (2006) 'IL-23 is essential for T cell-mediated colitis and promotes inflammation via IL-17 and IL-6', *The Journal of clinical investigation*, 116(5), pp. 1310–1316. Available at: https://doi.org/10.1172/JCI21404.

Yin, X. *et al.* (2014) 'Niche-independent high-purity cultures of Lgr5 + intestinal stem cells and their progeny', *Nature Methods*, 11(1), pp. 106–112. Available at: https://doi.org/10.1038/nmeth.2737.

Yu, T. *et al.* (2012) 'Krüppel-like factor 4 regulates intestinal epithelial cell morphology and polarity', *PLoS ONE*, 7(2), pp. 1–9. Available at: https://doi.org/10.1371/journal.pone.0032492.

Yurkovetskiy, L. *et al.* (2013) 'Gender bias in autoimmunity is influenced by microbiota', *Immunity*, 39(2), pp. 400–412. Available at: https://doi.org/10.1016/J.IMMUNI.2013.08.013.

Zaki, M.H., Lamkanfi, M. and Kanneganti, T.D. (2011) 'The Nlrp3 inflammasome: contributions to intestinal homeostasis', *Trends in immunology*, 32(4), pp. 171–179. Available at: https://doi.org/10.1016/J.IT.2011.02.002.

Zamani, S. *et al.* (2017) 'Detection of enterotoxigenic Bacteroides fragilis in patients with ulcerative colitis', *Gut Pathogens*, 9(1). Available at: https://doi.org/10.1186/S13099-017-0202-0.

Zampini, A. *et al.* (2019) 'Defining Dysbiosis in Patients with Urolithiasis', *Scientific Reports 2019 9:1*, 9(1), pp. 1–13. Available at: https://doi.org/10.1038/s41598-019-41977-6.

Zeissig, S. *et al.* (2007) 'Changes in expression and distribution of claudin 2, 5 and 8 lead to discontinuous tight junctions and barrier dysfunction in active Crohn's disease', *Gut*, 56(1), pp. 61–72. Available at: https://doi.org/10.1136/GUT.2006.094375.

Zenewicz, L.A., Antov, A. and Flavell, R.A. (2009) 'CD4 T-cell differentiation and inflammatory bowel disease', *Trends in molecular medicine*, 15(5), pp. 199–207. Available at: https://doi.org/10.1016/J.MOLMED.2009.03.002.

Zhang, Y. and Que, J. (2020) 'BMP Signaling in Development, Stem Cells, and Diseases of the Gastrointestinal Tract', *Annual Review of Physiology*, 82, pp. 251–273. Available at: https://doi.org/10.1146/annurev-physiol-021119-034500.

Zhong, H. *et al.* (2019) 'Impact of early events and lifestyle on the gut microbiota and metabolic phenotypes in young school-age children', *Microbiome*, 7(1), pp. 1–14. Available at: https://doi.org/10.1186/S40168-018-0608-Z/FIGURES/4.

Zhou, Y. and Zhi, F. (2016a) 'Lower Level of Bacteroides in the Gut Microbiota Is Associated with Inflammatory Bowel Disease: A Meta-Analysis', *BioMed Research International*, 2016. Available at: https://doi.org/10.1155/2016/5828959.

Zhou, Y. and Zhi, F. (2016b) 'Lower Level of Bacteroides in the Gut Microbiota Is Associated with Inflammatory Bowel Disease: A Meta-Analysis', *BioMed research international*, 2016. Available at: https://doi.org/10.1155/2016/5828959.

Zhu, C. *et al.* (2021) '24-Norursodeoxycholic acid reshapes immunometabolism in CD8 + T cells and alleviates hepatic inflammation', *Journal of hepatology*, 75(5), pp. 1164–1176. Available at: https://doi.org/10.1016/J.JHEP.2021.06.036.

Zimmermann, P. and Curtis, N. (2020) 'Breast milk microbiota: A complex microbiome with multiple impacts and conditioning factors.', *undefined*, 81(1), pp. 17–47. Available at: https://doi.org/10.1016/J.JINF.2020.01.023.